JEFF

**SANDIA REPORT** SAND84—1471 • Unlimited Release • UC—70
Printed December 1984

# Fracture and Matrix Hydrologic Characteristics of Tuffaceous Materials from Yucca Mountain, Nye County, Nevada

R. R. Peters, E. A. Klavetter, I. J. Hall,
S. C. Blair, P. R. Heller, G. W. Gee

**Prepared by**
**Sandia National Laboratories**
**Albuquerque, New Mexico 87185 and Livermore, California 94550**
**for the United States Department of Energy**
**under Contract DE-AC04-76DP00789**

#144

HYDROLOGY DOCUMENT NUMBER 144

SF2900Q(8-81)

Printed in the United States of America
Available from
National Technical Information Service
U.S. Department of Commerce
5285 Port Royal Road
Springfield, VA 22161

NTIS price codes
Printed copy: A09
Microfiche copy: A01

Distribution
Category UC-70

SAND84-1471
Unlimited Release
Printed December 1984

# FRACTURE AND MATRIX HYDROLOGIC CHARACTERISTICS OF TUFFACEOUS MATERIALS FROM YUCCA MOUNTAIN, NYE COUNTY, NEVADA

Sandia National Laboratories
R. R. Peters
E. A. Klavetter
I. J. Hall

Pacific Northwest Laboratory
S. C. Blair
P. R. Heller
G. W. Gee

## ABSTRACT

The geological formations in the unsaturated zone at Yucca Mountain, on and adjacent to the Nevada Test Site (NTS), are currently being studied for consideration as the host for a radioactive-waste repository; the U.S. Department of Energy is carrying out these studies through the Nevada Nuclear Waste Storage Investigations project. The formations are composed of tuffaceous (tuff) materials that must be evaluated to estimate the rate at which radionuclides would migrate to the accessible environment. According to the available evidence, the flux of water in the unsaturated zone beneath the Yucca Mountain site is low; quantifying such low flow rates through direct measurements is difficult. To help provide data that can be used to assess unsaturated flow, Pacific Northwest Laboratory (PNL), under contract to Sandia National Laboratories (SNL), performed hydrologic tests on tuffaceous samples from 48 different locations in Yucca Mountain.

The primary purpose of this document is to provide a compilation of the testing procedures used and the hydrologic data obtained. The results of the testing indicate the following:

1. There are wide variations in water-retention characteristics for the tuffaceous materials tested. Nonwelded, nonzeolitized samples tended to drain readily, while welded samples and nonwelded, zeolitized samples stayed near saturation at relatively high suction head values (10 to 50 m). The water retention characteristic curves (pressure vs saturation), in general, were replicated by mercury-intrusion tests on similar samples.
2. The measured saturated hydraulic conductivities for welded tuff samples were low, ranging from $10^{-10}$ to $10^{-14}$ m/s. Most of the nonwelded, zeolitized samples exhibited low conductivities similar to those of welded samples. The nonwelded, nonzeolitized samples exhibited conductivities ranging from $10^{-6}$ to $10^{-10}$ m/s, values that compare with silts and clay-type soils.
3. The fracture saturated conductivity was significantly higher than the matrix conductivity on all samples tested and flow through all fractured and unfractured samples was reduced at elevated effective pressure. The degree of welding of the matrix and the fracture surface characteristics influenced the response of fractured samples to elevated pressure.

This report contains the entire set of psychrometer measurements of desaturation curves for tuffs from Yucca Mountain as well as a substantial number of saturated conductivity measurements. It is, to the best of the authors' knowledge, the most complete set of published, unsaturated, hydrologic data for any hard rock.

ACKNOWLEDGMENTS

The authors wish to acknowledge the efforts of other individuals who were instrumental to this study. B. M. Schwartz of Sandia National Laboratories (SNL) contributed to document and procedures review. J. H. Gauthier (SNL) provided valuable support for much of the graphics. C. E. Haines, of Pacific Northwest Laboratories (PNL), provided technical assistance in parameter measurement.

TABLE OF CONTENTS

TABLE OF CONTENTS (continued)

FIGURES

FIGURES (continued)

FIGURES (concluded)

TABLES

TABLES (Continued)

## INTRODUCTION

The geological formations in the unsaturated zone at Yucca Mountain, on and adjacent to the Nevada Test Site (NTS), are currently being studied for consideration as the host for a radioactive-waste repository; the U.S. Department of Energy is carrying out these studies through the Nevada Nuclear Waste Storage Investigations project. Because water flow through unsaturated rock is the principal mechanism for the transport of soluble radionuclides and other contaminants from a repository to the biosphere at an arid site, characterization of the hydrologic system within Yucca Mountain is an essential portion of the evaluation of this location. At Yucca Mountain, rates of flow in the unsaturated zone have been shown to be low, but must be quantified or bounded if the site is to be characterized for possible use as a waste repository. However, the quantification of low flow rates deep within any arid formation is difficult, and few direct measurements of unsaturated flow rates have been made (Winograd, 1981). An alternative to direct measurement of the low flow rates in Yucca Mountain is to estimate the flow rate indirectly by using models that account for the dependence of hydraulic properties on water content. Unsaturated-flow codes, combined with the hydrologic properties of tuffaceous (tuff) materials at Yucca Mountain under unsaturated conditions, can be used to predict pressure-head profiles and water content as a function of depth and water flux. These predicted pressure profiles can be compared with pressure profiles and water content determined by field measurements to determine the flow rate within Yucca Mountain. Modeling flow in the unsaturated zone is currently receiving considerable attention. A good introduction to this topic is provided by several authors including Narasimhan (1982).

In a previous contract, Pacific Northwest Laboratory (PNL) provided Sandia National Laboratories (SNL) with data on the relationship between water content and pressure head for tuffs tested in the pressure-head range of 0 to -30,000 m.[a] However, because of limitations of the test apparatus, little water-retention data were collected in the range of -10 to -1000 m of pressure head (which is equivalent to negative suction head). To determine the hydraulic properties in the range of -10 to -1000 m, tests were run on 19 samples of tuff taken from drill hole USW GU-3 and 29 samples taken from drill hole USW G-4 on the NTS. Direct measurement of unsaturated conductivities of tuff within a reasonable time period is currently impossible because of limitations of test equipment. However, theoretical models of unsaturated flow (e.g., Mualem, 1976) allow one to calculate the unsaturated conductivity if water-retention data and saturated-conductivity data are available. Four samples of unfractured tuff from drill hole USW GU-3 were tested at elevated confining pressures to determine the saturated conductivity, and five fractured samples taken from drill hole USW G-4 were tested at elevated confining pressures to determine saturated conductivity. This report discusses the methods used to characterize the hydraulic properties of the tuffs, documents the results of those tests, and provides analysis of those results.

---

(a) Gee, G. W., P. R. Heller, and M. E. Dodson. 1982. "Laboratory Report on the Unsaturated Flow Characteristics of Core Samples from Nevada Test Site Well-USW GU-3 (NTS)." Letter Report, October 1982, Pacific Northwest Laboratory, Richland, Washington.

## MATERIALS AND METHODS

Tuffaceous core materials for testing on this project were taken from drill holes USW GU-3 and USW G-4 in Yucca Mountain. Table 1 presents a summary of the functional stratigraphies found in these two drill holes. The functional stratigraphies were developed by Ortiz (1984) and are based on logs of the drill holes and mineralogical work. Table 2 presents the PNL code, drill hole depth, and functional unit for core samples tested from drill holes USW GU-3 and USW G-4, respectively.

Three types of tests were performed by PNL. They include 1) water-retention tests, 2) unconfined, saturated hydraulic conductivity tests, and 3) confined, saturated hydraulic conductivity tests. Mercury-intrusion tests were performed by Micromeritics[a] so that water-retention curves determined by the mercury intrusion measurements could be compared with those determined by the psychrometric measurements made by PNL.

All 48 samples selected by SNL were tested for water-retention characteristics. The tests were run on cylinders 1.4 x 1.2 cm (diameter x length) that were subcored from the original core samples. The water solution used in testing the hydraulic properties was of low ionic strength and had a composition similar to that of ground water sampled near the test well. Table 3 lists the chemical composition of the test solution.

Unconfined saturated-conductivity tests were also run on the 1.4 x 1.2 cm cylinders. Saturated conductivities at elevated confining pressures were measured on the fractured and unfractured samples listed in Table 4.

---

(a) Micromeritics Instr. Corp., Norcross, Georgia 30093
Tests done on Auto-Pore 9200 Porosimeter to 60,000 psi.

TABLE 1. Description of Units

| Unit | GU-3 Depth[a] (ft) | G-4 Depth (ft) | Hydrologic Unit | Description |
|---|---|---|---|---|
| I-A | 0-343 | 22-118 | Tiva Canyon welded unit | Moderately to densely welded, devitrified ash-flow tuff in the Tiva Canyon Member of the Paintbrush Tuff. |
| I-B | 343-430 | 118-243 | Paintbrush nonwelded unit | Partially welded to nonwelded, vitric and occasionally devitrified tuffs of the Tiva Canyon, Yucca Mountain, Pah Canyon, and Topopah Spring Members of the Paintbrush Tuff. |
| II-L | 430-690 | 243-670 | Topopah Spring welded unit | Moderately to densely welded, devitrified zone of the Topopah Spring Member of the Paintbrush Tuff that contains more than approximately 10% by volume of vugs. |
| II-NL | 690-1187 | 670-1293 | Topopah Spring welded unit | Moderately to densely welded, devitrified zone of the Topopah Spring Member of the Paintbrush Tuff that contains less than approximately 10% by volume of vugs. This is the potential repository unit. |
| III | 1187-1269 | 1293-1345 | Basal Vitrophyre of the Topopah Spring welded unit | Basal Vitrophyre of the Topopah Spring Member. |
| IV-A-v[b] | 1269-1507 | 1345-1360 | Vitric Calico Hills nonwelded unit | Nonwelded ashflows, bedded and reworked tuffs, vitric and primarily nonzeolitized Topopah Spring Member and/or the Calico Hills. |

(a) Sample depths reported in feet are primary data supplied by Sandia National Laboratories.
(b) The lower case "v" or "z" in a unit number (e.g., IV-A-v) indicates whether the unit is vitric or water-induced zeolitization has occurred.

TABLE 1. Description of Units (continued)

| Unit | GU-3 Depth[a] (ft) | G-4 Depth (ft) | Hydrologic Unit | Description |
|---|---|---|---|---|
| IV-B-v | 1507-1560 | Missing | Vitric Calico Hills nonwelded unit | Basal, bedded and reworked zone of the vitric tuffs and tuffaceous sandstones of the Calico Hills. |
| IV-C-v | 1560-1601 | Missing | Vitric Calico Hills non-welded unit | Upper vitric zone of the Prow Pass Member of the Crater Flat Tuff. |
| IV-A-z | Missing | 1360-1706 | Zeolitized Calico Hills nonwelded unit | Nonwelded ashflows, bedded and reworked tuffs, primarily zeolitized, from the Topopah Spring Member and/or the Calico Hills. |
| IV-B-z | Missing | 1706-1761 | Zeolitized Calico Hills nonwelded unit | Basal, bedded and reworked zone of the zeolitized tuffs and tuffaceous sandstones of the Calico Hills. |
| IV-C-z | Missing | 1761-1792 | Zeolitized Calico Hills nonwelded unit | Upper zeolitized zone of the Prow Pass Member of the Crater Flat Tuff. |
| V | 1601-1746 | 1792-1960 | Prow Pass welded unit | Moderately welded, devitrified zone of the Prow Pass Member of the Crater Flat Tuff. |
| VI | 1746-2069 | 1960-2250 | Crater Flat nonwelded unit | Zeolitized portions of the lower Prow Pass Member and of the upper Bullfrog Member of the Crater Flat Tuff. |
| VII | 2069-2508 | 2250-2698 | Bullfrog welded unit | Welded devitrified zone of the Bullfrog Member of the Crater Flat Tuff. |

TABLE 2. Information Concerning Samples Taken from Drill Holes USW G-4 and USW GU-3

| Drill Hole USW G-4 | PNL Sample Code | Depth Below Surface, ft | Unit |
|---|---|---|---|
| | G4-1 | 43 | I-A |
| | G4-2 | 124 | I-B |
| | G4-3 | 208 | I-B |
| | G4-4 | 247 | II-L |
| | G4-5 | 864 (dark section) | II-NL |
| | G4-24 | 864 (light section) | II-NL |
| | G4-6 | 1158 | II-NL |
| | G4-1F | 1215 | II-NL |
| | G4-7 | 1256 | II-NL |
| | G4-2F | 1278 | II-NL |
| | G4-8 | 1299 | III |
| | G4-9 | 1324 | III |
| | G4-3F | 1359 | IV-A-v |
| | G4-10 | 1405 | IV-A-z |
| | G4-11 | 1548 | IV-A-z |
| | G4-4F | 1551 | IV-A-z |
| | G4-12 | 1686 | IV-A-z |
| | G4-13 | 1728 | IV-B-z |
| | G4-14 | 1737 | IV-B-z |
| | G4-15 | 1769 | IV-C-z |
| | G4-16 | 1778 | IV-C-z |
| | G4-5F | 1778 | IV-C-z |
| | G4-17 | 1787 | IV-C-z |
| | G4-18 | 1899 | V |
| | G4-19 | 2006 | VI |
| | G4-20 | 2101 | VI |
| | G4-21 | 2401 | VII |
| | G4-22 | 2407 | VII |
| | G4-23 | (a) | |

TABLE 2. (continued)

| Drill Hole USW GU-3 | PNL Sample Code | Depth Below Surface, ft | Unit |
|---|---|---|---|
| | GU3-1 | 82 | I-A |
| | GU3-2 | 120 | I-A |
| | GU3-3 | 155 | I-A |
| | GU3-4 | 257 | I-A |
| | GU3-5 | 316 | I-A |
| | GU3-6 | 374 | I-B |
| | GU3-7 | 378 | I-B |
| | GU3-8 | 397 | I-B |
| | GU3-9 | 1132 | II-NL |
| | GU3-10 | 1197 | III |
| | GU3-11 | 1245 | III |
| | GU3-12 | 1311 | IV-A-v |
| | GU3-13 | 1331 | IV-A-v |
| | GU3-14 | 1440 | IV-A-v |
| | GU3-15 | 1499 | IV-A-v |
| | GU3-16 | 1555 | IV-B-v |
| | GU3-17 | 1628 | V |
| | GU3-18 | 1680 | V |
| | GU3-19 | 1730 | V |

(a) Sandia Sample Code 1010A (commercial clinoptilolite).

TABLE 3. Constituent Concentration of J-13 Well Water[a] Used in Saturation and Conductivity Tests

| Constituent | mg/L |
|---|---|
| Al | <0.1 |
| Si | 31.35 |
| Fe | 0.05 |
| Mg | 1.98 |
| Ca | 12.93 |
| Sr | 0.04 |
| Li | 0.04 |
| Na | 48.00 |
| K | 4.69 |
| $CO_3$ | 71.70 |
| $HCO_3$ | 0.0 |
| Cl | 3.7 |
| $SO_4$ | 9.3 |
| $NO_3$ | 1.5 |
| $PO_4$ | 0.02 |

(a) pH = 8.10

TABLE 4. Samples Tested for Conductivity at Elevated Confining Pressure

| Unfractured Samples | Fractured Samples |
|---|---|
| GU3-2 | G4-1F |
| GU3-3 | G4-2F |
| GU3-11 | G4-3F |
| GU3-15 | G4-4F |
| | G4-5F |

Unfractured samples tested at elevated confining pressure were wafers 5.4 x 1.9 cm (diameter x length).

The criteria for selecting the fractured core samples were

1. That the fracture be natural, or at least not be obviously caused by the drilling process.
2. That the orientation of the fracture allow testing.

The second criterion indicated that it would be advantageous to look for core containing a single fracture oriented approximately parallel to the core axis. A fracture with this orientation is a member of the vertical fracture set, which is thought to be the predominant fracture set at Yucca Mountain (Scott, 1983). Therefore, all the fractured core selected for testing contained a single fracture oriented approximately parallel to the core axis; the fracture divided the sample into two discrete pieces. Fractured samples were right circular cylinders 6 x 8 or 6 x 15 cm (diameter x length). Photographs of fractured core samples from depths of 1215 (G4-1F) and 1778 (G4-5F) ft in drill hole USW G-4 are presented in Figure 1. Table 5 gives a brief description of each fractured sample tested.

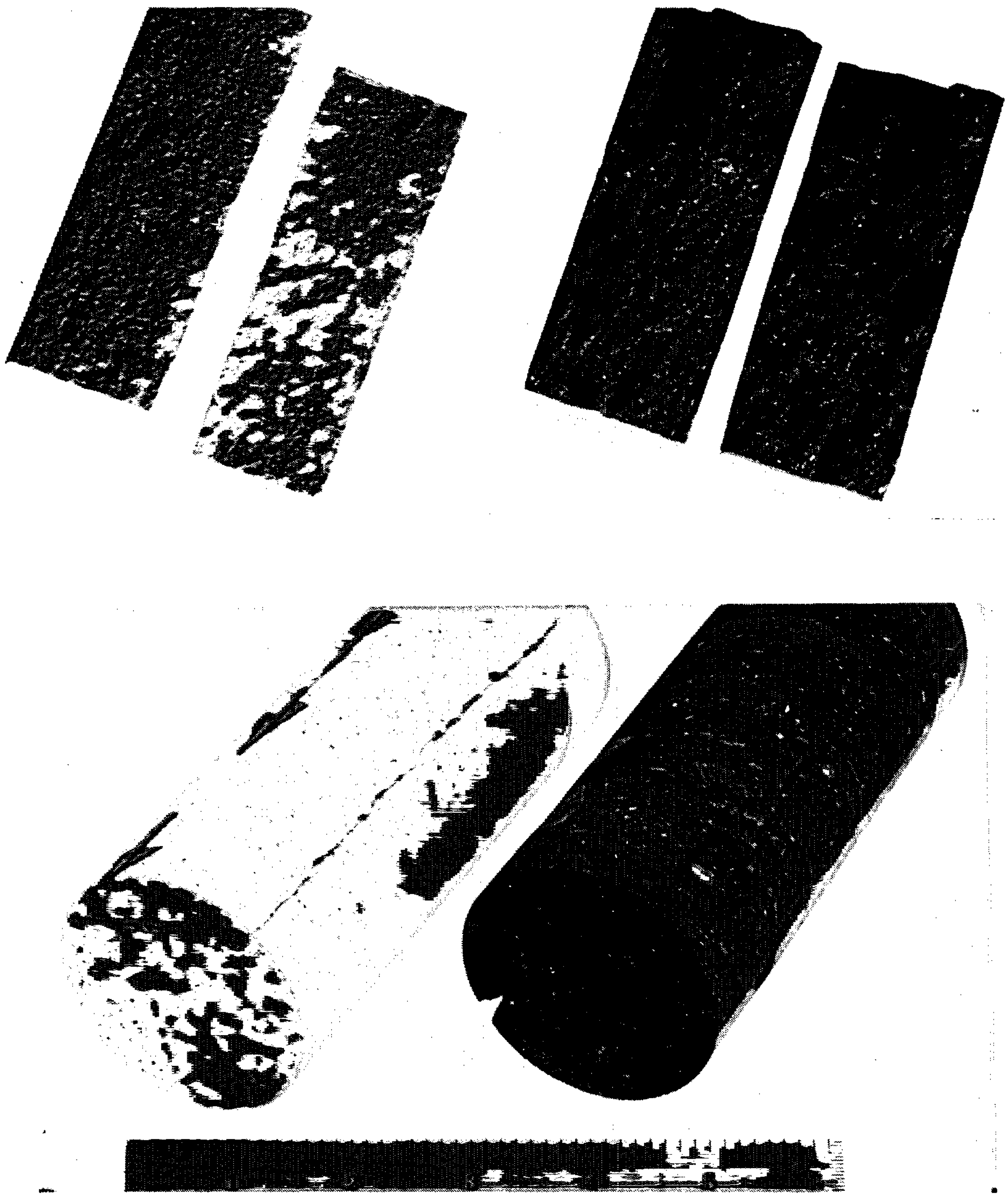

G4-1F

FIGURE 1. Photographs of Two Fractured Core Samples from Drill Hole USW G-4. Fracture surfaces for sample G4-5F mate extremely well while fracture surfaces for G4-1F mate poorly.

TABLE 5. Characterization of Fractured Tuff Cores from Hole USW G-4

| Sample | Sample Depth, ft | Description | Length, cm | Diameter, cm | Crack Width, cm | Fracture Surface | Fracture Mating | Comments |
|---|---|---|---|---|---|---|---|---|
| G4-1F | 1215 | Densely welded tuff, Brown color | 15.29 | 6.08 | 6.05 | Rough, but planar surface Oriented parallel to core axis | Poor | Asperities on surface oriented parallel to core axis Fracture has poor fit and largest aperture Missing chips along fracture surface |
| G4-2F | 1278 | Densely welded tuff, Brown color | 7.67 | 6.10 | 5.80 | Smooth, curved surface Subparallel to axis | Fair | Obvious voids along surface, flow channels visible, one large chip loose at end of core |
| G4-3F | 1359 | Densely welded tuff, Dark grey | 15.28 | 6.07 | 6.05 | Smooth, planar surface Parallel to core axis | Good | |
| G4-4F | 1551 | Moderately consolidated, Whitish matrix with angular black fragments | 7.72 | 5.99 | 5.89 | Undulating surface Subparallel to core axis | Fair | Lithic fragments, (~0.5-0.8 cm dia.) present throught rock |
| G4-5F | 1778 | Moderately consolidated tuff, Pink in color | 15.27 | 6.10 | 4.95 | Planar surface Parallel to core axis | Excellent | Fracture surfaces mate extremely well |

## TESTING METHODS--WATER RETENTION

This section describes the testing methods used to obtain data concerning the functional relationship between sample saturation and pressure head. This relationship is one of the two "characteristic curves" required by unsaturated hydrology models. The data, when combined with the saturated hydraulic conductivity, can be used to estimate the functional relationship between sample unsaturated conductivity and pressure head--the second characteristic curve required by the models. (The calculation of the unsaturated conductivity is discussed in the Results section.)

Two methods were used to obtain the water-retention curve. The first is a direct method using a thermocouple psychrometer. The second is a somewhat indirect one using the results of mercury-intrusion tests.

All samples were vacuum saturated before testing with the thermocouple psychrometer. The samples were placed in a vacuum chamber, which was then filled with J-13 well water to just cover the samples. The chamber was pumped for 45 minutes and the samples were allowed to saturate inside the closed chamber for 24 hours before testing. Grain density and bulk density were measured for each sample to determine porosity. Samples were tested using a thermocouple psychrometer, yielding data for water retention as a function of pressure.

### Psychrometer Tests

A commercial thermocouple psychrometer[a] was used to measure water potential (used to estimate the suction head, h,) of the matrix water in the range from 10 to 10,000 m (Figure 2). The samples were wiped clean of any free water, placed in a preweighed bottle, weighed, and transferred to a small

(a) Decagon, Inc., Pullman, Washington.

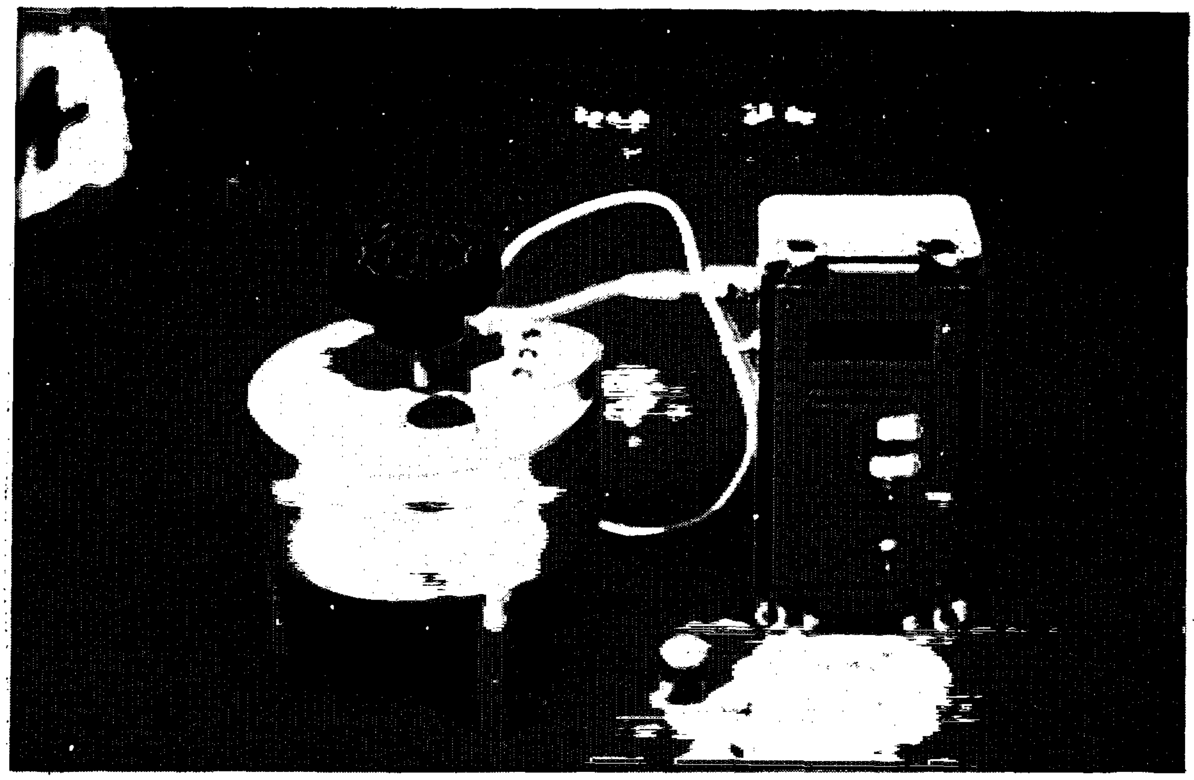

FIGURE 2. Thermocouple Psychrometer Sample Changer, Small Chamber, and Direct Readout Unit

cup that fit into a vapor-tight chamber in the thermocouple psychrometer. After approximately 1 hour, during which time the samples and chamber were allowed to equilibrate thermally, the relative humidity was measured with a miniature thermocouple psychrometer. The samples were removed, dried slightly (for about 30 seconds) in a microwave oven and allowed to cool; the process was then repeated. Moisture content was determined gravimetrically, and the water potential was determined from the measured humidity.

Microwave drying (Gee and Dodson, 1981) was used to desaturate the samples in a stepwise fashion because it saved time and dried the samples more uniformly than drying in a conventional electric oven. Some welded samples did not dry completely using this technique, apparently because water was trapped in the pores. Other samples were incompletely saturated and dried too quickly. These latter samples were then resaturated and the entire process repeated. In all cases, heating in a conventional electric oven was used to determine the final oven-dry weight. Samples were dried at 105°C for a minimum of 24 hr before weighing.

Humidity readings were taken until the sample reached a predesignated suction head, usually between 1000 and 3000 m. The data points corresponding to suction heads greater than 3000 m were obtained by allowing the samples to air dry and weighing the samples. An Assmann psychrometer[a] was used to measure the relative humidity of the air and, hence the sample. For all humidity measurements three subsamples for each sample depth (e.g., G4-1) in USW G-4 and two subsamples for each sample depth in USW GU-3 were tested to determine the homogeneity of subsamples as well as the consistency of tests, and to gather more data in the pressure range where the sample water content changed quickly.

---

(a)Weather Measure Corp., Sacramento, California.

A standard salt solution (0.5 M NaCl) with a water potential of 233 m at 25°C was used for calibrating the psychrometer. The psychrometer was considered to be functioning correctly when the measured value of water potential of the salt solution was within 10 m of the standard value. This test result also indicated that thermal equilibrium was being maintained in the sample chamber, since a sample temperature control of approximately 0.01°C is required to attain reproducibility of 10 m (Brown and Van Haveren, 1972). The inside walls of the sample cup were coated with paraffin to prevent water from adsorbing on the cup walls.

Estimation of Suction Head From Psychrometric Measurements

The psychrometer measures the wet-bulb depression (humidity) in a closed chamber directly above the sample using a miniature thermocouple connected to a microvolt sensing unit. The equilibrium vapor pressure and relative humidity can be related directly to the water potential of the water in the sample (Campbell, 1977). The relationship between the total water potential and relative humidity can be written as

$$\psi = \frac{-RT}{M} \ln (RH/100) \qquad (1)$$

where $\psi$ = total water potential

$R$ = universal gas constant

$T$ = Kelvin temperature

$M$ = molecular weight of water

$RH$ = relative humidity (percent).

Numerous references (e.g., Hillel, 1981; Papendick and Campbell 1980) detail the relationship of total water potential to individual component potentials and to sample suction. The total water potential of the water in the sample is the sum of the individual water-potential components as follows:

$$\psi = \psi_{os} + \psi_m + \psi_g + \psi_p + \psi_{ov} \qquad (2)$$

where $\psi_{os}$, $\psi_m$, $\psi_g$, $\psi_p$, $\psi_{ov}$ are osmotic, matrix, gravitational, pressure and overburden potential components, respectively.

For an unsaturated tuffaceous rock sample at atmospheric pressure, the major components of the total potential are $\psi_{os}$ and $\psi_m$. Because the J-13 well water used in the tests was low in salts, it was assumed that $\psi_{os}$ was negligible; hence, $\psi$ is approximately equal in magnitude to the matrix potential, $\psi_m$. The value of $\psi$ or $\psi_m$ can be expressed either in terms of pressure units (Pascals or bars) or head units (m) (Campbell and Van Schilfgaarde, 1981). The suction head, h, is equal to $-\psi_m$ and represents the water head created by capillary and surface adsorptive forces of the matrix material. The water potential readings (negative bars) from the psychrometer were converted to suction head values (m) by multiplying by -10.2.

Mercury-Intrusion Tests

Mercury intrusion tests were performed on samples from USW G-4. Sample size was approximately 1.2 x 2.0 cm (diameter x length). The Micromeritics AutoPore 9200 testing apparatus was used with standard testing procedures. The sample and chamber were evacuated before testing began. The pressure range during the mercury-intrusion testing was 1.5 to 60,000 psi. The approximate range of pore sizes corresponding to this pressure range is 120 to

0.003 microns based on capillary bundle theory (e.g., Hillel, 1982). The primary result of these tests is the measured relationship between pressure and intruded mercury volume. The intruded mercury volume data is converted to mercury-saturaton data by dividing each data point by the maximum value of intruded mercury volume. The manner in which the mercury-saturation data points are used is explained below.

The adjustment for the differences in the properties of mercury and water was based on capillary bundle theory (e.g., see Hillel, 1982) with the suction head for water calculated as:

$$h_w = \frac{P_{Hg}}{\rho_w g} \frac{\sigma_w \cos(\gamma_w)}{\sigma_{Hg} \cos\left(\gamma_{Hg}\right)} \tag{3}$$

where

$P$ = pressure

$\sigma$ = surface tension between the fluid and tuff

$\gamma$ = contact angle between the fluid and tuff.

$\rho_w$ = density of water

$g$ = acceleration of gravity

The "w" and "Hg" subscripts refer to water and mercury, respectively. The specific values used for sigma and gamma were estimates based on information contained in a variety of sources (e.g., Hillel, 1982) and are listed below.

$\sigma_w$ = 72 dynes/cm $\gamma_w$ = 15°

$\sigma_{Hg}$ = 484 dynes/cm $\gamma_{Hg}$ = 130°.

The water saturation corresponding to this adjusted pressure is 1 minus the mercury saturation determined in the intrusion tests. Thus, at zero pressure the mercury saturation of the sample is zero and the corresponding water saturation is 100%. At the maximum recorded pressure, corresponding to an $h_w$ of about $1.0 \times 10^4$ m of water, the mercury content of the sample is a maximum, the mercury saturation is assumed to be 100%, and the corresponding water saturation is 0%.

## TESTING METHODS--SATURATED HYDRAULIC CONDUCTIVITY

The saturated hydraulic conductivity testing consists of

1. Unconfined matrix-conductivity testing of the small samples used in the water-retention tests and of larger, core samples.
2. Confined, matrix-conductivity testing of core samples.
3. Confined, conductivity testing of fractured core samples.

All samples were saturated in the manner described previously.

### Unconfined Matrix Testing

Unconfined, saturated hydraulic conductivity was measured by a constant head method. This method measures conductivity by determining the time necessary for a given amount of liquid at room temperature (20 to 22°C) to pass through the core under a fixed pressure gradient. All 29 samples from drill hole USW G-4 were tested using the Ruska permeameter;[a] for about half of the samples more than one subsample was tested. Cross-sectional samples from drill hole USW GU-3 and six samples from USW G-4 were tested using a permeameter designed to accommodate the core samples.

#### Ruska Permeameter Tests

Tuff matrix samples were cut to size (1.4 x 1.2 cm), vacuum saturated, and inserted into the core holder. The core holder and buret above the sample were filled with test liquid to a level slightly above the upper index mark. A 2-bar (20.4-m) pressure gradient was applied on the test liquid from the top of the buret. The time necessary for the liquid level in the buret to drop

(a) Model No. 1013-801-00, Ruska Instr. Corp., Houston, Texas.

from the upper to the lower index mark was determined and the saturated hydraulic conductivity calculated using Darcy's law for laminar flow in a right circular cylinder:

$$K = (Q/At)(L/\Delta H) \tag{4}$$

where $K$ = saturated hydraulic conductivity (m/s)

$Q$ = volume of water passing through the sample ($m^3$)

$A$ = cross-sectional area of the sample ($m^2$)

$t$ = time (seconds)

$L$ = length of sample (m)

$\Delta H$ = hydraulic head difference (m).

Note: At 20°C, with water's density at 1 g/$cm^3$, the relationship between the permeability unit of "darcy" and the conductivity unit of "m/s" is 1 darcy = $1.02 \times 10^{-5}$ m/s.

Core Permeameter Tests

Because the cores were not uniform, cross sections were taken from selected core samples to represent the heterogeneity of the entire core cross section. Cross sections in the form of wafers 6 x 2 cm (diameter x length) were taken from six of the core samples from drill hole USW G-4, (G4-5, G4-11, G4-13, G4-14, G4-17, and G4-18). The dimensions of the USW GU-3 samples were 6 x 5 cm. These samples were positioned in a specially built, rigid-wall, plastic permeameter and sealed in place with a silicone rubber compound to prevent water flow between the sample and the permeameter wall. The samples were then vacuum saturated and allowed to soak a minimum of 24 hr before testing. For these constant-head tests, elevated pressures up to 3 bars (30.6 m equivalent head) were applied to the permeant solution (J-13 well water). The effluent from each sample and the time required to collect it were recorded, and Equation 4 was used to determine the conductivity of the sample.

Confined Matrix Testing

This section describes conductivity tests performed on relatively thin (1.9 cm) samples of unfractured tuff under saturated conditions and confining stresses. The purpose of these measurements was to measure hydraulic conductivity under conditions that simulated the overburden stress encountered at depth. The sample was placed between two metal endcaps and coated with silicon rubber and shrink tubing as shown in Figure 3. The sample stack was then assembled into the base plate of the pressure vessel and vacuum saturated with J-13 well water. The base plate was then raised into a pressure vessel. The high-pressure apparatus is shown pictorially in Figure 4 and is described in detail by Blair and Stottlemyre (1981).

To determine the flow through unfractured tuff, the confining fluid pressure was raised to 100 bars and upstream pore pressure maintained at 50 bars. A high-pressure positive-displacement pump was used to supply pore fluid to the sample at a constant rate and a gas-backed accumulator was used to maintain a constant pressure on the downstream pore fluid reservoir. A differential pressure transducer was used to monitor pressure drop across the sample. The conductivity test apparatus is shown schematically in Figure 5a. The fluid supply rate was adjusted until steady-state flow was obtained. This

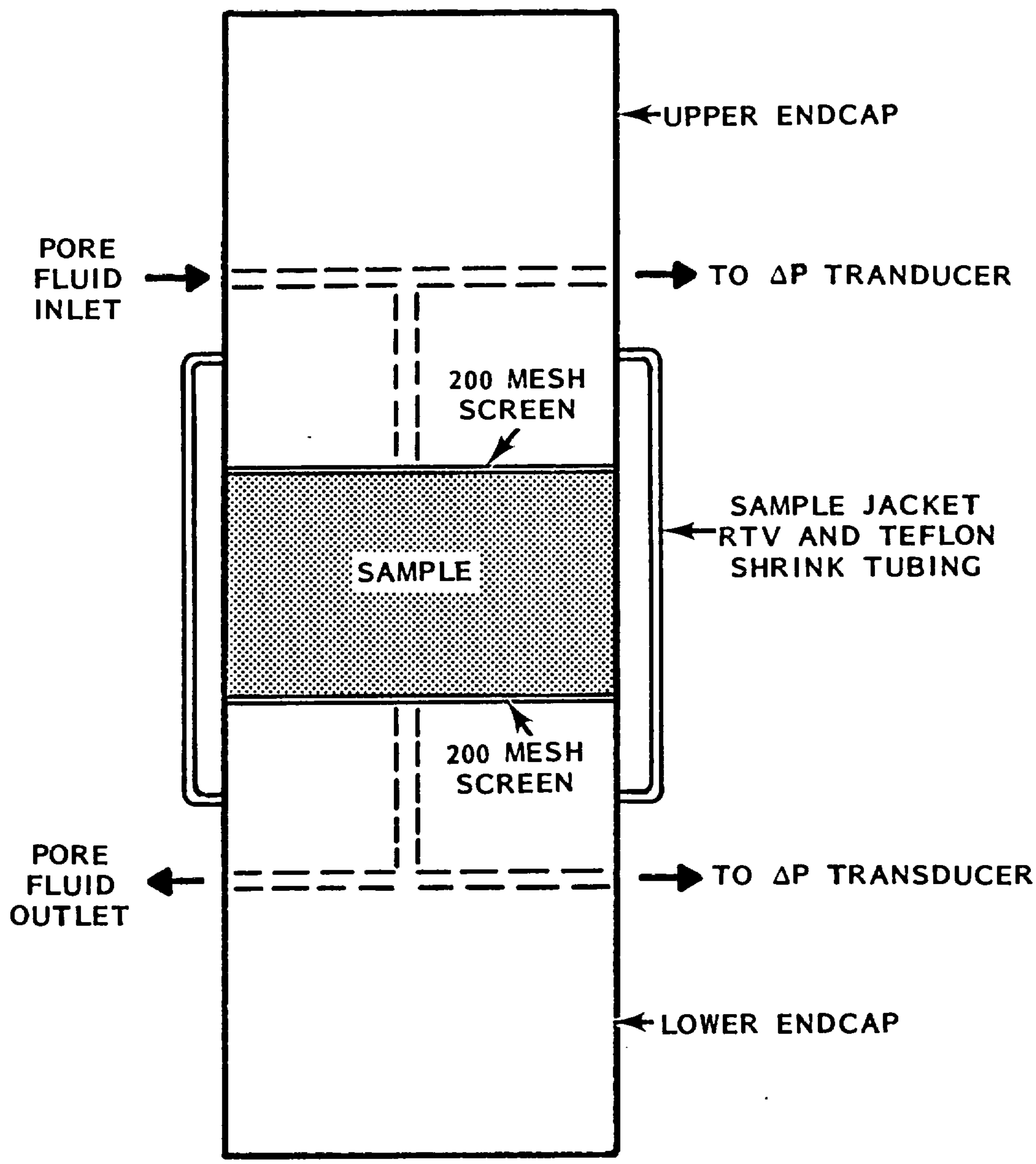


FIGURE 3. Schematic of Sample Assembly for High-Pressure Testing

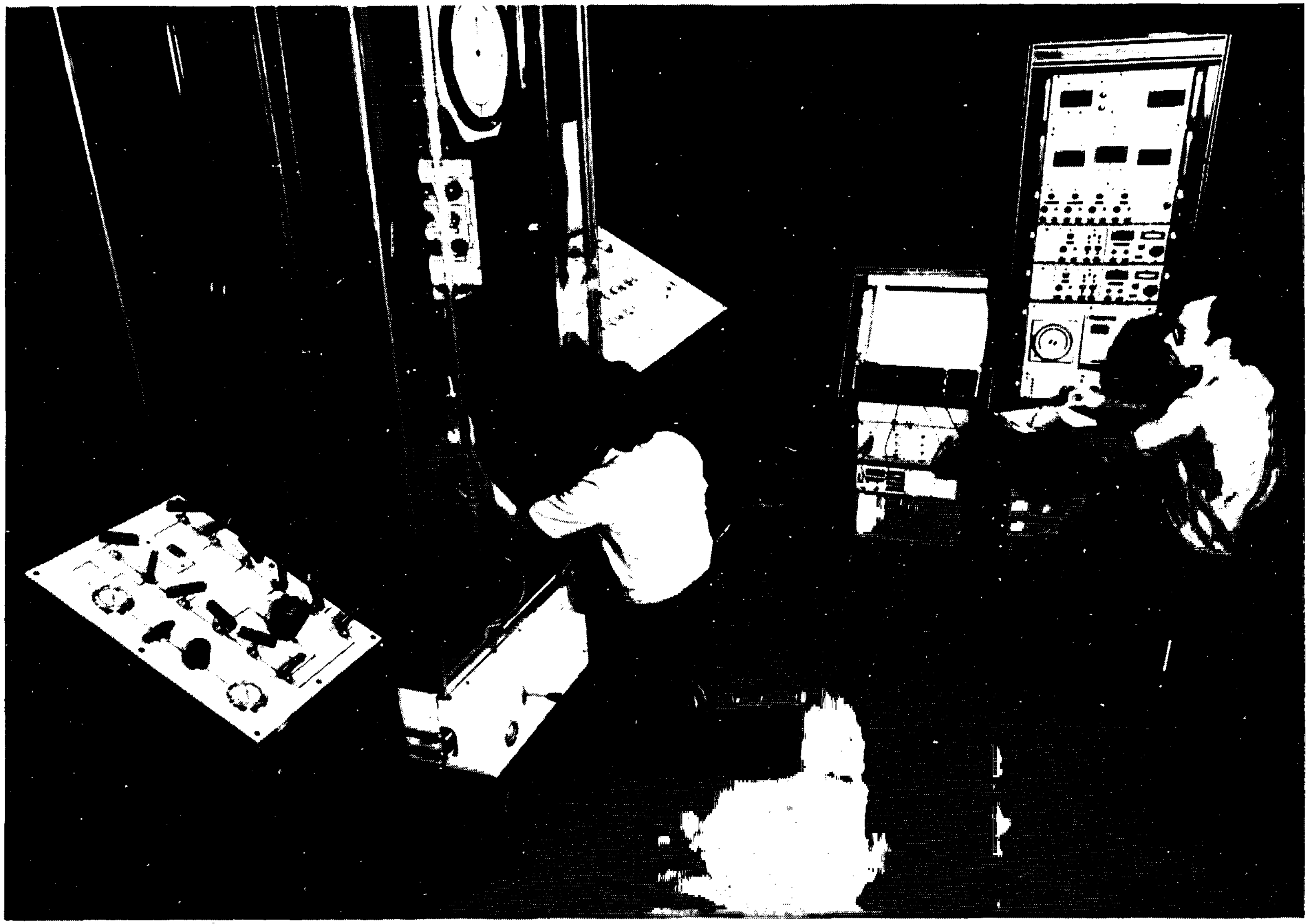

FIGURE 4. High-Pressure Testing Apparatus

was determined by monitoring upstream and downstream pressure as well as pressure drop across the sample. Steady-state flow was assumed when all pressure values (confining fluid, pore fluid inlet, etc) remained constant over a reasonable time period (on the order of minutes to hours). The exact length of time required to reach steady-state is dependent on many factors with the major one being the sample's saturated conductivity. Five different parameters were digitally recorded during the tests. These parameters, along with their estimated accuracy, are listed in Table 6. An analog chart recorder was also used to monitor various parameters throughout the testing.

Saturated conductivity measurements at increasing effective pressures (stresses) were conducted by increasing the confining fluid pressure and then reducing the fluid supply rate to attain a desired effective pressure. The saturated conductivity was calculated using Darcy's law for a laminar flow (Equation 4).

The effective pressure is a measure of the average confining stress on the sample and is calculated as

$$P_{eff} = P_c - \frac{[P_i + P_o]}{2} \qquad (5)$$

where

$P_c$ = confining fluid pressure

$P_i$ = pore fluid pressure at sample inlet

$P_o$ = pore fluid pressure at sample outlet

The effective pressure applied to a sample in the testing apparatus is approximately equivalent to the in situ confining stress.

Confined Fracture Testing

This section describes the saturated hydraulic conductivity testing performed on large (6 x 8 or 6 x 15 cm long) cylindrical samples of fractured tuff. Dimensions of each sample were measured, the fracture surfaces were examined, and the characteristics were documented (see Table 5). The sample was prepared in the same manner as that used for the saturated hydraulic conductivity testing of matrix samples under confining stress (discussed in the previous section).

To test fractured samples, the confining pressure and pore pressure were initially raised to 35 and 30 bars, respectively. The pore pressure was kept at approximately 30 bars throughout all tests, while the confining pressure was varied over a range of 35 to 150 bars. A pressure differential was introduced across the sample and flow through the sample was measured using one of two methods. For samples accommodating high flow rates (greater than 0.1 mL/s), flow was measured using a flow meter downstream of the sample, and back pressure was maintained through the use of a metering valve. This configuration is shown schematically in Figure 5b. For samples that were less permeable, the system was configured as shown in Figure 5a, and flow rate was calculated from piston displacement in the pore-fluid supply pump. In both methods, a differential pressure transducer was used to measure pressure drop across the sample. Data for confining pressure, upstream and downstream fluid pressure, differential pressure, pump displacement, flow rate, and temperature were recorded digitally. The accuracy of measurement of all parameters, except temperature, is listed in Table 6 (Blair and Stottlemyre, 1981). Sample temperature was that of the ambient conditions (22°C).

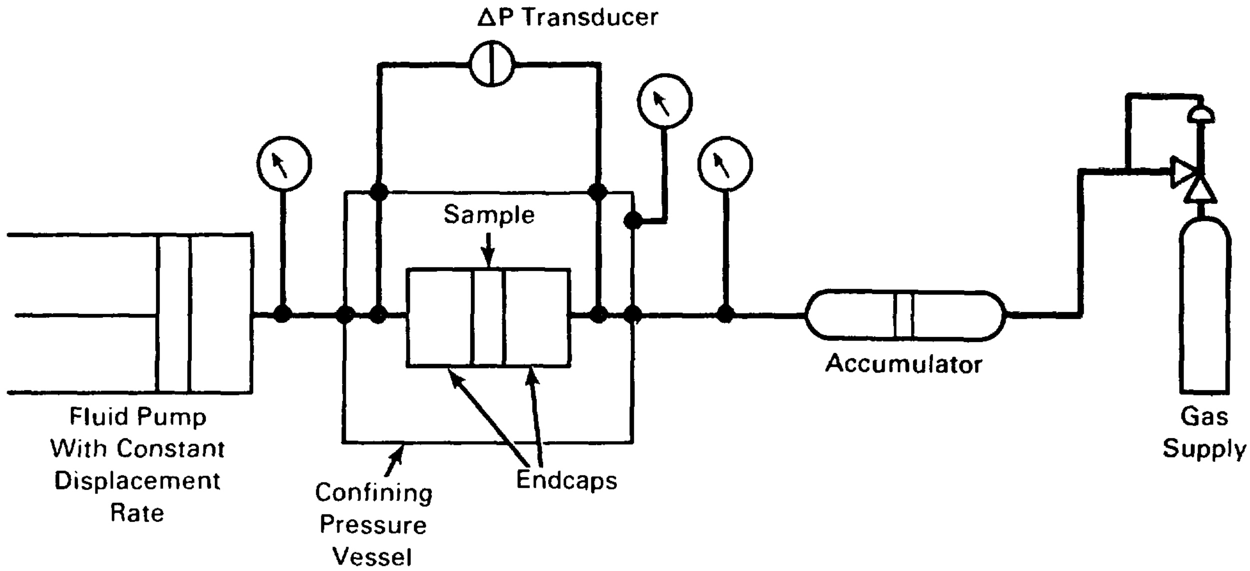


5a - Unfractured Samples and Fractured Samples with Flow Rates Less than 0.1 mL/s

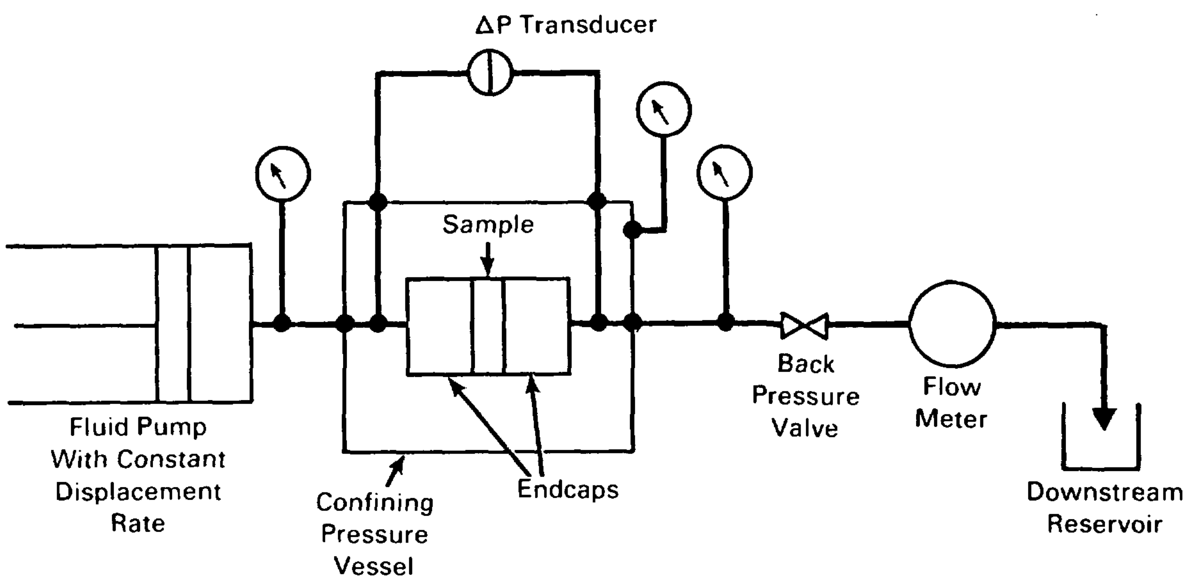


5b - Fractured Samples with Flow Rates Greater than 0.1 mL/s

FIGURE 5. Conductivity Test Apparatus

TABLE 6. Accuracy of Parameters Digitally Recorded During Experiment

| Parameter | Accuracy (Better Than) |
|---|---|
| Fluid pump displacement | $4.6 \times 10^{-5}$ mL |
| Upstream pore fluid pressure | 1% |
| Downstream pore fluid pressure | 1% |
| Differential pressure across sample | 1.4% |
| Confining fluid pressure | 0.25% |

For all tests, data for confining pressure were recorded manually in a notebook, and data for pore pressure were recorded on an analog recorder. A detailed procedure for the laboratory testing is provided in Appendix A in Figure A.1. For all samples, saturated conductivity was calculated only for intervals where flow was judged to be steady state.

The cubic law approximation for steady-state laminar flow between parallel plates was used to reduce the laboratory fracture-flow data. This approximation for flow in a crack is given by Gale (1975) as

$$\frac{Q}{t} = \frac{e^3 w}{12 \mu L} \Delta P \qquad (6)$$

where

$e$ = effective parallel-plate hydraulic fracture aperture (m)

$\mu$ = fluid viscosity $\left( \frac{Ns}{m^2} = 10 \text{ poise} \right)$

$w$ = fracture width (m).

The effect of surface roughness was not included in this analysis. The ratio of physical aperture to effective parallel-plate hydraulic aperture (e) appears to generally be in the range of 2 to 7 (Barton, et al., 1983). Laboratory data were used to solve for e and then a fracture conductivity, $K_f$, was calculated by using the approximation (Gale, 1975):

$$K_f = \frac{e^2 \rho g}{12\mu} \quad (7)$$

where

$\rho$ = fluid density (kg/m$^3$)

All measurements were conducted at 22°C, and a fluid viscosity of $\mu = 0.9548 \times 10^{-2}$ poise was used in all calculations.

# RESULTS

In this section, we discuss the data obtained by testing the water-retention characteristics, the hydraulic conductivities of the tuff matrix, and the hydraulic conductivity of the matrix and fractures at elevated confining pressures. These data are listed in tabular form in Appendix A.

## RESULTS OF WATER RETENTION TESTING

### Psychrometer Water Retention Data

Table A.1 in Appendix A presents the water-retention characteristics at various suction heads in the range from 0 to about 10,000 m. Appendix B contains plots based on these data. Three individual subsamples were tested for each USW G-4 depth (e.g., depth of 43' denoted as sample G4-1) and two individual subsamples were tested for each USW GU-3 depth. The relative humidity was converted to water potential using Equation 1. Table A.2 (Appendix A) summarizes the densities and hydraulic conductivities. The total porosity (Tables A.1 and A.2) was calculated using the bulk density data (Table A.1) and the grain density (Table A.2).

The total porosity and maximum measured water content ("vol/vol" column) listed in Table A.1 for each subsample are approximately the same value (i.e., the subsample was almost completely saturated--see G4-2a). There are two possible causes for those cases where the maximum water content and porosity differ greatly (e.g., G4-12a or G4-9a).

1. The porosity determined from the subsample's bulk density and a single grain-density measurement for that sample depth is inaccurate because tuff variability within that sample.

2) When the subsample's maximum water content is much less than the porosity (e.g., G4-9a), the sample may contain many very small and/or disconnected pores that could not be saturated by a vacuum saturation technique within a reasonable amount of time. It can be assumed that these pores will not contribute significantly to water flow.

For these reasons, the maximum volumetric water content rather than the porosity was used as a basis on which the relative saturation was computed. The data plotted in Appendix B are the volumetric water content divided by the volumetric water content when the sample is "saturated." This quantity will be referred to as the saturation.

Comparison with Mercury-Intrusion Tests

The results of mercury-intrusion tests have also been used to estimate the shape of the saturation curve. Mercury-intrusion tests were run on almost all of the G-4 samples. Appendix C contains 23 figures showing a comparison of the saturation data derived from the psychrometer tests and its curve fit (discussed in the next section) with the adjusted mercury-intrusion data. Table A.3 summarizes the ancillary data on porosity, bulk density, and grain density supplied by Micromeritics.

The plots in Appendix C indicate that the saturation curves derived from the mercury-intrusion data are in qualitative agreement with the psychrometer-derived saturation curves at suction-head values less than about $2 \times 10^3$ m of water. Above this suction head it becomes very difficult to push mercury into the extremely small pores, and so the water saturation, derived from the mercury-intrusion tests, at high suction heads drops to zero. In some cases there are significant differences between the mercury-intrusion results and the psychrometer test results at all suction heads (e.g., G4-3 and G4-22). The conclusions drawn from the figures in Appendix C are

1. The mercury-intrusion data and the psychrometer data generally support each other over the pressure range where both tests are valid. Thus, the confidence in the results obtained from both testing methods is increased.
2. In a few cases there is significant disagreement both qualitatively and quantitatively. It should be noted, however, that the two fluids used in the testing procedures are fundamentally different, with mercury being a nonwetting fluid and water being a wetting fluid. The assumptions made to convert the mercury intrusion data to water saturation data are quite simplistic and may miss important effects (due to sample structure or mineralogy) that may be present in some samples and not in others. The psychrometer data are a much more direct measurement of the desired information and so they should be more reliable.

Fitting the Water-Retention Data

Many different functions have been suggested to be used to fit water retention data. A discussion of these may be found in a paper by Van Genuchten (1978). Several different functions were tried; functions suggested by Haverkamp (1977) and Van Genuchten appeared the most promising.

The Van Genuchten curve was used to fit the saturation data because it gave as good a fit as other methods and it yields an analytical expression when the relative hydraulic conductivity is calculated by the method of Mualem

(1976) (McKeon et al., 1983). A discussion of a comparison of Van Genuchten and Haverkamp fits of the data may be found in Appendix D. The conclusion of this comparison is that when the curve is well defined by the data points, the two curve fits provide nearly identical results.

The equation for the saturation (or equivalently, moisture content) is:

$$S = (S_s - S_r)\left[\frac{1}{1 + |\alpha h|^{\beta}}\right]^{\lambda} + S_r \qquad (8)$$

The equation for the unsaturated conductivity using the Van Genuchten fit and the method of Mualem (1976) is:

$$K(h) = K_s\left(\frac{[1 - |\alpha h|^{\beta-1} \cdot (1 + |\alpha h|^{\beta})^{-\lambda}]^2}{(1 + |\alpha h|^{\beta})^{\lambda/2}}\right) \qquad (9)$$

α : suction head $-\frac{P_c}{\rho g}$

The values of $K_s$, α, β, and $S_r$ for each sample are listed in Table A.2. Estimates of the parameters were calculated using the SOILGEN computer codes described by McKeon et al. (1983).

The method of Mualem for calculating unsaturated conductivities has been shown to work well for a variety of soils, but the authors have not found any evidence of any methods which have proven validity over the large suction head ranges and low unsaturated conductivities characteristic of the tuff samples tested. There is currently no direct way to measure low unsaturated conductivities ($<10^{-10}$ m/s) for liquid flow in a reasonable time period. Therefore, this calculational method was determined to be acceptable to meet current needs.

## Discussion of Water-Retention Results by Unit

The water retention data and curve fits have been collected for each rock unit in Figures 6-14 (for definition of the units see Table 1). The figure for each unit has the data points for all the samples belonging to that unit plotted in the upper half of the figure with the corresponding fitted curves plotted in the lower half of the figure. These plots, together with Table 2, may be examined to gain understanding of the homogeneity of a unit and the similarities and differences between the units. The accuracy of the psychrometer data is of the order of 10 m of suction head; a fact which should be considered during examination of Figures 6-14. The information in Figures 6-14 also was used to attempt to pick representative samples for each unit for use in future hydrologic computations. The representative sample was chosen on the basis of the following criteria which are listed in order of decreasing importance.

1. Saturation curve shape.
2. Saturated conductivity.
3. Porosity and other bulk properties.

As information resulting from upcoming tests becomes available an attempt will be made to apply statistical methods to this larger data set to more rigorously quantify the definition of a representative sample, the variation in parameter values, etc. This rigorous definition of property variability will be necessary for calculations required as a part of the licensing process.

Figure 6 shows a consistent pattern for Unit I-A (the welded, devitrified Tiva Canyon). A representative sample for the samples tested in this unit is G4-1.

Unit I-B (Figure 7) looks self-consistent except for G4-2 which, according to the tables, has a relatively low porosity (0.27) when compared to the other samples (0.40 to 0.65). X-ray diffraction tests of G4-2 show that it is a devitrified, partially welded sample. Thus, its saturation curve is dissimilar to the rest of the samples which are vitric, partially welded to nonwelded tuffs. A representative sample for the samples tested in this unit is GU3-7.

The saturation curves of Units II-L and II-NL were combined in Figure 8 because the matrix of the two units should be very similar in chemical composition and bulk properties. The curves appear fairly self-consistent. X-ray diffraction testing of samples G4-5 and G4-24 show no significant differences in the major constituents of the samples. A representative sample for the samples tested in this unit is G4-6.

The saturation curves (Figure 9) for Unit III are fairly self-consistent for a unit consisting of a vitrophyre that may be locally altered. The plot of the data points shows much more consistency than the plot of the fitted curves. The porosities for this unit are very low (0.02 to 0.11) and it was difficult to saturate the samples. G4-8 has a typical or average curve shape and saturated hydraulic conductivity; however, its porosity is the highest. There appears to be no sample that can qualify as representative or average for the samples tested in this unit. GU3-10 or GU3-11 could be used in calculations.

In Figure 10, Units IV-A-v through IV-C-v were combined into Unit IV-v which is a nonwelded, vitric unit with occasional zeolitization. The major difference between Unit IV-v and Unit IV-z is the prevalence of zeolitization. The variability of the unit is also seen in the plot of the saturation curves with some of the curves appearing to be similar to those of Unit I-B (a vitric, nonzeolitized unit). Other curves tend to resemble those of Unit IV-z (a zeolitized unit). Inspection of the Unit IV-v curves together

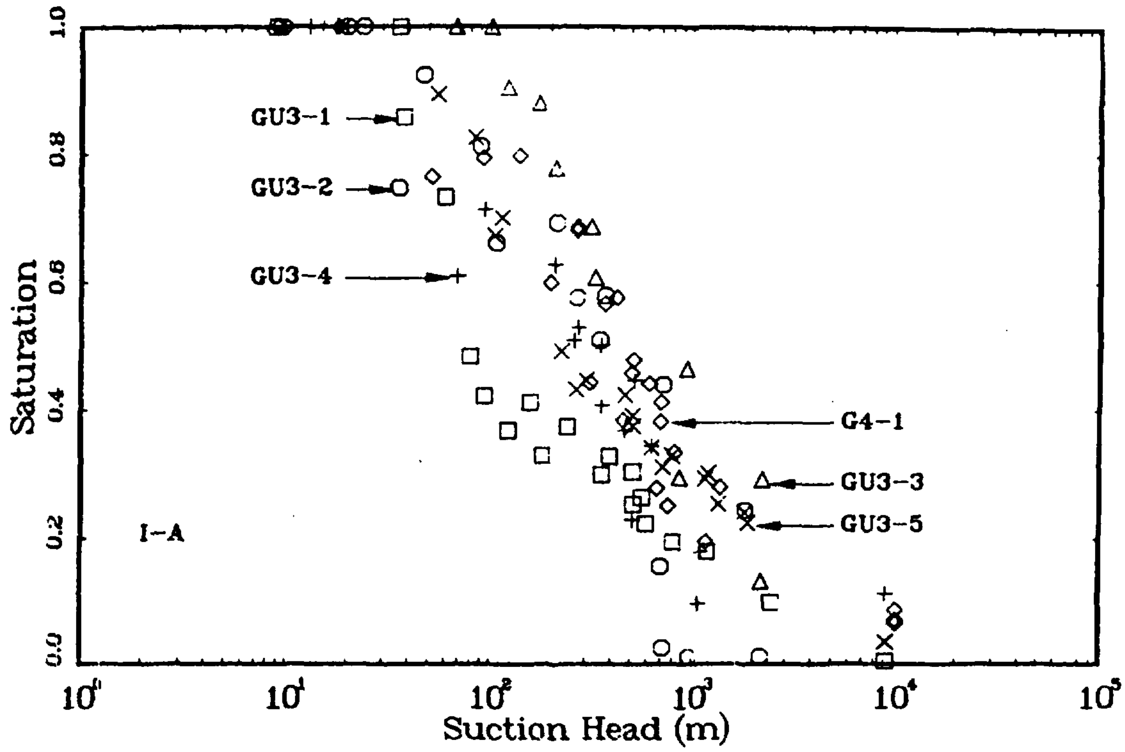


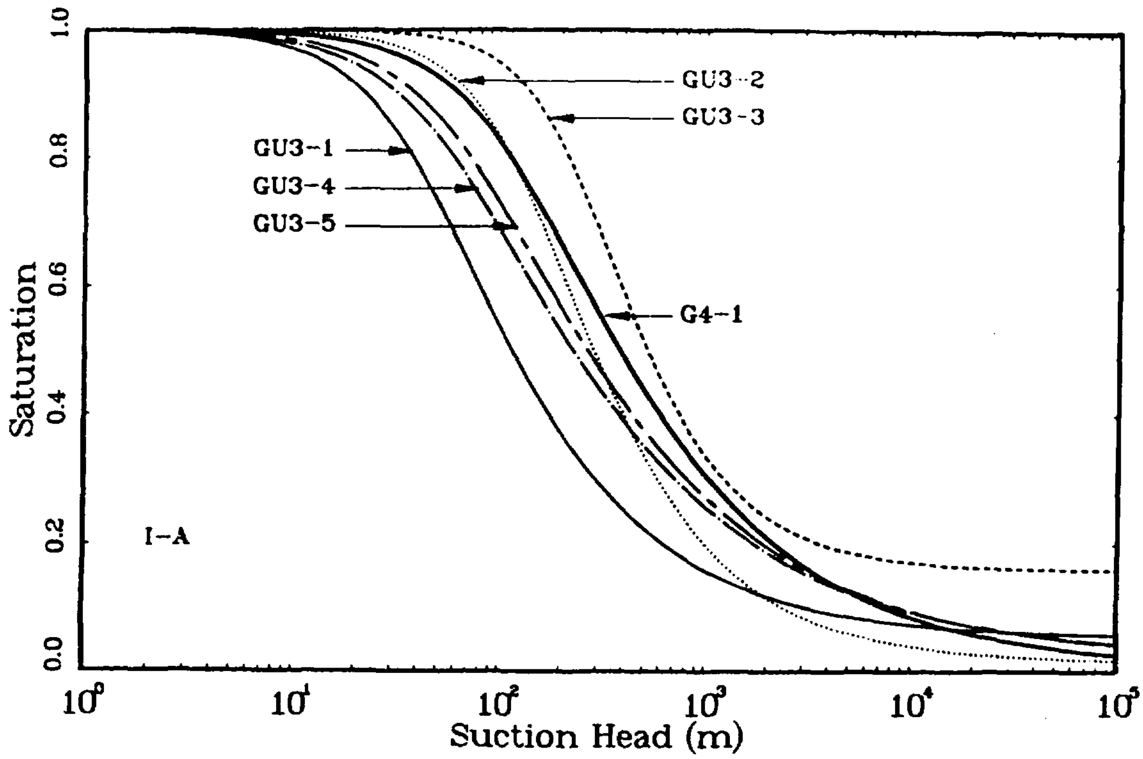


**Figure 6 Tiva Canyon Welded Unit I-A**

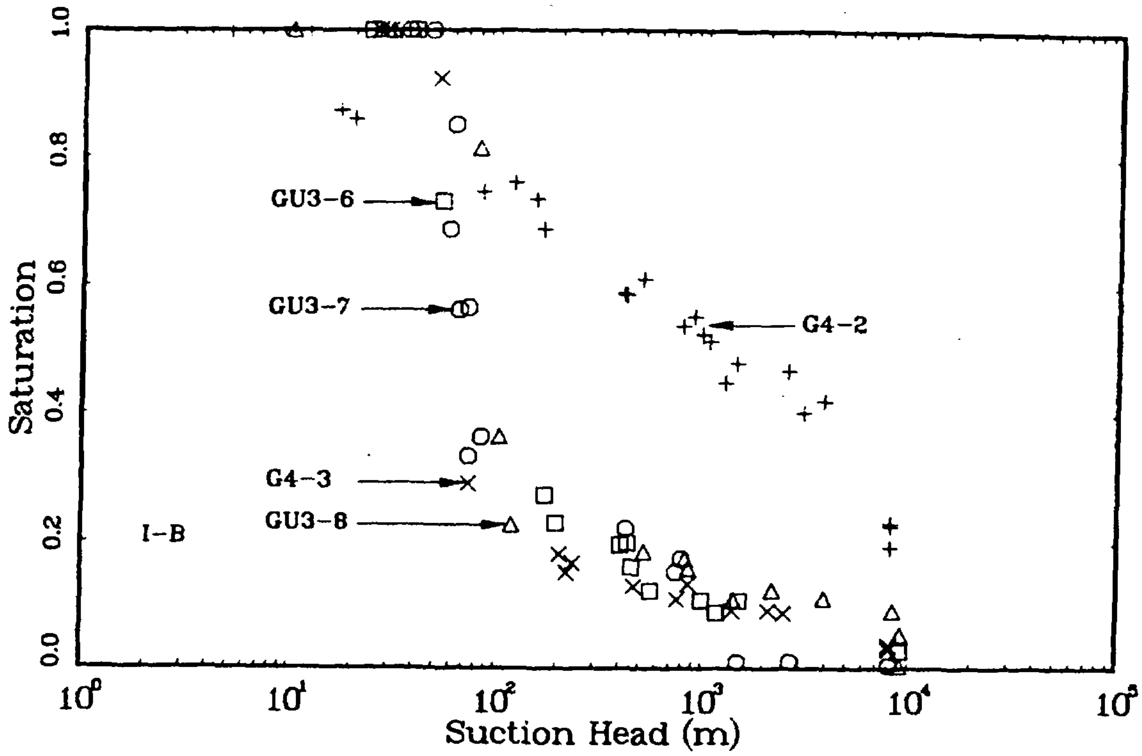


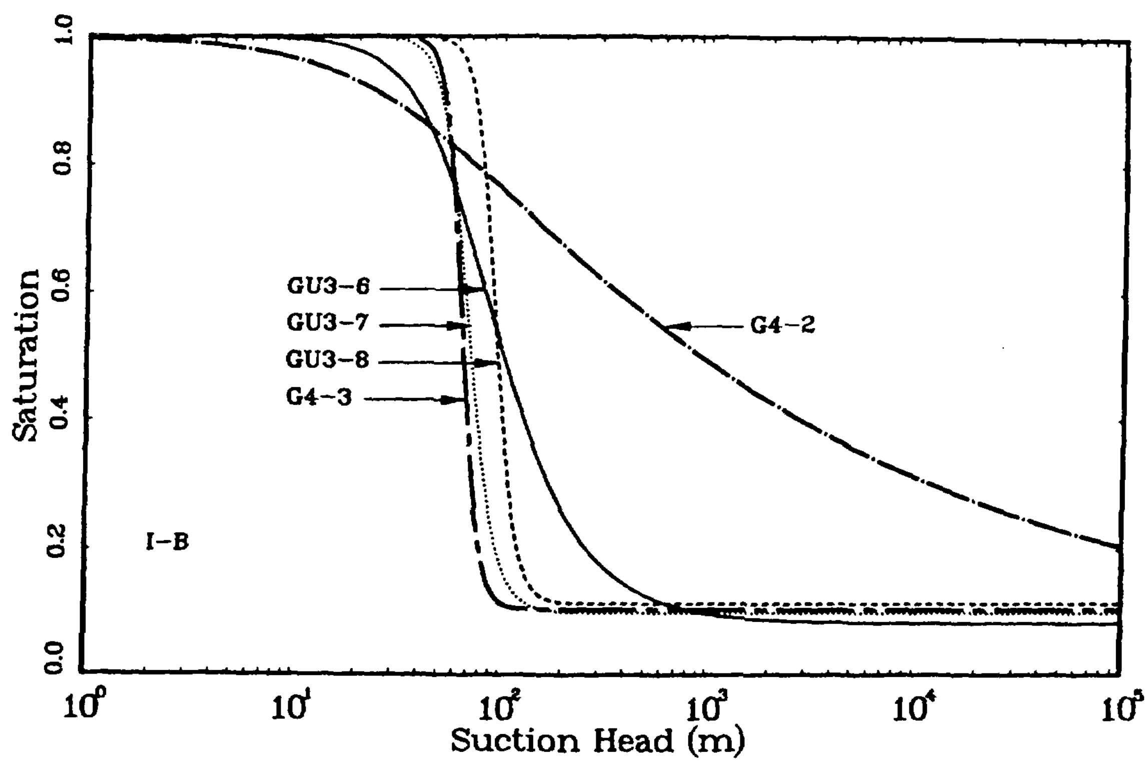


**Figure 7 Paintbrush Nonwelded Unit I-B**

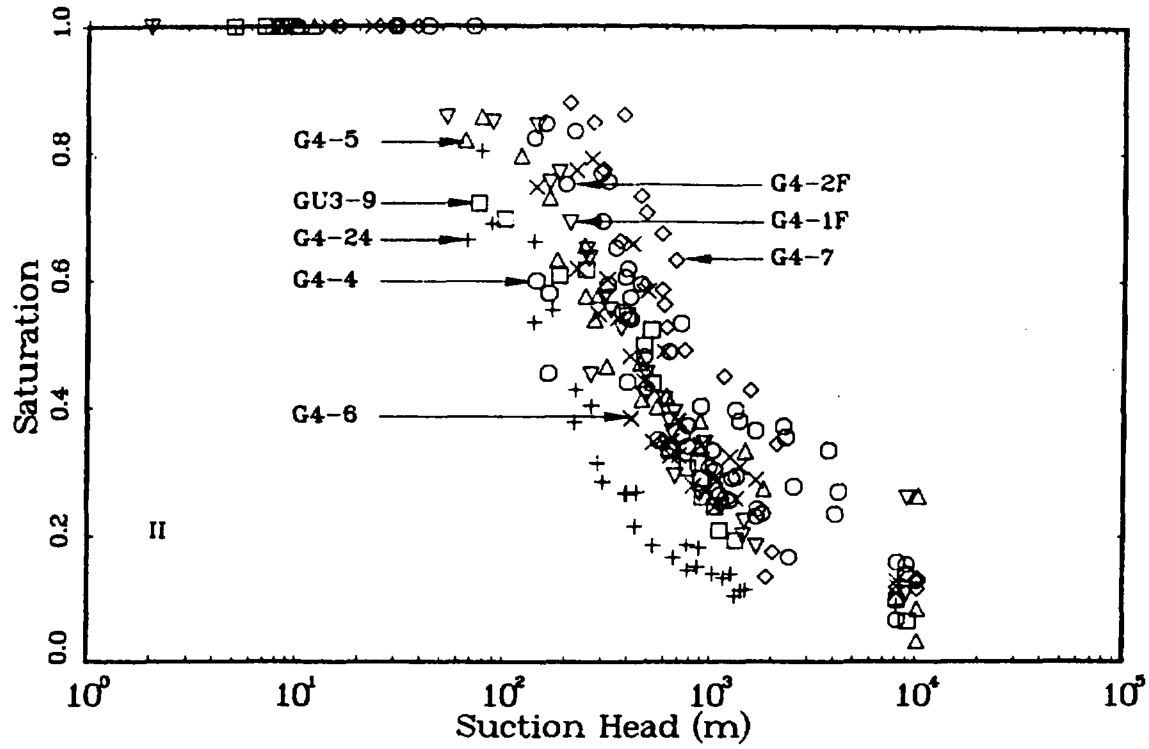


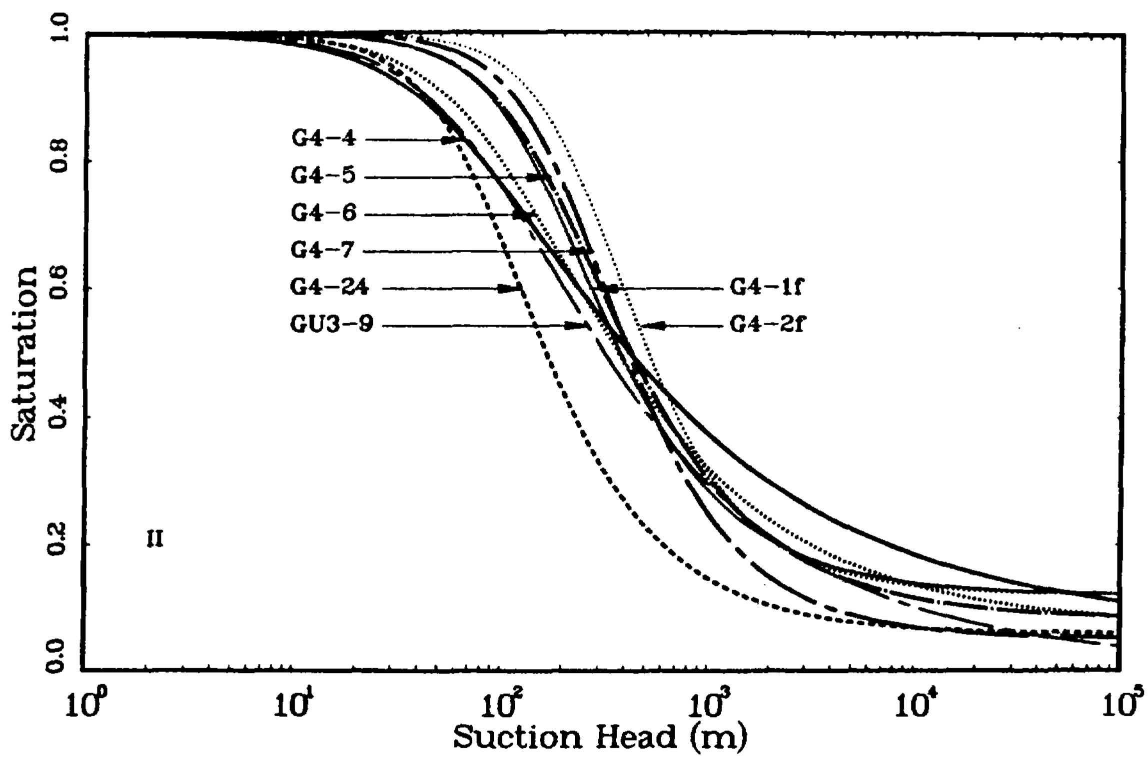


**Figure 8 Topopah Spring Welded Unit II**

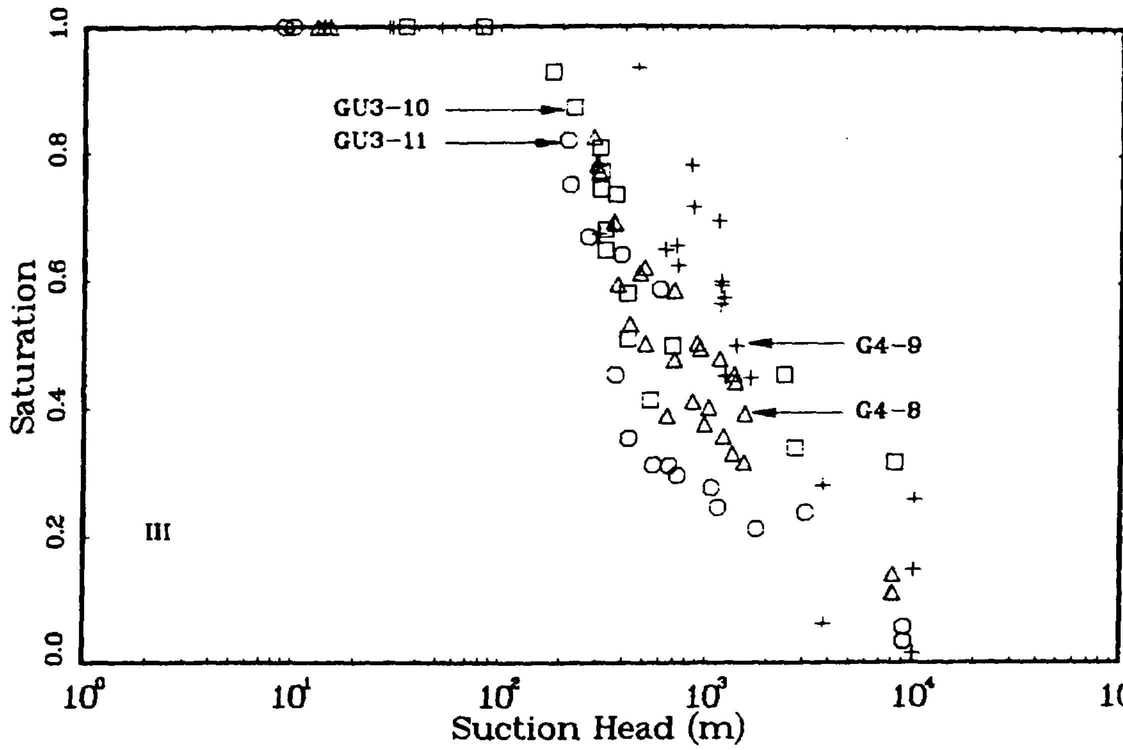


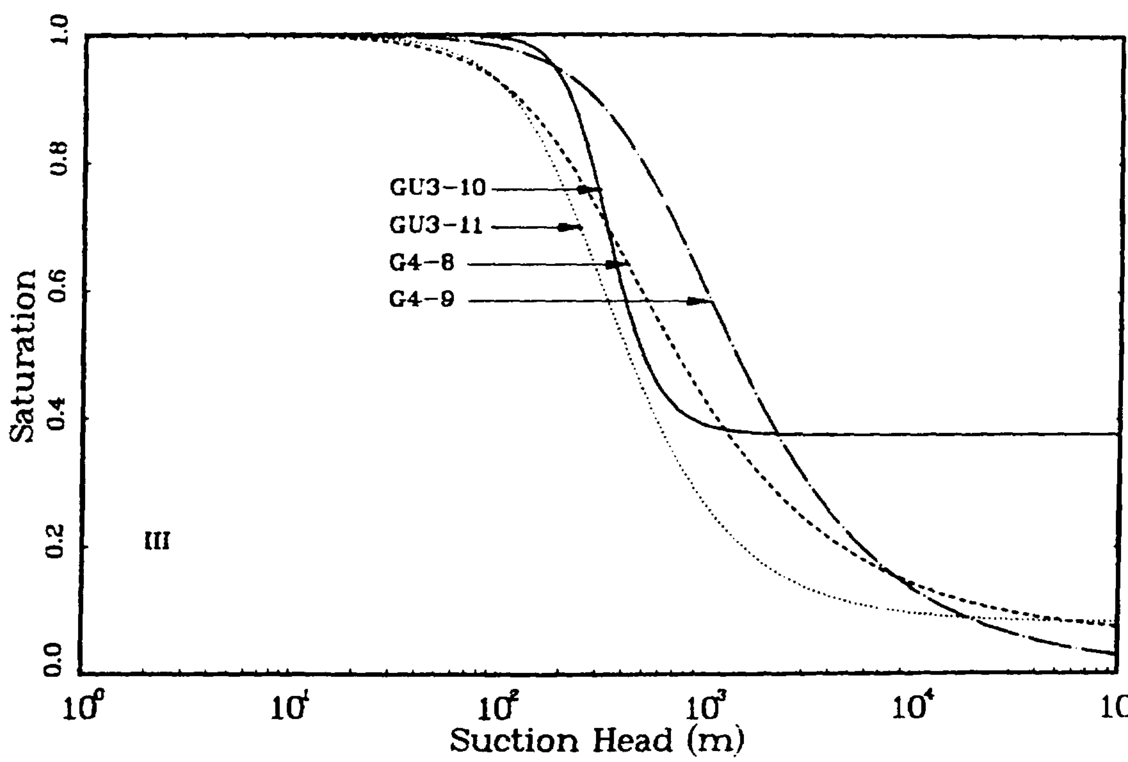


**Figure 9 Basal Vitrophyre of Topopah Spring Welded Unit III**

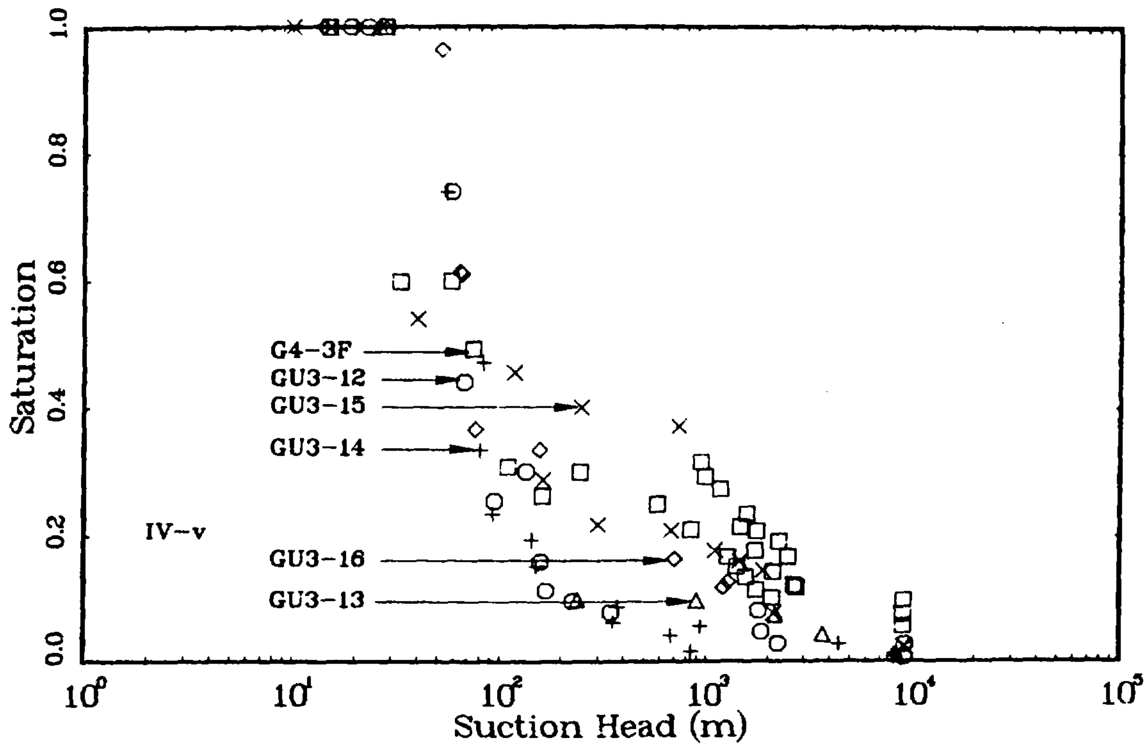


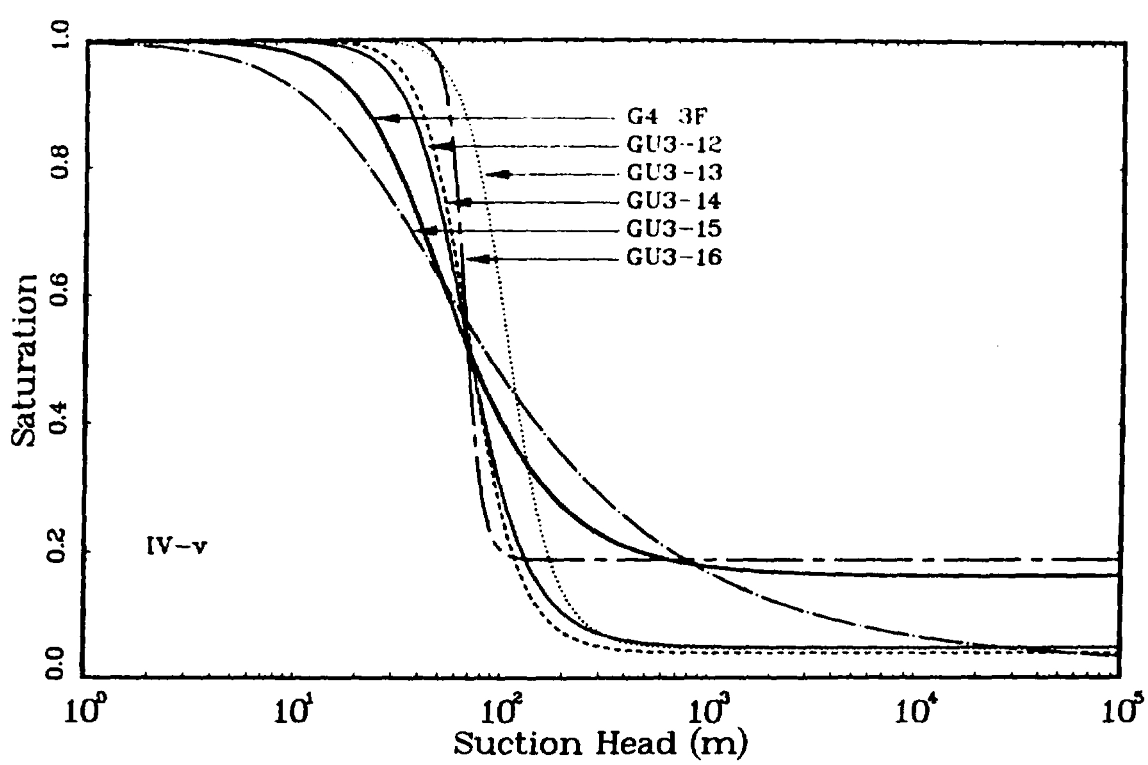


**Figure 10 Vitric Calico Hills Nonwelded Unit IV-v**

with Table A.2 reveals that the saturated hydraulic conductivities appear to generally correlate with the curve shape. Curves with gentle slopes (small betas) have small conductivities (e.g., G4-3F), while those with steep slopes (large betas) have high conductivities (e.g., GU3-14). This qualitative correlation appears to hold for the nonwelded units. A representative sample for the samples tested in this unit is GU3-14, which was chosen primarily on the basis of the relatively large amount of data in the region where the saturation decreases rapidly. The values of the other parameters describing GU3-14 appear consistent with those of the other Unit IV-v samples.

Unit IV-z curves in Figure 11 appear to be fairly self-consistent. That G4-10 is somewhat anomalous is not entirely unexpected, because it comes from the upper boundary of this unit. A representative sample for the samples tested in this unit is G4-11.

Samples were taken from Units V, VI, and VII for completeness. There are some portions of Yucca Mountain where Unit V occurs above the water table. In Figure 12 we see that samples from Unit V are fairly self-consistent. These samples were taken from locations below the water table, and their data appear somewhat different from those for samples taken from welded, devitrified units above the water table (I-A and II). In particular, they generally have a steeper slope and a larger conductivity than those of samples from Units I-A and II. G4-18 appears to be representative for the samples tested in this unit.

Data from Unit VI (Figure 13) are typical of those from a nonwelded, zeolitized unit, although the saturated hydraulic conductivities for this unit are somewhat larger than those measured for samples from Unit IV-z.

Unit VII is a welded devitrified unit below the water table. The saturation curves and the saturated hydraulic conductivities are presented in

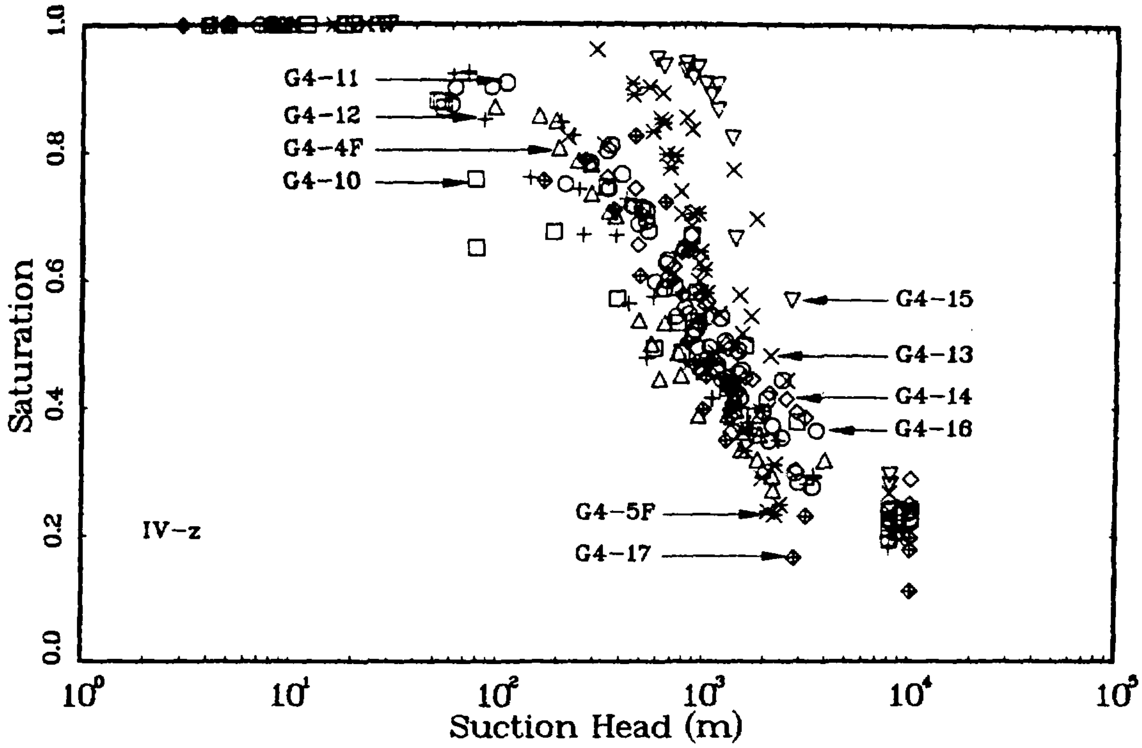


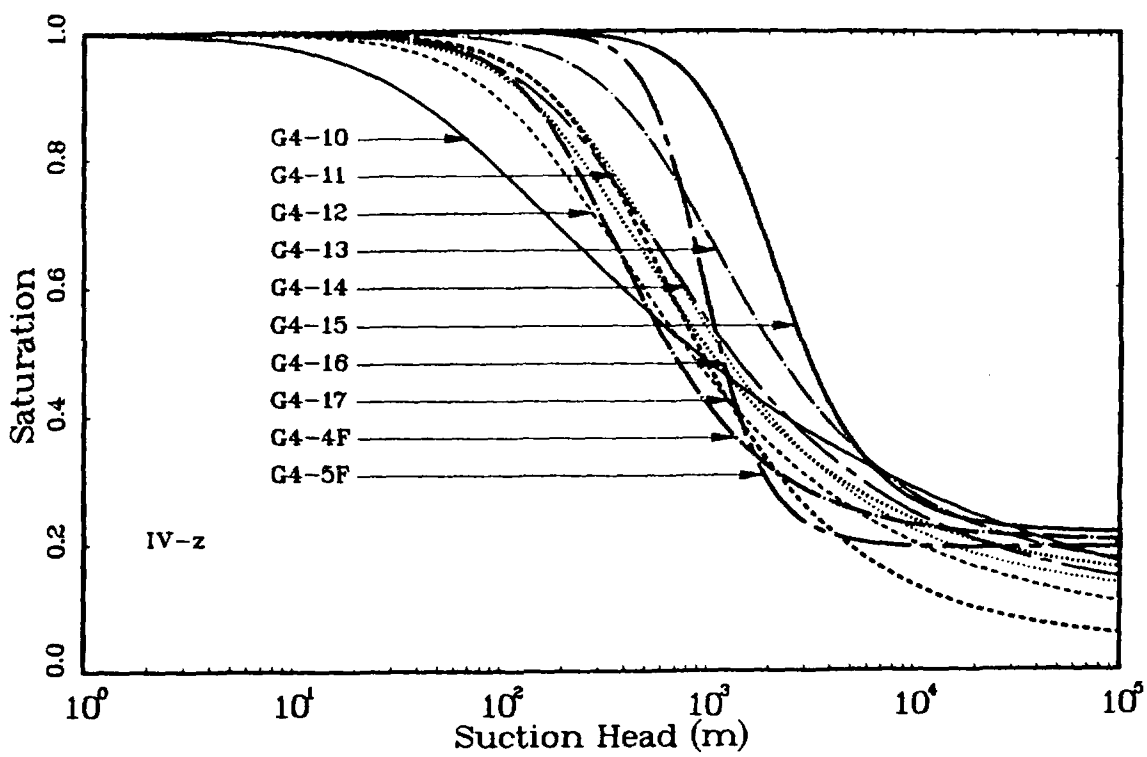


**Figure 11 Zeolitized Calico Hills Nonwelded Unit IV-z**

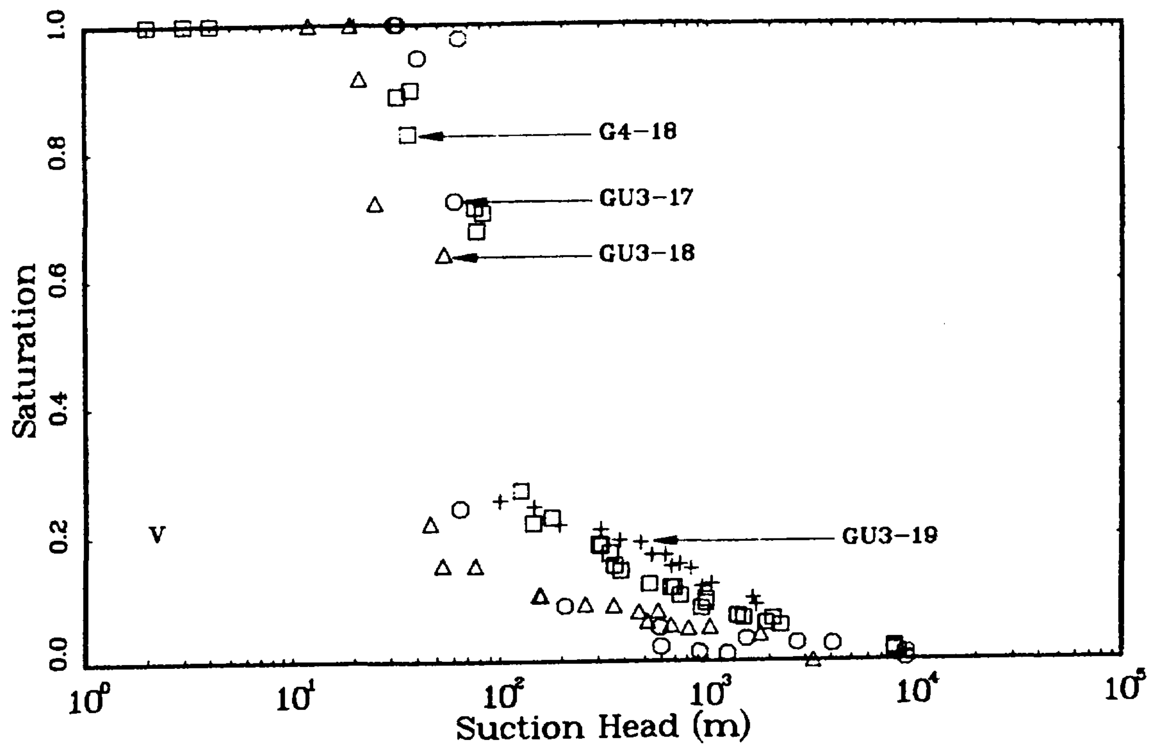


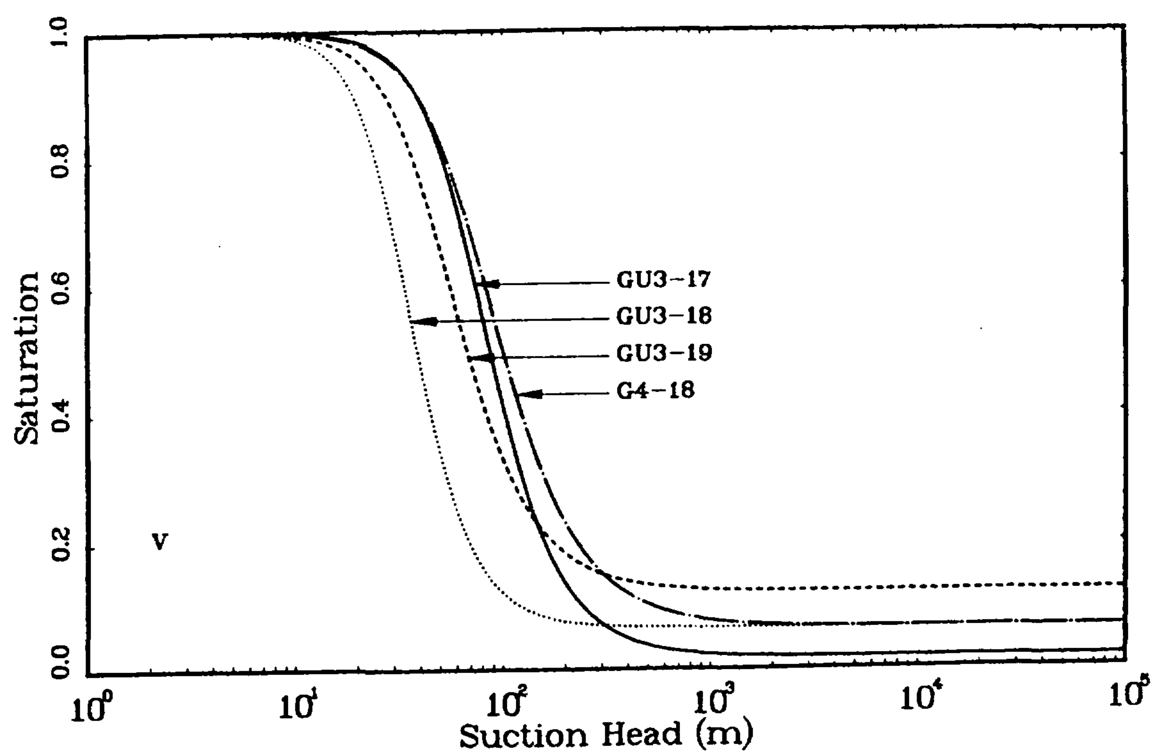


**Figure 12  Prow Pass Welded Unit  V**

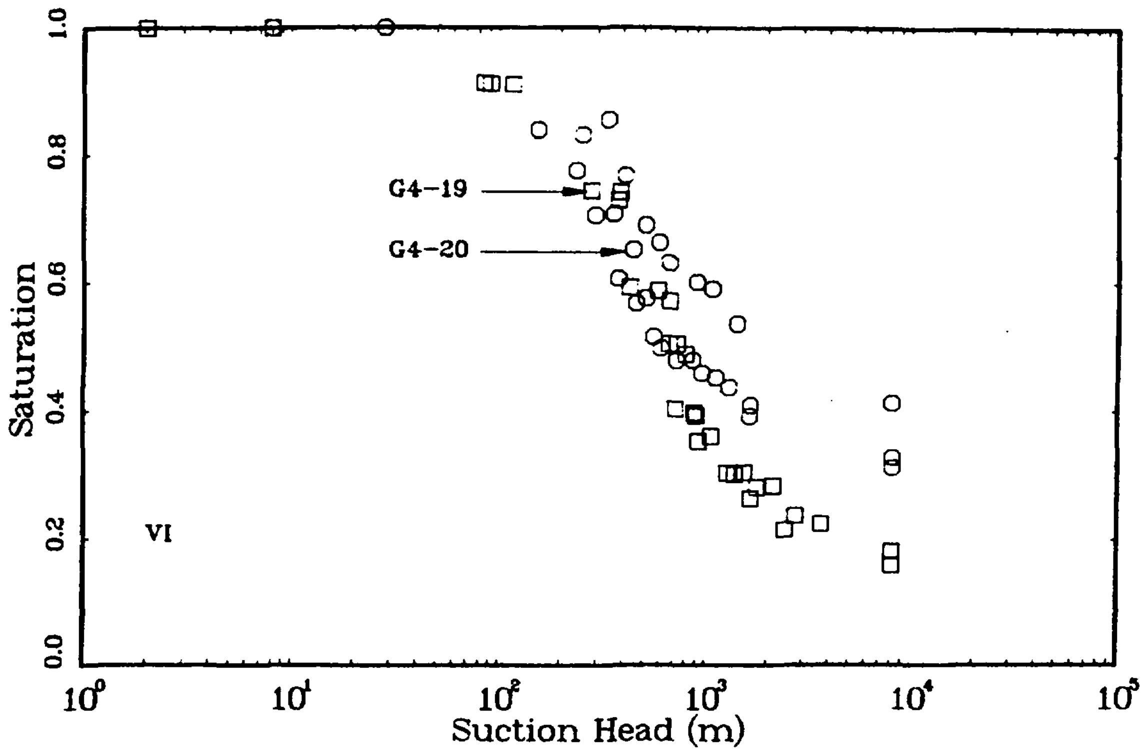


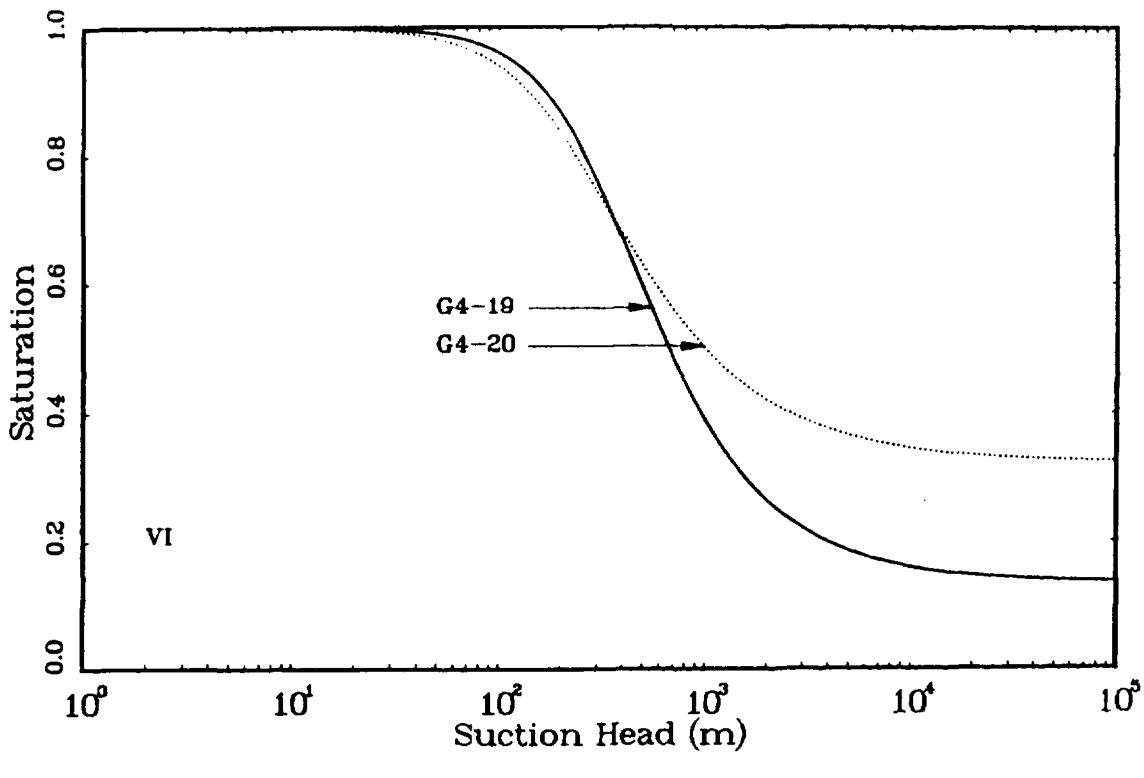


**Figure 13 Crater Flat Nonwelded Unit VI**

Figure 14 for this unit and visually appear different than those seen for Units I-A and II. The data visually appear to be similar to those for the Unit V samples, which were also taken from a location below the water table.

## RESULTS OF SATURATED HYDRAULIC CONDUCTIVITY TESTING

This section contains the results of unconfined and confined saturated hydraulic conductivity testing of the tuff matrix and confined saturated conductivity testing of five fractured core samples.

### Unconfined Matrix-Testing Results

Table A.4 in Appendix A gives the conductivities of all samples tested in the Ruska permeameter and in the core permeameter (referred to as "Large Disk" in Table A.4). It should be noted in Table A.4 that there is no statistically significant difference between the conductivity values of the small (Ruska permeameter) and large disk samples except possible for samples G4-13 and G4-17.

The following visual observations of the samples are relevant to the saturated hydraulic conductivity data.

> From visual observations of the cross-sectional samples (G4-5, G4-17, G4-11, G4-13, G4-14, and G4-18), it appeared that in samples G4-5 and G4-17 the flow occurred through microsized cracks in the core samples. The texture of samples G4-11, G4-13, G4-14, and G4-18 was very coarse, and several different types of material were cemented together. Observations confirmed that water flow was through the matrix of the material. However, it could not be determined whether the water flowed through a single type of material or through all of the matrix within a sample.

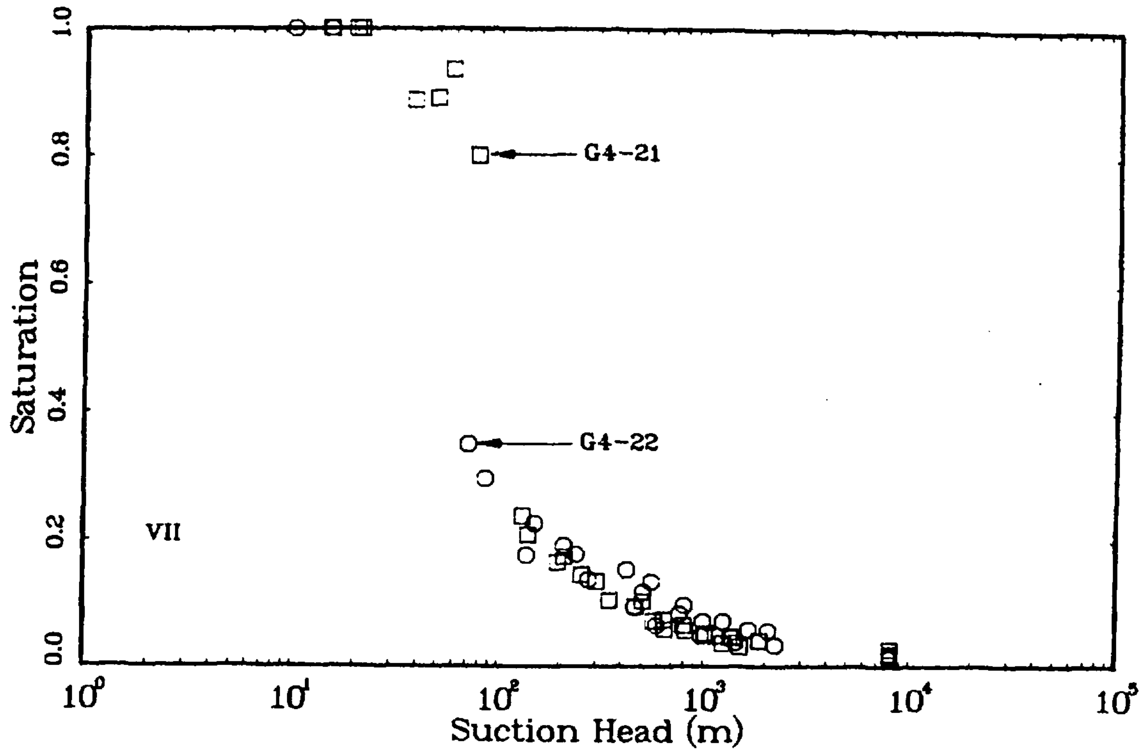


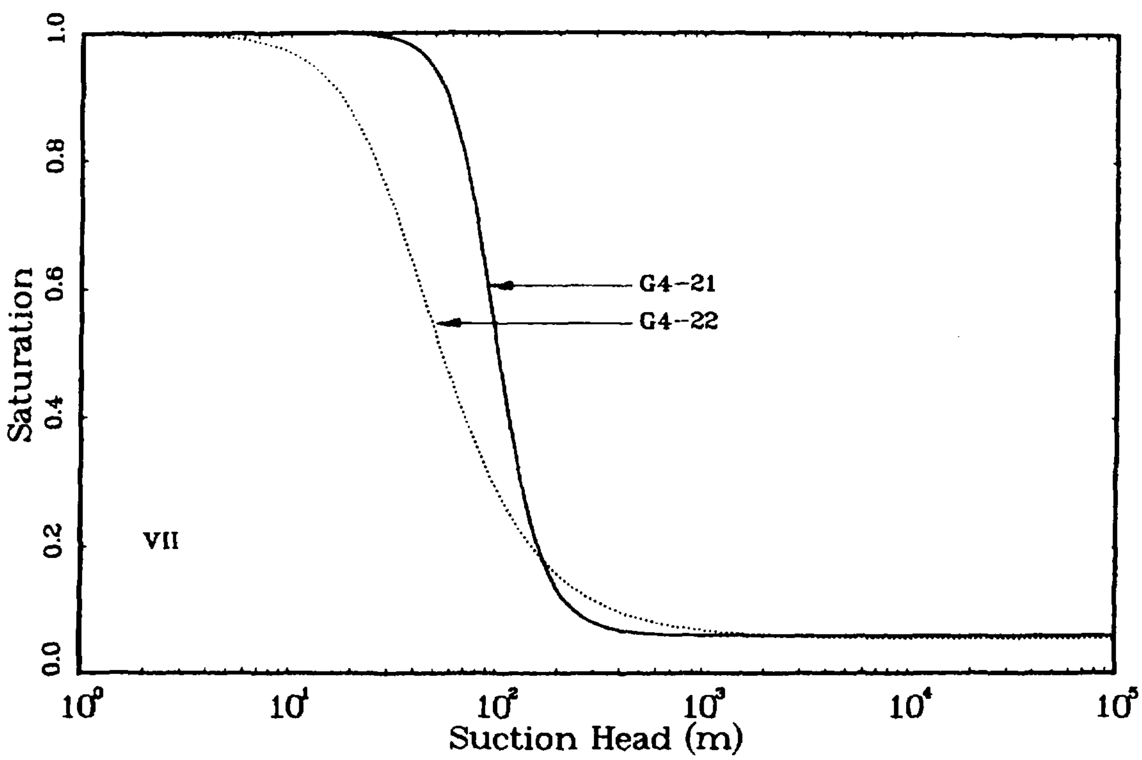


**Figure 14 Bullfrog Welded Unit VII**

Sample G4-3 was very fragile and loosely compacted and crumbled easily, especially when saturated. When a slight pressure head was applied to determine the conductivity, several samples cracked before a measurement could be taken. The subsample tested had no apparent cracks at the end of the run.

Samples G4-1, G4-1F, G4-2F, G4-4, G4-5, G4-6, G4-7, G4-8, G4-9, G4-19, G4-20, G4-21, G4-22, G4-23, G4-24, GU3-1, GU3-2, GU3-3, GU3-4, GU3-5, GU3-9, GU3-10, and GU3-11 were all welded, small-grained samples of apparently uniform material. In general, flow probably would occur only through microsized cracks in these samples. The remaining samples appeared to be less welded, lighter in weight, and of nonuniform coarse material. Flow probably occurs through the matrix of these samples.

Figure 15 contains plots of each sample's average unconfined saturated hydraulic conductivity versus average porosity, with these data organized according to the four rock types found at Yucca Mountain. The type of symbol (e.g., a square) indicates the unit from which the saturated sample was taken. The bars indicate the measured range of porosity and saturated hydraulic conductivity for each sample depth. Bars that extend to the bottom of the plot indicate a test where the result indicated only an upper limit on the saturated conductivity (e.g., $<1.3 \times 10^{-11}$ m/s). These plots indicate the conductivities for the welded samples and the nonwelded, vitric samples appear to be positively correlated with porosity, while the nonwelded, zeolitized samples appear to have no correlation. The zeolitized samples all exhibit low saturated hydraulic conductivities, presumably due to the higher microporosity relative to the nonzeolitized samples.

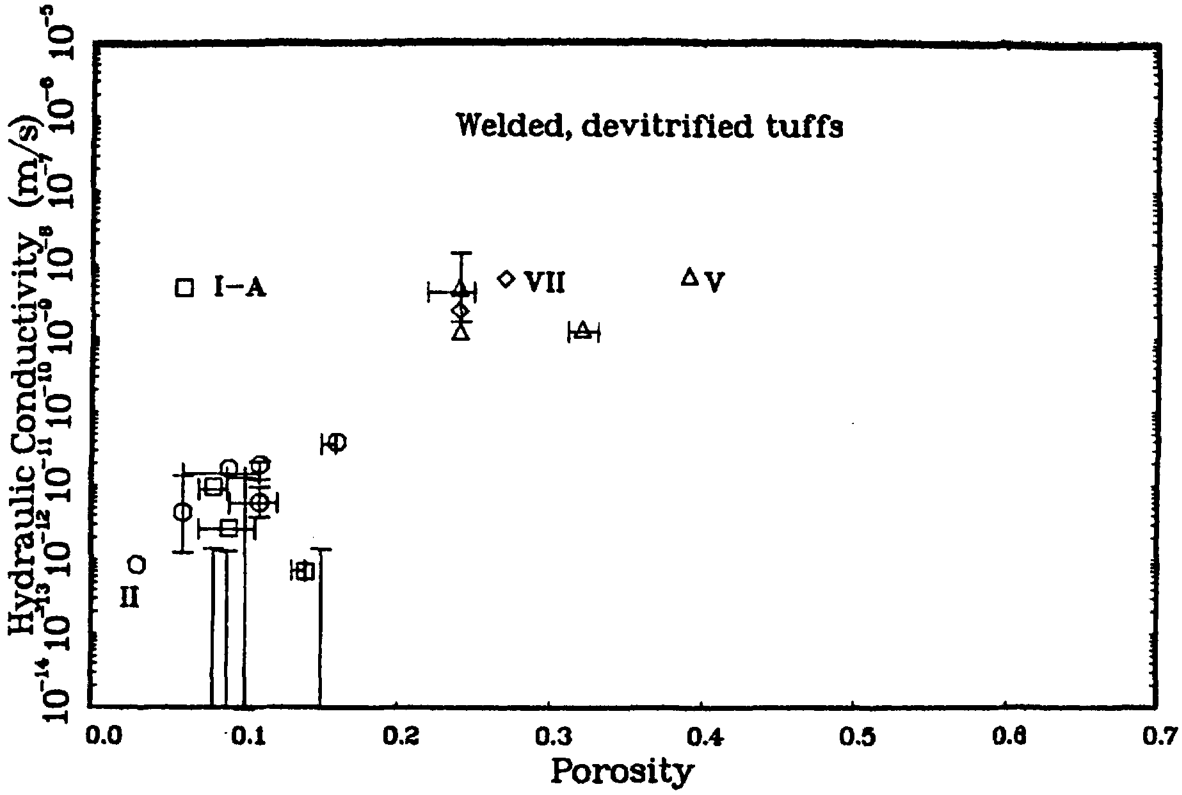


**Figure 15a Correlation Between Porosity and Saturated Hydraulic Conductivity**

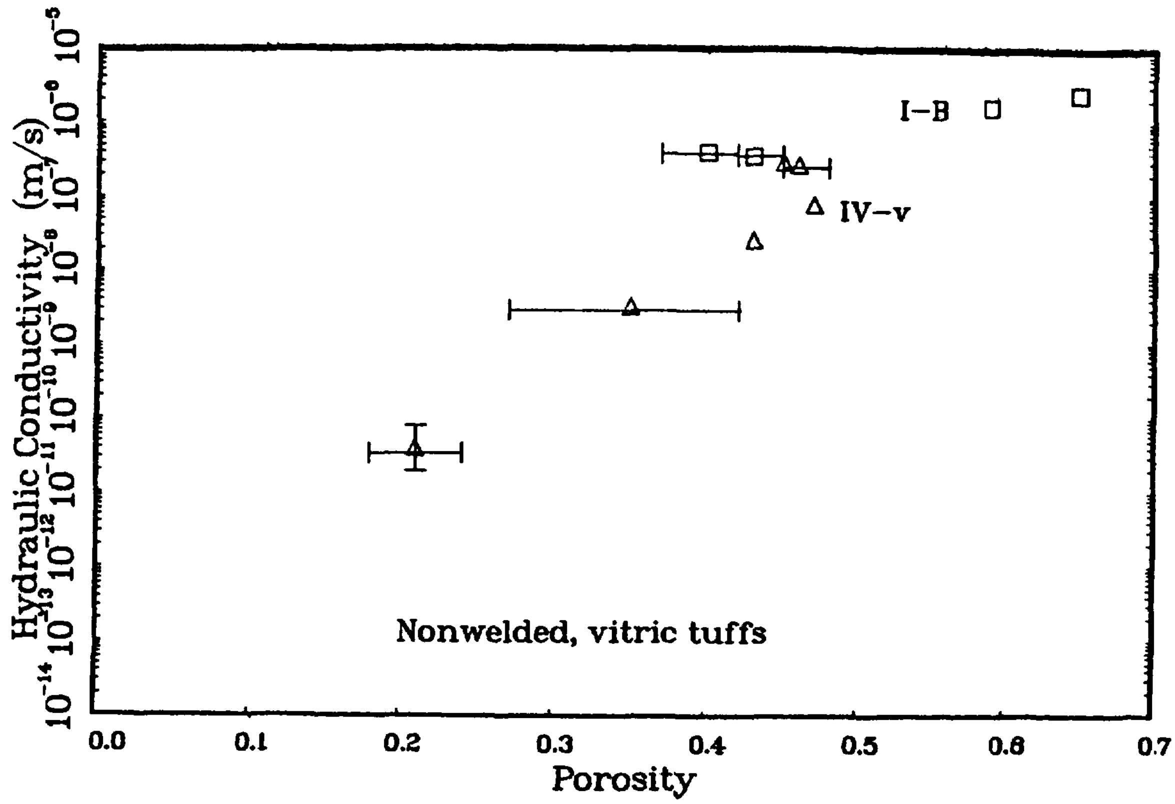


**Figure 15b Correlation Between Porosity and Saturated Hydraulic Conductivity**

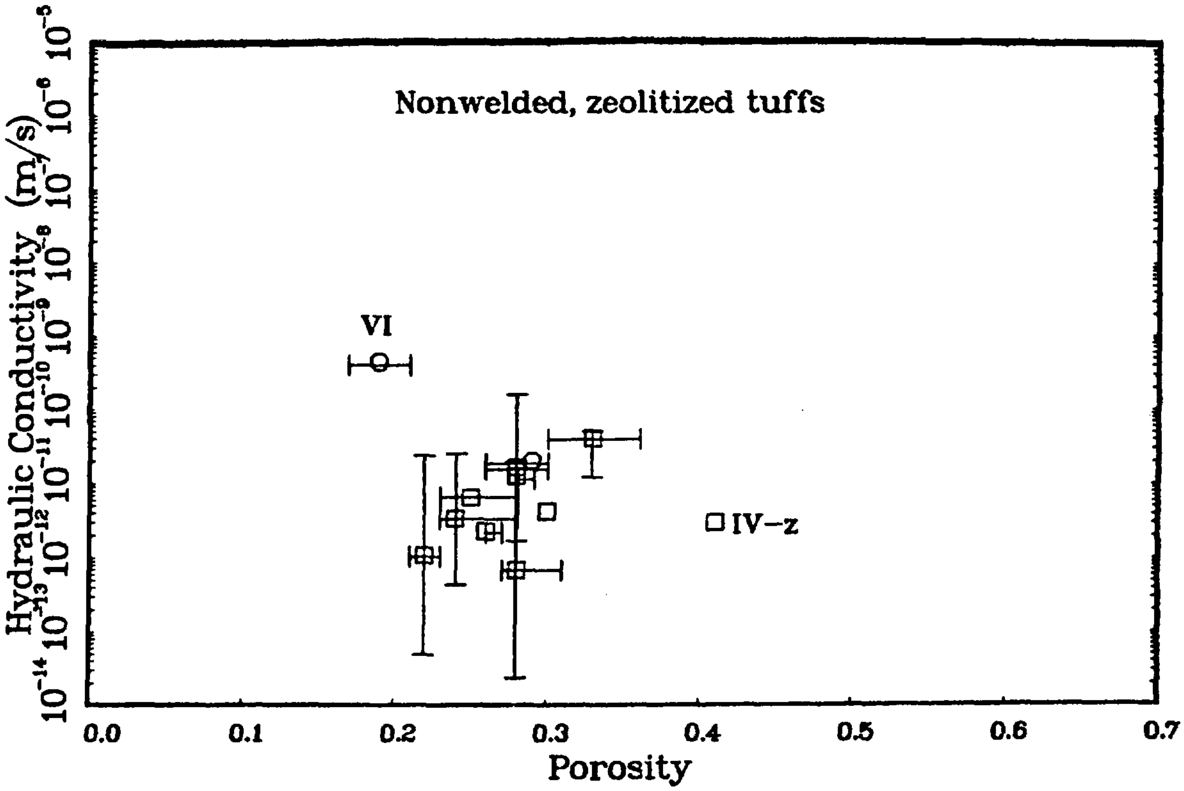


Figure 15c Correlation Between Porosity and Saturated Hydraulic Conductivity

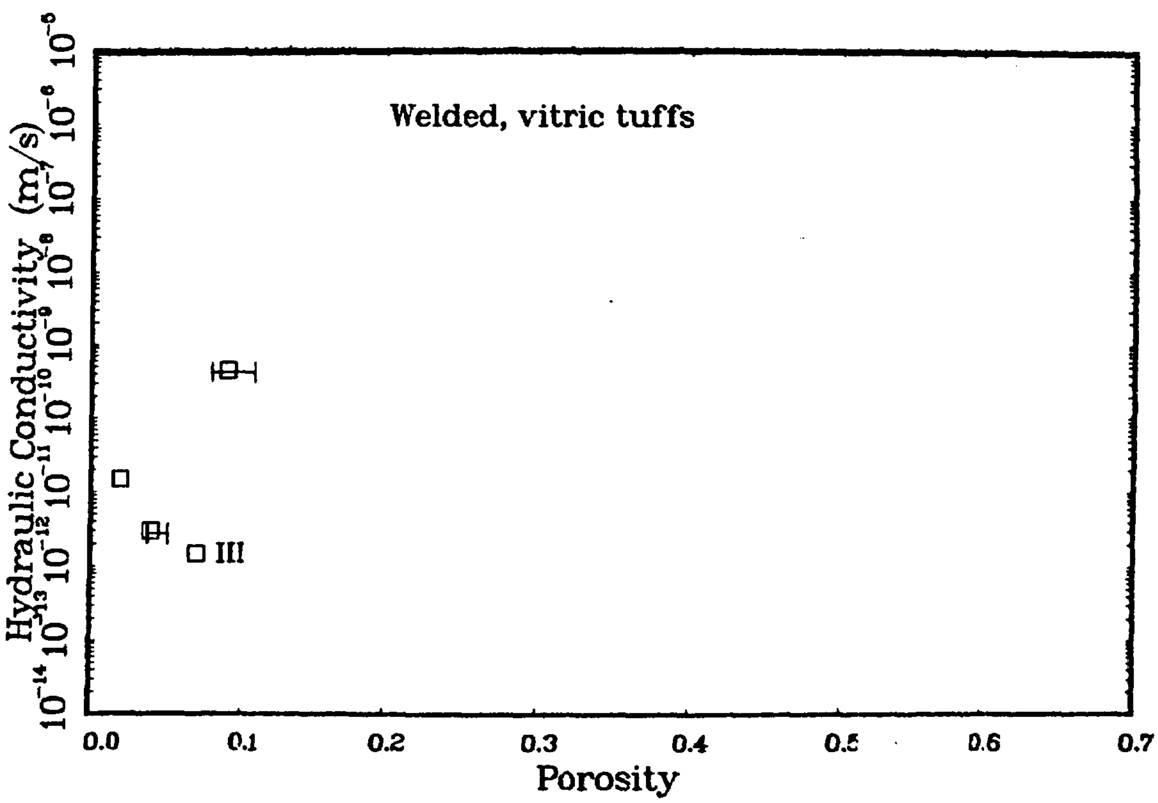


Figure 15d Correlation Between Porosity and Saturated Hydraulic Conductivity

Confined Matrix-Testing Results

Conductivity measurements of unfractured samples at elevated effective pressures were made on four unfractured tuff core samples from drill hole USW GU-3 at the NTS. These experiments measured conductivity as a function of increasing effective pressure at ambient temperature in order to begin gathering data concerning the affect of confining stress on saturated conductivity. As a point of reference, the vertical stress at the water table under Yucca Mountain is about 130 bars. Higher confining stresses were investigated to gain further understanding of rock behavior. A discussion of the results for each sample follows.

GU3-2

Data for sample GU3-2 are shown in Figure E.1 (also see Table A.5, Appendix A). This sample displays a loss of conductivity in the effective pressure range of 50 to 350 bars that is typical of microcrack closure. At higher effective pressures the loss of conductivity for this sample is probably associated with inelastic sample deformation that was observed after testing was completed.

GU3-15

Data for sample GU3-15 are also shown in Figure E.1 (see Table A.6, Appendix A). This sample displays a loss of conductivity very similar to sample GU3-2 for the range 50 to 150 bars. However, when effective pressure was increased between 150 and 550 bars, conductivity for this sample decreased sharply, losing 90% of its conductivity. GU3-15 is a high porosity, low density, nonwelded sample and much of the conductivity reduction above 150 bars is due to inelastic sample compaction.

GU3-11

Conductivity of sample GU3-11 was $10^{-13}$ m/s at initial conditions of pressure. As pressure was increased, conductivity of this sample decreased to below our detection limit ($\sim 10^{-13}$ m/s).

GU3-3

Sample GU3-3 was tested in a slightly different way from the above samples. For this sample, effective pressure was cycled during testing as shown in Figure E.2 (also see Table A.7, Appendix A). The effective pressure was cycled to determine the amount of hysteresis in conductivity loss with increasing effective pressure. Conductivity data for this sample are plotted versus effective pressure in Figure E.3. Sample GU3-3 showed a more rapid decrease in conductivity at low effective pressures (<150 bars) than either of the other samples. The major portion of the conductivity loss was irrecoverable when effective pressure was lowered to 50 bars. When the second pressure cycle was imposed (maximum $P_{eff}$ = 250 bars), conductivity decreased linearly at a rapid rate, and 50% of the loss was unrecoverable. Subsequent pressure cycles showed conductivity to decrease with increasing pressure in a recoverable fashion.

The results of testing on this sample were unexpected, especially the rapid and irrecoverable loss of conductivity noted at pressures between 50 and 150 bars. Close inspection of this sample after testing revealed a well-developed, through-going crack. This rapid and unrecoverable loss of conductivity with increasing effective pressure is consistent with crack closure and deformation of asperities along the crack with increasing pressure (Johnson, 1983). Thus, the conductivity data for this sample should be interpreted as data for a fractured tuff sample.

Laboratory conductivity data indicate that all four samples had very low conductivity, and data for GU3-2 and GU3-15 indicate that in the pressure range that simulates repository conditions ($P_{eff}$ = 0 - 150 bars) conductivity decreased approximately 10%, probably because of the closure of microcracks in the samples. This decrease in conductivity is small compared to that due to other factors (e.g., variability within a unit or saturation).

Confined Fracture-Testing Results

Conductivities of five fractured tuff samples were measured at a series of elevated confining fluid pressures between 35 and 150 bars, with the average pore pressure held constant at 30 bars. Effective pressures ranged from 5 to 120 bars for these samples.

Each sample behaved differently during the flow testing, and a discussion of each sample's results is presented below.

Sample G4-1F

This sample is a highly welded tuff and the surfaces of the fracture are rough and display a poor fit when compared to the other samples (see Figure 1). Laboratory data and calculated parameters are listed in Table A.8. Figures E.4 through E.6 show that calculated aperture and relative conductivity for the sample decreased evenly with increasing pressure over the entire pressure range. The sample also displayed the least amount of change in relative conductivity.

Because the fracture surfaces were rough and poorly mated, it is likely that flow through this sample occurred mainly in channels with relatively large apertures and that the increased pressure may have reduced the size of these channels, but did not close them. When effective pressure was reduced the sample regained 74% of its original calculated fracture conductivity. The hysteresis evident in the plots can be attributed to 1) mechanical (frictional) bonding of the fracture during pressurization, and 2) asperity mating or breaking of asperities during pressurization.

**Sample G4-2F**

This sample is a highly welded tuff containing a fracture with a relatively smooth surface. Data and calculated parameters for the sample are listed in Table A.9 and are plotted in Figures E.7 through E.9. Computed aperture and fracture conductivity decreased as effective pressure was increased to 70 bars; they then remained nearly constant as effective pressure was increased to approximately 120 bars. The rock recovered at least 50% of its initial fracture conductivity (Figure E.9). Upon removal from the pressure vessel, a small thin chip about 1 $cm^2$ in size was found in place, but broken from the fracture surface. Hysteresis evident in the plots may be caused by plastic deformation along the fracture surface.

**Sample G4-3F**

This is a dense, strong tuff containing a very planar fracture with smooth, well-matched surfaces. The sample displayed the largest relative change in computed aperture and fracture conductivity, with most of the decrease occurring as $P_{eff}$ was increased from 20 to 60 bars (see Table A.10 and Figures E.10 through E.12). Although the computed fracture conductivity decreased to 10% of the original value, it recovered to 83% of the original value when effective pressure was reduced to 10 bars. Hysteresis in plots for this sample is attributed to mechanisms mentioned previously for sample G4-1F.

Sample G4-4F

This sample is a nonwelded tuff. Laboratory data and calculated parameters are listed in Table A.11 and plots of computed aperture, normalized aperture, and normalized fracture conductivity are shown in Figures E.13 through E.15. Fracture conductivity decreased with increasing pressure over the entire pressure range; however, conductivity decreased more rapidly as effective pressure was increased over the range of 10 to 60 bars. It is also interesting to note that the conductivity of this sample only returned to 36% of the original conductivity when pressure was reduced. This permanent loss of conductivity may be due in part to a plastic deformation along the fracture surface that improved mating between the fracture surfaces as pressure was increased. Also, the sample matrix contained several voids that were deformed as pressure was increased; however, this probably had little effect on fracture conductivity because the low conductivity of the matrix severely restricted flow through the internal voids.

Sample G4-5F

This is a nonwelded tuff sample with a planar fracture oriented parallel to the core axis. The surfaces of the fracture are extremely well matched (see Figure 1). Laboratory data and selected calculated parameters are listed in Table A.12. Computed aperture, normalized aperture, and normalized fracture conductivity are shown as a function of effective pressure in Figures E.16 through E.18, respectively. These figures show that, as effective pressure was increased from 10 to 20 bars, computed aperture and conductivity decreased rapidly. Conductivity of the fracture continued to decrease with increasing effective pressure to a value of 20% of the initial conductivity. Conductivity returned to 100% of the original value when effective pressure was lowered. Data for this sample exhibit much less hysteresis than other samples during the entire pressurization cycle, probably because of the extremely good mating between the two surfaces of the fracture.

Summary of Fracture Testing Results

Table 7 contains a summary of the data obtained from the G4-1F through G4-5F samples. The initial hydraulic aperture of the discrete fractures (at low effective confining pressures) ranges from 6 μm for samples G4-2F and G4-5F to 67 μm for sample G4-1F, with respective fracture conductivities of $3.0 \times 10^{-5}$ to $3.8 \times 10^{-3}$ m/s. It should be noted that the aperture calculated is an equivalent parallel-plate hydraulic aperture and may be significantly different from the physical, or real, effective fracture aperture, with the equivalent hydraulic aperture always being smaller because of the effects of the fracture surface roughness on flow through the fracture. The ratio of the effective physical aperture to the effective hydraulic aperture appears to be in the range of 2 to 7, with the effects of the surface roughness more significant at lower apertures (Barton et al., 1983).

Fitting the Confined Fracture-Conductivity Data

Normalized conductivity as a function of effective confining pressure is shown in Figures E.6, E.9, E.12, E.15, and E.18 for the five fractured core samples. Analyses by Walsh (1981) indicate that the cube root of the fracture conductivity should be linearly related to the logarithm of the effective confining pressure. The following relationship suggested by Walsh was used to fit both the loading and unloading laboratory data:

**TABLE 7.** Summary Data for Fractured Tuff Samples

| Sample Code | Fracture Aperture: Computed Initial Aperture | Normalized Minimum Aperture | Recovered Aperture | Fracture Conductivity: Computed Fracture Conductivity | Normalized Minimum Conductivity | Recovered Fracture Conductivity |
|---|---|---|---|---|---|---|
| | $e_o$ (microns) | (% $e_o$) | (% $e_o$) | $K_o$ ($10^{-5}$m/s) | (% $K_o$) | (% $K_o$) |
| G4-1F | 67 | 57% | 86% | 378 | 32% | 74% |
| G4-2F | 6 | 49% | 85% | 3.5 | 24% | 74% |
| G4-3F | 22 | 31% | 91% | 43 | 10% | 83% |
| G4-4F | 31 | 39% | 60% | 79 | 15% | 36% |
| G4-5F | 6 | 44% | 100% | 3.1 | 20% | 100% |

$$(K/K_{init})^{1/3} = a - b \cdot \ln(P_{eff}) \quad (10)$$

where

$K$ = fracture saturated conductivity

$K_{init}$ = fracture conductivity at the initial confining pressure

$P_{eff}$ = effective confining pressure, bars (see eq. 5)

a,b = determined constants, related to the fracture surface topography

Although at some high pressures the fracture saturated conductivity will reach a minimum value, it can be seen from the curves in Figures E.6, E.9, E.12, E.15 and E.18 that, even at 130 bars, the fracture conductivity is still decreasing for the samples. This is a result of both the rock strength and the surface topography.

The laboratory data were entered in a regression analysis routine which produced estimates of the parameters "a" and "b". The fitted curves are plotted in the Figures E.6, E.9, E.12, E.15, and E.18 showing the normalized conductivity for samples G4-1F thru G4-5F. These values are physically related to the topography of the fracture surface, with "b" proportional to the root-mean-square (RMS) value of the asperity height distribution and "a" inversely proportional to the normalizing conductivity $K_{init}$. The estimates of both parameters and the corresponding coefficient of determination, $R^2$, are shown in Table 8 for both the loading and unloading curves. When the parameter "b" is multiplied by the initial conductivity to yield a relative RMS value of the asperity height distribution, it can be seen that sample G4-1F has the largest value and G4-5F the smallest. This is consistent with the visual appearance of the fracture surfaces, with sample G4-1F described previously as having the roughest surface and worst fracture mating and sample G4-5F as having a nearly planar fracture with the fracture surfaces extremely well matched.

With values of both saturated fracture conductivities as a function of effective confining pressure (corresponding to overburden stress) for the welded and nonwelded tuff of the functional units in Yucca Mountain, and estimates of the frequency and size of fractures in those units provided by other NNWSI groups, it should be possible to estimate an effective, saturated conductivity for the rock mass.

Table 8. Regression Parameter Estimates for Confined-Fracture Conductivity Curve Fits

| Sample ID | Parameter a | Parameter b | $R^2$ | $K_{init} \times 10^3$ (m/s) |
|---|---|---|---|---|
| Loading Curve | | | | |
| G4-1F | 1.204 | 0.084 | 0.94 | 3.78 |
| G4-2F | 1.572 | 0.196 | 0.94 | 0.035 |
| G4-3F | 1.906 | 0.296 | 0.97 | 0.43 |
| G4-4F | 1.529 | 0.200 | 0.97 | 0.79 |
| G4-5F | 1.244 | 0.131 | 0.97 | 0.030 |
| Unloading Curve | | | | |
| G4-1F | 1.028 | 0.070 | 0.93 | 3.78 |
| G4-2F | 1.034 | 0.079 | 0.94 | 0.035 |
| G4-3F | 1.349 | 0.190 | 0.97 | 0.43 |
| G4-4F | 0.962 | 0.093 | 0.97 | 0.79 |
| G4-5F | 1.241 | 0.140 | 0.97 | 0.030 |

# SUMMARY

The testing and analysis of 48 samples taken from drill holes USW GU-3 and USW G-4 provide information required for hydrologic and radionuclide transport analyses to determine the suitability of the Yucca Mountain site as a location for a high-level nuclear waste repository. The results of these tests indicate:

## Matrix Water Retention

1) The relationship between water content and suction head for each individual sample is unique for the specific core matrix material and suggests that the matrix properties could be described reasonably well by the smooth curves.

2) A comparison of psychometric and mercury intrusion data for 22 individual samples indicates that the two testing methods give results that are, for the most part, in good qualitative agreement. There appears to be no general correlation between the type of rock and degree of agreement between the two testing methods. The psychrometric method is a much more direct measurement of the desired information and so appears more reliable.

3) The data on water content versus suction head data for the limited number of samples taken from a particular rock type (functional unit) form a reasonably coherent group.

4) Comparison of Haverkamp and Van Genuchten curve-fits of data for selected samples indicates that when the curve is well defined by the data points the two curve fits yield identical results. The Van Genuchten curve fit was

chosen because it is more convenient to use, as it yields an analytical expression when the unsaturated hydraulic conductivity is calculated by the method of Maulem (1976).

Matrix Saturated Hydraulic Conductivity

1) The nonwelded, vitric tuff samples had conductivities orders of magnitude higher than those of either the welded tuff samples or the nonwelded, zeolitic tuff samples.

2) As individual groups, the nonwelded, vitric tuff samples and the welded, devitrified samples appear to have a general correlation between the porosity of their samples and the hydraulic conductivity. The other two tuff types did not show any correlation.

3) The six core cross sections (diameter about 6.3 cm) tested for hydraulic conductivity generally had hydraulic conductivities equal to or lower than those for the cylindrical samples (diameter about 1.2 cm).

4) The reduction in conductivity, as confining pressure is increased to approximately the lithostatic load (maximum value of about 130 bars), is fairly small compared to the reduction due to other factors (e.g. saturation). For example, the reduction in saturated conductivity for the three samples for which we have data was less than 15% as the effective pressure was increased from 50 to 150 bars (see Tables A.5 to A.7). If the matrix saturation of sample GU3-2 is reduced from 100% to 90%, the calculated matrix conductivity will decrease by 75%.

The contrast in matrix properties between the unsaturated-zone hydrologic units may be seen in Table 9 and Figure 16, which contain information for samples "representative" of the individual units. Information contained in this paper indicates that the matrix data fall into three general groups:

1. Densely welded tuffs (Units I-A, II, and III).

2. Vitric, nonwelded tuffs (Units I-B and IV-v).

3. Zeolitized, nonwelded tuffs (Unit IV-z).

The information concerning the representative samples (contained in Table 9 and Figure 16) supports this conclusion. The representative samples are suggested for "first-cut" hydrologic calculations concerning Yucca Mountain. As additional information becomes available, an attempt will be made to apply statistical methods to this larger data set to more rigorously quantify the definition of a representative sample, the variation in parameter values, etc.

Fracture Saturated Hydraulic Conductivity

1) The saturated conductivity of the fractures is several orders of magnitude higher than that of the matrix.

2) Flow through all fractured samples was substantially reduced at elevated pressures; however, the response of a particular sample to pressure was influenced by the fracture surface characteristics and the mechanical strength of the sample.

3) Fractured samples that were composed of strong rock regained 75 to 100% of initial conductivity when pressure was lowered to initial levels, while a weaker sample recovered only 36% of its initial conductivity indicating that irreversible (plastic) mating of the fracture surfaces had occurred.

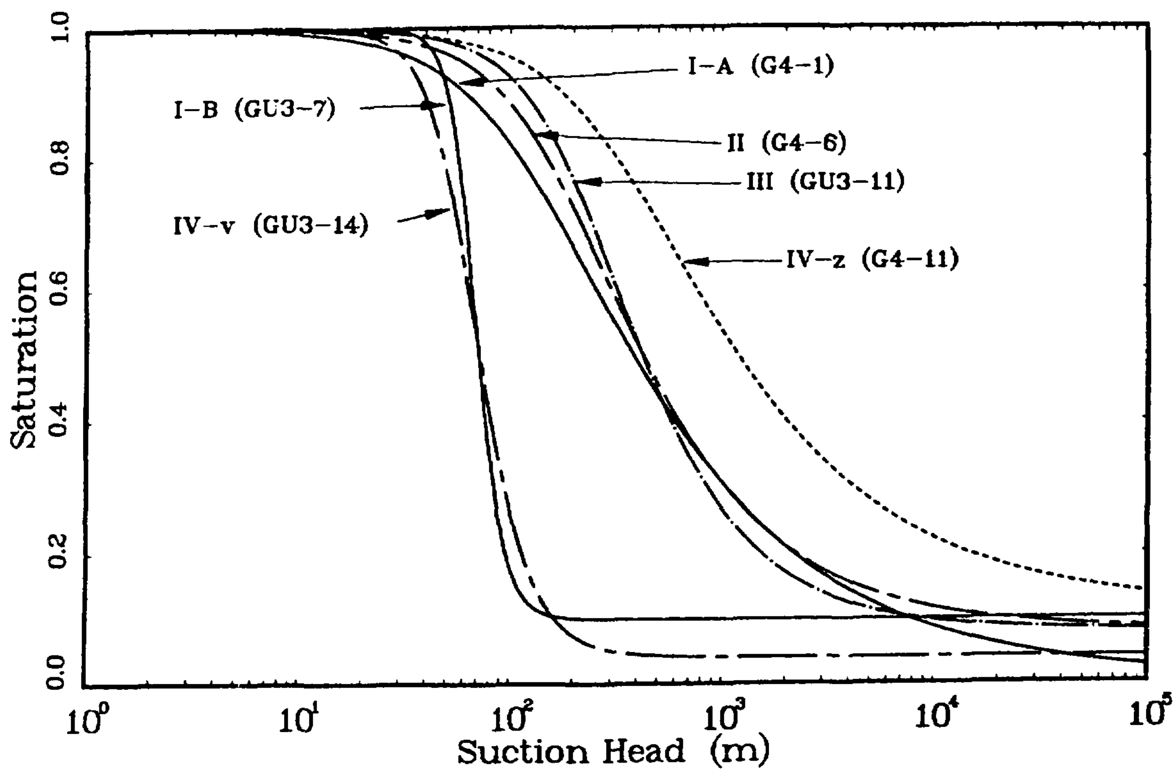


Figure 16. Representative Water-Retention Curves for the Unsaturated Zone Hydrologic Zone Units

Table 9. Properties for Representative Samples Taken From the Unsaturated Zone Hydrologic Units

| Unit | Sample Code | Grain Density ($g/cm^3$) | Porosity | Hydraulic Conductivity (m/s) | $S_r$ | Alpha (1/m) | Beta |
|---|---|---|---|---|---|---|---|
| I-A | G4-1 | 2.49 | 0.08 | 9.7E-12 | 0.0020 | 0.821E-02 | 1.558 |
| I-B | GU3-7 | 2.35 | 0.40 | 3.9E-07 | 0.1001 | 0.150E-01 | 6.872 |
| II | G4-6 | 2.58 | 0.11 | 1.9E-11 | 0.0801 | 0.567E-02 | 1.798 |
| III | GU3-11 | 2.38 | 0.07 | 1.5E-12 | 0.0804 | 0.441E-02 | 2.058 |
| IV-v | GU3-14 | 2.37 | 0.46 | 2.7E-09 | 0.0405 | 0.160E-01 | 3.872 |
| IV-z | G4-11 | 2.23 | 0.28 | 2.0E-11 | 0.1095 | 0.308E-02 | 1.602 |

REFERENCES


Barton, N., Bakhtar, K., and S. Bandis, "Rock Joint Description and Modeling for Prediction of Near-Field Repository Performance," Materials Res. Soc. Ann. Meeting 1983, Boston, Mass, Proc. Symp. D - "Scientific Basis for Nuclear Waste Management."

Blair, S. C., and J. A. Stottlemyre. 1981. "A New Laboratory Test Facility for Aquifer Materials." In Proceedings of the International Conference on Seasonal Thermal Energy Storage and Compressed Air Energy Storage, CONF-811066, Vol. 1, pp. 263-269, Pacific Northwest Laboratory, Richland, Washington.

Brown, R. W., and B. P. VanHaveren (ed). 1972. "Psychrometry in Water Relations Research." In Proceedings of the Symposium on Thermocouple Psychrometers. Utah Agricultural Experiment Station, Utah St. Univ., Logan, Utah.

Campbell, G. S., 1977. An Introduction to Environmental Biophysics, Springer-Verlag, New York, New York.

Campbell, G. S. and J. Van Schilfgaarde. 1981. "Use of SI Units in Soil Physics." J. of Agronomic Education 10:73-74.

Gale, J. E. 1975. "A Numerical Field and Laboratory Study of Flow in Rocks with Deformable Fractures." Ph.D. Thesis, p. 225, Univ. of Calif., Berkeley, California.

Gee, G. W., and M. E. Dodson. 1981. "Soil Water Content by Microwave Drying: A Routine Procedure." Soil Sci. Soc. Am. J. 45:1234-1237.

Haverkamp, R., Vauclin, M., Touma, J., Wierenga, P., and G. Vachaud. 1977. "A Comparison of Numerical Simulation Models for One-Dimensional Infiltration," Soil Sci. Soc. Am. J., Vol 41.

Hillel, D. 1982. Introduction to Soil Physics, Academic Press, New York, New York.

Johnson, B. 1983. "Permeability of a Simulated-Fracture as a Function of Normal Stress." In Proceedings of the 24th Symposium on Rock Mechanics, Association of Engineering Geologists, Short Hills, New Jersey.

McKeon, T. J., S. W. Tyler, D. W. Mayer, and A. E. Reisenauer. 1983. Trust-II Utility Package: Partially Saturated Soil Characterization, Grid Generation, and Advective Transport Analysis." NUREG/CR-3443 (PNL-4805), Nuclear Regulatory Commission, Washington, D.C.

Mualem, Y. 1976. "A New Model for Predicting the Hydraulic Conductivity of Unsaturated Porous Media," Water Resources Research 12(3):513-522.

Narasimhan, T. N., 1982. "Physics of Saturated-Unsaturated Subsurface Flow" in "Recent Trends in Hydrogeology" edited by T. N. Narasimhan, Special Paper 189, Geological Society of America, Boulder, Colorado.

Ortiz, T. S., Williams, R. L., Nimick, F. B., and B. C. Whittet. "A Three-Dimensional Model of Thermal-Mechanical Units at Yucca Mountain, Southern Nevada," SAND84-1076, Sandia National Laboratories, Albuquerque, New Mexico, In Preparation.

Papendick, R. I., and G. S. Campbell. 1980. "Theory and Measurement of Water Potential," J. F. Parr, W. R. Gardner, L. F. Ellion (Eds.), Water Potential Relations in Soil Microbiology, Soil Sci. Soc. Am., Madison, Wisconsin.

Scott, R. B., Spengler, R. W., Lappin, A. R., and M. P. Chornack, 1983. "Geologic Character of Tuffs in the Unsaturated Zone at Yucca Mountain, Southern Nevada," in "Role of the Unsaturated Zone in Radioactive and Hazardous Waste Disposal," edited by J. Mercer, Ann Arbor Science, Ann Arbor, Michigan.

Van Genuchten, R. 1978. "Calculating the Unsaturated Hydraulic Conductivity with a New Closed Form Analytical Model," Water Resources Bulletin, Princeton University Press, Princeton University, Princeton, New Jersey.

Walsh, J. B. 1981, "Effect of Pore Pressure and Confining Pressure on Fracture Permeability," Int.J. Rock Mech. Min. Sci. & Geomech. Abstr., Vol. 18, 429-435.

Winograd, I. J. 1981. "Radioactive Waste Disposal in Thick Unsaturated Zones." Sci. 212:1457-1464.

# APPENDIX A

## TEST RESULTS

This appendix contains the data gathered by PNL and is organized in the following manner:

| | |
|---|---|
| Table A.1 | Porosity and Water Retention Data for Samples from Drill Holes USW G-4 and USW GU-3 |
| Table A.2 | Properties of Samples Taken From USW G-4 and USW GU-3 |
| Table A.3 | Summary of Mercury-Intrusion Data Supplied by Micromeritics |
| Table A.4 | Unconfined Saturated Hydraulic Conductivity Data for Samples Taken From USW G-4 and USW GU-3 |
| Figure A.1 | Technique for Measuring Sample Saturated Conductivity as a Function of Elevated Confining Pressure |
| Table A.5 | Data and Calculated Values for Confined, Saturated Conductivity Tests of Sample GU3-2 |
| Table A.6 | Data and Calculated Values for Confined, Saturated Conductivity Tests of Sample GU3-15 |
| Table A.7 | Data and Calculated Values for Confined, Saturated Conductivity Tests of Sample GU3-3 |

TABLE A.1. Porosity and Water Retention Data for Samples from Drill Holes USW G-4 and USW GU-3

| Sample | Depth (ft) | Unit | Bulk Density ($g/cm^3$) | Porosity | Head (m) | Water Content g/g | Water Content vol/vol |
|---|---|---|---|---|---|---|---|
| G4-1a | 43 | I-A | 2.26 | .09 | 0 | 0.0322 | 0.07 |
| | | | | | 9 | 0.0322 | 0.07 |
| | | | | | 52 | 0.0246 | 0.06 |
| | | | | | 199 | 0.0193 | 0.04 |
| | | | | | 314 | 0.0143 | 0.04 |
| | | | | | 459 | 0.0124 | 0.03 |
| | | | | | 670 | 0.0090 | 0.02 |
| | | | | | 757 | 0.0081 | 0.02 |
| | | | | | 1183 | 0.0063 | 0.01 |
| | | | | | 10200 | 0.0023 | 0.005 |
| G4-1b | 43 | I-A | 2.31 | .07 | 0 | 0.0242 | 0.06 |
| | | | | | 10 | 0.0242 | 0.06 |
| | | | | | 92 | 0.0192 | 0.04 |
| | | | | | 270 | 0.0165 | 0.04 |
| | | | | | 372 | 0.0137 | 0.03 |
| | | | | | 505 | 0.0111 | 0.03 |
| | | | | | 699 | 0.0100 | 0.02 |
| | | | | | 816 | 0.0081 | 0.02 |
| | | | | | 1387 | 0.0068 | 0.02 |
| | | | | | 10200 | 0.0016 | 0.004 |
| G4-1c | 43 | I-A | 2.32 | .07 | 0 | 0.0217 | 0.05 |
| | | | | | 18 | 0.0217 | 0.05 |
| | | | | | 138 | 0.0173 | 0.04 |
| | | | | | 272 | 0.0149 | 0.03 |
| | | | | | 423 | 0.0125 | 0.03 |
| | | | | | 515 | 0.0104 | 0.02 |
| | | | | | 612 | 0.0096 | 0.02 |
| | | | | | 699 | 0.0083 | 0.02 |
| | | | | | 10200 | 0.0019 | 0.004 |
| G4-2a | 124 | I-B | 1.72 | .28 | 0 | 0.1420 | 0.24 |
| | | | | | 5 | 0.1420 | 0.24 |
| | | | | | 20 | 0.1220 | 0.21 |
| | | | | | 83 | 0.1061 | 0.13 |
| | | | | | 408 | 0.0837 | 0.14 |
| | | | | | 973 | 0.0746 | 0.13 |
| | | | | | 1436 | 0.0683 | 0.12 |
| | | | | | 3825 | 0.0598 | 0.10 |
| | | | | | 8109 | 0.0330 | 0.06 |
| G4-2b | 124 | I-B | 1.72 | .28 | 0 | 0.1434 | 0.25 |
| | | | | | 12 | 0.1434 | 0.25 |
| | | | | | 151 | 0.1055 | 0.18 |
| | | | | | 418 | 0.0841 | 0.15 |
| | | | | | 785 | 0.0773 | 0.13 |
| | | | | | 2550 | 0.0672 | 0.12 |
| | | | | | 3060 | 0.0579 | 0.10 |
| | | | | | 8109 | 0.0327 | 0.05 |
| G4-2c | 124 | I-B | 1.80 | .25 | 0 | 0.1199 | 0.22 |
| | | | | | 5 | 0.1199 | 0.22 |
| | | | | | 17 | 0.1046 | 0.19 |
| | | | | | 118 | 0.0913 | 0.16 |
| | | | | | 165 | 0.0826 | 0.15 |
| | | | | | 500 | 0.0733 | 0.13 |
| | | | | | 890 | 0.0663 | 0.12 |
| | | | | | 1056 | 0.0618 | 0.11 |
| | | | | | 1265 | 0.0539 | 0.10 |
| | | | | | 8109 | 0.0233 | 0.04 |

TABLE A.1. (cont)

| Sample | Depth (ft) | Unit | Bulk Density ($g/cm^3$) | Porosity | Head (m) | Water Content g/g | Water Content vol/vol |
|---|---|---|---|---|---|---|---|
| G4-3a | 208 | I-B | 0.85 | .65 | 0 | 0.5359 | 0.45 |
| | | | | | 26 | 0.5359 | 0.45 |
| | | | | | 51 | 0.4945 | 0.42 |
| | | | | | 237 | 0.0901 | 0.08 |
| | | | | | 467 | 0.0704 | 0.06 |
| | | | | | 2499 | 0.0481 | 0.05 |
| | | | | | 8109 | 0.0169 | 0.001 |
| G4-3b | 208 | I-B | 0.85 | .65 | 0 | 0.5446 | 0.46 |
| | | | | | 26 | 0.5446 | 0.46 |
| | | | | | 73 | 0.1591 | 0.14 |
| | | | | | 222 | 0.0833 | 0.07 |
| | | | | | 757 | 0.0606 | 0.05 |
| | | | | | 1409 | 0.0510 | 0.04 |
| | | | | | 8109 | 0.0196 | 0.02 |
| G4-3c | 208 | I-B | 0.85 | .65 | 0 | 0.4947 | 0.42 |
| | | | | | 29 | 0.4947 | 0.42 |
| | | | | | 204 | 0.0901 | 0.08 |
| | | | | | 856 | 0.0668 | 0.06 |
| | | | | | 2107 | 0.0463 | 0.04 |
| | | | | | 8109 | 0.0189 | 0.02 |
| G4-4a | 247 | II-L | 2.49 | .031* | 0 | 0.0131 | 0.033 |
| | | | | | 30 | 0.0131 | 0.033 |
| | | | | | 166 | 0.0076 | 0.019 |
| | | | | | 397 | 0.0058 | 0.014 |
| | | | | | 900 | 0.0053 | 0.013 |
| | | | | | 1377 | 0.0050 | 0.012 |
| | | | | | 1650 | 0.0048 | 0.012 |
| | | | | | 3743 | 0.0044 | 0.011 |
| | | | | | 4055 | 0.0031 | 0.003 |
| | | | | | 8109 | 0.0013 | 0.003 |
| G4-4b | 247 | II-L | 2.49 | .031* | 0 | 0.0118 | 0.029 |
| | | | | | 43 | 0.0118 | 0.029 |
| | | | | | 318 | 0.0070 | 0.017 |
| | | | | | 377 | 0.0065 | 0.016 |
| | | | | | 713 | 0.0063 | 0.016 |
| | | | | | 1329 | 0.0047 | 0.012 |
| | | | | | 2251 | 0.0044 | 0.011 |
| | | | | | 2319 | 0.0042 | 0.010 |
| | | | | | 2550 | 0.0033 | 0.008 |
| | | | | | 8109 | 0.0008 | 0.002 |
| G4-4c | 247 | II-L | 2.49 | .031* | 0 | 0.0125 | 0.031 |
| | | | | | 71 | 0.0125 | 0.031 |
| | | | | | 144 | 0.0075 | 0.019 |
| | | | | | 165 | 0.0057 | 0.014 |
| | | | | | 561 | 0.0044 | 0.010 |
| | | | | | 1051 | 0.0038 | 0.009 |
| | | | | | 1341 | 0.0037 | 0.009 |
| | | | | | 4212 | 0.0034 | 0.008 |
| | | | | | 8109 | 0.0020 | 0.005 |
| G4-5a | 864 (dark) | II-NL | 2.26 | .11 | 0 | 0.0482 | 0.11 |
| | | | | | 10 | 0.0482 | 0.11 |
| | | | | | 65 | 0.0395 | 0.09 |
| | | | | | 181 | 0.0305 | 0.07 |
| | | | | | 275 | 0.0260 | 0.06 |
| | | | | | 466 | 0.0200 | 0.04 |
| | | | | | 589 | 0.0169 | 0.03 |
| | | | | | 1140 | 0.0127 | 0.02 |
| | | | | | 10200 | 0.0016 | 0.01 |

* - The porosity value listed is an estimate based on the grain density from a nearby sample; see Table A.2 for further information.

TABLE A.1. (cont)

| Sample | Depth (ft) | Unit | Bulk Density (g/cm$^3$) | Porosity | Head (m) | Water Content g/g | Water Content vol/vol |
|---|---|---|---|---|---|---|---|
| G4-5b | 864 | II-NL | 2.30 | .09 | 0 | 0.0362 | 0.08 |
| | | | | | 12 | 0.0362 | 0.08 |
| | | | | | 121 | 0.0288 | 0.07 |
| | | | | | 245 | 0.0237 | 0.05 |
| | | | | | 287 | 0.0209 | 0.05 |
| | | | | | 456 | 0.0171 | 0.04 |
| | | | | | 612 | 0.0152 | 0.03 |
| | | | | | 887 | 0.0138 | 0.03 |
| | | | | | 1474 | 0.0121 | 0.02 |
| | | | | | 10200 | 0.0096 | 0.004 |
| G4-5c | 864 | II-NL | 2.38 | .06 | 0 | 0.0493 | 0.12 |
| | | | | | 8 | 0.0493 | 0.12 |
| | | | | | 78 | 0.0422 | 0.10 |
| | | | | | 167 | 0.0360 | 0.09 |
| | | | | | 249 | 0.0284 | 0.07 |
| | | | | | 315 | 0.0230 | 0.05 |
| | | | | | 553 | 0.0199 | 0.04 |
| | | | | | 882 | 0.0169 | 0.03 |
| | | | | | 1822 | 0.0136 | 0.03 |
| | | | | | 10200 | 0.0042 | 0.01 |
| G4-24a | 864 (light) | II-NL | 2.21 | .16 | 0 | 0.0586 | 0.13 |
| | | | | | 9 | 0.0586 | 0.13 |
| | | | | | 87 | 0.0404 | 0.09 |
| | | | | | 172 | 0.0325 | 0.07 |
| | | | | | 224 | 0.0252 | 0.06 |
| | | | | | 303 | 0.0168 | 0.04 |
| | | | | | 392 | 0.0158 | 0.04 |
| | | | | | 529 | 0.0109 | 0.02 |
| | | | | | 667 | 0.0098 | 0.02 |
| | | | | | 780 | 0.0086 | 0.02 |
| | | | | | 1166 | 0.0079 | 0.02 |
| | | | | | 1326 | 0.0062 | 0.01 |
| | | | | | 8109 | 0.0052 | 0.01 |
| G4-24b | 864 | II-NL | 2.23 | .15 | 0 | 0.0545 | 0.12 |
| | | | | | 2 | 0.0545 | 0.12 |
| | | | | | 67 | 0.0362 | 0.08 |
| | | | | | 140 | 0.0292 | 0.07 |
| | | | | | 220 | 0.0207 | 0.05 |
| | | | | | 285 | 0.0172 | 0.04 |
| | | | | | 394 | 0.0146 | 0.03 |
| | | | | | 433 | 0.0118 | 0.03 |
| | | | | | 771 | 0.0102 | 0.02 |
| | | | | | 867 | 0.0083 | 0.02 |
| | | | | | 1261 | 0.0077 | 0.02 |
| | | | | | 1492 | 0.0063 | 0.01 |
| | | | | | 8109 | 0.0050 | 0.01 |
| G4-24c | 864 | II-NL | 2.21 | .16 | 0 | 0.0558 | 0.12 |
| | | | | | 1 | 0.0558 | 0.12 |
| | | | | | 78 | 0.0448 | 0.09 |
| | | | | | 140 | 0.0369 | 0.08 |
| | | | | | 267 | 0.0226 | 0.05 |
| | | | | | 442 | 0.0151 | 0.03 |
| | | | | | 882 | 0.0102 | 0.02 |
| | | | | | 1032 | 0.0079 | 0.02 |
| | | | | | 1415 | 0.0064 | 0.01 |
| | | | | | 8109 | 0.0050 | 0.01 |
| G4-6a | 1158 | II-NL | 2.30 | .11 | 0 | 0.0399 | 0.09 |
| | | | | | 27 | 0.0399 | 0.09 |
| | | | | | 144 | 0.0298 | 0.07 |
| | | | | | 226 | 0.0247 | 0.06 |
| | | | | | 286 | 0.0219 | 0.05 |
| | | | | | 353 | 0.0216 | 0.05 |
| | | | | | 414 | 0.0154 | 0.04 |
| | | | | | 528 | 0.0139 | 0.03 |
| | | | | | 642 | 0.0131 | 0.03 |
| | | | | | 828 | 0.0112 | 0.03 |
| | | | | | 949 | 0.0109 | 0.03 |
| | | | | | 1054 | 0.0099 | 0.02 |
| | | | | | 8109 | 0.0044 | 0.01 |

TABLE A.1. (cont)

| Sample | Depth (ft) | Unit | Bulk Density (g/cm$^3$) | Porosity | Head (m) | Water Content g/g | Water Content vol/vol |
|---|---|---|---|---|---|---|---|
| G4-6b | 1158 | II-NL | 2.30 | .11 | 0 | 0.0406 | 0.09 |
| | | | | | 14 | 0.0406 | 0.09 |
| | | | | | 224 | 0.0314 | 0.07 |
| | | | | | 418 | 0.0267 | 0.06 |
| | | | | | 497 | 0.0237 | 0.06 |
| | | | | | 592 | 0.0199 | 0.05 |
| | | | | | 645 | 0.0142 | 0.03 |
| | | | | | 702 | 0.0133 | 0.03 |
| | | | | | 1061 | 0.0120 | 0.03 |
| | | | | | 1076 | 0.0117 | 0.03 |
| | | | | | 1342 | 0.0106 | 0.02 |
| | | | | | 8109 | 0.0053 | 0.01 |
| G4-6c | 1158 | II-NL | 2.30 | .11 | 0 | 0.0445 | 0.10 |
| | | | | | 23 | 0.0445 | 0.10 |
| | | | | | 266 | 0.0352 | 0.08 |
| | | | | | 316 | 0.0268 | 0.06 |
| | | | | | 408 | 0.0215 | 0.05 |
| | | | | | 476 | 0.0198 | 0.05 |
| | | | | | 696 | 0.0170 | 0.04 |
| | | | | | 901 | 0.0153 | 0.04 |
| | | | | | 1242 | 0.0145 | 0.03 |
| | | | | | 1394 | 0.0138 | 0.03 |
| | | | | | 1666 | 0.0129 | 0.03 |
| | | | | | 8109 | 0.0054 | 0.01 |
| G4-1Fa | 1215 | II-NL | 2.28 | .12* | 0 | 0.0395 | 0.09 |
| | | | | | 9 | 0.0395 | 0.09 |
| | | | | | 88 | 0.0335 | 0.08 |
| | | | | | 167 | 0.0298 | 0.07 |
| | | | | | 258 | 0.0251 | 0.06 |
| | | | | | 328 | 0.0219 | 0.05 |
| | | | | | 369 | 0.0208 | 0.05 |
| | | | | | 671 | 0.0156 | 0.04 |
| | | | | | 934 | 0.0137 | 0.03 |
| | | | | | 1145 | 0.0099 | 0.02 |
| | | | | | 1443 | 0.0080 | 0.02 |
| | | | | | 1681 | 0.0073 | 0.02 |
| | | | | | 9027 | 0.0043 | 0.01 |
| G4-1Fb | 1215 | II-NL | 2.28 | .12* | 0 | 0.0395 | 0.09 |
| | | | | | 8 | 0.0395 | 0.09 |
| | | | | | 53 | 0.0338 | 0.07 |
| | | | | | 185 | 0.0304 | 0.07 |
| | | | | | 251 | 0.0256 | 0.06 |
| | | | | | 307 | 0.0227 | 0.05 |
| | | | | | 487 | 0.0180 | 0.04 |
| | | | | | 598 | 0.0164 | 0.04 |
| | | | | | 630 | 0.0151 | 0.03 |
| | | | | | 676 | 0.0117 | 0.03 |
| | | | | | 1464 | 0.0089 | 0.02 |
| | | | | | 9027 | 0.0044 | 0.01 |
| G4-1Fc | 1215 | II-NL | 2.36 | .09* | 0 | 0.0324 | 0.08 |
| | | | | | 2 | 0.0324 | 0.08 |
| | | | | | 144 | 0.0273 | 0.07 |
| | | | | | 209 | 0.0224 | 0.05 |
| | | | | | 265 | 0.0147 | 0.04 |
| | | | | | 489 | 0.0137 | 0.03 |
| | | | | | 652 | 0.0118 | 0.03 |
| | | | | | 893 | 0.0087 | 0.02 |
| | | | | | 9027 | 0.0085 | 0.01 |
| G4-7a | 1256 | II-NL | 2.30 | .09 | 0 | 0.0341 | 0.08 |
| | | | | | 30 | 0.0341 | 0.08 |
| | | | | | 270 | 0.0289 | 0.07 |
| | | | | | 459 | 0.0250 | 0.06 |
| | | | | | 577 | 0.0230 | 0.05 |
| | | | | | 581 | 0.0200 | 0.05 |
| | | | | | 609 | 0.0180 | 0.04 |
| | | | | | 2020 | 0.0060 | 0.01 |
| | | | | | 10200 | 0.0040 | 0.01 |

* - The porosity value listed is an estimate based on the grain density from a nearby sample; see Table A.2 for further information.

TABLE A.1. (cont)

| Sample | Depth (ft) | Unit | Bulk Density (g/cm$^3$) | Porosity | Head (m) | Water Content g/g | Water Content vol/vol |
|---|---|---|---|---|---|---|---|
| G4-7b | 1256 | II-NL | 2.28 | .10 | 0 | 0.0321 | 0.07 |
| | | | | | 38 | 0.0321 | 0.07 |
| | | | | | 379 | 0.0276 | 0.06 |
| | | | | | 486 | 0.0227 | 0.05 |
| | | | | | 675 | 0.0203 | 0.05 |
| | | | | | 747 | 0.0158 | 0.04 |
| | | | | | 1161 | 0.0145 | 0.03 |
| | | | | | 1564 | 0.0138 | 0.03 |
| | | | | | 2105 | 0.0111 | 0.03 |
| | | | | | 10200 | 0.0043 | 0.01 |
| G4-7c | 1256 | II-NL | 2.27 | .10 | 0 | 0.0403 | 0.09 |
| | | | | | 16 | 0.0403 | 0.09 |
| | | | | | 209 | 0.0354 | 0.08 |
| | | | | | 302 | 0.0312 | 0.07 |
| | | | | | 362 | 0.0267 | 0.06 |
| | | | | | 477 | 0.0239 | 0.05 |
| | | | | | 596 | 0.0227 | 0.05 |
| | | | | | 1887 | 0.0055 | 0.01 |
| | | | | | 10200 | 0.0052 | 0.01 |
| G4-2Fa | 1278 | II-NL | 2.35 | .060 | 0 | 0.0294 | 0.07 |
| | | | | | 10 | 0.0294 | 0.07 |
| | | | | | 140 | 0.0242 | 0.06 |
| | | | | | 294 | 0.0226 | 0.05 |
| | | | | | 396 | 0.0182 | 0.04 |
| | | | | | 457 | 0.0175 | 0.04 |
| | | | | | 628 | 0.0144 | 0.03 |
| | | | | | 776 | 0.0110 | 0.03 |
| | | | | | 1277 | 0.0086 | 0.02 |
| | | | | | 1703 | 0.0072 | 0.02 |
| | | | | | 9027 | 0.0046 | 0.01 |
| G4-2Fb | 1278 | II-NL | 2.34 | .064 | 0 | 0.0310 | 0.07 |
| | | | | | 30 | 0.0310 | 0.07 |
| | | | | | 159 | 0.0262 | 0.06 |
| | | | | | 200 | 0.0233 | 0.06 |
| | | | | | 299 | 0.0215 | 0.05 |
| | | | | | 347 | 0.0202 | 0.05 |
| | | | | | 408 | 0.0178 | 0.04 |
| | | | | | 487 | 0.0134 | 0.03 |
| | | | | | 774 | 0.0106 | 0.03 |
| | | | | | 988 | 0.0096 | 0.02 |
| | | | | | 1249 | 0.0080 | 0.02 |
| | | | | | 1673 | 0.0072 | 0.02 |
| | | | | | 2427 | 0.0052 | 0.01 |
| | | | | | 9027 | 0.0044 | 0.01 |
| G4-2Fc | 1278 | II-NL | 2.36 | .056 | 0 | 0.0307 | 0.07 |
| | | | | | 10 | 0.0307 | 0.07 |
| | | | | | 219 | 0.0256 | 0.06 |
| | | | | | 319 | 0.0232 | 0.06 |
| | | | | | 387 | 0.0186 | 0.04 |
| | | | | | 409 | 0.0166 | 0.04 |
| | | | | | 478 | 0.0148 | 0.04 |
| | | | | | 730 | 0.0110 | 0.03 |
| | | | | | 1028 | 0.0103 | 0.02 |
| | | | | | 1114 | 0.0082 | 0.02 |
| | | | | | 1799 | 0.0073 | 0.02 |
| | | | | | 9027 | 0.0043 | 0.01 |

TABLE A.1. (cont)

| Sample | Depth (ft) | Unit | Bulk Density (g/cm³) | Porosity | Head (m) | Water Content g/g | vol/vol |
|---|---|---|---|---|---|---|---|
| G4-8a | 1299 | III | 2.23 | .11 | 0 | 0.0371 | 0.08 |
| | | | | | 13 | 0.0371 | 0.08 |
| | | | | | 292 | 0.0290 | 0.06 |
| | | | | | 370 | 0.0221 | 0.05 |
| | | | | | 424 | 0.0198 | 0.04 |
| | | | | | 505 | 0.0187 | 0.04 |
| | | | | | 646 | 0.0145 | 0.03 |
| | | | | | 979 | 0.0140 | 0.03 |
| | | | | | 1212 | 0.0133 | 0.03 |
| | | | | | 1342 | 0.0123 | 0.03 |
| | | | | | 1531 | 0.0118 | 0.03 |
| | | | | | 8109 | 0.0042 | 0.01 |
| G4-8b | 1299 | III | 2.28 | .09 | 0 | 0.0246 | 0.06 |
| | | | | | 14 | 0.0246 | 0.06 |
| | | | | | 283 | 0.0203 | 0.05 |
| | | | | | 357 | 0.0170 | 0.04 |
| | | | | | 498 | 0.0153 | 0.03 |
| | | | | | 694 | 0.0144 | 0.03 |
| | | | | | 896 | 0.0124 | 0.03 |
| | | | | | 928 | 0.0122 | 0.03 |
| | | | | | 1155 | 0.0118 | 0.03 |
| | | | | | 1364 | 0.0112 | 0.03 |
| | | | | | 1382 | 0.0109 | 0.02 |
| | | | | | 8109 | 0.0035 | 0.01 |
| G4-8c | 1299 | III | 2.31 | .08 | 0 | 0.0320 | 0.07 |
| | | | | | 15 | 0.0320 | 0.07 |
| | | | | | 300 | 0.0247 | 0.06 |
| | | | | | 355 | 0.0222 | 0.05 |
| | | | | | 473 | 0.0196 | 0.05 |
| | | | | | 696 | 0.0153 | 0.04 |
| | | | | | 856 | 0.0132 | 0.03 |
| | | | | | 1025 | 0.0129 | 0.03 |
| | | | | | 1539 | 0.0126 | 0.03 |
| | | | | | 8109 | 0.0036 | 0.01 |
| G4-9a | 1324 | III | 2.28 | .038 | 0 | 0.0040 | 0.009 |
| | | | | | 30 | 0.0040 | 0.009 |
| | | | | | 301 | 0.0027 | 0.006 |
| | | | | | 624 | 0.0026 | 0.005 |
| | | | | | 1168 | 0.0024 | 0.005 |
| | | | | | 1209 | 0.0023 | 0.005 |
| | | | | | 1391 | 0.0020 | 0.005 |
| | | | | | 1633 | 0.0018 | 0.002 |
| | | | | | 10200 | 0.0006 | 0.001 |
| G4-9b | 1324 | III | 2.25 | .051 | 0 | 0.0046 | 0.010 |
| | | | | | 52 | 0.0046 | 0.010 |
| | | | | | 459 | 0.0043 | 0.010 |
| | | | | | 836 | 0.0036 | 0.010 |
| | | | | | 857 | 0.0033 | 0.007 |
| | | | | | 1132 | 0.0032 | 0.007 |
| | | | | | 1162 | 0.0026 | 0.006 |
| | | | | | 3700 | 0.0013 | 0.003 |
| | | | | | 10200 | 0.0012 | 0.003 |
| G4-9c | 1324 | III | 2.27 | .042 | 0 | 0.0064 | 0.015 |
| | | | | | 29 | 0.0064 | 0.015 |
| | | | | | 298 | 0.0050 | 0.011 |
| | | | | | 711 | 0.0042 | 0.010 |
| | | | | | 724 | 0.0040 | 0.009 |
| | | | | | 1173 | 0.0038 | 0.009 |
| | | | | | 1234 | 0.0029 | 0.007 |
| | | | | | 3784 | 0.0004 | 0.001 |
| | | | | | 10200 | 0.0001 | 0.0002 |

TABLE A.1. (cont)

| Sample | Depth (ft) | Unit | Bulk Density (g/cm$^3$) | Porosity | Head (m) | Water Content g/g | Water Content vol/vol |
|---|---|---|---|---|---|---|---|
| G4-3Fa | 1359 | IV-A-v | 1.88 | .21* | 0 | 0.0992 | 0.19 |
| | | | | | 15 | 0.0992 | 0.19 |
| | | | | | 33 | 0.0595 | 0.11 |
| | | | | | 245 | 0.0299 | 0.06 |
| | | | | | 578 | 0.0249 | 0.05 |
| | | | | | 1461 | 0.0214 | 0.04 |
| | | | | | 1730 | 0.0176 | 0.03 |
| | | | | | 2118 | 0.0143 | 0.03 |
| | | | | | 2673 | 0.0122 | 0.02 |
| | | | | | 2740 | 0.0119 | 0.02 |
| | | | | | 9027 | 0.0076 | 0.01 |
| G4-3Fb | 1359 | IV-A-v | 1.82 | .24* | 0 | 0.1196 | 0.22 |
| | | | | | 15 | 0.1196 | 0.22 |
| | | | | | 58 | 0.0718 | 0.13 |
| | | | | | 109 | 0.0370 | 0.07 |
| | | | | | 161 | 0.0316 | 0.06 |
| | | | | | 840 | 0.0252 | 0.05 |
| | | | | | 1264 | 0.0201 | 0.04 |
| | | | | | 1410 | 0.0183 | 0.03 |
| | | | | | 1558 | 0.0162 | 0.03 |
| | | | | | 1748 | 0.0138 | 0.03 |
| | | | | | 2098 | 0.0123 | 0.02 |
| | | | | | 9027 | 0.0069 | 0.01 |
| G4-3Fc | 1359 | IV-A-v | 1.97 | .18* | 0 | 0.0666 | 0.13 |
| | | | | | 28 | 0.0666 | 0.13 |
| | | | | | 74 | 0.0329 | 0.07 |
| | | | | | 936 | 0.0211 | 0.04 |
| | | | | | 986 | 0.0196 | 0.04 |
| | | | | | 1164 | 0.0183 | 0.04 |
| | | | | | 1574 | 0.0157 | 0.03 |
| | | | | | 1762 | 0.0139 | 0.03 |
| | | | | | 2256 | 0.0128 | 0.03 |
| | | | | | 2498 | 0.0112 | 0.02 |
| | | | | | 9027 | 0.0066 | 0.01 |
| G4-10a | 1405 | IV-A-z | 1.39 | .41* | 0 | 0.2723 | 0.38 |
| | | | | | 12 | 0.2723 | 0.38 |
| | | | | | 51 | 0.2395 | 0.33 |
| | | | | | 78 | 0.2063 | 0.29 |
| | | | | | 187 | 0.1839 | 0.26 |
| | | | | | 711 | 0.1601 | 0.22 |
| | | | | | 750 | 0.1452 | 0.20 |
| | | | | | 784 | 0.1327 | 0.18 |
| | | | | | 1163 | 0.1256 | 0.17 |
| | | | | | 1786 | 0.1058 | 0.15 |
| | | | | | 8109 | 0.0580 | 0.08 |
| G4-10b | 1405 | IV-A-v | 1.39 | .41* | 0 | 0.2231 | 0.31 |
| | | | | | 20 | 0.2231 | 0.31 |
| | | | | | 53 | 0.1959 | 0.27 |
| | | | | | 79 | 0.1452 | 0.20 |
| | | | | | 381 | 0.1275 | 0.18 |
| | | | | | 577 | 0.1102 | 0.15 |
| | | | | | 992 | 0.1019 | 0.14 |
| | | | | | 1306 | 0.0963 | 0.13 |
| | | | | | 2867 | 0.0846 | 0.12 |
| | | | | | 8109 | 0.0442 | 0.06 |
| G4-10c | 1405 | IV-A-z | 1.39 | .41* | 0 | 0.2453 | 0.34 |
| | | | | | 18 | 0.2453 | 0.34 |
| | | | | | 55 | 0.2131 | 0.30 |
| | | | | | 336 | 0.1829 | 0.25 |
| | | | | | 861 | 0.1643 | 0.23 |
| | | | | | 918 | 0.1426 | 0.20 |
| | | | | | 938 | 0.1313 | 0.18 |
| | | | | | 1586 | 0.1221 | 0.17 |
| | | | | | 8109 | 0.0590 | 0.08 |

* - The porosity value listed is an estimate based on the grain density from a nearby sample; see Table A.2 for further information.

TABLE A.1. (cont)

| Sample | Depth (ft) | Unit | Bulk Density (g/cm³) | Porosity | Head (m) | Water Content g/g | Water Content vol/vol |
|---|---|---|---|---|---|---|---|
| G4-11a | 1548 | IV-A-z | 1.63 | .27 | 0 | 0.1708 | 0.28 |
| | | | | | 5 | 0.1708 | 0.28 |
| | | | | | 338 | 0.1370 | 0.22 |
| | | | | | 523 | 0.1212 | 0.20 |
| | | | | | 664 | 0.1079 | 0.17 |
| | | | | | 1212 | 0.0924 | 0.15 |
| | | | | | 1471 | 0.0837 | 0.14 |
| | | | | | 2413 | 0.0759 | 0.12 |
| | | | | | 2820 | 0.0512 | 0.08 |
| | | | | | 10200 | 0.0412 | 0.07 |
| G4-11b | 1548 | IV-A-z | 1.61 | .28 | 0 | 0.1840 | 0.30 |
| | | | | | 8 | 0.1840 | 0.30 |
| | | | | | 399 | 0.1407 | 0.23 |
| | | | | | 536 | 0.1246 | 0.20 |
| | | | | | 665 | 0.1104 | 0.18 |
| | | | | | 1275 | 0.0928 | 0.15 |
| | | | | | 1535 | 0.0845 | 0.14 |
| | | | | | 2044 | 0.0762 | 0.12 |
| | | | | | 2918 | 0.0526 | 0.08 |
| | | | | | 10200 | 0.0420 | 0.07 |
| G4-11c | 1548 | IV-A-z | 1.55 | .31 | 0 | 0.1974 | 0.31 |
| | | | | | 4 | 0.1974 | 0.31 |
| | | | | | 110 | 0.1794 | 0.28 |
| | | | | | 352 | 0.1601 | 0.25 |
| | | | | | 446 | 0.1413 | 0.22 |
| | | | | | 639 | 0.1159 | 0.18 |
| | | | | | 912 | 0.1031 | 0.16 |
| | | | | | 1461 | 0.0897 | 0.14 |
| | | | | | 3417 | 0.0549 | 0.09 |
| | | | | | 10200 | 0.0441 | 0.07 |
| G4-4Fa | 1551 | IV-A-z | 1.51 | .36* | 0 | 0.2307 | 0.35 |
| | | | | | 10 | 0.2307 | 0.35 |
| | | | | | 97 | 0.2007 | 0.30 |
| | | | | | 198 | 0.1859 | 0.28 |
| | | | | | 286 | 0.1695 | 0.26 |
| | | | | | 485 | 0.1241 | 0.19 |
| | | | | | 609 | 0.1029 | 0.16 |
| | | | | | 945 | 0.0896 | 0.14 |
| | | | | | 1553 | 0.0837 | 0.13 |
| | | | | | 1962 | 0.0703 | 0.11 |
| | | | | | 2203 | 0.0629 | 0.10 |
| | | | | | 9027 | 0.0479 | 0.07 |
| G4-4Fb | 1551 | IV-A-z | 1.62 | .32* | 0 | 0.1825 | 0.30 |
| | | | | | 8 | 0.1825 | 0.30 |
| | | | | | 159 | 0.1563 | 0.25 |
| | | | | | 245 | 0.1436 | 0.23 |
| | | | | | 344 | 0.1291 | 0.21 |
| | | | | | 645 | 0.0974 | 0.16 |
| | | | | | 756 | 0.0890 | 0.14 |
| | | | | | 954 | 0.0849 | 0.14 |
| | | | | | 1387 | 0.0763 | 0.12 |
| | | | | | 1441 | 0.0724 | 0.12 |
| | | | | | 1877 | 0.0654 | 0.11 |
| | | | | | 3905 | 0.0582 | 0.09 |
| | | | | | 9027 | 0.0448 | 0.07 |

* - The porosity value listed is an estimate based on the grain density from a nearby sample; see Table A.2 for further information.

TABLE A.1. (cont)

| Sample | Depth (ft) | Unit | Bulk Density (g/cm$^3$) | Porosity | Head (m) | Water Content g/g | Water Content vol/vol |
|---|---|---|---|---|---|---|---|
| G4-4Fc | 1551 | IV-A-z | 1.65 | .30* | 0 | 0.1737 | 0.29 |
| | | | | | 5 | 0.1737 | 0.29 |
| | | | | | 192 | 0.1473 | 0.24 |
| | | | | | 284 | 0.1357 | 0.22 |
| | | | | | 370 | 0.1216 | 0.20 |
| | | | | | 559 | 0.0870 | 0.14 |
| | | | | | 774 | 0.0785 | 0.13 |
| | | | | | 1303 | 0.0678 | 0.11 |
| | | | | | 1527 | 0.0582 | 0.10 |
| | | | | | 1839 | 0.0556 | 0.09 |
| | | | | | 2182 | 0.0511 | 0.08 |
| | | | | | 9027 | 0.0412 | 0.07 |
| G4-12a | 1686 | IV-A-z | 1.57 | .30 | 0 | 0.2334 | 0.37 |
| | | | | | 16 | 0.2334 | 0.37 |
| | | | | | 61 | 0.2153 | 0.34 |
| | | | | | 86 | 0.1986 | 0.31 |
| | | | | | 144 | 0.1774 | 0.28 |
| | | | | | 260 | 0.1568 | 0.25 |
| | | | | | 433 | 0.1316 | 0.21 |
| | | | | | 529 | 0.1119 | 0.18 |
| | | | | | 1095 | 0.0972 | 0.15 |
| | | | | | 1632 | 0.0882 | 0.14 |
| | | | | | 1685 | 0.0840 | 0.13 |
| | | | | | 3457 | 0.0690 | 0.11 |
| | | | | | 8109 | 0.0428 | 0.07 |
| G4-12b | 1686 | IV-A-z | 1.57 | .30 | 0 | 0.2143 | 0.34 |
| | | | | | 27 | 0.2143 | 0.34 |
| | | | | | 72 | 0.1976 | 0.31 |
| | | | | | 202 | 0.1813 | 0.28 |
| | | | | | 248 | 0.1591 | 0.25 |
| | | | | | 374 | 0.1437 | 0.23 |
| | | | | | 570 | 0.1232 | 0.19 |
| | | | | | 813 | 0.1014 | 0.16 |
| | | | | | 1110 | 0.0890 | 0.14 |
| | | | | | 1682 | 0.0809 | 0.13 |
| | | | | | 1916 | 0.0765 | 0.12 |
| | | | | | 3188 | 0.0605 | 0.09 |
| | | | | | 8109 | 0.0428 | 0.07 |
| G4-12c | 1686 | IV-A-z | 1.57 | .30 | 0 | 0.1901 | 0.30 |
| | | | | | 24 | 0.1901 | 0.30 |
| | | | | | 72 | 0.1759 | 0.28 |
| | | | | | 232 | 0.1570 | 0.25 |
| | | | | | 421 | 0.1381 | 0.22 |
| | | | | | 782 | 0.1105 | 0.17 |
| | | | | | 993 | 0.1010 | 0.16 |
| | | | | | 1529 | 0.0763 | 0.12 |
| | | | | | 1740 | 0.0703 | 0.11 |
| | | | | | 2313 | 0.0666 | 0.10 |
| | | | | | 3448 | 0.0557 | 0.09 |
| | | | | | 8109 | 0.0385 | 0.06 |
| G4-13a | 1728 | IV-B-z | 1.78 | .23 | 0 | 0.1665 | 0.30 |
| | | | | | 23 | 0.1665 | 0.30 |
| | | | | | 300 | 0.1599 | 0.28 |
| | | | | | 624 | 0.1485 | 0.26 |
| | | | | | 817 | 0.1421 | 0.25 |
| | | | | | 870 | 0.1390 | 0.25 |
| | | | | | 1380 | 0.1287 | 0.23 |
| | | | | | 1788 | 0.1159 | 0.21 |
| | | | | | 8109 | 0.0400 | 0.07 |

* - The porosity value listed is an estimate based on the grain density from a nearby sample; see Table A.2 for further information.

TABLE A.1. (cont)

| Sample | Depth (ft) | Unit | Bulk Density (g/cm³) | Porosity | Head (m) | Water Content g/g | vol/vol |
|---|---|---|---|---|---|---|---|
| G4-13b | 1728 | IV-B-z | 1.84 | .21 | 0 | 0.1421 | 0.26 |
| | | | | | 16 | 0.1421 | 0.26 |
| | | | | | 219 | 0.1170 | 0.22 |
| | | | | | 770 | 0.1050 | 0.19 |
| | | | | | 862 | 0.0973 | 0.18 |
| | | | | | 948 | 0.0891 | 0.16 |
| | | | | | 1490 | 0.0820 | 0.15 |
| | | | | | 1698 | 0.0773 | 0.14 |
| | | | | | 2126 | 0.0685 | 0.13 |
| | | | | | 8109 | 0.0381 | 0.07 |
| G4-13c | 1728 | IV-B-z | 1.83 | .21 | 0 | 0.1534 | 0.28 |
| | | | | | 23 | 0.1534 | 0.28 |
| | | | | | 330 | 0.1244 | 0.23 |
| | | | | | 770 | 0.1079 | 0.20 |
| | | | | | 862 | 0.1005 | 0.18 |
| | | | | | 944 | 0.0918 | 0.19 |
| | | | | | 1186 | 0.0840 | 0.15 |
| | | | | | 1545 | 0.0792 | 0.15 |
| | | | | | 2536 | 0.0680 | 0.12 |
| | | | | | 10200 | 0.0375 | 0.07 |
| G4-14a | 1737 | IV-B-z | 1.67 | .28 | 0 | 0.1478 | 0.25 |
| | | | | | 8 | 0.1478 | 0.25 |
| | | | | | 442 | 0.1056 | 0.18 |
| | | | | | 714 | 0.0919 | 0.15 |
| | | | | | 1017 | 0.0828 | 0.14 |
| | | | | | 1459 | 0.0719 | 0.12 |
| | | | | | 2098 | 0.0626 | 0.10 |
| | | | | | 3137 | 0.0570 | 0.10 |
| | | | | | 10200 | 0.0429 | 0.01 |
| G4-14b | 1737 | IV-B-z | 1.80 | .23 | 0 | 0.1345 | 0.24 |
| | | | | | 9 | 0.1345 | 0.24 |
| | | | | | 464 | 0.1000 | 0.18 |
| | | | | | 776 | 0.0867 | 0.16 |
| | | | | | 959 | 0.0774 | 0.14 |
| | | | | | 1288 | 0.0673 | 0.12 |
| | | | | | 1591 | 0.0603 | 0.11 |
| | | | | | 2842 | 0.0530 | 0.10 |
| | | | | | 10200 | 0.0338 | 0.07 |
| G4-14c | 1737 | IV-B-z | 1.80 | .23 | 0 | 0.1416 | 0.25 |
| | | | | | 8 | 0.1416 | 0.25 |
| | | | | | 342 | 0.1076 | 0.19 |
| | | | | | 477 | 0.0928 | 0.17 |
| | | | | | 790 | 0.0818 | 0.15 |
| | | | | | 1316 | 0.0698 | 0.13 |
| | | | | | 1729 | 0.0631 | 0.11 |
| | | | | | 2535 | 0.0587 | 0.11 |
| | | | | | 2856 | 0.0430 | 0.08 |
| | | | | | 10200 | 0.0335 | 0.06 |
| G4-15a | 1769 | IV-C-z | 1.77 | .26 | 0 | 0.1406 | 0.25 |
| | | | | | 20 | 0.1406 | 0.25 |
| | | | | | 585 | 0.1329 | 0.24 |
| | | | | | 878 | 0.1288 | 0.23 |
| | | | | | 1078 | 0.1251 | 0.23 |
| | | | | | 1162 | 0.1217 | 0.22 |
| | | | | | 1365 | 0.1156 | 0.20 |
| | | | | | 1418 | 0.0936 | 0.17 |
| | | | | | 2677 | 0.0801 | 0.14 |
| | | | | | 8109 | 0.0396 | 0.07 |
| G4-15b | 1769 | IV-C-z | 1.75 | .26 | 0 | 0.1379 | 0.24 |
| | | | | | 30 | 0.1379 | 0.24 |
| | | | | | 635 | 0.1289 | 0.23 |
| | | | | | 807 | 0.1279 | 0.22 |
| | | | | | 1009 | 0.1250 | 0.22 |
| | | | | | 8109 | 0.0409 | 0.07 |

TABLE A.1. (cont)

| Sample | Depth (ft) | Unit | Bulk Density (g/cm$^3$) | Porosity | Head (m) | Water Content g/g | Water Content vol/vol |
|---|---|---|---|---|---|---|---|
| G4-15c | 1769 | IV-C-z | 1.74 | .27 | 0 | 0.1391 | 0.24 |
| | | | | | 28 | 0.1391 | 0.24 |
| | | | | | 811 | 0.1305 | 0.23 |
| | | | | | 927 | 0.1297 | 0.23 |
| | | | | | 1149 | 0.1259 | 0.22 |
| | | | | | 8109 | 0.0391 | 0.07 |
| G4-16a | 1778 | IV-C-z | 1.75 | .24 | 0 | 0.1480 | 0.26 |
| | | | | | 7 | 0.1480 | 0.26 |
| | | | | | 60 | 0.1293 | 0.23 |
| | | | | | 280 | 0.1159 | 0.20 |
| | | | | | 500 | 0.1057 | 0.18 |
| | | | | | 792 | 0.0962 | 0.17 |
| | | | | | 844 | 0.0810 | 0.14 |
| | | | | | 889 | 0.0760 | 0.13 |
| | | | | | 1068 | 0.0734 | 0.13 |
| | | | | | 1290 | 0.0663 | 0.12 |
| | | | | | 1953 | 0.0583 | 0.10 |
| | | | | | 3558 | 0.0541 | 0.09 |
| | | | | | 8109 | 0.0362 | 0.06 |
| G4-16b | 1778 | IV-C-z | 1.69 | .27 | 0 | 0.1673 | 0.28 |
| | | | | | 4 | 0.1673 | 0.28 |
| | | | | | 62 | 0.1506 | 0.25 |
| | | | | | 213 | 0.1255 | 0.21 |
| | | | | | 478 | 0.1151 | 0.19 |
| | | | | | 578 | 0.1001 | 0.17 |
| | | | | | 732 | 0.0909 | 0.15 |
| | | | | | 933 | 0.0828 | 0.14 |
| | | | | | 1220 | 0.0745 | 0.13 |
| | | | | | 1413 | 0.0709 | 0.12 |
| | | | | | 2081 | 0.0584 | 0.10 |
| | | | | | 8109 | 0.0383 | 0.06 |
| G4-16c | 1778 | IV-C-z | 1.78 | .23 | 0 | 0.1499 | 0.27 |
| | | | | | 9 | 0.1499 | 0.27 |
| | | | | | 93 | 0.1351 | 0.24 |
| | | | | | 344 | 0.1114 | 0.20 |
| | | | | | 521 | 0.1038 | 0.18 |
| | | | | | 654 | 0.0940 | 0.17 |
| | | | | | 811 | 0.0836 | 0.15 |
| | | | | | 1047 | 0.0716 | 0.13 |
| | | | | | 1164 | 0.0687 | 0.12 |
| | | | | | 1312 | 0.0654 | 0.12 |
| | | | | | 1514 | 0.0623 | 0.11 |
| | | | | | 2171 | 0.0559 | 0.10 |
| | | | | | 2416 | 0.0531 | 0.09 |
| | | | | | 8109 | 0.0337 | 0.06 |
| G4-5Fa | 1778 | IV-C-z | 1.67 | .28 | 0 | 0.1711 | 0.29 |
| | | | | | 9 | 0.1711 | 0.29 |
| | | | | | 445 | 0.1552 | 0.26 |
| | | | | | 611 | 0.1457 | 0.24 |
| | | | | | 652 | 0.1363 | 0.23 |
| | | | | | 870 | 0.1203 | 0.20 |
| | | | | | 959 | 0.0994 | 0.17 |
| | | | | | 1047 | 0.0951 | 0.17 |
| | | | | | 1145 | 0.0834 | 0.15 |
| | | | | | 1315 | 0.0750 | 0.12 |
| | | | | | 1392 | 0.0679 | 0.11 |
| | | | | | 1574 | 0.0622 | 0.10 |
| | | | | | 2240 | 0.0534 | 0.09 |
| | | | | | 2382 | 0.0428 | 0.07 |
| | | | | | 9027 | 0.0361 | 0.06 |

TABLE A.1. (cont)

| Sample | Depth (ft) | Unit | Bulk Density (g/cm$^3$) | Porosity | Head (m) | Water Content g/g | Water Content vol/vol |
|---|---|---|---|---|---|---|---|
| G4-5Fb | 1778 | IV-C-z | 1.65 | .29 | 0 | 0.1623 | 0.27 |
| | | | | | 10 | 0.1623 | 0.27 |
| | | | | | 540 | 0.1463 | 0.24 |
| | | | | | 636 | 0.1372 | 0.23 |
| | | | | | 717 | 0.1290 | 0.21 |
| | | | | | 927 | 0.1144 | 0.19 |
| | | | | | 957 | 0.1047 | 0.17 |
| | | | | | 1029 | 0.0943 | 0.16 |
| | | | | | 1384 | 0.0715 | 0.12 |
| | | | | | 1909 | 0.0642 | 0.11 |
| | | | | | 2084 | 0.0388 | 0.06 |
| | | | | | 9027 | 0.0317 | 0.05 |
| G4-5Fc | 1778 | IV-C-z | 1.67 | .28 | 0 | 0.1686 | 0.28 |
| | | | | | 4 | 0.1686 | 0.28 |
| | | | | | 451 | 0.1500 | 0.25 |
| | | | | | 562 | 0.1403 | 0.23 |
| | | | | | 686 | 0.1308 | 0.22 |
| | | | | | 1000 | 0.1040 | 0.17 |
| | | | | | 1081 | 0.0788 | 0.13 |
| | | | | | 1362 | 0.0632 | 0.11 |
| | | | | | 1600 | 0.0563 | 0.09 |
| | | | | | 1947 | 0.0492 | 0.08 |
| | | | | | 2254 | 0.0395 | 0.07 |
| | | | | | 9027 | 0.0352 | 0.06 |
| G4-17a | 1787 | IV-C-z | 1.64 | .29 | 0 | 0.1815 | 0.30 |
| | | | | | 5 | 0.1815 | 0.30 |
| | | | | | 265 | 0.1429 | 0.24 |
| | | | | | 494 | 0.1278 | 0.21 |
| | | | | | 699 | 0.1091 | 0.18 |
| | | | | | 836 | 0.0915 | 0.15 |
| | | | | | 1028 | 0.0818 | 0.14 |
| | | | | | 1346 | 0.0723 | 0.12 |
| | | | | | 10200 | 0.0361 | 0.06 |
| G4-17b | 1787 | IV-C-z | 1.71 | .26 | 0 | 0.1573 | 0.27 |
| | | | | | 3 | 0.1573 | 0.27 |
| | | | | | 464 | 0.1297 | 0.22 |
| | | | | | 648 | 0.1136 | 0.19 |
| | | | | | 838 | 0.1016 | 0.17 |
| | | | | | 939 | 0.0837 | 0.14 |
| | | | | | 1055 | 0.0741 | 0.13 |
| | | | | | 1464 | 0.0673 | 0.12 |
| | | | | | 3192 | 0.0365 | 0.06 |
| | | | | | 10200 | 0.0282 | 0.05 |
| G4-17c | 1787 | IV-C-z | 1.63 | .30 | 0 | 0.1887 | 0.31 |
| | | | | | 3 | 0.1887 | 0.31 |
| | | | | | 168 | 0.1425 | 0.23 |
| | | | | | 365 | 0.1341 | 0.22 |
| | | | | | 490 | 0.1147 | 0.19 |
| | | | | | 903 | 0.0883 | 0.14 |
| | | | | | 997 | 0.0752 | 0.12 |
| | | | | | 1291 | 0.0661 | 0.11 |
| | | | | | 2806 | 0.0315 | 0.05 |
| | | | | | 10200 | 0.0214 | 0.04 |
| G4-18a | 1899 | V | 1.94 | .25 | 0 | 0.1224 | 0.24 |
| | | | | | 2 | 0.1224 | 0.24 |
| | | | | | 37 | 0.1096 | 0.21 |
| | | | | | 75 | 0.0872 | 0.17 |
| | | | | | 126 | 0.0332 | 0.06 |
| | | | | | 144 | 0.0270 | 0.05 |
| | | | | | 339 | 0.0211 | 0.04 |
| | | | | | 385 | 0.0178 | 0.03 |
| | | | | | 666 | 0.0145 | 0.03 |
| | | | | | 987 | 0.0115 | 0.02 |
| | | | | | 1407 | 0.0089 | 0.02 |
| | | | | | 8109 | 0.0026 | 0.01 |

TABLE A.1. (cont)

| Sample | Depth (ft) | Unit | Bulk Density (g/cm³) | Porosity | Head (m) | Water Content g/g | Water Content vol/vol |
|---|---|---|---|---|---|---|---|
| G4-18b | 1899 | V | 2.02 | .22 | 0 | 0.1049 | 0.21 |
| | | | | | 3 | 0.1049 | 0.21 |
| | | | | | 32 | 0.0929 | 0.19 |
| | | | | | 77 | 0.0709 | 0.14 |
| | | | | | 178 | 0.0240 | 0.05 |
| | | | | | 301 | 0.0196 | 0.04 |
| | | | | | 694 | 0.0124 | 0.03 |
| | | | | | 989 | 0.0105 | 0.02 |
| | | | | | 1504 | 0.0073 | 0.02 |
| | | | | | 1935 | 0.0064 | 0.01 |
| | | | | | 8109 | 0.0017 | 0.003 |
| G4-18c | 1899 | V | 1.94 | .25 | 0 | 0.1218 | 0.24 |
| | | | | | 4 | 0.1218 | 0.24 |
| | | | | | 36 | 0.1007 | 0.20 |
| | | | | | 82 | 0.0858 | 0.17 |
| | | | | | 307 | 0.0225 | 0.04 |
| | | | | | 359 | 0.0187 | 0.04 |
| | | | | | 527 | 0.0151 | 0.03 |
| | | | | | 741 | 0.0128 | 0.02 |
| | | | | | 935 | 0.0104 | 0.02 |
| | | | | | 2084 | 0.0083 | 0.02 |
| | | | | | 2268 | 0.0070 | 0.01 |
| | | | | | 8109 | 0.0023 | 0.01 |
| G4-19a | 2006 | VI | 1.60 | .30 | 0 | 0.1996 | 0.32 |
| | | | | | 2 | 0.1996 | 0.32 |
| | | | | | 117 | 0.1818 | 0.29 |
| | | | | | 386 | 0.1483 | 0.24 |
| | | | | | 585 | 0.1175 | 0.19 |
| | | | | | 665 | 0.1011 | 0.16 |
| | | | | | 719 | 0.0808 | 0.13 |
| | | | | | 1072 | 0.0723 | 0.12 |
| | | | | | 1275 | 0.0609 | 0.10 |
| | | | | | 2150 | 0.0569 | 0.09 |
| | | | | | 3686 | 0.0450 | 0.07 |
| | | | | | 8109 | 0.0364 | 0.06 |
| G4-19b | 2006 | VI | 1.61 | .30 | 0 | 0.1959 | 0.32 |
| | | | | | 8 | 0.1959 | 0.32 |
| | | | | | 91 | 0.1786 | 0.29 |
| | | | | | 379 | 0.1431 | 0.23 |
| | | | | | 666 | 0.1122 | 0.18 |
| | | | | | 798 | 0.0960 | 0.15 |
| | | | | | 887 | 0.0781 | 0.13 |
| | | | | | 931 | 0.0694 | 0.11 |
| | | | | | 1550 | 0.0599 | 0.10 |
| | | | | | 1791 | 0.0554 | 0.09 |
| | | | | | 2760 | 0.0467 | 0.08 |
| | | | | | 8109 | 0.0356 | 0.06 |
| G4-19c | 2006 | VI | 1.69 | .26 | 0 | 0.1729 | 0.29 |
| | | | | | 2 | 0.1729 | 0.29 |
| | | | | | 85 | 0.1579 | 0.27 |
| | | | | | 280 | 0.1288 | 0.22 |
| | | | | | 428 | 0.1027 | 0.17 |
| | | | | | 726 | 0.0875 | 0.15 |
| | | | | | 907 | 0.0681 | 0.12 |
| | | | | | 1393 | 0.0524 | 0.09 |
| | | | | | 1669 | 0.0459 | 0.08 |
| | | | | | 2459 | 0.0374 | 0.06 |
| | | | | | 8109 | 0.0277 | 0.05 |
| G4-20a | 2101 | VI | 1.76 | .21 | 0 | 0.1143 | 0.20 |
| | | | | | 28 | 0.1143 | 0.20 |
| | | | | | 336 | 0.0978 | 0.17 |
| | | | | | 408 | 0.0879 | 0.15 |
| | | | | | 513 | 0.0790 | 0.14 |
| | | | | | 597 | 0.0759 | 0.13 |
| | | | | | 666 | 0.0723 | 0.13 |
| | | | | | 903 | 0.0688 | 0.12 |
| | | | | | 1073 | 0.0676 | 0.12 |
| | | | | | 1422 | 0.0614 | 0.11 |
| | | | | | 8109 | 0.0473 | 0.08 |

TABLE A.1. (cont)

| Sample | Depth (ft) | Unit | Bulk Density (g/cm³) | Porosity | Head (m) | Water Content g/g | Water Content vol/vol |
|---|---|---|---|---|---|---|---|
| G4-20b | 2101 | VI | 1.85 | .17 | 0 | 0.1173 | 0.22 |
| | | | | | 28 | 0.1173 | 0.22 |
| | | | | | 253 | 0.0976 | 0.18 |
| | | | | | 360 | 0.0832 | 0.15 |
| | | | | | 447 | 0.0766 | 0.14 |
| | | | | | 514 | 0.0677 | 0.13 |
| | | | | | 606 | 0.0586 | 0.11 |
| | | | | | 720 | 0.0564 | 0.10 |
| | | | | | 1123 | 0.0532 | 0.10 |
| | | | | | 1669 | 0.0481 | 0.09 |
| | | | | | 8109 | 0.0387 | 0.07 |
| G4-20c | 2101 | VI | 1.82 | .19 | 0 | 0.1198 | 0.22 |
| | | | | | 8 | 0.1198 | 0.22 |
| | | | | | 154 | 0.1006 | 0.18 |
| | | | | | 238 | 0.0931 | 0.17 |
| | | | | | 294 | 0.0847 | 0.15 |
| | | | | | 376 | 0.0728 | 0.13 |
| | | | | | 460 | 0.0682 | 0.12 |
| | | | | | 557 | 0.0620 | 0.11 |
| | | | | | 864 | 0.0576 | 0.10 |
| | | | | | 956 | 0.0552 | 0.10 |
| | | | | | 1311 | 0.0525 | 0.10 |
| | | | | | 1655 | 0.0471 | 0.09 |
| | | | | | 8109 | 0.0376 | 0.07 |
| G4-21a | 2401 | VII | 2.00 | .24 | 0 | 0.1156 | 0.23 |
| | | | | | 20 | 0.1156 | 0.23 |
| | | | | | 38 | 0.1025 | 0.21 |
| | | | | | 77 | 0.0925 | 0.19 |
| | | | | | 132 | 0.0276 | 0.06 |
| | | | | | 211 | 0.0202 | 0.04 |
| | | | | | 303 | 0.0157 | 0.03 |
| | | | | | 509 | 0.0121 | 0.02 |
| | | | | | 801 | 0.0076 | 0.02 |
| | | | | | 1023 | 0.0061 | 0.01 |
| | | | | | 1407 | 0.0053 | 0.01 |
| | | | | | 8109 | 0.0032 | 0.01 |
| G4-21b | 2401 | VII | 1.97 | .25 | 0 | 0.1250 | 0.25 |
| | | | | | 21 | 0.1250 | 0.25 |
| | | | | | 49 | 0.1112 | 0.22 |
| | | | | | 141 | 0.0262 | 0.05 |
| | | | | | 256 | 0.0183 | 0.04 |
| | | | | | 351 | 0.0132 | 0.03 |
| | | | | | 641 | 0.0094 | 0.02 |
| | | | | | 820 | 0.0072 | 0.01 |
| | | | | | 1159 | 0.0061 | 0.01 |
| | | | | | 1252 | 0.0047 | 0.01 |
| | | | | | 1517 | 0.0040 | 0.01 |
| | | | | | 8109 | 0.0026 | 0.01 |
| G4-21c | 2401 | VII | 1.97 | .25 | 0 | 0.1177 | 0.23 |
| | | | | | 15 | 0.1177 | 0.23 |
| | | | | | 58 | 0.1101 | 0.21 |
| | | | | | 196 | 0.0196 | 0.04 |
| | | | | | 469 | 0.0114 | 0.02 |
| | | | | | 573 | 0.0086 | 0.02 |
| | | | | | 650 | 0.0070 | 0.01 |
| | | | | | 1355 | 0.0056 | 0.01 |
| | | | | | 1892 | 0.0049 | 0.01 |
| | | | | | 8109 | 0.0033 | 0.01 |
| G4-22a | 2407 | VII | 1.92 | .27 | 0 | 0.1215 | 0.23 |
| | | | | | 10 | 0.1215 | 0.23 |
| | | | | | 71 | 0.0425 | 0.08 |
| | | | | | 151 | 0.0276 | 0.05 |
| | | | | | 240 | 0.0217 | 0.04 |
| | | | | | 510 | 0.0145 | 0.03 |
| | | | | | 806 | 0.0119 | 0.02 |
| | | | | | 996 | 0.0088 | 0.02 |
| | | | | | 1664 | 0.0072 | 0.01 |
| | | | | | 8109 | 0.0016 | 0.01 |

TABLE A.1. (cont)

| Sample | Depth (ft) | Unit | Bulk Density (g/cm³) | Porosity | Head (m) | Water Content g/g | Water Content vol/vol |
|---|---|---|---|---|---|---|---|
| G4-22b | 2407 | VII | 1.93 | .27 | 0 | 0.1202 | 0.23 |
| | | | | | 10 | 0.1202 | 0.23 |
| | | | | | 86 | 0.0356 | 0.07 |
| | | | | | 210 | 0.0231 | 0.05 |
| | | | | | 422 | 0.0186 | 0.04 |
| | | | | | 557 | 0.0163 | 0.03 |
| | | | | | 765 | 0.0101 | 0.02 |
| | | | | | 1248 | 0.0087 | 0.02 |
| | | | | | 2080 | 0.0069 | 0.01 |
| | | | | | 8109 | 0.0021 | 0.01 |
| G4-22c | 2407 | VII | 1.92 | .27 | 0 | 0.1305 | 0.25 |
| | | | | | 15 | 0.1305 | 0.25 |
| | | | | | 138 | 0.0231 | 0.04 |
| | | | | | 277 | 0.0181 | 0.03 |
| | | | | | 464 | 0.0124 | 0.02 |
| | | | | | 592 | 0.0086 | 0.02 |
| | | | | | 979 | 0.0064 | 0.01 |
| | | | | | 1446 | 0.0050 | 0.01 |
| | | | | | 2256 | 0.0045 | 0.01 |
| | | | | | 8109 | 0.0027 | 0.01 |
| G4-23a | | Commercial Clinoptilolite | 1.60 | .37 | 0 | 0.1824 | 0.29 |
| | | | | | 6 | 0.1824 | 0.29 |
| | | | | | 61 | 0.1481 | 0.24 |
| | | | | | 142 | 0.1349 | 0.22 |
| | | | | | 241 | 0.1261 | 0.20 |
| | | | | | 432 | 0.1070 | 0.17 |
| | | | | | 700 | 0.0870 | 0.14 |
| | | | | | 1116 | 0.0799 | 0.13 |
| | | | | | 1472 | 0.0740 | 0.12 |
| | | | | | 2829 | 0.0695 | 0.11 |
| | | | | | 8109 | 0.0565 | 0.09 |
| G4-23b | | Commercial Clinoptilolite | 1.50 | .41 | 0 | 0.1600 | 0.24 |
| | | | | | 15 | 0.1600 | 0.24 |
| | | | | | 76 | 0.1361 | 0.20 |
| | | | | | 247 | 0.1361 | 0.16 |
| | | | | | 472 | 0.0973 | 0.15 |
| | | | | | 627 | 0.0890 | 0.13 |
| | | | | | 1088 | 0.0818 | 0.12 |
| | | | | | 1367 | 0.0745 | 0.11 |
| | | | | | 2191 | 0.0631 | 0.09 |
| | | | | | 3369 | 0.0620 | 0.09 |
| | | | | | 8109 | 0.0585 | 0.09 |
| G4-23c | | Commercial Clinoptilolite | 1.46 | .42 | 0 | 0.2284 | 0.33 |
| | | | | | 15 | 0.2284 | 0.33 |
| | | | | | 76 | 0.2041 | 0.30 |
| | | | | | 115 | 0.1649 | 0.24 |
| | | | | | 209 | 0.1517 | 0.22 |
| | | | | | 277 | 0.1412 | 0.21 |
| | | | | | 464 | 0.1141 | 0.17 |
| | | | | | 580 | 0.1048 | 0.15 |
| | | | | | 1239 | 0.0899 | 0.13 |
| | | | | | 2866 | 0.0827 | 0.12 |
| | | | | | 8109 | 0.0592 | 0.09 |
| GU3-1a | 82 | I-A | 2.11 | .15 | 0 | 0.0594 | 0.13 |
| | | | | | 9 | 0.0594 | 0.13 |
| | | | | | 38 | 0.0509 | 0.11 |
| | | | | | 94 | 0.0251 | 0.05 |
| | | | | | 123 | 0.0219 | 0.05 |
| | | | | | 181 | 0.0196 | 0.04 |
| | | | | | 359 | 0.0178 | 0.04 |
| | | | | | 514 | 0.0151 | 0.03 |
| | | | | | 592 | 0.0133 | 0.03 |
| | | | | | 803 | 0.0116 | 0.02 |
| | | | | | 1200 | 0.0107 | 0.02 |
| | | | | | 9180 | 0.0003 | 0.001 |

TABLE A.1. (cont)

| Sample | Depth (ft) | Unit | Bulk Density (g/cm³) | Porosity | Head (m) | Water Content g/g | Water Content vol/vol |
|---|---|---|---|---|---|---|---|
| GU3-1b | 82 | I-A | 2.11 | .15 | 0 | 0.0604 | 0.13 |
| | | | | | 36 | 0.0604 | 0.13 |
| | | | | | 60 | 0.0443 | 0.09 |
| | | | | | 80 | 0.0293 | 0.06 |
| | | | | | 158 | 0.0249 | 0.05 |
| | | | | | 244 | 0.0226 | 0.05 |
| | | | | | 392 | 0.0198 | 0.04 |
| | | | | | 512 | 0.0184 | 0.04 |
| | | | | | 567 | 0.0160 | 0.03 |
| | | | | | 2557 | 0.0060 | 0.01 |
| | | | | | 9180 | 0.0003 | 0.001 |
| GU3-2a | 121 | I-A | 2.16 | .13 | 0 | 0.0404 | 0.09 |
| | | | | | 24 | 0.0404 | 0.09 |
| | | | | | 47 | 0.0373 | 0.08 |
| | | | | | 89 | 0.0328 | 0.07 |
| | | | | | 214 | 0.0280 | 0.06 |
| | | | | | 371 | 0.0234 | 0.05 |
| | | | | | 714 | 0.0178 | 0.04 |
| | | | | | 1877 | 0.0099 | 0.02 |
| | | | | | 2265 | 0.0005 | 0.01 |
| GU3-2b | 121 | I-A | 2.14 | .14 | 0 | 0.0420 | 0.09 |
| | | | | | 20 | 0.0420 | 0.09 |
| | | | | | 36 | 0.0314 | 0.07 |
| | | | | | 107 | 0.0278 | 0.06 |
| | | | | | 271 | 0.0242 | 0.05 |
| | | | | | 349 | 0.0214 | 0.05 |
| | | | | | 701 | 0.0066 | 0.01 |
| | | | | | 721 | 0.0011 | 0.01 |
| | | | | | 969 | 0.0005 | 0.01 |
| GU3-3a | 155 | I-A | 2.31 | .071 | 0 | 0.0135 | 0.03 |
| | | | | | 68 | 0.0135 | 0.03 |
| | | | | | 121 | 0.0122 | 0.03 |
| | | | | | 211 | 0.0105 | 0.02 |
| | | | | | 331 | 0.0082 | 0.02 |
| | | | | | 859 | 0.0040 | 0.01 |
| | | | | | 2279 | 0.0018 | 0.01 |
| GU3-3b | 155 | I-A | 2.22 | .11 | 0 | 0.0208 | 0.05 |
| | | | | | 101 | 0.0208 | 0.05 |
| | | | | | 172 | 0.0183 | 0.04 |
| | | | | | 317 | 0.0143 | 0.03 |
| | | | | | 933 | 0.0097 | 0.02 |
| | | | | | 2294 | 0.0061 | 0.01 |
| GU3-4a | 257 | I-A | 2.33 | .065 | 0 | 0.0255 | 0.06 |
| | | | | | 15 | 0.0255 | 0.06 |
| | | | | | 94 | 0.0182 | 0.04 |
| | | | | | 209 | 0.0160 | 0.04 |
| | | | | | 260 | 0.0130 | 0.03 |
| | | | | | 352 | 0.0128 | 0.03 |
| | | | | | 520 | 0.0114 | 0.03 |
| | | | | | 630 | 0.0088 | 0.02 |
| | | | | | 1115 | 0.0046 | 0.01 |
| | | | | | 9180 | 0.0029 | 0.01 |
| GU3-4b | 257 | I-A | 2.33 | .065 | 0 | 0.0287 | 0.07 |
| | | | | | 13 | 0.0287 | 0.07 |
| | | | | | 69 | 0.0175 | 0.04 |
| | | | | | 274 | 0.0152 | 0.04 |
| | | | | | 359 | 0.0117 | 0.03 |
| | | | | | 467 | 0.0106 | 0.02 |
| | | | | | 510 | 0.0066 | 0.02 |
| | | | | | 1085 | 0.0028 | 0.003 |

TABLE A.1. (cont)

| Sample | Depth (ft) | Unit | Bulk Density (g/cm$^3$) | Porosity | Head (m) | Water Content g/g | Water Content vol/vol |
|---|---|---|---|---|---|---|---|
| GU3-5a | 316 | I-A | 2.26 | .089 | 0 | 0.0298 | 0.07 |
| | | | | | 84 | 0.0246 | 0.06 |
| | | | | | 114 | 0.0209 | 0.05 |
| | | | | | 225 | 0.0147 | 0.03 |
| | | | | | 268 | 0.0129 | 0.03 |
| | | | | | 512 | 0.0112 | 0.03 |
| | | | | | 630 | 0.0102 | 0.03 |
| | | | | | 714 | 0.0093 | 0.02 |
| | | | | | 1204 | 0.0090 | 0.02 |
| | | | | | 1358 | 0.0076 | 0.02 |
| | | | | | 9180 | 0.0011 | 0.01 |
| GU3-5b | 316 | I-A | 2.27 | .085 | 0 | 0.0306 | 0.07 |
| | | | | | 19 | 0.0306 | 0.07 |
| | | | | | 55 | 0.0273 | 0.06 |
| | | | | | 105 | 0.0206 | 0.05 |
| | | | | | 301 | 0.0137 | 0.03 |
| | | | | | 466 | 0.0130 | 0.03 |
| | | | | | 512 | 0.0120 | 0.03 |
| | | | | | 793 | 0.0101 | 0.02 |
| | | | | | 1168 | 0.0090 | 0.02 |
| | | | | | 1871 | 0.0074 | 0.02 |
| | | | | | 1938 | 0.0069 | 0.02 |
| | | | | | 9180 | 0.0011 | 0.003 |
| GU3-6a | 374 | I-B | 1.00 | .59 | 0 | 0.3807 | 0.38 |
| | | | | | 39 | 0.3807 | 0.38 |
| | | | | | 196 | 0.0880 | 0.09 |
| | | | | | 403 | 0.0750 | 0.08 |
| | | | | | 455 | 0.0616 | 0.06 |
| | | | | | 562 | 0.0475 | 0.05 |
| | | | | | 1178 | 0.0342 | 0.03 |
| | | | | | 9180 | 0.0107 | 0.01 |
| GU3-6b | 374 | I-B | 1.00 | .59 | 0 | 0.3904 | 0.39 |
| | | | | | 24 | 0.3904 | 0.39 |
| | | | | | 53 | 0.2855 | 0.29 |
| | | | | | 171 | 0.1074 | 0.11 |
| | | | | | 435 | 0.0783 | 0.08 |
| | | | | | 995 | 0.0428 | 0.04 |
| | | | | | 1518 | 0.0428 | 0.03 |
| | | | | | 9180 | 0.0113 | 0.01 |
| GU3-7a | 378 | I-B | 1.48 | .37 | 0 | 0.2560 | 0.38 |
| | | | | | 47 | 0.2560 | 0.38 |
| | | | | | 58 | 0.1763 | 0.26 |
| | | | | | 65 | 0.1441 | 0.21 |
| | | | | | 84 | 0.0932 | 0.14 |
| | | | | | 425 | 0.0570 | 0.08 |
| | | | | | 788 | 0.0450 | 0.07 |
| | | | | | 1511 | 0.0027 | 0.004 |
| | | | | | 8160 | 0.0015 | 0.002 |
| GU3-7b | 378 | I-B | 1.36 | .42 | 0 | 0.3209 | 0.44 |
| | | | | | 36 | 0.3209 | 0.44 |
| | | | | | 61 | 0.2731 | 0.37 |
| | | | | | 72 | 0.1816 | 0.25 |
| | | | | | 73 | 0.1073 | 0.15 |
| | | | | | 745 | 0.0495 | 0.07 |
| | | | | | 2713 | 0.0038 | 0.01 |
| GU3-8a | 397 | I-B | 1.42 | .42 | 0 | 0.2998 | 0.43 |
| | | | | | 10 | 0.2998 | 0.43 |
| | | | | | 80 | 0.2441 | 0.35 |
| | | | | | 103 | 0.1096 | 0.16 |
| | | | | | 822 | 0.0526 | 0.07 |
| | | | | | 2189 | 0.0378 | 0.05 |
| | | | | | 3896 | 0.0339 | 0.05 |
| | | | | | 8402 | 0.0281 | 0.04 |
| | | | | | 9180 | 0.0166 | 0.02 |

TABLE A.1. (cont)

| Sample | Depth (ft) | Unit | Bulk Density (g/cm³) | Porosity | Head (m) | Water Content g/g | Water Content vol/vol |
|---|---|---|---|---|---|---|---|
| GU3-8b | 397 | I-B | 1.34 | .45 | 0 | 0.3239 | 0.43 |
| | | | | | 30 | 0.3239 | 0.43 |
| | | | | | 119 | 0.0740 | 0.10 |
| | | | | | 520 | 0.0604 | 0.08 |
| | | | | | 859 | 0.0518 | 0.07 |
| | | | | | 1425 | 0.0358 | 0.05 |
| | | | | | 9180 | 0.0014 | 0.002 |
| GU3-9a | 1132 | II-NL | 2.33 | .082 | 0 | 0.0304 | 0.07 |
| | | | | | 5 | 0.0304 | 0.07 |
| | | | | | 101 | 0.0212 | 0.05 |
| | | | | | 186 | 0.0185 | 0.04 |
| | | | | | 395 | 0.0166 | 0.04 |
| | | | | | 475 | 0.0152 | 0.04 |
| | | | | | 527 | 0.0134 | 0.03 |
| | | | | | 631 | 0.0103 | 0.02 |
| | | | | | 877 | 0.0096 | 0.02 |
| | | | | | 921 | 0.0080 | 0.02 |
| | | | | | 1109 | 0.0064 | 0.02 |
| | | | | | 9180 | 0.0020 | 0.005 |
| GU3-9b | 1132 | II-NL | 2.33 | .082 | 0 | 0.0298 | 0.07 |
| | | | | | 7 | 0.0298 | 0.07 |
| | | | | | 76 | 0.0215 | 0.05 |
| | | | | | 250 | 0.0184 | 0.04 |
| | | | | | 514 | 0.0156 | 0.04 |
| | | | | | 640 | 0.0100 | 0.02 |
| | | | | | 778 | 0.0092 | 0.02 |
| | | | | | 900 | 0.0087 | 0.02 |
| | | | | | 1056 | 0.0074 | 0.02 |
| | | | | | 1331 | 0.0058 | 0.01 |
| GU3-10a | 1197 | III | 2.33 | .026 | 0 | 0.0110 | 0.03 |
| | | | | | 35 | 0.0110 | 0.03 |
| | | | | | 179 | 0.0102 | 0.02 |
| | | | | | 302 | 0.0089 | 0.02 |
| | | | | | 306 | 0.0085 | 0.02 |
| | | | | | 361 | 0.0081 | 0.02 |
| | | | | | 413 | 0.0064 | 0.02 |
| | | | | | 683 | 0.0055 | 0.01 |
| | | | | | 2382 | 0.0050 | 0.01 |
| GU3-10b | 1197 | III | 2.34 | .021 | 0 | 0.0094 | 0.02 |
| | | | | | 82 | 0.0094 | 0.02 |
| | | | | | 227 | 0.0082 | 0.02 |
| | | | | | 306 | 0.0070 | 0.02 |
| | | | | | 322 | 0.0064 | 0.02 |
| | | | | | 323 | 0.0061 | 0.01 |
| | | | | | 416 | 0.0048 | 0.01 |
| | | | | | 537 | 0.0039 | 0.01 |
| | | | | | 2708 | 0.0032 | 0.01 |
| | | | | | 8190 | 0.0030 | 0.01 |
| GU3-11a | 1246 | III | 2.22 | .066 | 0 | 0.0121 | 0.03 |
| | | | | | 9 | 0.0121 | 0.03 |
| | | | | | 218 | 0.0091 | 0.02 |
| | | | | | 267 | 0.0081 | 0.02 |
| | | | | | 363 | 0.0055 | 0.01 |
| | | | | | 423 | 0.0043 | 0.01 |
| | | | | | 554 | 0.0038 | 0.01 |
| | | | | | 724 | 0.0036 | 0.01 |
| | | | | | 1146 | 0.0030 | 0.01 |
| | | | | | 3055 | 0.0029 | 0.006 |
| | | | | | 9180 | 0.0007 | 0.002 |
| GU3-11b | 1246 | III | 2.20 | .074 | 0 | 0.0201 | 0.04 |
| | | | | | 10 | 0.0201 | 0.04 |
| | | | | | 212 | 0.0165 | 0.04 |
| | | | | | 385 | 0.0129 | 0.03 |
| | | | | | 593 | 0.0118 | 0.03 |
| | | | | | 661 | 0.0063 | 0.01 |
| | | | | | 1060 | 0.0056 | 0.01 |
| | | | | | 1765 | 0.0043 | 0.01 |
| | | | | | 9180 | 0.0007 | 0.002 |

TABLE A.1. (cont)

| Sample | Depth (ft) | Unit | Bulk Density (g/cm³) | Porosity | Head (m) | Water Content g/g | Water Content vol/vol |
|---|---|---|---|---|---|---|---|
| GU3-12a | 1311 | IV-A-v | 1.72 | .27 | 0 | 0.1359 | 0.23 |
| | | | | | 23 | 0.1359 | 0.23 |
| | | | | | 67 | 0.0601 | 0.10 |
| | | | | | 134 | 0.0411 | 0.07 |
| | | | | | 168 | 0.0155 | 0.03 |
| | | | | | 346 | 0.0107 | 0.02 |
| | | | | | 1867 | 0.0065 | 0.01 |
| | | | | | 9180 | 0.0038 | 0.01 |
| GU3-12b | 1311 | IV-A-v | 1.37 | .42 | 0 | 0.2885 | 0.40 |
| | | | | | 19 | 0.2885 | 0.40 |
| | | | | | 58 | 0.2136 | 0.29 |
| | | | | | 94 | 0.0739 | 0.10 |
| | | | | | 158 | 0.0462 | 0.06 |
| | | | | | 227 | 0.0281 | 0.04 |
| | | | | | 1800 | 0.0236 | 0.03 |
| | | | | | 2243 | 0.0083 | 0.01 |
| | | | | | 9180 | 0.0020 | 0.003 |
| GU3-13a | 1331 | IV-A-v | 1.29 | .45 | 0 | 0.1929 | 0.25 |
| | | | | | 26 | 0.1929 | 0.25 |
| | | | | | 239 | 0.0192 | 0.02 |
| | | | | | 2179 | 0.0145 | 0.02 |
| | | | | | 8190 | 0.0024 | 0.003 |
| GU3-13b | 1331 | IV-A-v | 1.29 | .45 | 0 | 0.2009 | 0.26 |
| | | | | | 28 | 0.2009 | 0.26 |
| | | | | | 899 | 0.0197 | 0.03 |
| | | | | | 3713 | 0.0087 | 0.01 |
| | | | | | 8190 | 0.0025 | 0.003 |
| GU3-14a | 1440 | IV-A-v | 1.30 | .45 | 0 | 0.3185 | 0.41 |
| | | | | | 20 | 0.3185 | 0.41 |
| | | | | | 55 | 0.2355 | 0.31 |
| | | | | | 80 | 0.1069 | 0.14 |
| | | | | | 92 | 0.0750 | 0.10 |
| | | | | | 143 | 0.0620 | 0.08 |
| | | | | | 373 | 0.0280 | 0.04 |
| | | | | | 940 | 0.0180 | 0.02 |
| | | | | | 4436 | 0.0090 | 0.01 |
| | | | | | 8190 | 0.0040 | 0.005 |
| GU3-14b | 1440 | IV-A-v | 1.24 | .48 | 0 | 0.3850 | 0.48 |
| | | | | | 30 | 0.3850 | 0.48 |
| | | | | | 83 | 0.1818 | 0.23 |
| | | | | | 151 | 0.0590 | 0.07 |
| | | | | | 355 | 0.0240 | 0.03 |
| | | | | | 674 | 0.0160 | 0.02 |
| | | | | | 844 | 0.0060 | 0.01 |
| | | | | | 8160 | 0.0030 | 0.003 |
| GU3-15a | 1499 | IV-A-v | 1.33 | .43 | 0 | 0.2777 | 0.37 |
| | | | | | 15 | 0.2777 | 0.37 |
| | | | | | 162 | 0.0803 | 0.11 |
| | | | | | 298 | 0.0607 | 0.08 |
| | | | | | 672 | 0.0582 | 0.08 |
| | | | | | 1102 | 0.0494 | 0.07 |
| | | | | | 1457 | 0.0447 | 0.06 |
| | | | | | 1895 | 0.0406 | 0.05 |
| | | | | | 9180 | 0.0070 | 0.01 |
| GU3-15b | 1499 | IV-A-v | 1.33 | .43 | 0 | 0.3073 | 0.41 |
| | | | | | 10 | 0.3073 | 0.41 |
| | | | | | 40 | 0.1664 | 0.22 |
| | | | | | 117 | 0.1405 | 0.19 |
| | | | | | 247 | 0.1236 | 0.16 |
| | | | | | 731 | 0.1144 | 0.15 |
| | | | | | 2137 | 0.0238 | 0.03 |
| | | | | | 9180 | 0.0070 | 0.01 |

TABLE A.1. (cont)

| | | | | | | | |
|---|---|---|---|---|---|---|---|
| GU3-16a | 1555 | IV-B-v | 1.29 | .47 | 0 | 0.2814 | 0.36 |
| | | | | | 14 | 0.2814 | 0.36 |
| | | | | | 65 | 0.1722 | 0.38 |
| | | | | | 156 | 0.0944 | 0.12 |
| | | | | | 699 | 0.0463 | 0.06 |
| | | | | | 1209 | 0.0336 | 0.04 |
| GU3-16b | 1555 | IV-B-v | 1.29 | .47 | 0 | 0.2707 | 0.35 |
| | | | | | 52 | 0.2607 | 0.35 |
| | | | | | 64 | 0.1663 | 0.21 |
| | | | | | 76 | 0.0996 | 0.13 |
| | | | | | 1280 | 0.0347 | 0.04 |
| GU3-17a | 1628 | V | 1.57 | .39 | 0 | 0.2243 | 0.35 |
| | | | | | 31 | 0.2243 | 0.35 |
| | | | | | 63 | 0.2193 | 0.33 |
| | | | | | 207 | 0.0200 | 0.01 |
| | | | | | 592 | 0.0120 | 0.01 |
| | | | | | 1553 | 0.0080 | 0.01 |
| | | | | | 2740 | 0.0065 | 0.01 |
| | | | | | 4065 | 0.0060 | 0.01 |
| | | | | | 9180 | 0.0027 | 0.004 |
| GU3-17b | 1628 | V | 1.57 | .39 | 0 | 0.2392 | 0.38 |
| | | | | | 32 | 0.2392 | 0.38 |
| | | | | | 40 | 0.2263 | 0.36 |
| | | | | | 60 | 0.1729 | 0.27 |
| | | | | | 64 | 0.0583 | 0.09 |
| | | | | | 600 | 0.0054 | 0.01 |
| | | | | | 918 | 0.0035 | 0.01 |
| | | | | | 1254 | 0.0028 | 0.004 |
| | | | | | 9180 | 0.0007 | 0.001 |
| GU3-18a | 1680 | V | 1.73 | .33 | 0 | 0.1755 | 0.30 |
| | | | | | 12 | 0.1755 | 0.30 |
| | | | | | 21 | 0.1605 | 0.28 |
| | | | | | 25 | 0.1266 | 0.22 |
| | | | | | 46 | 0.0388 | 0.07 |
| | | | | | 53 | 0.0272 | 0.05 |
| | | | | | 156 | 0.0189 | 0.03 |
| | | | | | 260 | 0.0161 | 0.03 |
| | | | | | 470 | 0.0140 | 0.02 |
| | | | | | 516 | 0.0112 | 0.02 |
| | | | | | 1031 | 0.0096 | 0.02 |
| | | | | | 3284 | 2.83E-5 | 4.90E-5 |
| GU3-18b | 1680 | V | 1.76 | .31 | 0 | 0.1392 | 0.25 |
| | | | | | 19 | 0.1392 | 0.25 |
| | | | | | 54 | 0.0890 | 0.16 |
| | | | | | 76 | 0.0215 | 0.04 |
| | | | | | 158 | 0.0148 | 0.03 |
| | | | | | 356 | 0.0125 | 0.02 |
| | | | | | 580 | 0.0112 | 0.02 |
| | | | | | 670 | 0.0080 | 0.02 |
| | | | | | 813 | 0.0073 | 0.01 |
| | | | | | 1817 | 0.0060 | 0.01 |
| GU3-19a | 1730 | V | 1.91 | .24 | 0 | 0.1170 | 0.22 |
| | | | | | 20 | 0.1170 | 0.22 |
| | | | | | 100 | 0.0299 | 0.06 |
| | | | | | 194 | 0.0255 | 0.05 |
| | | | | | 378 | 0.0226 | 0.04 |
| | | | | | 538 | 0.0199 | 0.04 |
| | | | | | 672 | 0.0178 | 0.03 |
| | | | | | 944 | 0.0140 | 0.03 |
| | | | | | 1734 | 0.0106 | 0.02 |
| | | | | | 9180 | 0.0013 | 0.002 |
| GU3-19b | 1730 | V | 1.92 | .24 | 0 | 0.1152 | 0.22 |
| | | | | | 20 | 0.1152 | 0.22 |
| | | | | | 146 | 0.0283 | 0.05 |
| | | | | | 306 | 0.0242 | 0.05 |
| | | | | | 474 | 0.0219 | 0.04 |
| | | | | | 624 | 0.0196 | 0.04 |
| | | | | | 734 | 0.0179 | 0.03 |
| | | | | | 836 | 0.0171 | 0.03 |
| | | | | | 1049 | 0.0144 | 0.03 |
| | | | | | 1668 | 0.0117 | 0.02 |
| | | | | | 9180 | 0.0015 | 0.003 |

TABLE A.2. Properties for Samples Taken from USW G-4 and USW GU-3

| Sample Code | Depth (ft) | Unit | Grain Density (g/cm$^3$) | Porosity | Sat. Hydraulic Conductivity (m/s) | $S_r$ | Alpha (1/m) | Beta |
|---|---|---|---|---|---|---|---|---|
| G4-1 | 43 | I-A [a] | 2.49 | .08 [b] | 9.7E-12 | 0.0020 | 0.821E-02 | 1.558 |
| G4-2 | 124 | I-B [c] | 2.40 | .27 | 2.6E-11 - 2.9E-12 | 0.0400 | 0.305E-01 | 1.220 |
| G4-3 | 208 | I-B | 2.45 | .65 | 2.4E-6 | 0.1053 | 0.158E-01 | 10.563 |
| G4-4 | 247 | II-L | 2.57 [d] | .03 | 8.6E-13 | 0.0600 | 0.152E-01 | 1.400 |
| G4-5 | 864 (dark) | II-NL | 2.54 | .09 | 2.2E-11 - 1.3E-11 [e] | 0.0662 | 0.985E-02 | 1.561 |
| G4-24 | 864 (lt.) | II-NL | 2.47 | .16 | 3.9E-11 | 0.0578 | 0.119E-01 | 1.945 |
| G4-6 | 1158 | II-NL | 2.58 | .11 | 1.9E-11 | 0.0801 | 0.567E-02 | 1.798 |
| G4-1F | 1215 | II-NL | 2.58 [f] | .11 | 9.2E-12 - 3.8E-12 | 0.1199 | 0.602E-02 | 1.916 |
| G4-7 | 1256 | II-NL | 2.53 | .10 | <1.3E-11 [g] | 0.0704 | 0.258E-02 | 1.907 |
| G4-2F | 1278 | II-NL | 2.50 | .06 | 1.5E-11 - 1.3E-12 | 0.1198 | 0.372E-02 | 2.116 |
| G4-8 | 1299 | III | 2.50 | .09 | 4.5E-10 | 0.0517 | 0.419E-02 | 1.622 |
| G4-9 | 1324 | III | 2.37 | .04 | 3.0E-12 | 0.0026 | 0.169E-02 | 1.708 |
| G4-3F | 1359 | IV-A-v | 2.39 [h] | .21 | 8.0E-11 - 2.0E-11 | 0.1638 | 0.265E-01 | 2.223 |
| G4-10 | 1405 | IV-A-z | 2.35 [i] | .41 | 3.0E-12 | 0.0100 | 0.220E-01 | 1.236 |
| G4-11 | 1548 | IV-A-z | 2.23 | .28 | 2.0E-11 - 2.4E-14 | 0.1095 | 0.308E-02 | 1.602 |
| G4-4F | 1551 | IV-A-z | 2.37 [j] | .33 | 5.1E-11 - 1.3E-11 | 0.2017 | 0.415E-02 | 1.894 |

Notes: a) Mineralogical analyses indicate probable vapor-phase alteration of matrix.
b) Average value listed, see Table A.1 for values.
c) Mineralogical analyses indicate devitrified, nonwelded sample.
d) Value estimated based on grain density test of G-4 sample from 251 feet of depth.
e) If multiple tests were made, the range is indicated, see Table A.4.
f) Value estimated based on grain density test of G-4 sample from 1241 feet of depth.
g) Actual value below this limit.
h) Value estimated based on grain density test of G-4 sample from 1373 feet of depth.
i) Value estimated based on grain density test of G-4 sample from 1410 feet of depth.
j) Value estimated based on grain density test of G-4 sample from 1550 feet of depth.

TABLE A.2. (cont)

| Sample Code | Depth (ft) | Unit | Grain Density (g/cm$^3$) | Porosity | Sat. Hydraulic Conductivity (m/s) | $S_r$ | Alpha (1/m) | Beta |
|---|---|---|---|---|---|---|---|---|
| G4-12 | 1686 | IV-A-z | 2.25 | .30 | 4.24E-12 | 0.0600 | 0.600E-02 | 1.460 |
| G4-13 | 1728 | IV-B-z | 2.32 | .22 | 2.5E-11 - 4.7E-14 | 0.1500 | 0.158E-02 | 1.685 |
| G4-14 | 1737 | IV-B-z | 2.33 | .24 | 2.5E-11 - 4.6E-13 | 0.1000 | 0.370E-02 | 1.496 |
| G4-15 | 1769 | IV-C-z | 2.38 | .26 | 2.3E-12 | 0.2154 | 0.605E-03 | 2.487 |
| G4-16 | 1778 | IV-C-z | 2.31 | .25 | 6.5E-12 | 0.1330 | 0.425E-02 | 1.560 |
| G4-5F | 1778 | IV-C-z | 2.31 | .28 | 2.3E-11 - 6.9E-12 | 0.1939 | 0.120E-02 | 3.322 |
| G4-17 | 1787 | IV-C-z | 2.32 | .28 | 1.6E-10 - 1.7E-12 | 0.0370 | 0.286E-02 | 1.675 |
| G4-18 | 1899 | V | 2.59 | .24 | 1.4E-8 - 1.6E-9 | 0.0658 | 0.141E-01 | 2.639 |
| G4-19 | 2006 | VI | 2.29 | .29 | 2.0E-11 | 0.1346 | 0.316E-02 | 2.019 |
| G4-20 | 2101 | VI | 2.24 | .19 | 4.4E-10 | 0.3217 | 0.448E-02 | 1.872 |
| G4-21 | 2401 | VII | 2.62 | .24 | 2.3E-9 | 0.0608 | 0.112E-01 | 4.148 |
| G4-22 | 2407 | VII | 2.63 | .27 | 6.3E-9 | 0.0559 | 0.293E-01 | 2.257 |
| G4-23 | --- | --- | 2.53 | .40 | <1.3E-11 | 0.1897 | 0.134E-01 | 1.407 |

Anaconda 1010A, Commercial Clinoptilolite

| Sample Code | Depth (ft) | Unit | Grain Density (g/cm$^3$) | Porosity | Sat. Hydraulic Conductivity (m/s) | $S_r$ | Alpha (1/m) | Beta |
|---|---|---|---|---|---|---|---|---|
| GU3-1 | 82 | I-A | 2.49 | .15 | <1.5E-12 | 0.0535 | 0.231E-01 | 1.693 |
| GU3-2 | 121 | I-A | 2.49 | .14 | 7.0E-13 | 0.0139 | 0.701E-02 | 1.851 |
| GU3-3 | 155 | I-A | 2.49 | .09 | 2.7E-12 | 0.1600 | 0.389E-02 | 2.130 |
| GU3-4 | 257 | I-A | 2.49 | .06 | 4.8E-09 [k] | 0.0200 | 0.168E-01 | 1.500 |
| GU3-5 | 316 | I-A | 2.48 | .09 | <1.5E-12 | 0.0180 | 0.137E-01 | 1.513 |
| GU3-6 | 374 | I-B | 2.41 | .59 | 1.6E-06 | 0.0835 | 0.144E-01 | 2.528 |
| GU3-7 | 378 | I-B | 2.35 | .40 | 3.9E-07 | 0.1001 | 0.150E-01 | 6.872 |
| GU3-8 | 397 | I-B | 2.44 | .43 | 3.5E-07 | 0.1145 | 0.110E-01 | 8.878 |
| GU3-9 | 1132 | II-NL | 2.54 | .08 | <1.5E-12 | 0.0075 | 0.123E-01 | 1.488 |
| GU3-10 | 1197 | III | 2.39 | .02 | 1.5E-11 | 0.3757 | 0.328E-02 | 4.118 |
| GU3-11 | 1246 | III | 2.38 | .07 | 1.5E-12 | 0.0804 | 0.441E-02 | 2.058 |
| GU3-12 | 1311 | IV-A-v | 2.37 | .35 [l] | 3.2E-09 | 0.0497 | 0.172E-01 | 3.283 |
| GU3-13 | 1331 | IV-A-v | 2.36 | .45 | 2.9E-07 | 0.0479 | 0.103E-01 | 4.203 |
| GU3-14 | 1440 | IV-A-v | 2.37 | .46 | 2.7E-07 | 0.0405 | 0.160E-01 | 3.872 |
| GU3-15 | 1499 | IV-A-v | 2.35 | .43 | 2.6E-08 | 0.0200 | 0.440E-01 | 1.496 |
| GU3-16 | 1555 | IV-B-v [m] | 2.44 | .47 | 7.9E-8 | 0.1892 | 0.155E-01 | 10.140 |
| GU3-17 | 1628 | V | 2.58 | .39 | 6.9E-09 | 0.0180 | 0.144E-01 | 2.964 |
| GU3-18 | 1680 | V | 2.57 | .32 | 1.3E-09 | 0.0665 | 0.314E-01 | 3.442 |
| GU3-19 | 1730 | V | 2.52 | .24 | 1.2E-09 [k] | 0.1239 | 0.211E-01 | 2.851 |

Notes: k) Flow pattern indicated cracks in sample.
l) Subsamples had porosities of .27 and .42.
m) Minerological analysis indicates this sample is a nonzeolitized, devitrified 'inclusion' in this unit.

**TABLE A.3.** Summary of Mercury Intrusion Data Supplied by Micromeritics[a]

| Sample | Bulk Density, $g/cm^3$ | Apparent (Skeletal) Density, $g/cm^3$ | Average Pore Diameter, μm |
|---|---|---|---|
| G4-1 | 5.1755 | 5.9929 | 0.0156 |
| G4-2 | 1.8715 | 2.6008 | 0.0259 |
| G4-3 | 1.2409 | 2.1764 | 0.2472 |
| G4-4 | | Data not available | |
| G4-5 | 2.3192 | 2.5902 | 0.0306 |
| G4-24 | 1.8512 | 2.5552 | 0.1311 |
| G4-6 | 2.3235 | 2.5922 | 0.0315 |
| G4-7 | 2.3579 | 2.5681 | 0.0180 |
| G4-8 | 2.2826 | 2.5104 | 0.0187 |
| G4-8[b] | 2.2724 | 2.5416 | 0.0153 |
| G4-9 | | Data not available | |
| G4-10 | 1.6501 | 2.2863 | 0.0177 |
| G4-11 | 1.6706 | 2.2648 | 0.0192 |
| G4-12 | 1.7101 | 2.3781 | 0.0217 |
| G4-13 | 1.7623 | 2.2773 | 0.0236 |
| G4-14 | 1.8813 | 2.3443 | 0.0198 |
| G4-15 | 1.8433 | 2.2440 | 0.0131 |
| G4-16 | 1.6577 | 2.2527 | 0.0204 |
| G4-17 | 1.6419 | 2.3662 | 0.0363 |
| G4-18 | 1.9570 | 2.6050 | 0.0284 |
| G4-19 | 1.5779 | 2.3005 | 0.0329 |
| G4-20 | 1.8792 | 2.2441 | 0.0307 |
| G4-21 | 2.5419 | 3.7244 | 0.0672 |
| G4-22 | 1.9541 | 2.6303 | 0.1360 |
| G4-23 | 1.5690 | 2.1422 | 0.0233 |

(a) Micromeritics Instrument Corporation
5680 Goshen Springs
Norcross, Georgia 30093

(b) Two G4-8 subsamples were tested by Micromeritics.

TABLE A.4 Unconfined Hydraulic Conductivity for Samples Taken from USW G-4 and USW GU-3

| Sample | Depth (ft) | Unit | Saturated Hydraulic Conductivity (m/s) | | | |
|---|---|---|---|---|---|---|
| | | | Ruska Permeameter | | | Large Disc |
| | | | Run #1 | Run #2 | Run #3 | |
| G4-1 | 43 | I-A | 9.68E-12 | | | |
| G4-2 | 124 | I-B | 2.63E-11 | 2.86E-12 | | |
| G4-3 | 208 | I-B | 2.35E-06 | | | |
| G4-4 | 247 | II-L | 8.60E-13 | | | |
| G4-5 | 864 (dark) | II-NL | 2.17E-11 | 1.31E-11 | 1.97E-11 | 2.17E-11 |
| G4-24 | 864 (light) | II-NL | 3.90E-11 | | | |
| G4-6 | 1158 | II-NL | 1.86E-11 | | | |
| G4-1F | 1215 | II-NL | 3.77E-12 | 7.11E-12 | 9.19E-12 | |
| G4-7 | 1256 | II-NL | <1.31E-11[a] | | | |
| G4-2F | 1278 | II-NL | 8.58E-12 | 1.34E-12 | 1.48E-11 | |
| G4-8 | 1299 | III | 4.47E-10 | | | |
| G4-9 | 1324 | III | 3.02E-12 | | | |
| G4-3F | 1359 | IV-A-v | 3.25E-11 | 1.99E-11 | 8.03E-11 | |
| G4-10 | 1405 | IV-A-z | 2.99E-12 | | | |
| G4-11 | 1548 | IV-A-z | <1.31E-11[a] | 5.9 E-12 | 1.97E-11 | 2.37E-14 |
| G4-4F | 1551 | IV-A-z | 5.06E-11 | 1.88E-11 | 1.33E-11 | |
| G4-12 | 1686 | IV-A-z | 4.24E-12 | | | |
| G4-13 | 1728 | IV-B-z | 1.86E-11 | 2.45E-11 | 1.97E-11 | 4.69E-14 |
| G4-14 | 1737 | IV-B-z | <1.31E-11[a] | 4.59E-13 | 2.48E-11 | 1.59E-12 |
| G4-15 | 1769 | IV-C-z | 2.30E-12 | | | |
| G4-16 | 1778 | IV-C-z | 6.47E-12 | | | |
| G4-5F | 1778 | IV-C-z | 6.89E-12 | 1.83E-11 | 2.25E-11 | |
| G4-17 | 1789 | IV-C-z | 1.61E-10 | 1.97E-11 | 1.24E-10 | 1.68E-12 |
| G4-18 | 1899 | V | 2.34E-09 | 1.38E-08 | 1.58E-09 | 4.46E-09 |
| G4-19 | 2006 | VI | 2.03E-11 | | | |
| G4-20 | 2101 | VI | 4.36E-10 | | | |
| G4-21 | 2401 | VII | 2.31E-09 | | | |
| G4-22 | 2407 | VII | 6.26E-09 | | | |
| G4-23 | Anaconda | 1010A | <1.31E-11[a] | | | |

[a] Indicates upper limit.

TABLE A.4. (cont)

| Sample | Depth (ft) | Unit | Saturated Hydraulic Conductivity (m/s) | | | |
|---|---|---|---|---|---|---|
| | | | Ruska Permeameter | | | Large Disc |
| | | | Run #1 | Run #2 | Run #3 | |
| GU3-1 | 82 | I-A | | | | <1.5 E-12[a] |
| GU3-2 | 121 | I-A | | | | 7.0 E-13 |
| GU3-3 | 155 | I-A | | | | 2.66E-12 |
| GU3-4 | 257 | I-A | | | | 4.83E-09 |
| GU3-5 | 316 | I-A | | | | <1.5 E-12[a] |
| GU3-6 | 374 | I-B | | | | 1.63E-06 |
| GU3-7 | 378 | I-B | | | | 3.90E-07 |
| GU3-8 | 379 | I-B | | | | 3.52E-07 |
| GU3-9 | 1132 | II-NL | | | | <1.5 E-12[a] |
| GU3-10 | 1197 | III | | | | 1.46E-11 |
| GU3-11 | 1246 | III | | | | 1.52E-12 |
| GU3-12 | 1311 | IV-A-v | | | | 3.15E-09 |
| GU3-13 | 1331 | IV-A-v | | | | 2.92E-07 |
| GU3-14 | 1440 | IV-A-v | | | | 2.68E-07 |
| GU3-15 | 1499 | IV-A-v | | | | 2.57E-08 |
| GU3-16 | 1555 | IV-B-v | | | | 7.90E-08 |
| GU3-17 | 1628 | V | | | | 6.92E-09 |
| GU3-18 | 1680 | V | | | | 1.28E-09 |
| GU3-19 | 1730 | V | | | | 1.18E-09 |

[a] Indicates upper limit.

FIGURE A.1. Technique for Measuring Sample Saturated Conductivity as a Function of Elevated Confining Pressure

1. Sample preparation.

   a. Measure sample length and diameter.

   b. Jacket sample with end caps as per standard procedure for low temperature samples.

2. Conductivity system preparation.
   Note: Concurrent with sample preparation.

   a. Clean system as necessary to remove contaminants.

   b. Configure permeability apparatus as per Figure 5a for normal permeability measurement or as per Figure 5b for low permeability measurement depending on anticipated sample permeability.

   c. Fill and flush system with J-13 well water.

   d. Pressurize accumulator with nitrogen gas to one half the pore fluid operating pressure specified by the test plan.

3. Sample Installation.

   a. Assemble sample stack and test apparatus as required by test plan on base plug as per standard procedure.

   b. Leak check sample stack and correct any leaks found.

   c. Vacuum saturate sample stack with J-13 well water.

   d. Install differential pressure transducer, calibrated for anticipated range.

   e. Raise base plug with sample stack into pressure vessel and complete connections as per standard operating procedure.

4. Vessel pressurization.

   a. Fill confinement pressure vessel as per standard operating procedure.

   b. Pressurize vessel to initial confining pressure specified by test plan as per standard operating procedure.

   c. Introduce pore fluid to sample and increase pore fluid pressure to specified value.

5. Test data collection.

   a. Start data collection using DAS and X-Y recorder.

   b. Adjust pore fluid pump speed and/or back pressure valve to obtain specified pore pressure and a reasonable flow or sample differential pressure.

   c. Vary confining pressure as per test plan and collect data at each pressure specified. Adjust pump speed or back pressure valve as necessary to obtain differential pressures within calibrated range.

6. System shutdown.

   a. Stop data collection.

   b. Depressurize sample pore fluid to atmospheric pressure.

   c. Depressurize pressure vessel as per standard operating procedure.

   d. Disengage sample stack assembly as per standard operating procedure.

**TABLE A.5** Data and Calculated Values for Confined, Saturated Conductivity Tests of Sample GU3-2

| P-C (Bars) | P-E (Bars) | Flow (mL/Sec) | D.P. (PSI) | K (Millidarcy) |
|---|---|---|---|---|
| 100 | 50 | 0.0043 | 172 | 0.031 |
| 200 | 150 | 0.0043 | 196 | 0.027 |
| 400 | 350 | 0.0043 | 217 | 0.024 |
| 700 | 650 | 0.0043 | 233 | 0.023 |
| 960 | 910 | 0.0043 | 265 | 0.020 |
| 700 | 650 | 0.0043 | 261 | 0.020 |
| 400 | 350 | 0.0043 | 255 | 0.021 |
| 200 | 150 | 0.0043 | 250 | 0.021 |
| 100 | 50 | 0.0043 | 235 | 0.022 |

Column Heading Explanation - Tables A.5 - A.7

P-C Confining fluid pressure

P-E Effective pressure

Flow Fluid flow rate through the sample

D.P. Pressure drop across the sample

K Calculated permeability

Note: At 20°C with water's density at 1 $g/cm^3$ the relationship between the permeability unit of "millidarcy" and the conductivity unit of "m/s" is: 1 millidarcy = $1.02 \times 10^{-8}$ m/s

**TABLE A.6** Data and Calculated Values for Confined, Saturated Conductivity Tests of Sample GU3-15

| P-C (Bars) | P-E (Bars) | Flow (mL/Sec) | D.P. (PSI) | K (Millidarcy) |
|---|---|---|---|---|
| 100 | 50 | 0.0055 | 3.5 | 20.2 |
| 200 | 150 | 0.0055 | 4.0 | 17.7 |
| 300 | 250 | 0.0055 | 5.1 | 13.9 |
| 400 | 350 | 0.0055 | 11.0 | 6.4 |
| 600 | 550 | 0.0055 | 34.0 | 2.1 |
| 800 | 750 | 0.0055 | 72.0 | 1.0 |
| 1000 | 950 | 0.0011 | 41.0 | 0.3 |
| 800 | 750 | 0.0011 | 41.0 | 0.3 |
| 600 | 550 | 0.0011 | 39.0 | 0.4 |
| 400 | 350 | 0.0011 | 38.0 | 0.4 |
| 200 | 150 | 0.0011 | 29.0 | 0.5 |
| 100 | 50 | 0.0011 | 23.0 | 0.6 |

(See Table A.5 for column headings explanation)

TABLE A.7 Data and Calculated Values for Confined, Saturated Conductivity Tests of Sample GU3-3

| P-C (Bars) | P-E (Bars) | Flow (mL/Sec) | D.P. (PSI) | K (Millidarcy) |
|---|---|---|---|---|
| 100 | 50 | 0.049 | 129 | 0.384 |
| 100 | 50 | 0.034 | 104 | 0.333 |
| 200 | 150 | 0.034 | 243 | 0.054 |
| 200 | 150 | 0.018 | 154 | 0.120 |
| 100 | 50 | 0.018 | 115 | 0.160 |
| 100 | 50 | 0.031 | 199 | 0.155 |
| 200 | 150 | 0.018 | 187 | 0.098 |
| 300 | 250 | 0.018 | 386 | 0.050 |
| 300 | 250 | 0.011 | 237 | 0.046 |
| 300 | 250 | 0.007 | 192 | 0.041 |
| 300 | 250 | 0.007 | 201 | 0.395 |
| 200 | 150 | 0.007 | 172 | 0.046 |
| 100 | 50 | 0.007 | 120 | 0.066 |
| 300 | 250 | 0.007 | 223 | 0.035 |
| 300 | 250 | 0.005 | 147 | 0.034 |
| 400 | 350 | 0.005 | 206 | 0.023 |
| 400 | 350 | 0.003 | 180 | 0.020 |
| 300 | 250 | 0.003 | 156 | 0.023 |
| 200 | 150 | 0.003 | 130 | 0.028 |
| 300 | 250 | 0.003 | 151 | 0.024 |
| 500 | 450 | 0.003 | 292 | 0.012 |
| 500 | 450 | 0.002 | 241 | 0.011 |
| 500 | 450 | 0.002 | 215 | 0.010 |
| 300 | 250 | 0.002 | 180 | 0.014 |
| 100 | 50 | 0.002 | 80 | 0.028 |
| 100 | 50 | 0.004 | 111 | 0.044 |
| 100 | 50 | 0.002 | 62 | 0.037 |
| 300 | 250 | 0.002 | 112 | 0.020 |
| 500 | 450 | 0.002 | 202 | 0.011 |
| 500 | 450 | 0.001 | 119 | 0.009 |
| 600 | 550 | 0.001 | 22 | 0.005 |
| 600 | 550 | 0.001 | 532 | 0.001 |

(See Table A.5 for column headings explanation)

**TABLE A.8** Laboratory Data and Calculated Parameters for Confined, Saturated Conductivity Tests of Sample G4-1F

| 0 | 1 P-C (BARS) | 2 P-UP (BARS) | 3 P-DN (BARS) | 4 DIFF-P | 5 FLOW (ML/SEC) | 6 P-P (BARS) | 7 P-EFF (BARS) | 8 APTR (MICRONS) | 9 NORM APTR | 10 PERM (DARCY) | 11 NORM PERM |
|---|---|---|---|---|---|---|---|---|---|---|---|
| 1 | 35 | 28 | 27 | 0.367 | 0.385 | 27 | 8 | 67 | 1.00 | 378 | 1.00 |
| 2 | 40 | 29 | 28 | 0.389 | 0.377 | 29 | 11 | 65 | 0.97 | 359 | 0.95 |
| 3 | 50 | 28 | 27 | 0.441 | 0.376 | 28 | 22 | 62 | 0.93 | 329 | 0.87 |
| 4 | 60 | 29 | 29 | 0.474 | 0.404 | 29 | 31 | 62 | 0.93 | 329 | 0.87 |
| 5 | 70 | 23 | 23 | 0.369 | 0.241 | 23 | 47 | 57 | 0.85 | 275 | 0.73 |
| 6 | 70 | 30 | 29 | 0.560 | 0.388 | 29 | 41 | 58 | 0.87 | 287 | 0.76 |
| 7 | 80 | 28 | 27 | 0.639 | 0.392 | 28 | 52 | 56 | 0.84 | 264 | 0.70 |
| 8 | 100 | 33 | 32 | 0.703 | 0.376 | 32 | 68 | 53 | 0.80 | 241 | 0.64 |
| 9 | 120 | 32 | 31 | 0.868 | 0.412 | 32 | 88 | 51 | 0.77 | 223 | 0.59 |
| 10 | 140 | 34 | 32 | 1.179 | 0.397 | 33 | 107 | 46 | 0.68 | 177 | 0.47 |
| 11 | 150 | 34 | 32 | 1.319 | 0.392 | 33 | 117 | 44 | 0.66 | 163 | 0.43 |
| 12 | 140 | 35 | 33 | 1.793 | 0.391 | 34 | 106 | 40 | 0.59 | 132 | 0.35 |
| 13 | 120 | 32 | 30 | 1.926 | 0.381 | 31 | 89 | 38 | 0.57 | 124 | 0.33 |
| 14 | 100 | 32 | 30 | 1.616 | 0.384 | 31 | 69 | 41 | 0.61 | 140 | 0.37 |
| 15 | 80 | 34 | 31 | 1.503 | 0.387 | 32 | 48 | 42 | 0.63 | 148 | 0.39 |
| 16 | 70 | 33 | 32 | 1.348 | 0.400 | 33 | 37 | 44 | 0.66 | 163 | 0.43 |
| 17 | 60 | 31 | 29 | 1.210 | 0.407 | 30 | 30 | 46 | 0.68 | 177 | 0.47 |
| 18 | 50 | 31 | 29 | 0.933 | 0.406 | 30 | 20 | 50 | 0.75 | 210 | 0.56 |
| 19 | 40 | 29 | 28 | 0.745 | 0.398 | 28 | 12 | 53 | 0.80 | 241 | 0.64 |
| 20 | 35 | 28 | 27 | 0.575 | 0.387 | 28 | 7 | 58 | 0.86 | 281 | 0.74 |

Column Heading Explanation - Tables A.8 - A.12

| | |
|---|---|
| P-C | Confining fluid pressure |
| P-UP | Upstream pore fluid pressure |
| P-DN | Downstream pore fluid pressure |
| DIFF-P | (P-UP - P-DN) Pressure drop across the sample |
| FLOW | Fluid flow rate through the sample |
| P-P | (P-UP + P-DN)/2 Sample's average pore pressure |
| P-EFF | (P-C - P-P) Effective confining pressure |
| APTR | Aperture calculated using "cubic law" (Equation 6) |
| NORM APTR | Normalized aperture |
| PERM | Calculated permeability (see Equation 7) |
| NORM PERM | Normalized permeability |

**TABLE A.9** Laboratory Data and Calculated Parameters for Confined, Saturated Conductivity Tests of Sample G4-2F

| 0 | 1 P-C (BARS) | 2 UP-P | 3 DN-P | 4 DIFF PRESS | 5 FLOW (ML/SEC) | 6 P-P (BARS) | 7 P-E (BARS) | 8 APTR (MICRONS) | 9 NORM APTR | 10 PERM (DARCY) | 11 NORM PERM |
|---|---|---|---|---|---|---|---|---|---|---|---|
| 1 | 38 | 20 | 16 | 3 | 0.00465 | 18 | 20 | 6 | 1.00 | 3.51 | 1.00 |
| 2 | 51 | 24 | 20 | 3 | 0.00465 | 22 | 29 | 6 | 0.95 | 3.14 | 0.89 |
| 3 | 56 | 28 | 23 | 4 | 0.00465 | 26 | 30 | 6 | 0.88 | 2.75 | 0.78 |
| 4 | 60 | 27 | 21 | 5 | 0.00465 | 24 | 36 | 5 | 0.82 | 2.36 | 0.67 |
| 5 | 68 | 30 | 24 | 5 | 0.00465 | 27 | 41 | 5 | 0.79 | 2.19 | 0.62 |
| 6 | 67 | 26 | 21 | 4 | 0.00232 | 23 | 44 | 4 | 0.69 | 1.67 | 0.47 |
| 7 | 83 | 25 | 20 | 4 | 0.00232 | 23 | 60 | 4 | 0.67 | 1.58 | 0.45 |
| 8 | 102 | 27 | 21 | 5 | 0.00116 | 24 | 78 | 3 | 0.49 | 0.85 | 0.24 |
| 9 | 104 | 27 | 21 | 5 | 0.00116 | 24 | 80 | 3 | 0.52 | 0.94 | 0.27 |
| 10 | 101 | 23 | 18 | 4 | 0.00116 | 20 | 81 | 4 | 0.56 | 1.12 | 0.32 |
| 11 | 120 | 24 | 19 | 4 | 0.00116 | 21 | 99 | 4 | 0.57 | 1.13 | 0.32 |
| 12 | 140 | 27 | 23 | 3 | 0.00116 | 25 | 115 | 4 | 0.60 | 1.26 | 0.36 |
| 13 | 148 | 30 | 25 | 3 | 0.00116 | 28 | 120 | 4 | 0.57 | 1.14 | 0.33 |
| 14 | 152 | 32 | 26 | 4 | 0.00116 | 29 | 123 | 3 | 0.53 | 1.00 | 0.29 |
| 15 | 130 | 33 | 29 | 4 | 0.00116 | 31 | 99 | 4 | 0.56 | 1.10 | 0.31 |
| 16 | 121 | 31 | 25 | 4 | 0.00116 | 28 | 93 | 4 | 0.56 | 1.12 | 0.32 |
| 17 | 99 | 33 | 29 | 3 | 0.00116 | 31 | 68 | 4 | 0.58 | 1.18 | 0.33 |
| 18 | 80 | 35 | 31 | 3 | 0.00116 | 33 | 47 | 4 | 0.61 | 1.32 | 0.38 |
| 19 | 71 | 37 | 33 | 3 | 0.00116 | 35 | 36 | 4 | 0.61 | 1.30 | 0.37 |
| 20 | 74 | 25 | 22 | 2 | 0.00116 | 24 | 50 | 4 | 0.65 | 1.47 | 0.42 |
| 21 | 62 | 28 | 24 | 2 | 0.00116 | 26 | 36 | 4 | 0.67 | 1.60 | 0.45 |
| 22 | 49 | 29 | 26 | 2 | 0.00116 | 27 | 22 | 5 | 0.73 | 1.89 | 0.54 |
| 23 | 42 | 30 | 28 | 1 | 0.00116 | 29 | 13 | 6 | 0.86 | 2.59 | 0.74 |
| 24 | 42 | 27 | 21 | 5 | 0.00232 | 24 | 18 | 4 | 0.66 | 1.51 | 0.43 |
| 25 | 36 | 25 | 19 | 4 | 0.00232 | 22 | 14 | 5 | 0.70 | 1.73 | 0.49 |

(See Table A.8 for explanation of column headings)

**TABLE A.10** Laboratory Data and Calculated Parameters for Confined, Saturated Conductivity Tests of Sample G4-3F

| 0 | 1 P-C (BARS) | 2 UP-P (BARS) | 3 DN-P | 4 DIFF PRESS | 5 FLOW (ML/SEC) | 6 P-P (BARS) | 7 P-E (BARS) | 8 APTR (MICRONS) | 9 NORM APTR | 10 PERM (DARCY) | 11 NORM PERM |
|---|---|---|---|---|---|---|---|---|---|---|---|
| 1 | 45 | 20 | 16 | 2.92 | 0.0870 | 18 | 27 | 22 | 0.91 | 35 | 0.82 |
| 2 | 40 | 22 | 19 | 2.18 | 0.0866 | 21 | 19 | 22 | 1.00 | 43 | 1.00 |
| 3 | 50 | 17 | 13 | 3.54 | 0.0860 | 15 | 35 | 19 | 0.85 | 31 | 0.72 |
| 4 | 50 | 28 | 25 | 2.45 | 0.0866 | 27 | 23 | 22 | 0.96 | 39 | 0.92 |
| 5 | 50 | 27 | 24 | 2.45 | 0.0860 | 25 | 25 | 22 | 0.96 | 39 | 0.92 |
| 6 | 60 | 28 | 24 | 3.33 | 0.0870 | 26 | 34 | 20 | 0.87 | 32 | 0.76 |
| 7 | 60 | 27 | 22 | 3.74 | 0.0850 | 24 | 36 | 19 | 0.83 | 29 | 0.69 |
| 8 | 60 | 26 | 20 | 4.22 | 0.0860 | 23 | 37 | 18 | 0.80 | 27 | 0.64 |
| 9 | 70 | 28 | 21 | 5.64 | 0.0866 | 24 | 46 | 16 | 0.73 | 23 | 0.53 |
| 10 | 70 | 29 | 25 | 3.06 | 0.0430 | 27 | 43 | 16 | 0.71 | 21 | 0.50 |
| 11 | 80 | 31 | 27 | 3.67 | 0.0430 | 29 | 51 | 15 | 0.67 | 19 | 0.44 |
| 12 | 80 | 31 | 24 | 5.85 | 0.0430 | 28 | 52 | 13 | 0.57 | 14 | 0.32 |
| 13 | 80 | 29 | 22 | 5.98 | 0.0429 | 25 | 55 | 13 | 0.56 | 14 | 0.32 |
| 14 | 80 | 28 | 24 | 2.92 | 0.0210 | 26 | 54 | 13 | 0.57 | 14 | 0.32 |
| 15 | 80 | 32 | 29 | 1.36 | 0.0100 | 30 | 50 | 13 | 0.57 | 14 | 0.32 |
| 16 | 80 | 24 | 22 | 1.70 | 0.0100 | 23 | 57 | 12 | 0.53 | 12 | 0.28 |
| 17 | 100 | 27 | 24 | 2.04 | 0.0100 | 25 | 75 | 11 | 0.50 | 11 | 0.25 |
| 18 | 120 | 30 | 26 | 2.99 | 0.0100 | 28 | 92 | 10 | 0.44 | 8 | 0.19 |
| 19 | 140 | 22 | 15 | 6.26 | 0.0100 | 18 | 122 | 8 | 0.34 | 5 | 0.12 |
| 20 | 140 | 25 | 23 | 1.84 | 0.0056 | 24 | 116 | 10 | 0.42 | 8 | 0.18 |
| 21 | 140 | 24 | 20 | 3.47 | 0.0055 | 22 | 118 | 8 | 0.34 | 5 | 0.12 |
| 22 | 150 | 29 | 25 | 3.40 | 0.0055 | 27 | 123 | 8 | 0.34 | 5 | 0.12 |
| 23 | 150 | 27 | 22 | 4.01 | 0.0056 | 25 | 125 | 7 | 0.33 | 5 | 0.11 |
| 24 | 140 | 30 | 26 | 3.33 | 0.0054 | 28 | 112 | 8 | 0.34 | 5 | 0.12 |
| 25 | 140 | 23 | 18 | 4.28 | 0.0053 | 21 | 119 | 7 | 0.31 | 4 | 0.10 |
| 26 | 120 | 24 | 20 | 3.33 | 0.0053 | 22 | 98 | 8 | 0.34 | 5 | 0.12 |
| 27 | 100 | 27 | 23 | 2.72 | 0.0057 | 25 | 75 | 8 | 0.37 | 6 | 0.14 |
| 28 | 80 | 28 | 25 | 1.90 | 0.0056 | 27 | 53 | 9 | 0.42 | 8 | 0.18 |
| 29 | 70 | 30 | 27 | 1.16 | 0.0055 | 28 | 42 | 11 | 0.49 | 10 | 0.24 |
| 30 | 70 | 31 | 29 | 1.36 | 0.0055 | 30 | 40 | 10 | 0.47 | 9 | 0.22 |
| 31 | 70 | 24 | 22 | 0.95 | 0.0052 | 23 | 47 | 12 | 0.52 | 11 | 0.27 |
| 32 | 70 | 23 | 20 | 1.50 | 0.0055 | 21 | 49 | 10 | 0.45 | 9 | 0.20 |
| 33 | 70 | 28 | 25 | 2.24 | 0.0109 | 27 | 43 | 11 | 0.50 | 10 | 0.25 |
| 34 | 70 | 21 | 17 | 2.72 | 0.0110 | 19 | 51 | 10 | 0.47 | 9 | 0.22 |
| 35 | 70 | 20 | 17 | 2.99 | 0.0111 | 18 | 52 | 10 | 0.45 | 9 | 0.21 |
| 36 | 70 | 27 | 20 | 5.51 | 0.0216 | 23 | 47 | 10 | 0.46 | 9 | 0.21 |
| 37 | 60 | 27 | 23 | 3.81 | 0.0217 | 25 | 35 | 12 | 0.52 | 12 | 0.27 |
| 38 | 50 | 27 | 23 | 2.45 | 0.0218 | 25 | 25 | 14 | 0.61 | 16 | 0.37 |
| 39 | 40 | 27 | 25 | 1.16 | 0.0217 | 26 | 14 | 17 | 0.78 | 26 | 0.61 |
| 40 | 40 | 22 | 18 | 3.20 | 0.0436 | 20 | 20 | 16 | 0.70 | 21 | 0.49 |
| 41 | 40 | 29 | 26 | 2.18 | 0.0431 | 28 | 12 | 18 | 0.79 | 27 | 0.63 |
| 42 | 40 | 29 | 24 | 4.22 | 0.0864 | 27 | 13 | 18 | 0.80 | 27 | 0.64 |
| 43 | 40 | 29 | 24 | 4.08 | 0.0871 | 26 | 14 | 18 | 0.81 | 28 | 0.66 |
| 44 | 40 | 23 | 17 | 5.64 | 0.0870 | 20 | 20 | 16 | 0.73 | 23 | 0.53 |
| 45 | 35 | 24 | 21 | 2.86 | 0.0864 | 23 | 12 | 21 | 0.91 | 36 | 0.83 |

(See Table A.8 for explanation of column headings)

**TABLE A.11** Laboratory Data and Calculated Parameters for Confined, Saturated Conductivity Tests of Sample G4-4F

| 0 | 1 P-C (BARS) | 2 UP-P | 3 DN-P | 4 DIFF PRESS | 5 FLOW (ML/SEC) | 6 P-P (BARS) | 7 P-E (BARS) | 8 APTR (MICRONS) | 9 NORM APTR | 10 PERM (DARCY) | 11 NORM PERM |
|---|---|---|---|---|---|---|---|---|---|---|---|
| 1 | 35 | 21 | 17 | 1.904 | 0.3687 | 19 | 16 | 31 | 1.00 | 79 | 1.00 |
| 2 | 35 | 24 | 20 | 2.108 | 0.3690 | 22 | 13 | 30 | 0.97 | 74 | 0.93 |
| 3 | 40 | 23 | 20 | 2.584 | 0.3692 | 22 | 18 | 28 | 0.90 | 65 | 0.82 |
| 4 | 50 | 20 | 16 | 2.788 | 0.3696 | 18 | 32 | 27 | 0.88 | 61 | 0.78 |
| 5 | 50 | 28 | 23 | 3.400 | 0.3687 | 25 | 25 | 25 | 0.82 | 54 | 0.68 |
| 6 | 50 | 22 | 17 | 3.740 | 0.3686 | 19 | 31 | 24 | 0.80 | 50 | 0.64 |
| 7 | 65 | 22 | 16 | 4.556 | 0.3691 | 19 | 46 | 23 | 0.75 | 44 | 0.56 |
| 8 | 56 | 23 | 17 | 4.556 | 0.3687 | 20 | 36 | 23 | 0.75 | 44 | 0.56 |
| 9 | 55 | 22 | 16 | 4.692 | 0.3695 | 19 | 36 | 23 | 0.74 | 43 | 0.55 |
| 10 | 60 | 21 | 14 | 6.256 | 0.3699 | 17 | 43 | 21 | 0.67 | 36 | 0.45 |
| 11 | 60 | 26 | 21 | 3.604 | 0.2214 | 24 | 36 | 21 | 0.68 | 37 | 0.47 |
| 12 | 60 | 23 | 18 | 4.080 | 0.2195 | 21 | 39 | 20 | 0.65 | 34 | 0.43 |
| 13 | 60 | 21 | 17 | 3.196 | 0.1746 | 19 | 41 | 20 | 0.66 | 34 | 0.43 |
| 14 | 60 | 22 | 19 | 1.700 | 0.0922 | 20 | 40 | 20 | 0.65 | 34 | 0.43 |
| 15 | 70 | 24 | 21 | 1.836 | 0.0922 | 23 | 47 | 20 | 0.64 | 32 | 0.41 |
| 16 | 80 | 24 | 21 | 1.972 | 0.0923 | 23 | 57 | 19 | 0.62 | 31 | 0.39 |
| 17 | 100 | 23 | 20 | 2.312 | 0.0919 | 21 | 79 | 18 | 0.59 | 28 | 0.35 |
| 18 | 100 | 24 | 19 | 3.400 | 0.0925 | 22 | 78 | 16 | 0.52 | 21 | 0.27 |
| 19 | 120 | 23 | 18 | 4.284 | 0.0926 | 20 | 100 | 15 | 0.48 | 18 | 0.23 |
| 20 | 140 | 26 | 19 | 5.304 | 0.0922 | 22 | 118 | 14 | 0.45 | 16 | 0.20 |
| 21 | 140 | 24 | 17 | 6.120 | 0.0924 | 20 | 120 | 13 | 0.43 | 14 | 0.18 |
| 22 | 140 | 25 | 20 | 3.740 | 0.0553 | 22 | 118 | 13 | 0.42 | 14 | 0.18 |
| 23 | 150 | 28 | 23 | 4.284 | 0.0548 | 26 | 124 | 12 | 0.40 | 13 | 0.16 |
| 24 | 150 | 23 | 17 | 4.964 | 0.0552 | 20 | 130 | 12 | 0.39 | 12 | 0.15 |
| 25 | 140 | 24 | 18 | 4.828 | 0.0550 | 21 | 119 | 12 | 0.39 | 12 | 0.15 |
| 26 | 120 | 24 | 19 | 4.420 | 0.0550 | 22 | 98 | 12 | 0.40 | 13 | 0.16 |
| 27 | 100 | 24 | 19 | 4.012 | 0.0554 | 22 | 78 | 13 | 0.41 | 14 | 0.17 |
| 28 | 100 | 29 | 23 | 4.284 | 0.0556 | 26 | 74 | 12 | 0.41 | 13 | 0.16 |
| 29 | 100 | 22 | 16 | 4.012 | 0.0557 | 19 | 81 | 13 | 0.42 | 14 | 0.17 |
| 30 | 80 | 25 | 21 | 3.536 | 0.0559 | 23 | 57 | 13 | 0.43 | 15 | 0.19 |
| 31 | 80 | 24 | 19 | 3.332 | 0.0553 | 21 | 59 | 13 | 0.44 | 15 | 0.19 |
| 32 | 70 | 27 | 22 | 3.128 | 0.0553 | 24 | 46 | 14 | 0.45 | 16 | 0.20 |
| 33 | 60 | 27 | 22 | 2.380 | 0.0557 | 25 | 35 | 15 | 0.49 | 19 | 0.24 |
| 34 | 60 | 21 | 17 | 2.720 | 0.0556 | 19 | 41 | 14 | 0.47 | 18 | 0.22 |
| 35 | 50 | 21 | 17 | 1.972 | 0.0554 | 19 | 31 | 16 | 0.53 | 22 | 0.28 |
| 36 | 40 | 21 | 18 | 1.428 | 0.0564 | 19 | 21 | 18 | 0.59 | 27 | 0.35 |
| 37 | 35 | 21 | 17 | 1.292 | 0.0550 | 19 | 16 | 18 | 0.60 | 29 | 0.36 |

(See Table A.8 for explanation of column headings)

**TABLE A.12** Laboratory Data and Calculated Parameters for Confined, Saturated Conductivity Tests of Sample G4-5F

| 0 | 1 P-C (BARS) | 2 UP-P | 3 DN-P | 4 DIFF -P (BARS) | 5 FLOW (ML/SEC) | 6 P-P (BARS) | 7 P-E (BARS) | 8 APTR (MICRONS) | 9 NORM APTR | 10 PERM (DARCY) | 11 NORM PERM |
|---|---|---|---|---|---|---|---|---|---|---|---|
| 1 | 37 | 30 | 26 | 3.214 | 0.001962 | 28 | 8.999 | 6.0 | 0.98 | 3.0 | 0.97 |
| 2 | 50 | 31 | 26 | 4.840 | 0.001156 | 29 | 21.274 | 4.4 | 0.72 | 1.6 | 0.52 |
| 3 | 38 | 29 | 24 | 4.180 | 0.001503 | 27 | 11.272 | 5.0 | 0.82 | 2.1 | 0.68 |
| 4 | 80 | 27 | 23 | 3.944 | 0.000558 | 25 | 55.316 | 3.7 | 0.60 | 1.1 | 0.37 |
| 5 | 80 | 27 | 23 | 4.284 | 0.000420 | 25 | 55.214 | 3.2 | 0.54 | 0.9 | 0.29 |
| 6 | 80 | 26 | 22 | 3.536 | 0.000793 | 24 | 55.622 | 4.3 | 0.70 | 1.5 | 0.50 |
| 7 | 120 | 26 | 22 | 3.672 | 0.000448 | 24 | 95.724 | 3.5 | 0.58 | 1.0 | 0.33 |
| 8 | 116 | 25 | 22 | 2.312 | 0.000206 | 23 | 92.574 | 3.1 | 0.52 | 0.8 | 0.27 |
| 9 | 115 | 24 | 22 | 1.836 | 0.000133 | 23 | 92.118 | 2.9 | 0.48 | 0.7 | 0.23 |
| 10 | 150 | 25 | 22 | 2.516 | 0.000159 | 23 | 126.778 | 2.8 | 0.46 | 0.7 | 0.21 |
| 11 | 150 | 25 | 22 | 2.992 | 0.000163 | 23 | 126.778 | 2.7 | 0.44 | 0.6 | 0.19 |
| 12 | 150 | 25 | 21 | 3.332 | 0.000000 | 23 | 126.710 | 0.0 | 0.00 | 0.0 | 0.00 |
| 13 | 120 | 25 | 21 | 3.536 | 0.000194 | 23 | 96.778 | 2.7 | 0.44 | 0.6 | 0.19 |
| 14 | 80 | 25 | 21 | 3.944 | 0.000305 | 23 | 56.846 | 3.0 | 0.49 | 0.8 | 0.24 |
| 15 | 54 | 23 | 21 | 1.632 | 0.000209 | 22 | 32.240 | 3.5 | 0.58 | 1.1 | 0.34 |
| 16 | 50 | 23 | 21 | 2.040 | 0.000615 | 22 | 28.138 | 4.7 | 0.78 | 1.9 | 0.61 |
| 17 | 50 | 29 | 25 | 3.196 | 0.000479 | 27 | 22.868 | 3.7 | 0.62 | 1.2 | 0.38 |
| 18 | 35 | 30 | 27 | 2.040 | 0.001306 | 28 | 6.678 | 6.1 | 1.00 | 3.1 | 1.00 |

(See Table A.8 for explanation of column headings)

## APPENDIX B
## SATURATION DATA PLOTS AND CURVE FITS

This appendix contains plots based on the psychrometer data contained in Table A.1. The saturation data points are, as discussed in the main body of the report, the water content divided by the maximum water content. The subsample data are keyed with all subsample "a" (e.g., G4-1a ) points plotted as circles, subsample "b" points plotted as triangles, and subsample "c" (G-4 samples only) points plotted as diamonds.

These data were fit using the Van Genuchten function . The fitted curve is plotted and the parameters are listed.

The "stars" indicate data points added to stabilize the curve fit routine at a reasonable result.

The plots are in the order listed in Table 2.

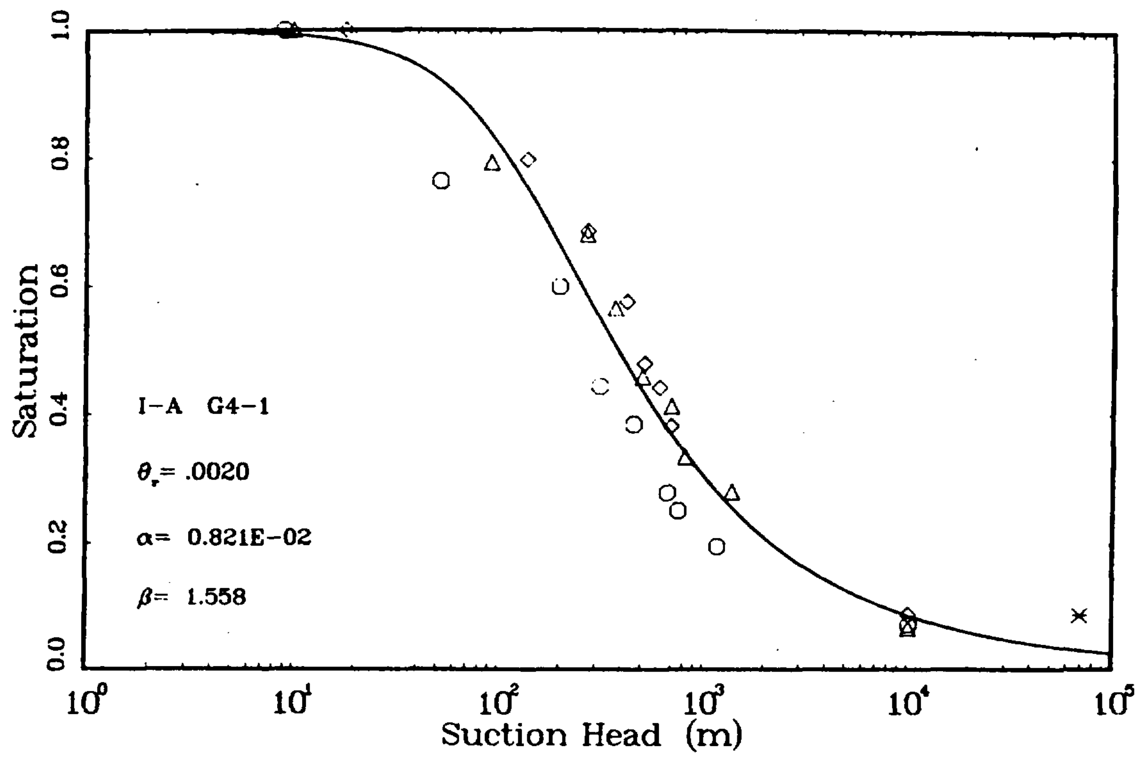


**Figure B.1**

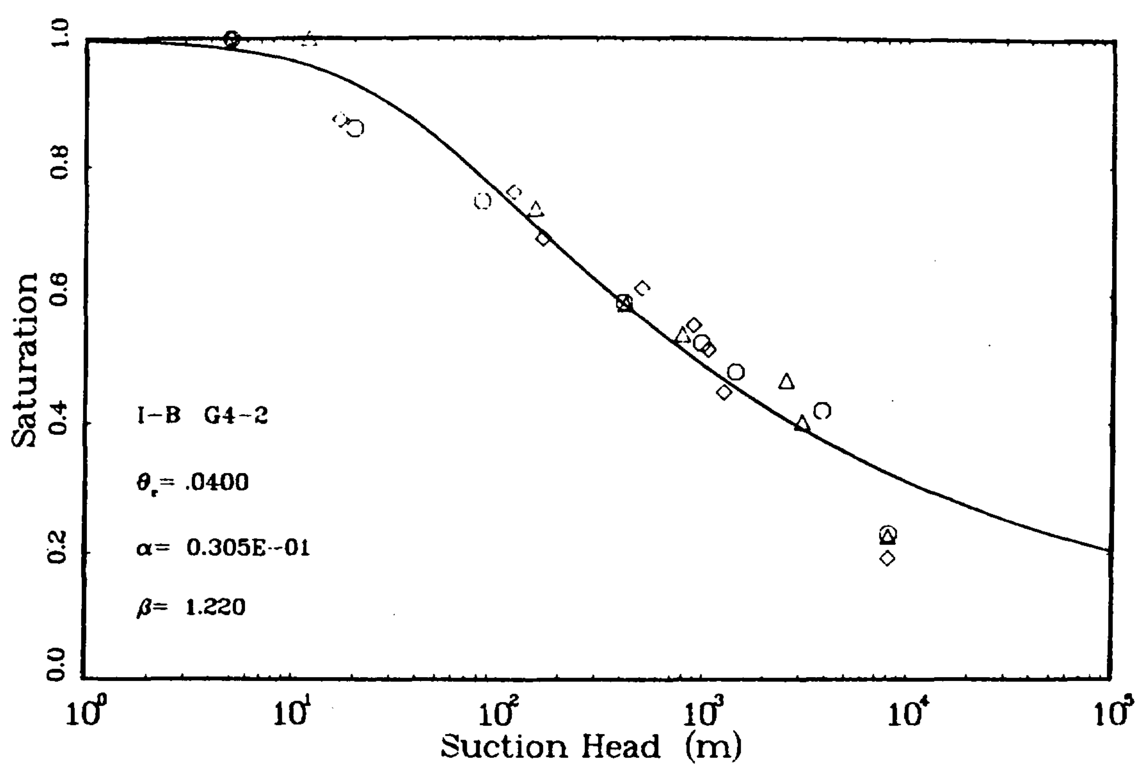


**Figure B.2**

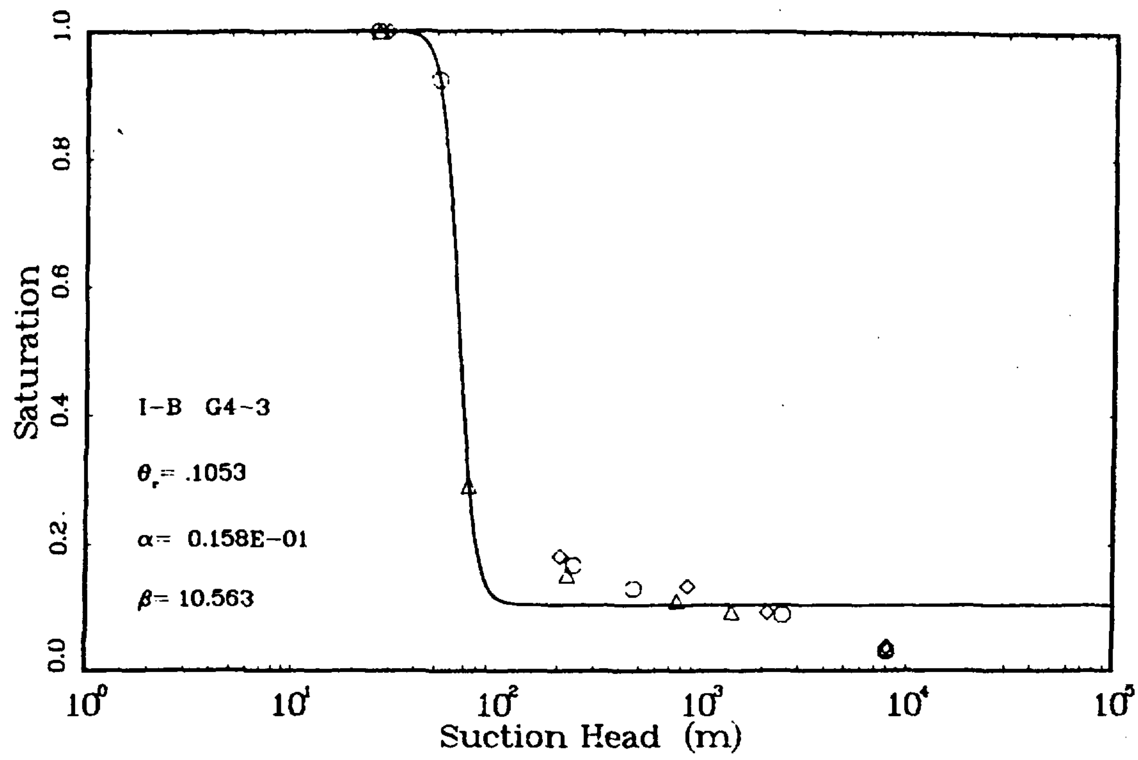


**Figure B.3**

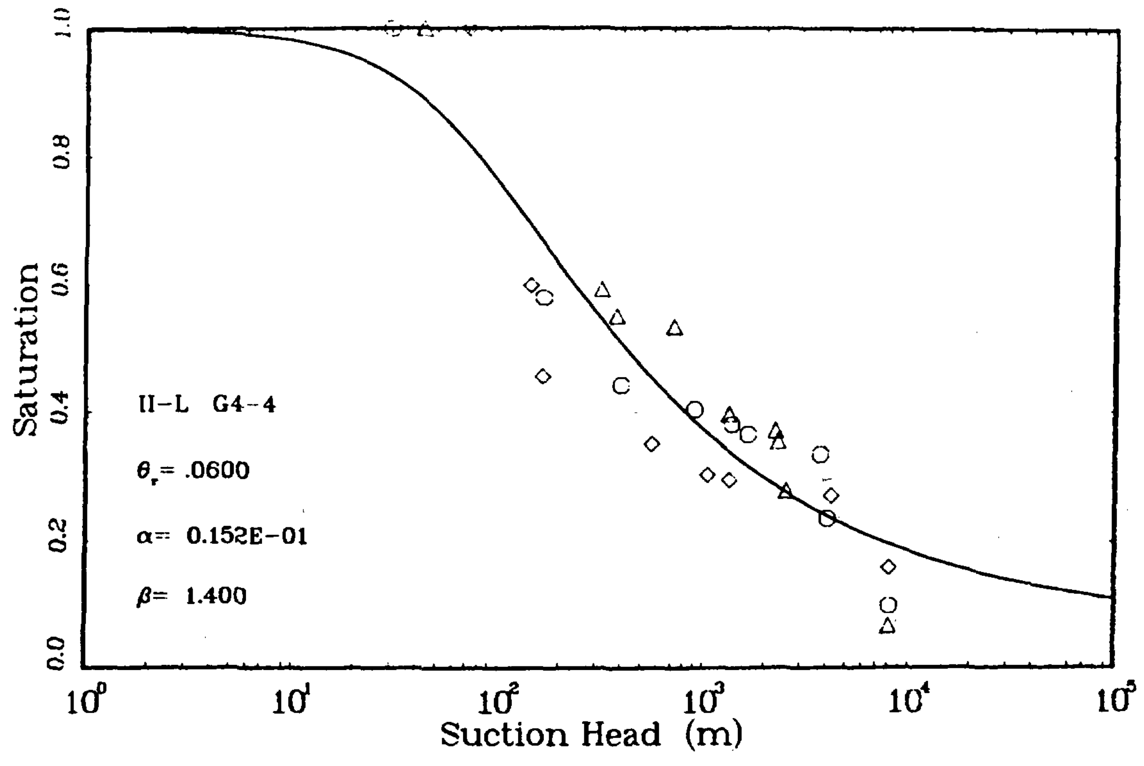


**Figure B.4**

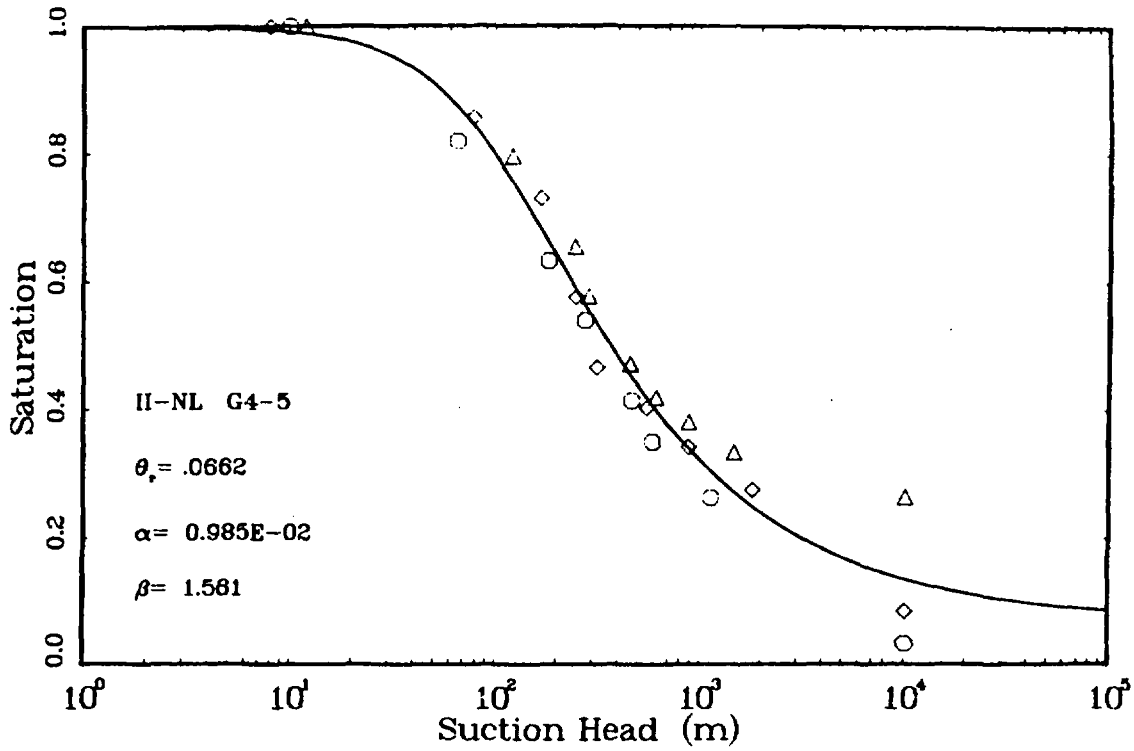


**Figure B.5**

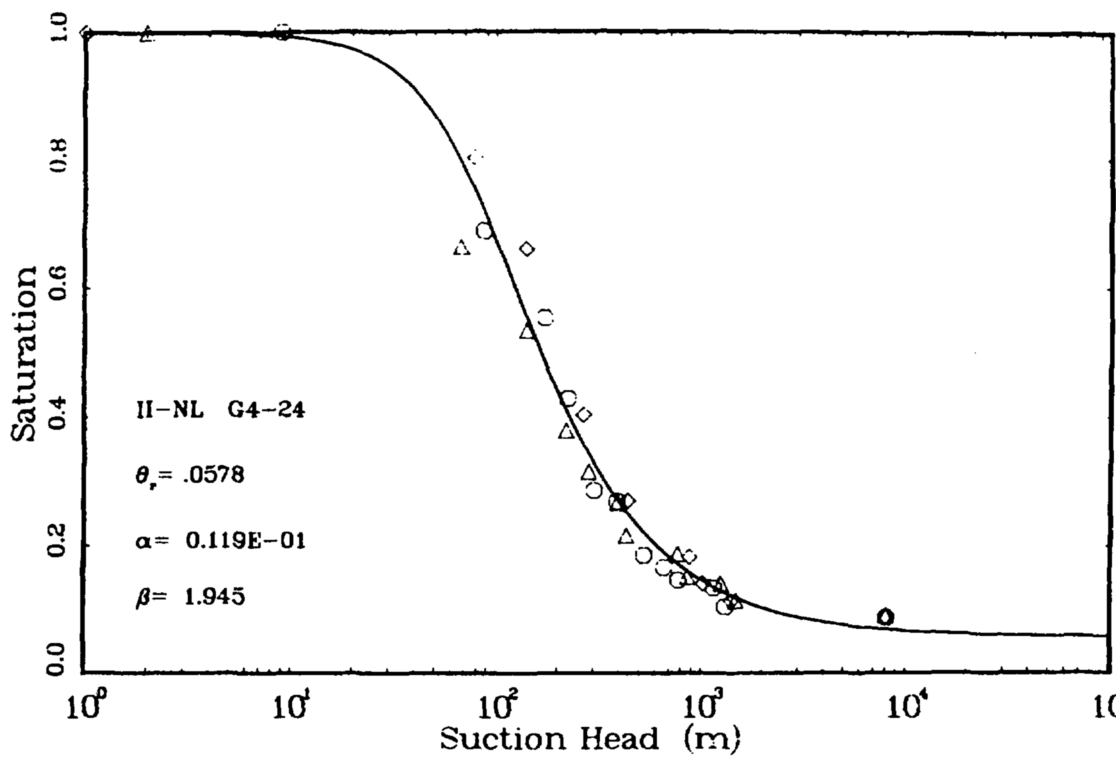


**Figure B.6**

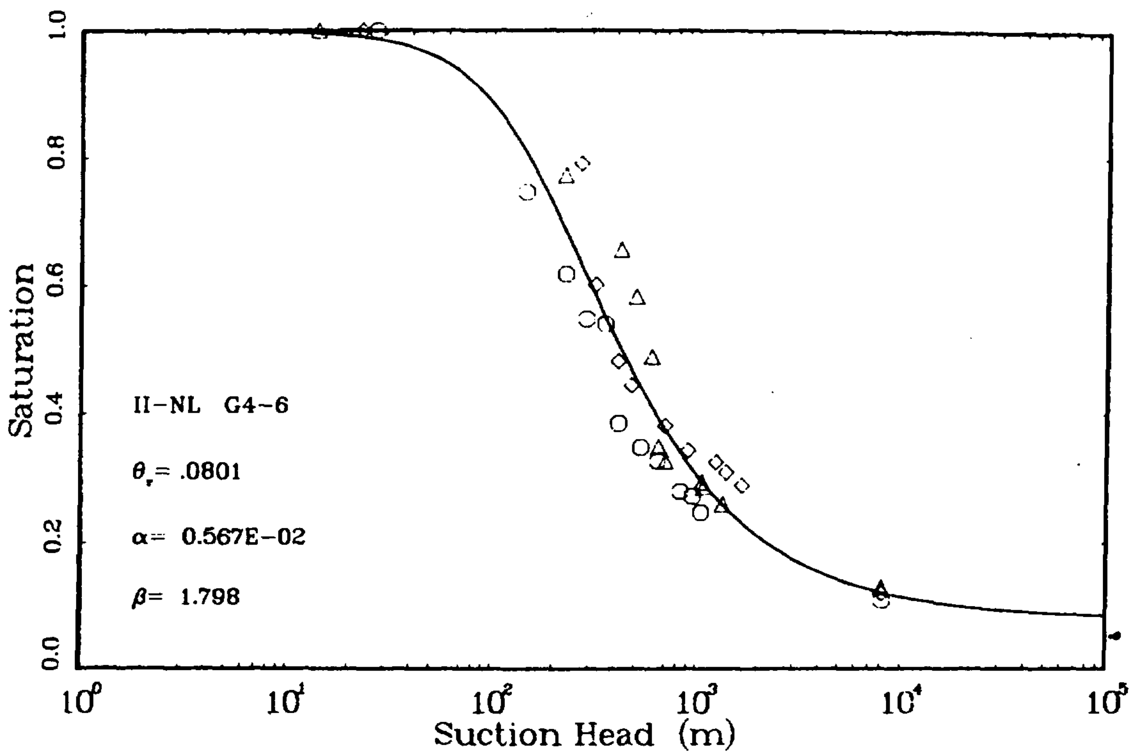


**Figure B.7**

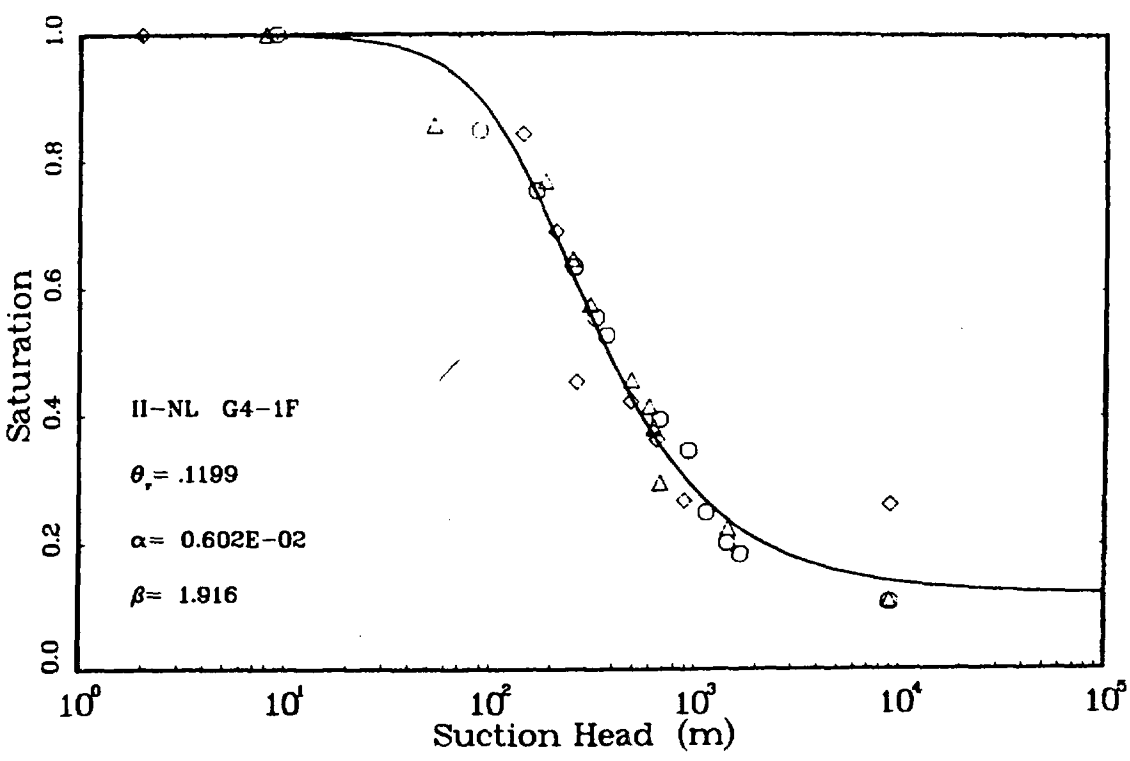


**Figure B.8**

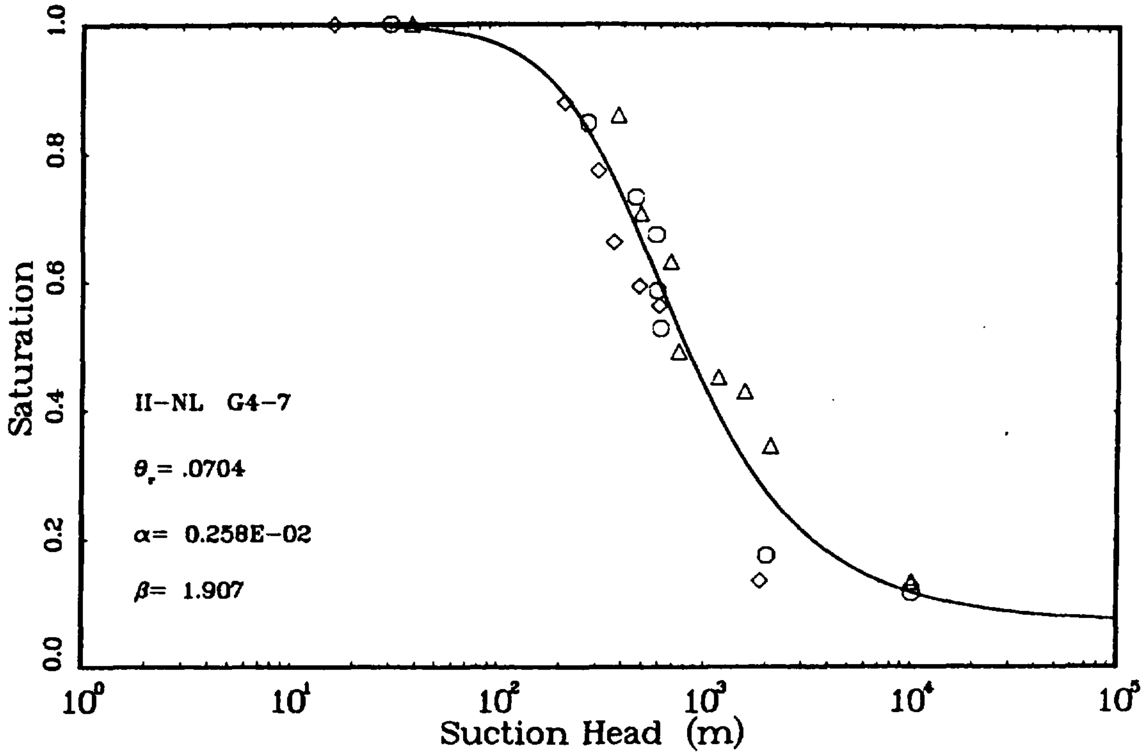


**Figure B.9**

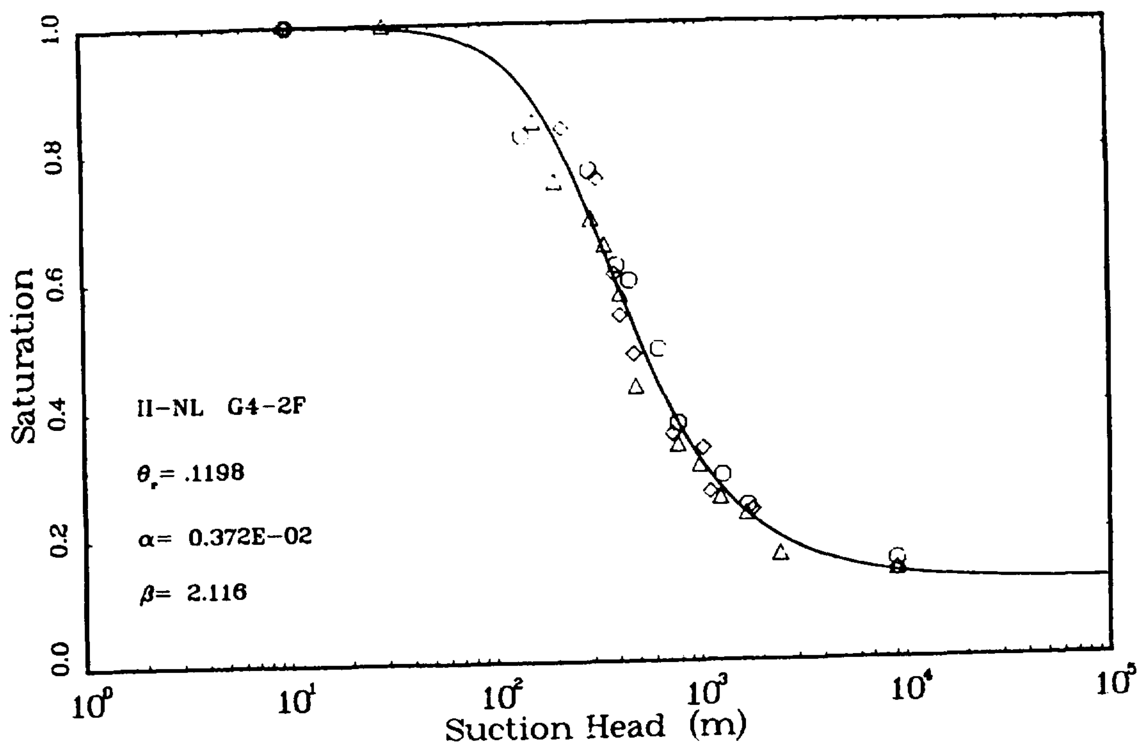


**Figure B.10**

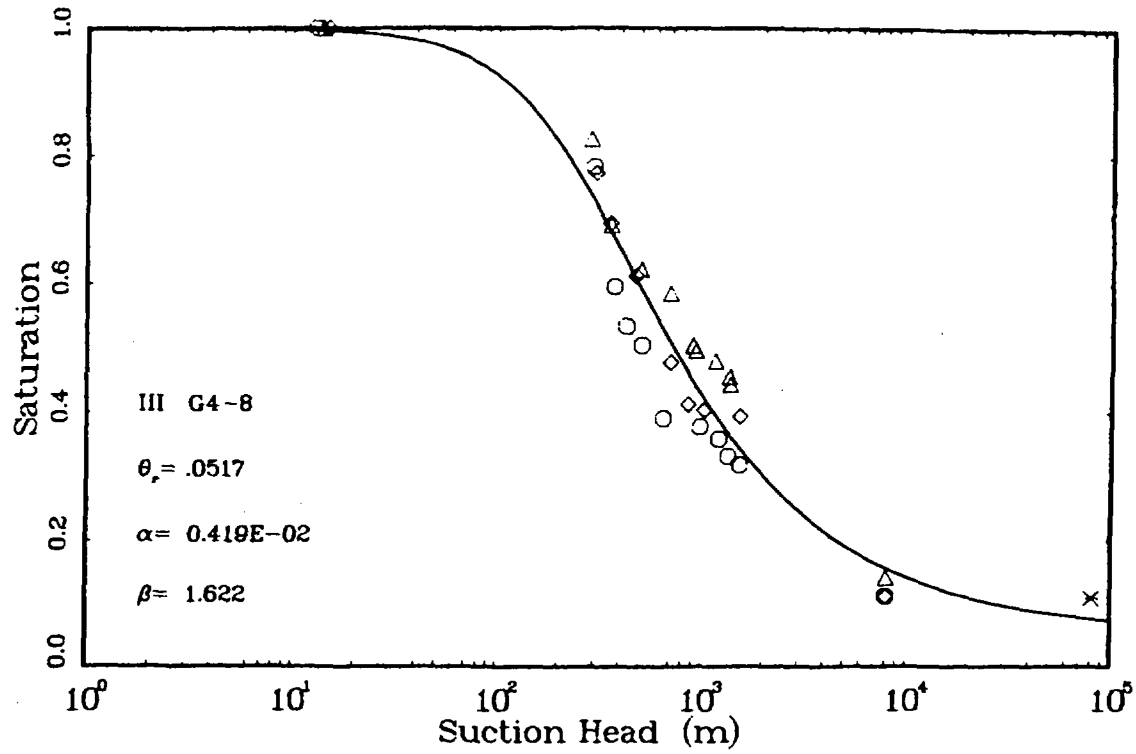


**Figure B.11**

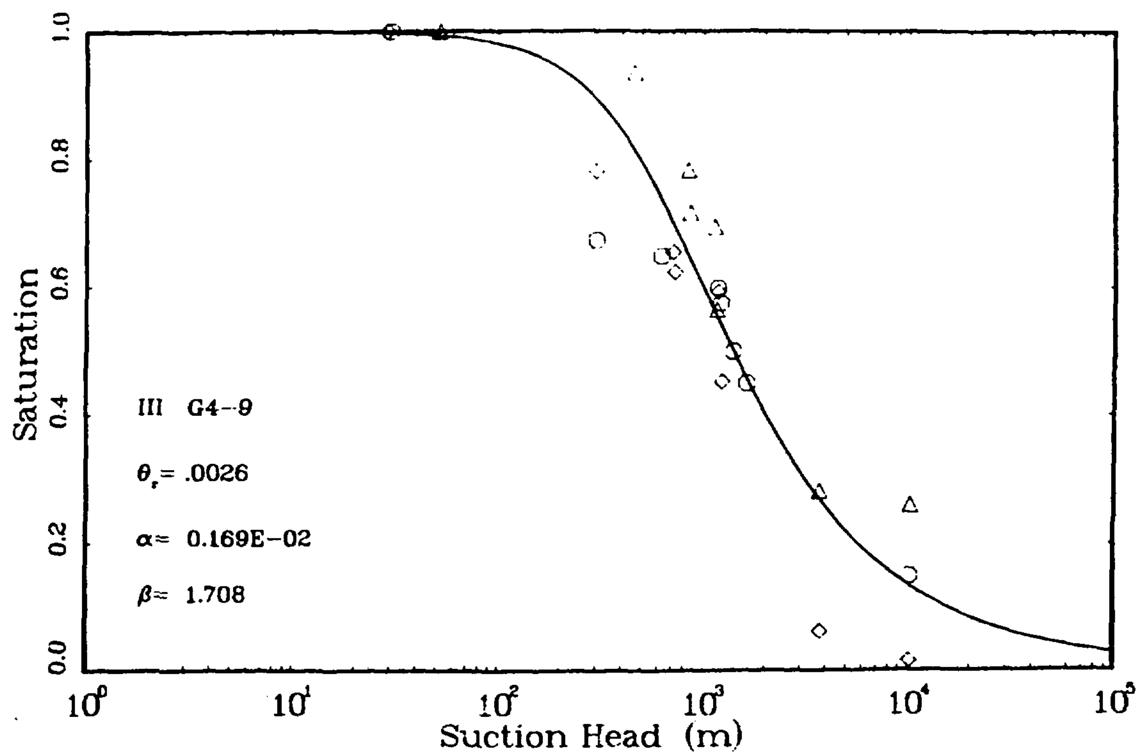


**Figure B.12**

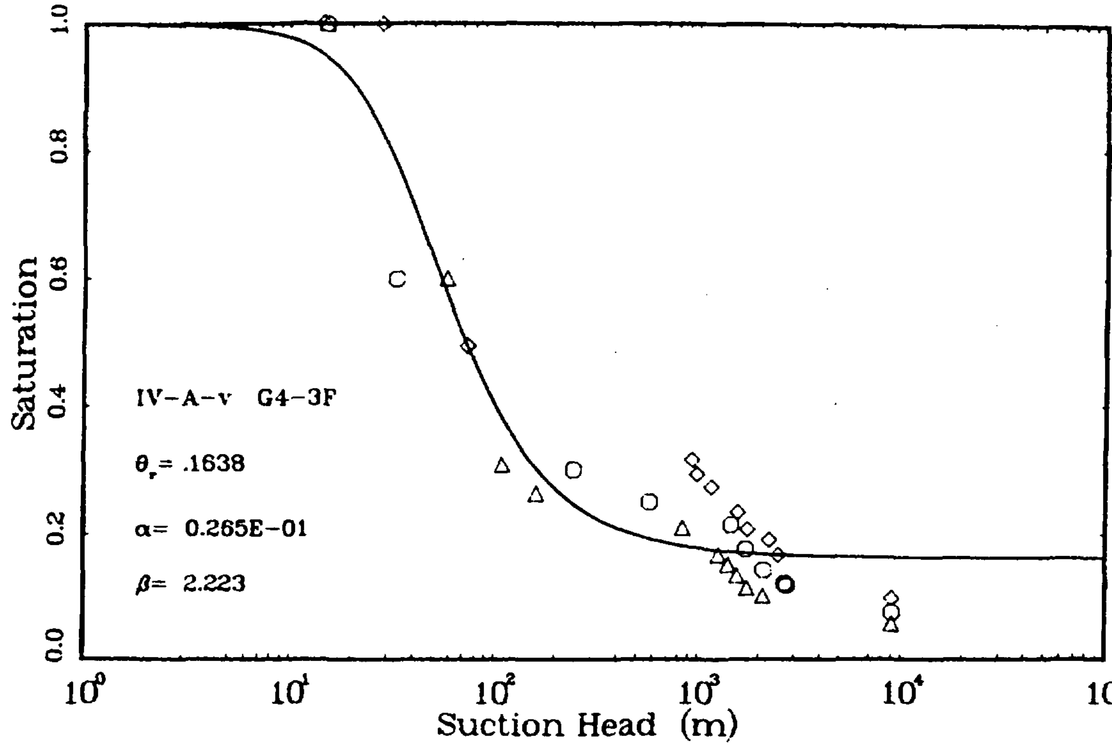


**Figure B.13**

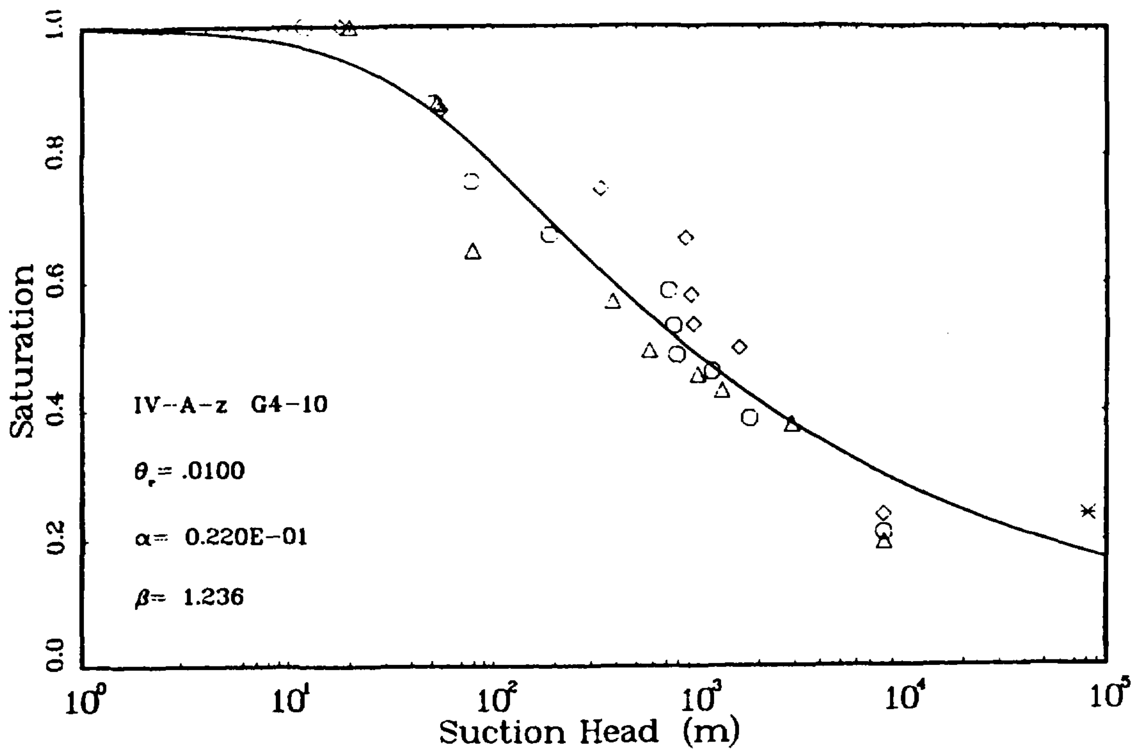


**Figure B.14**

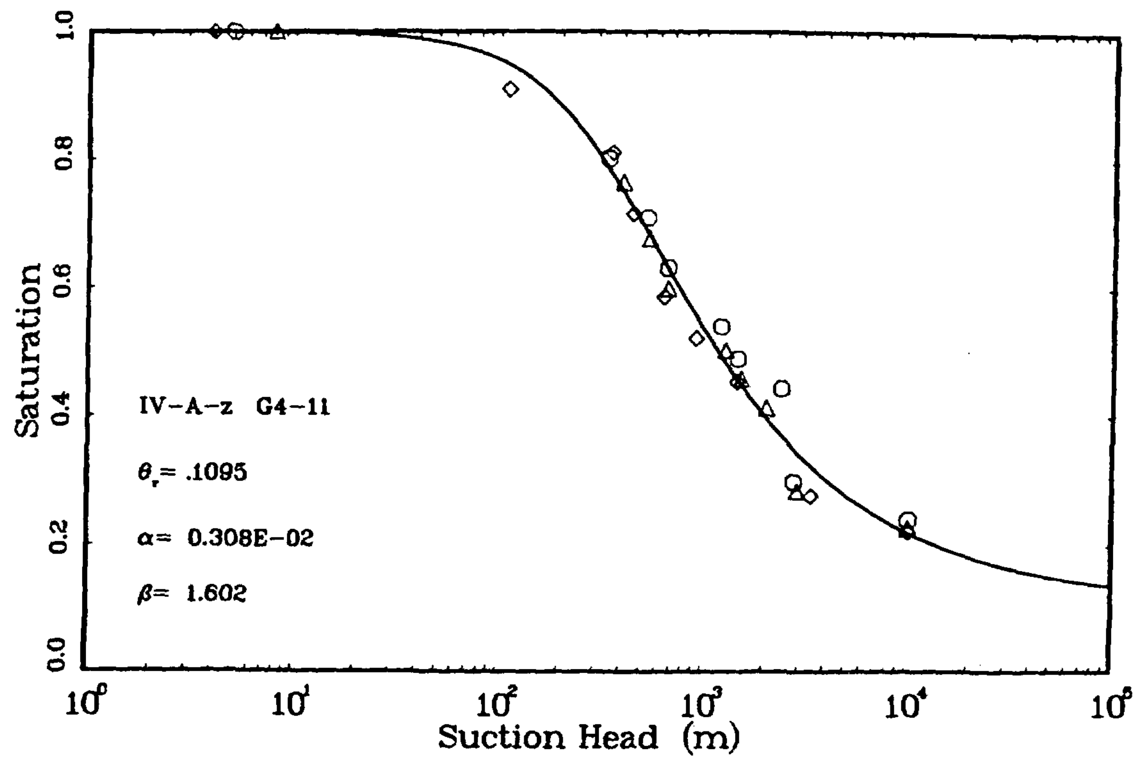


**Figure B.15**

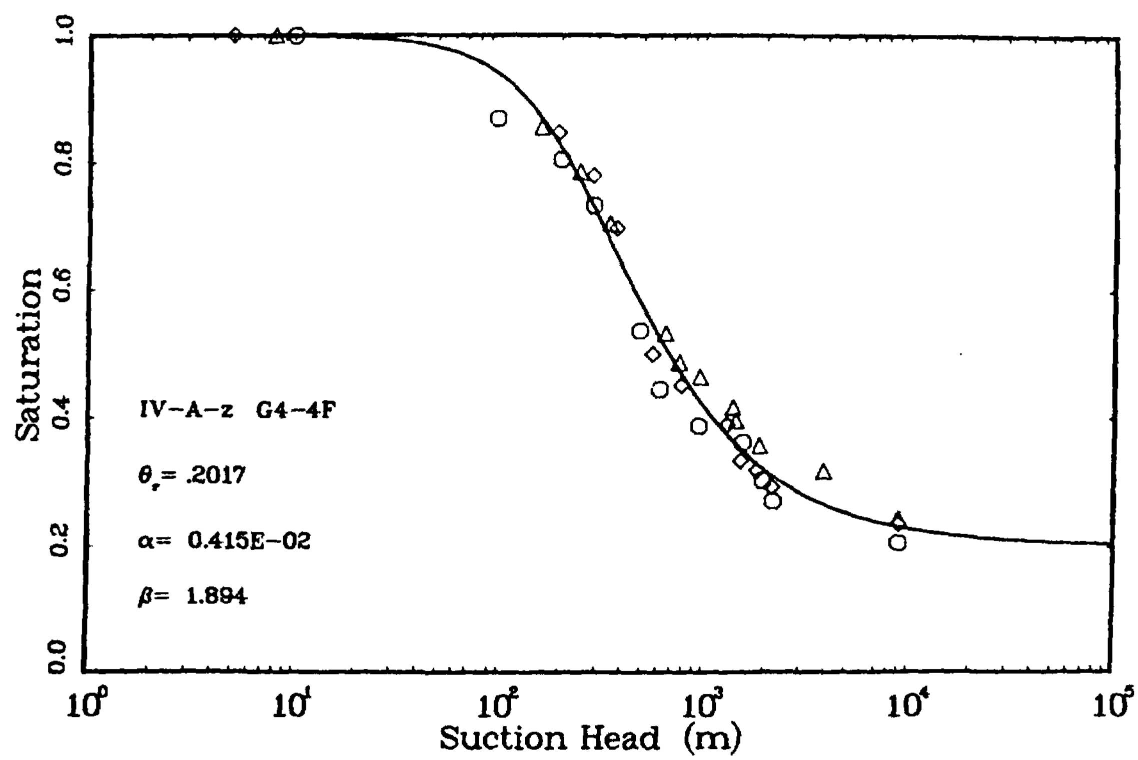


**Figure B.16**

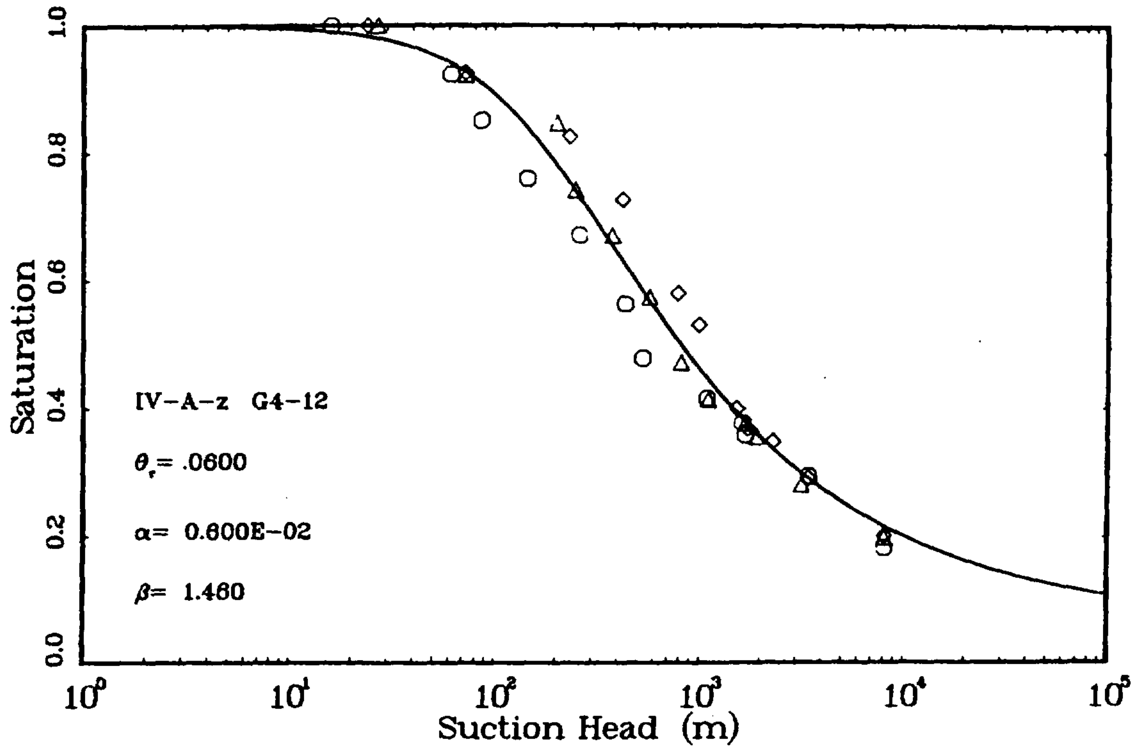


**Figure B.17**

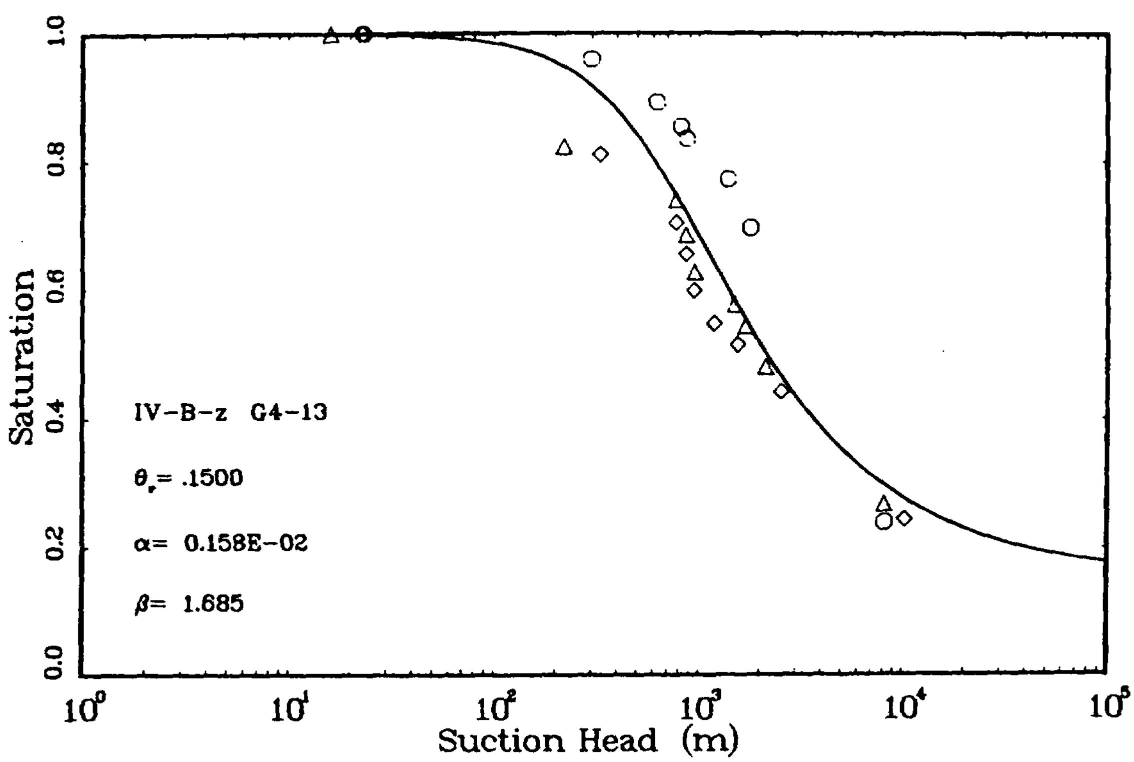


**Figure B.18**

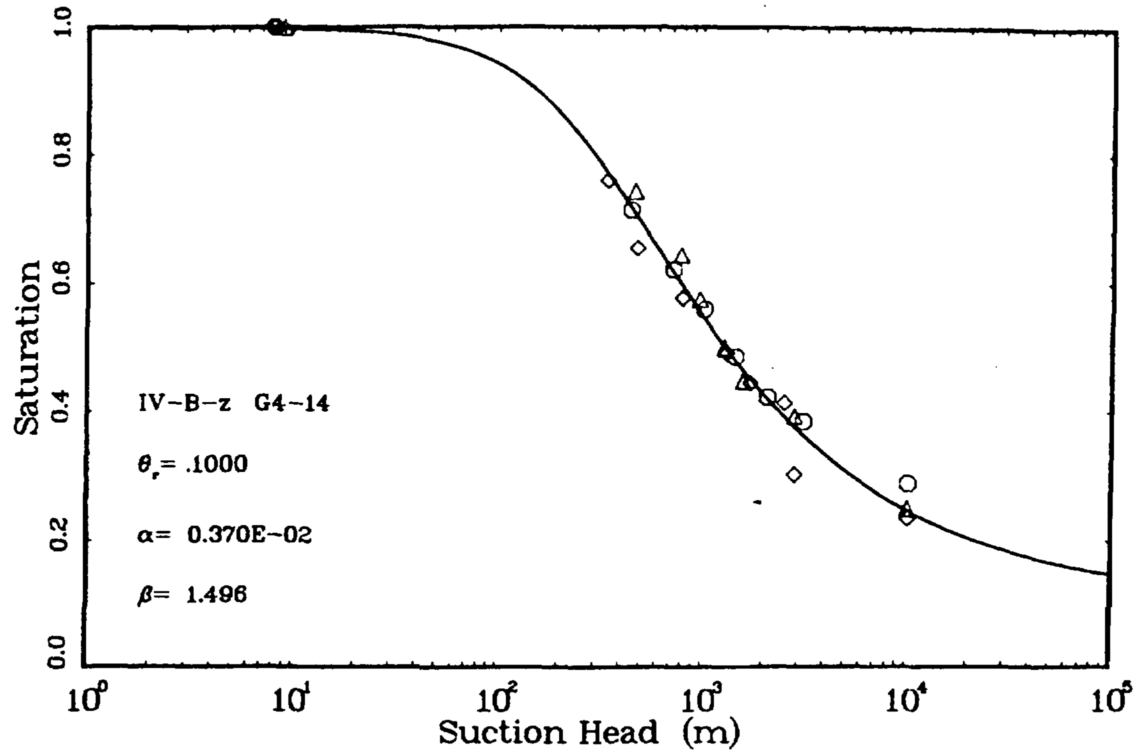


**Figure B.19**

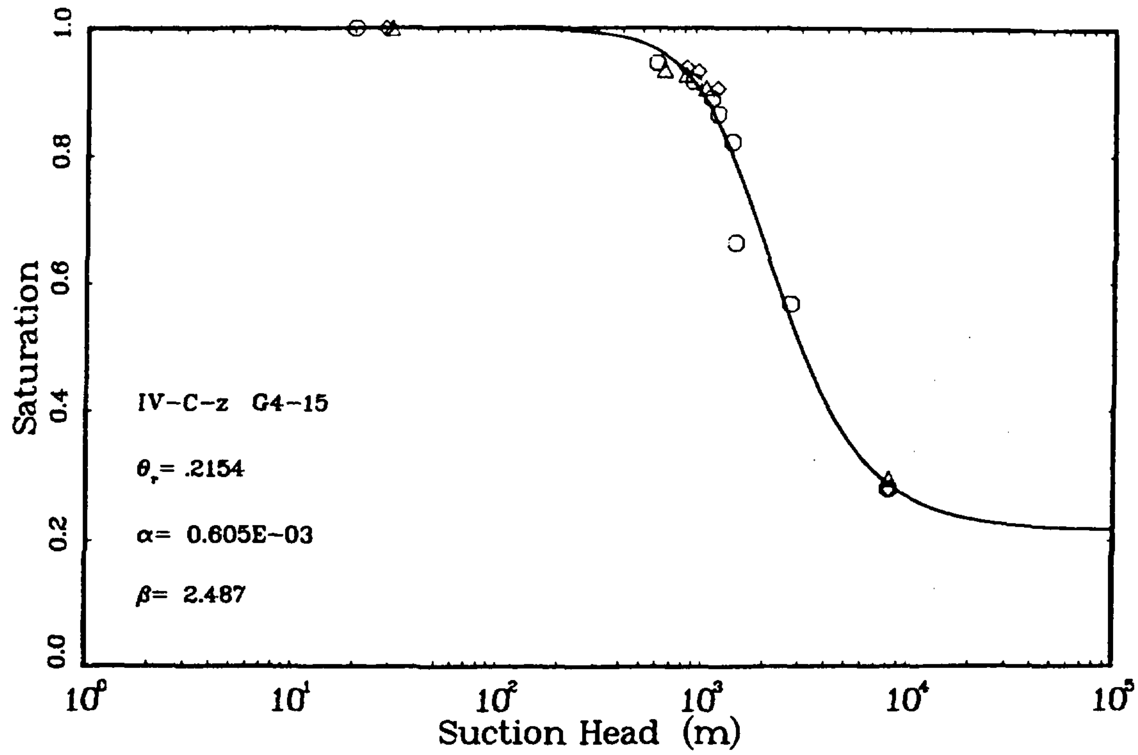


**Figure B.20**

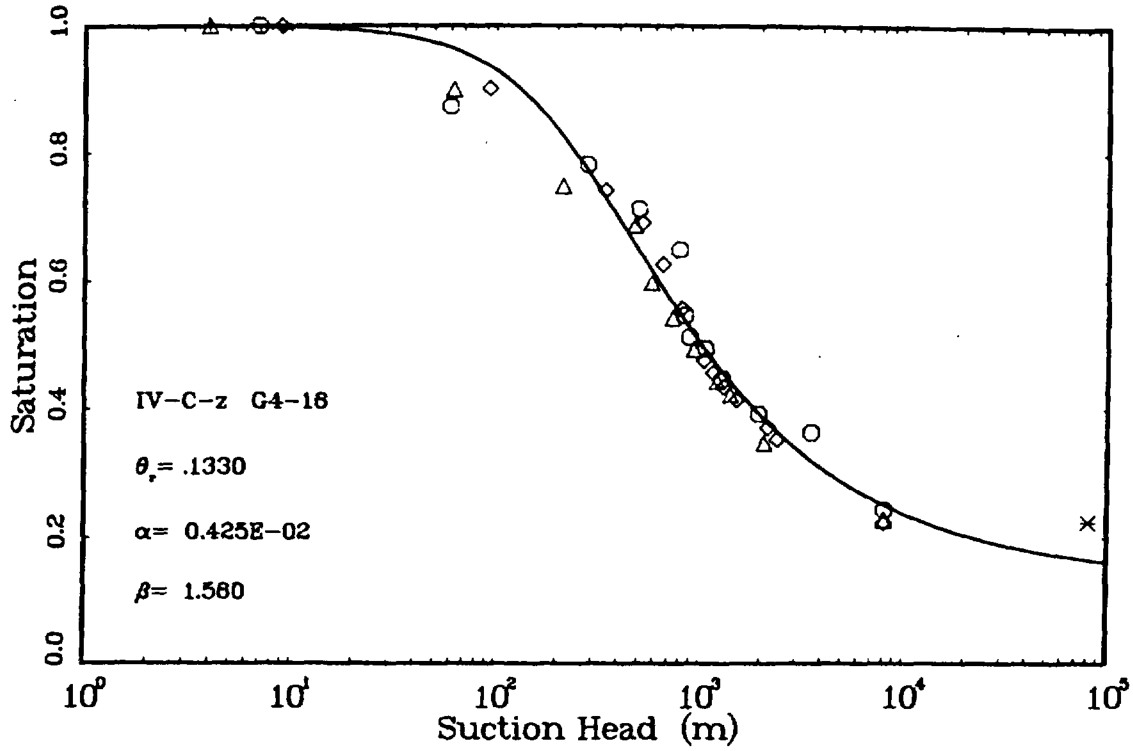


Figure B.21

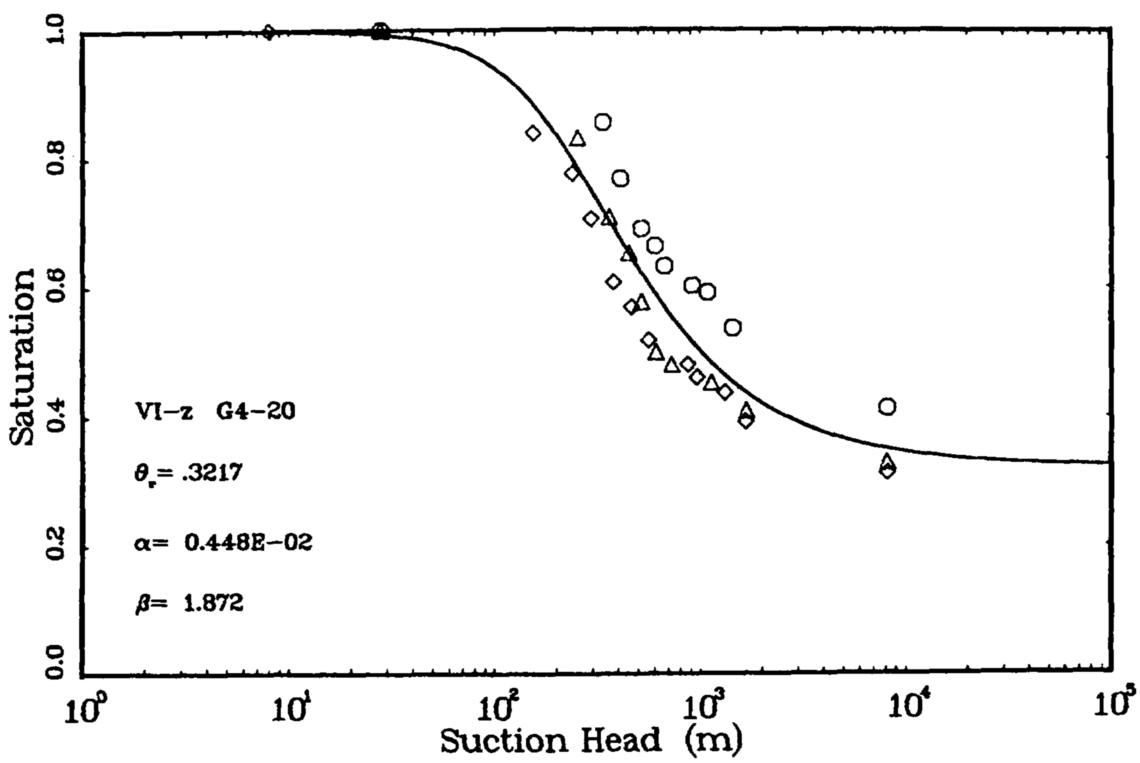


Figure B.22

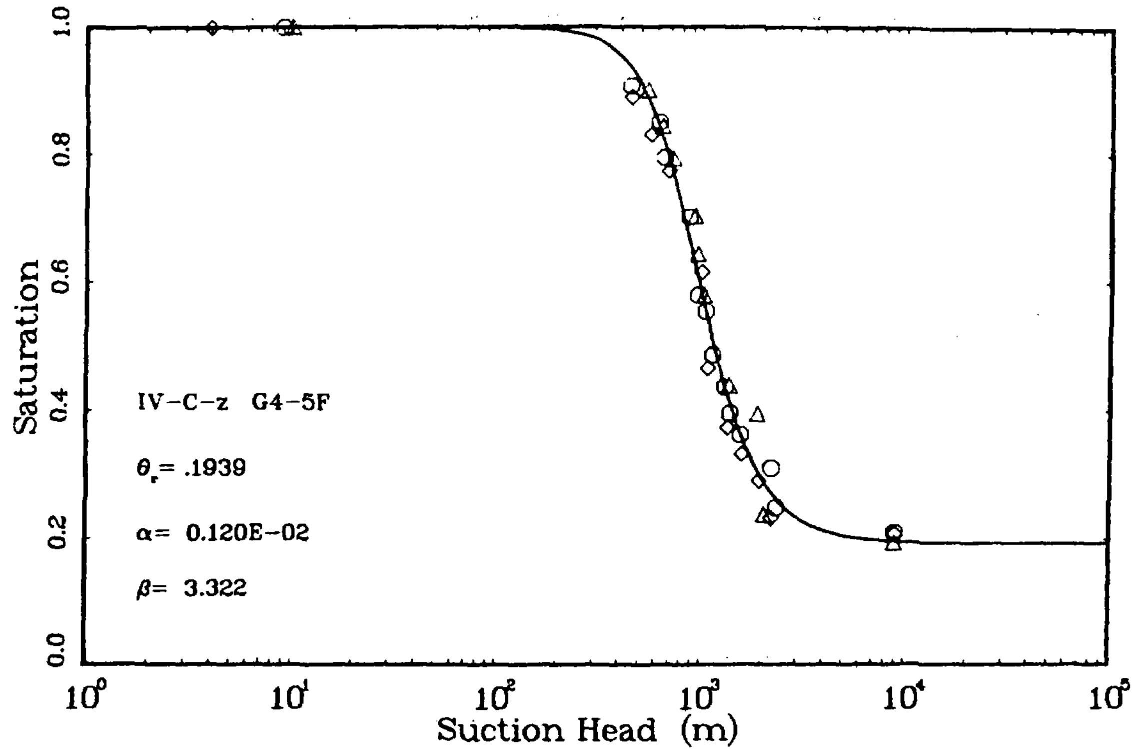


**Figure B.23**

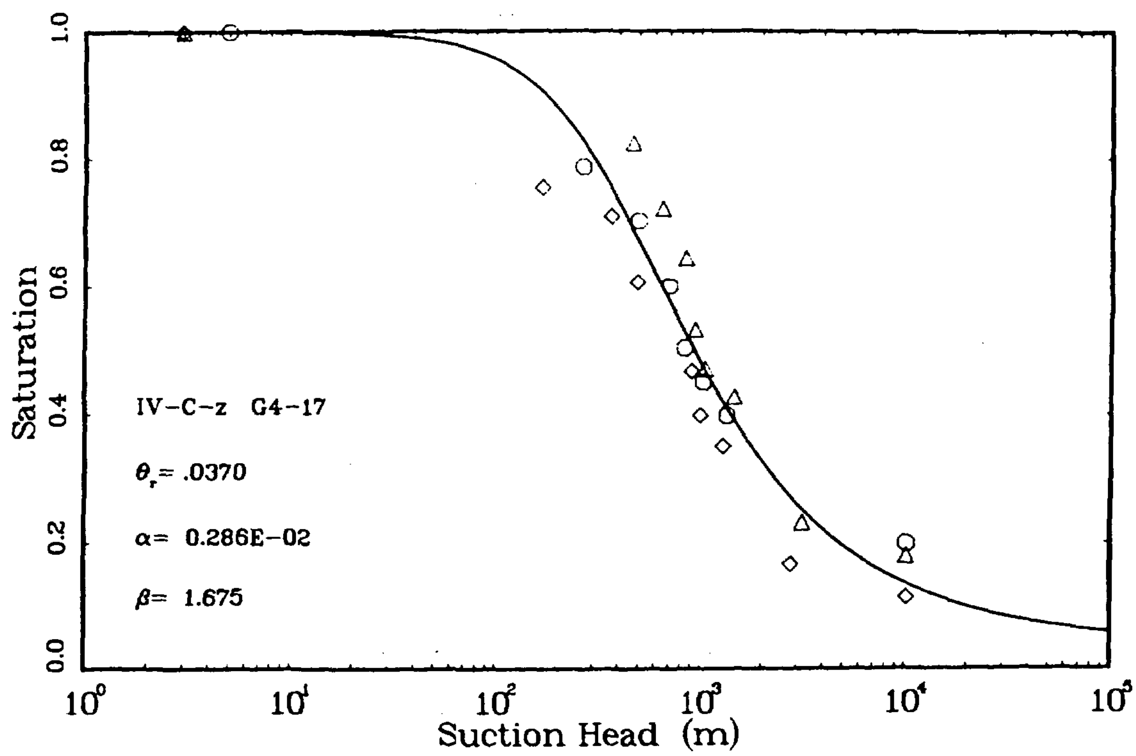


**Figure B.24**

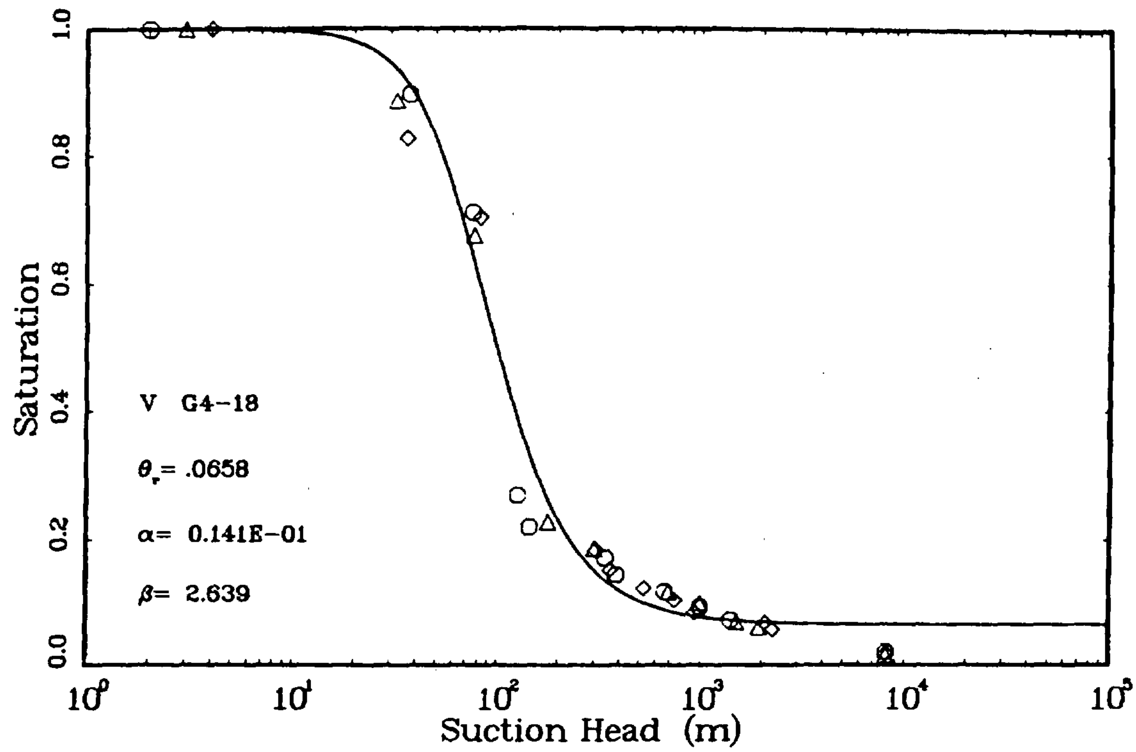


**Figure B.25**

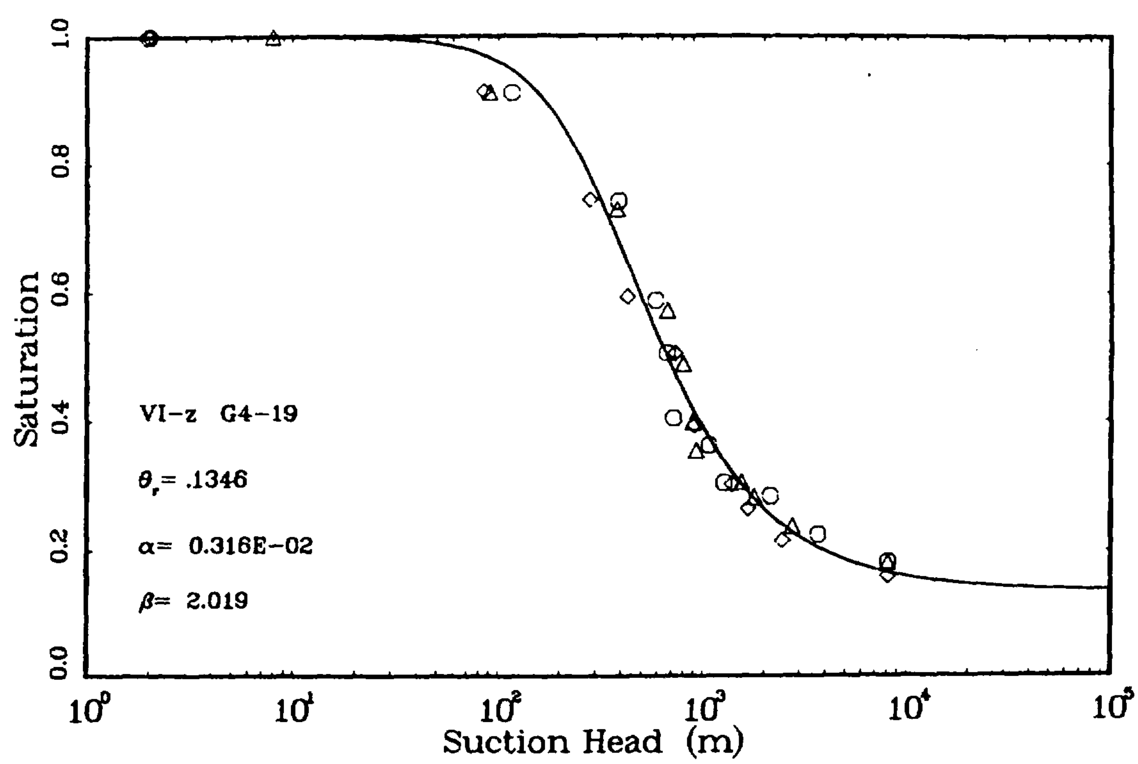


**Figure B.26**

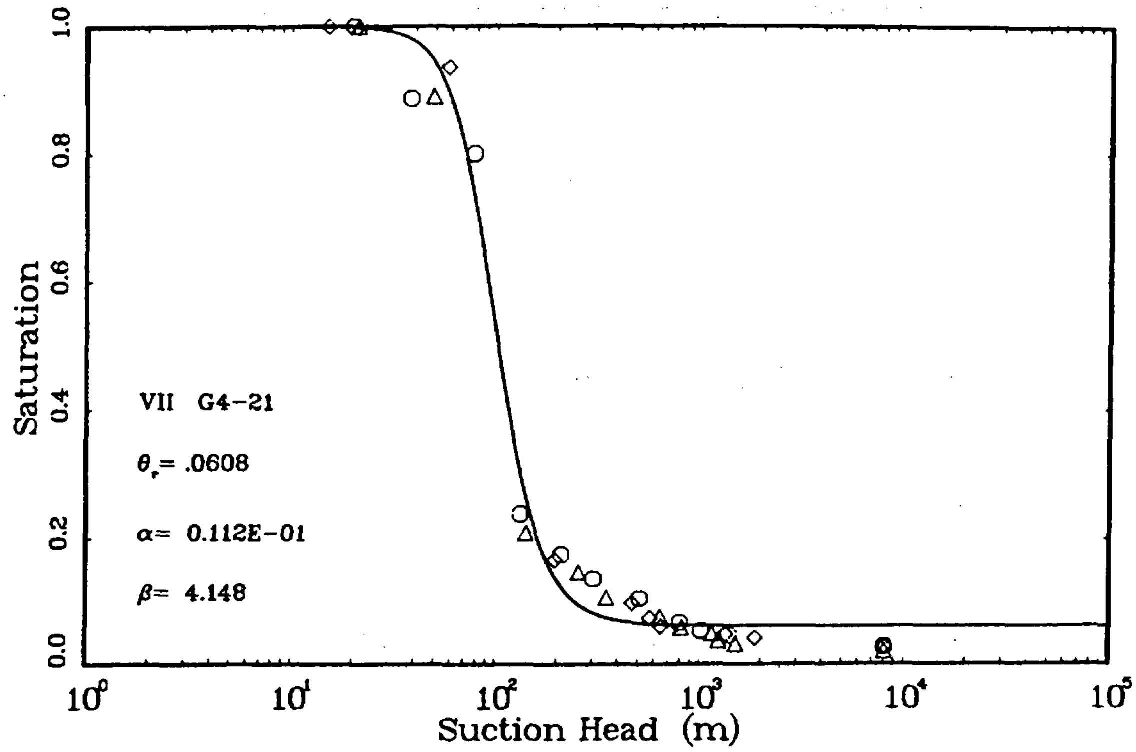


Figure B.27

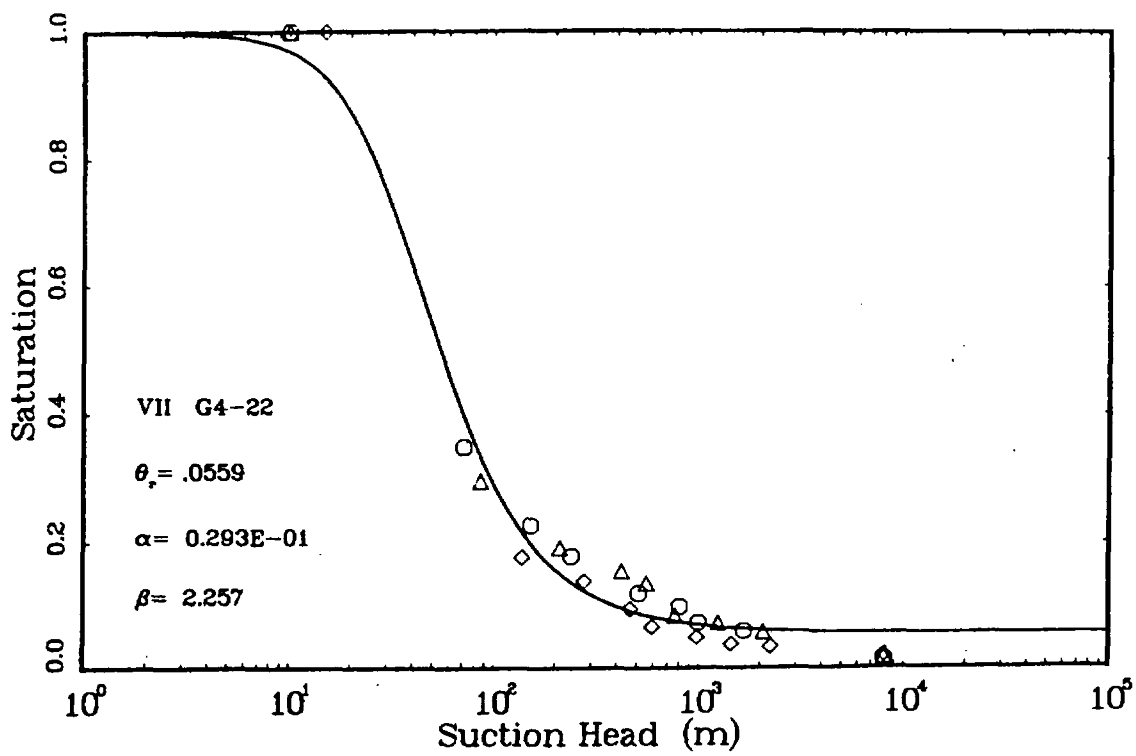


Figure B.28

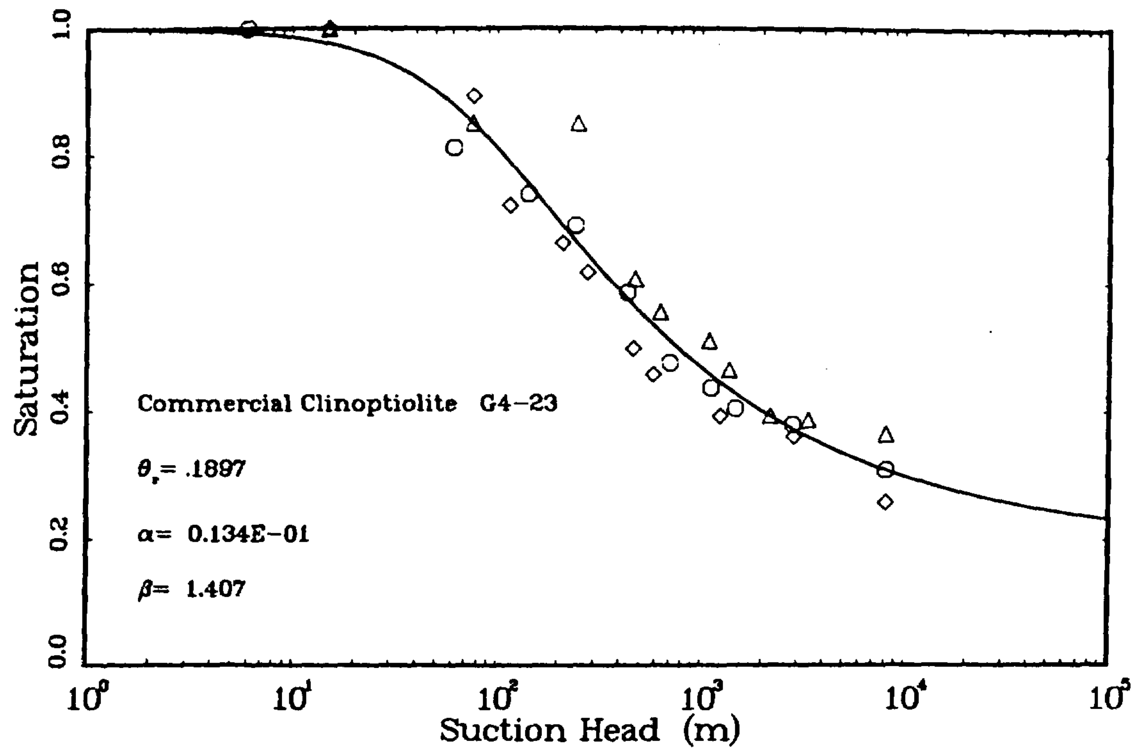


**Figure B.29**

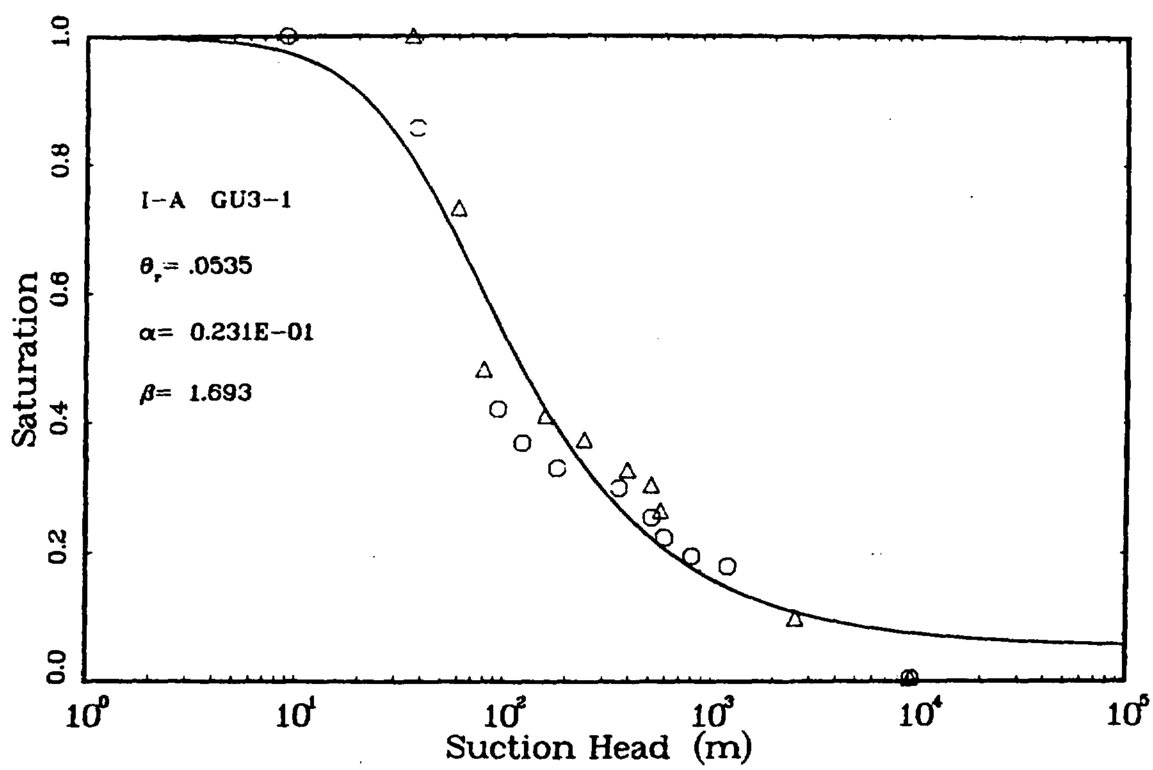


**Figure B.30**

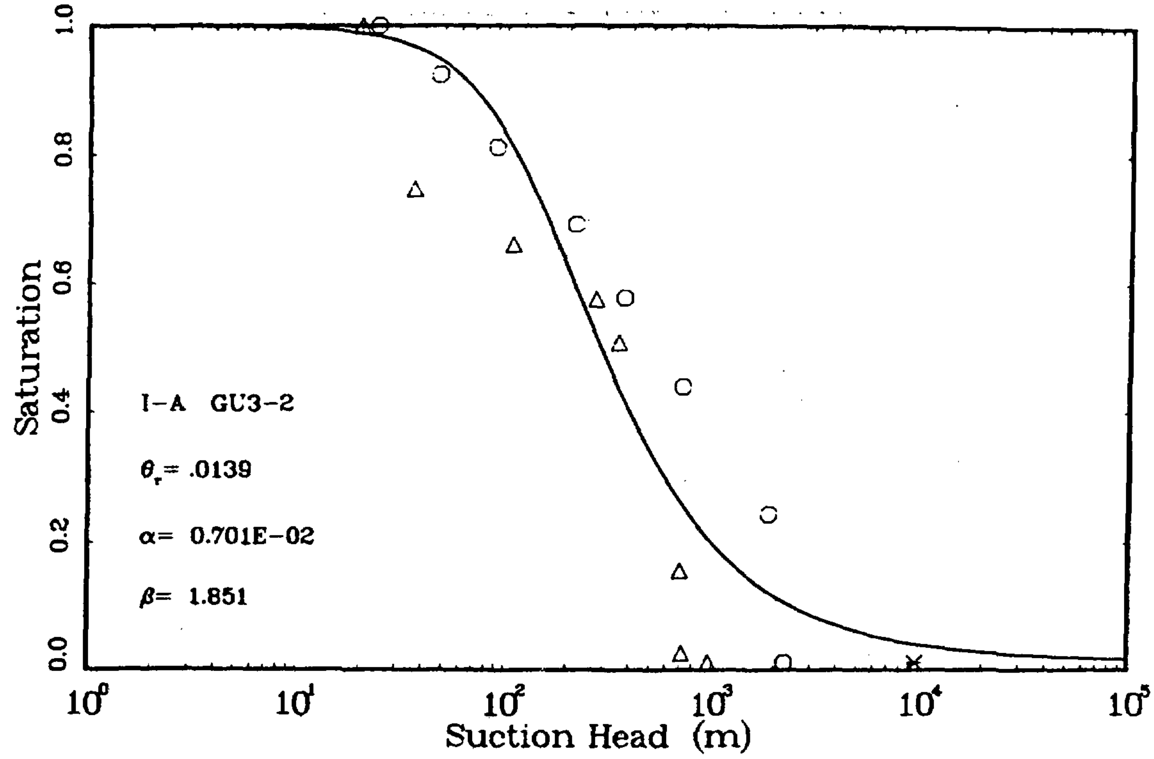


**Figure B.31**

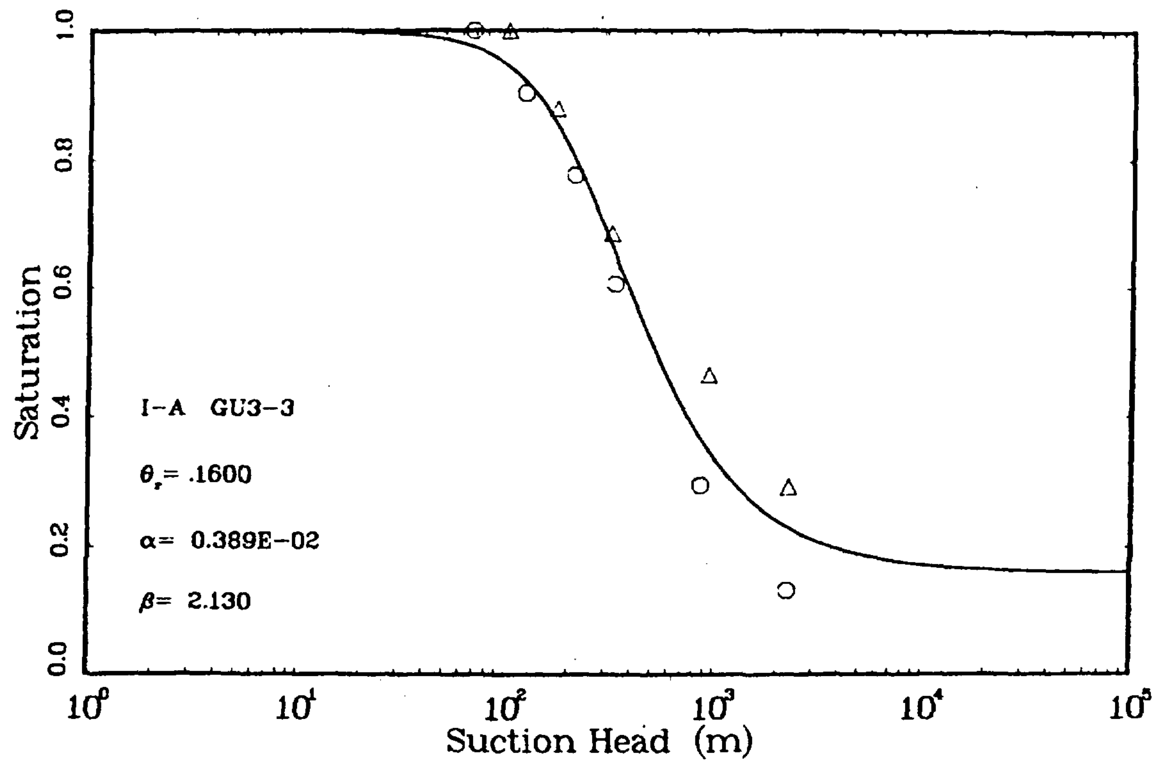


**Figure B.32**

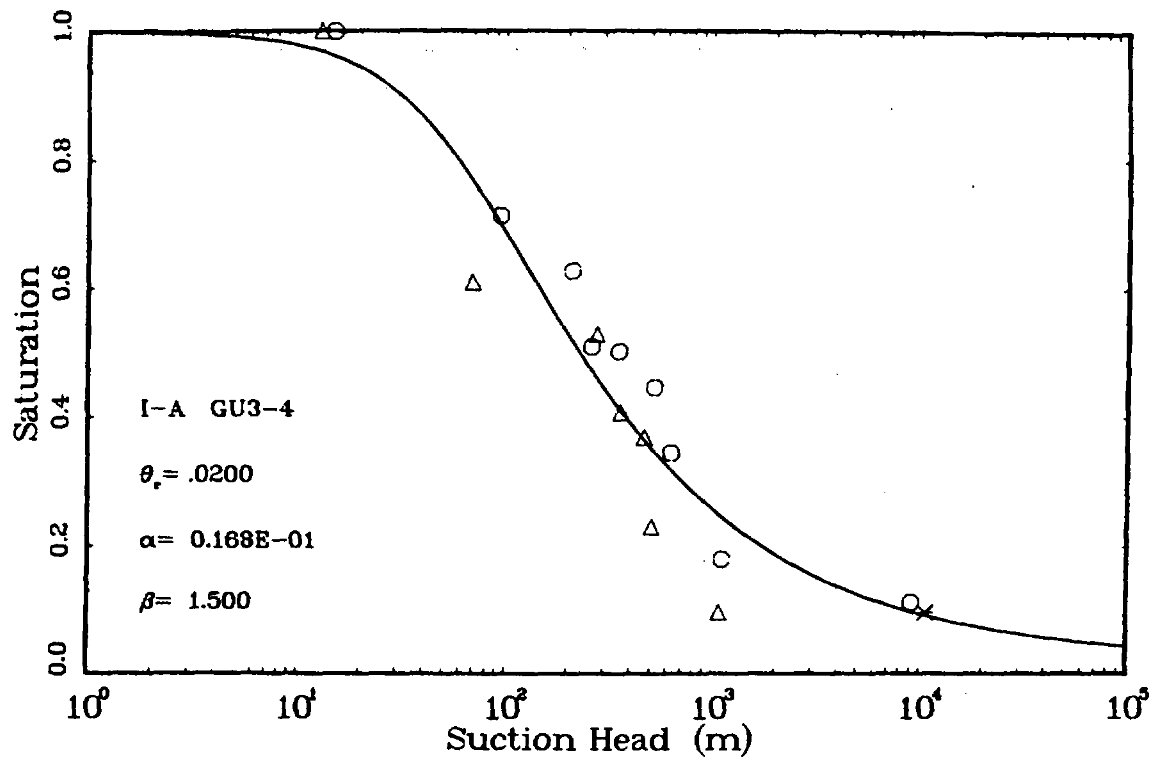


**Figure B.33**

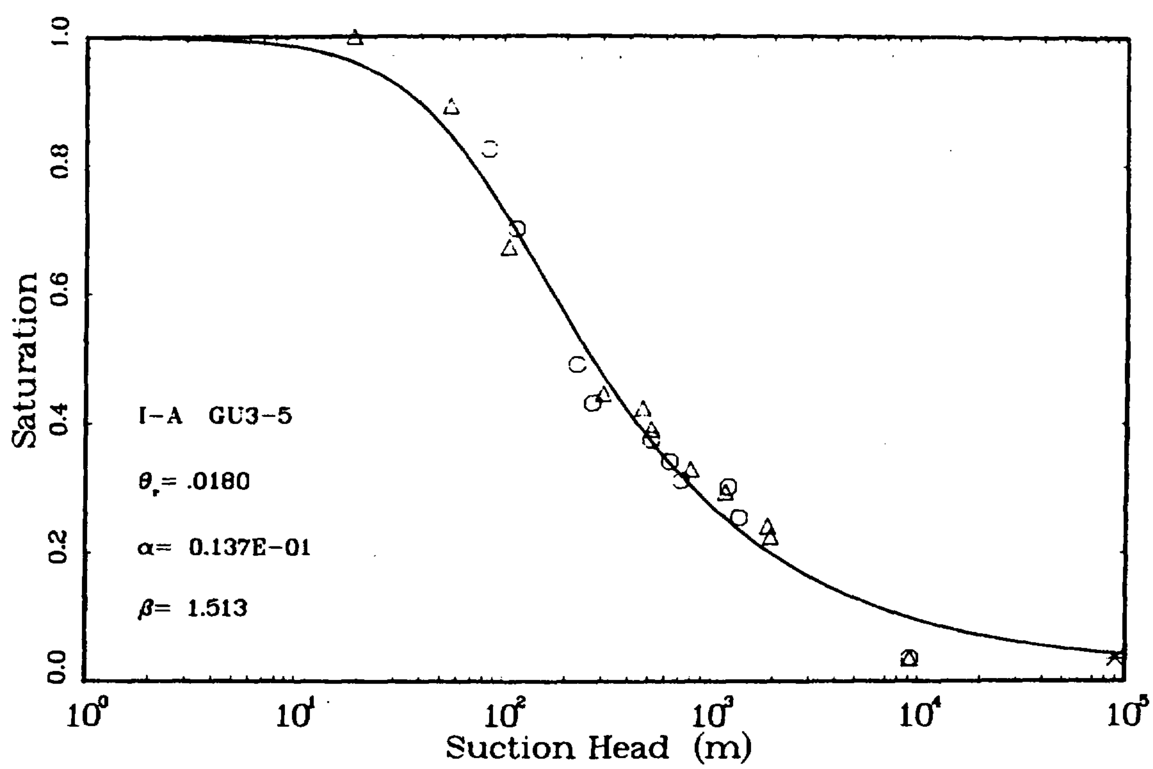


**Figure B.34**

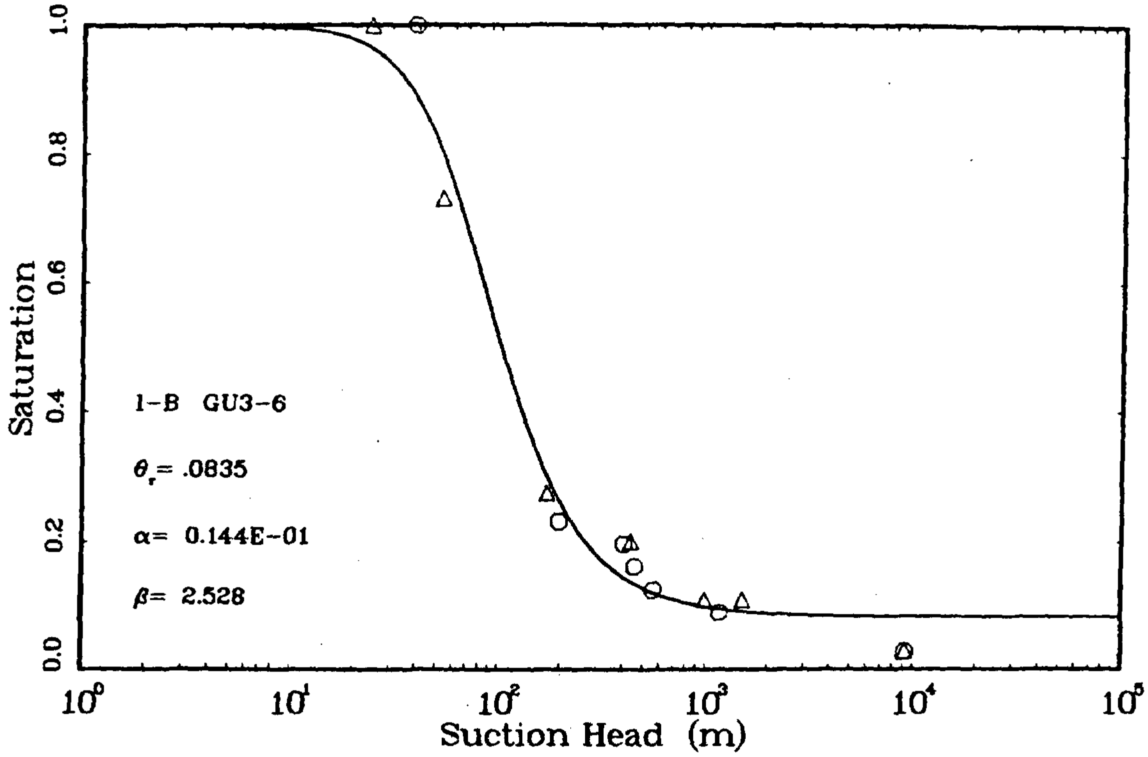


**Figure B.35**

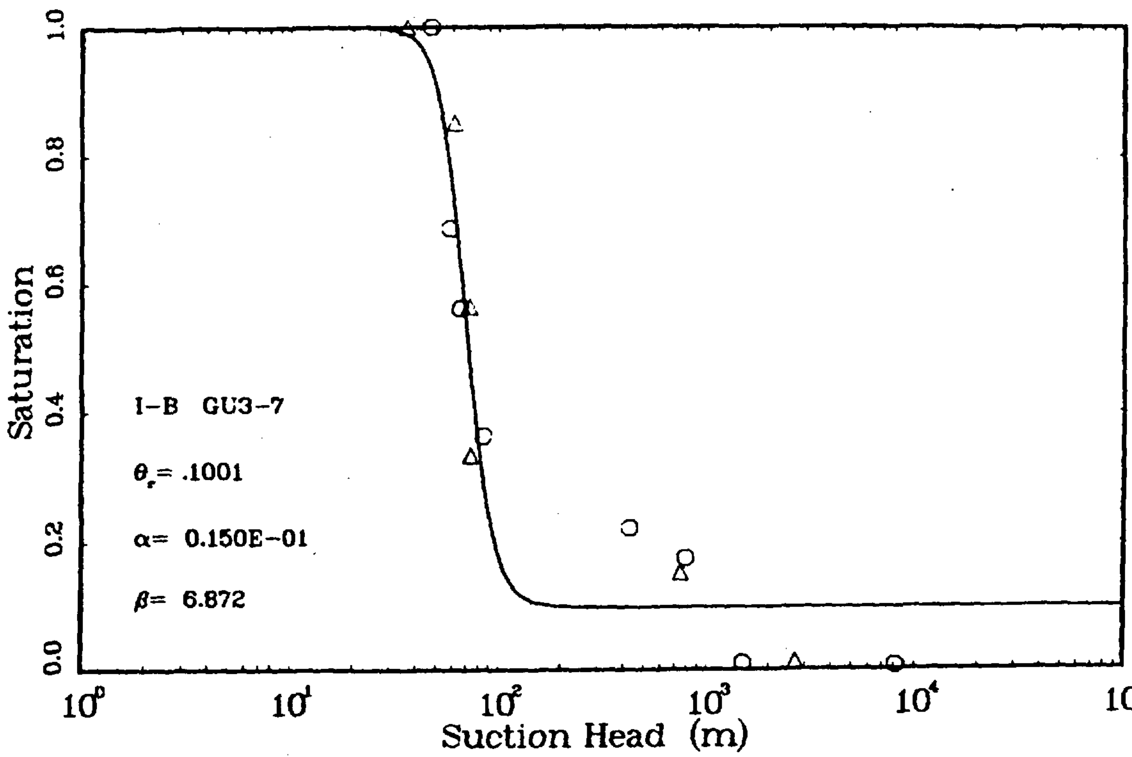


**Figure B.36**

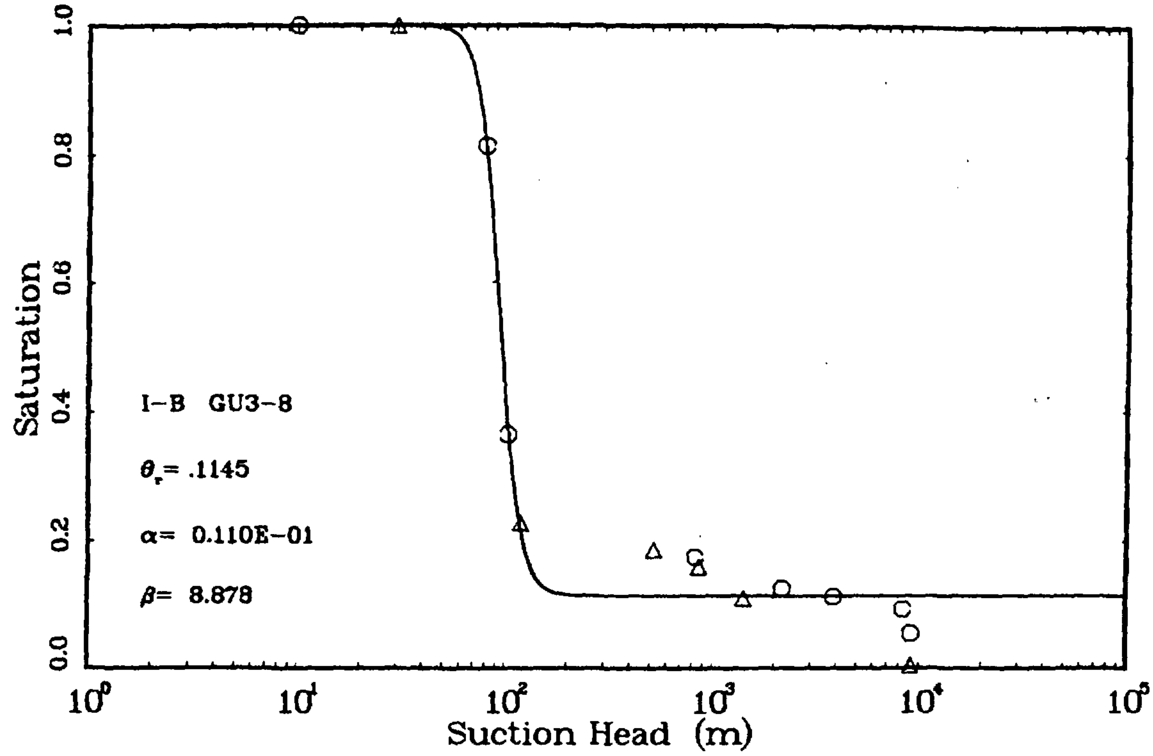


**Figure B.37**

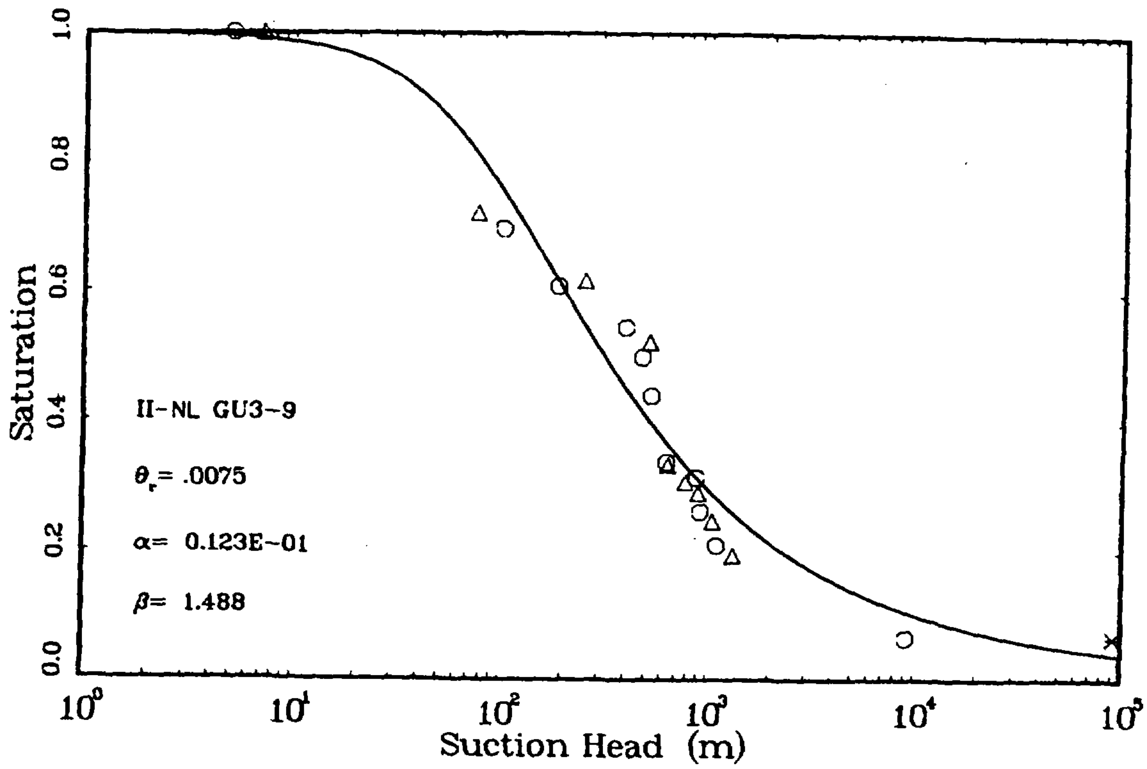


**Figure B.38**

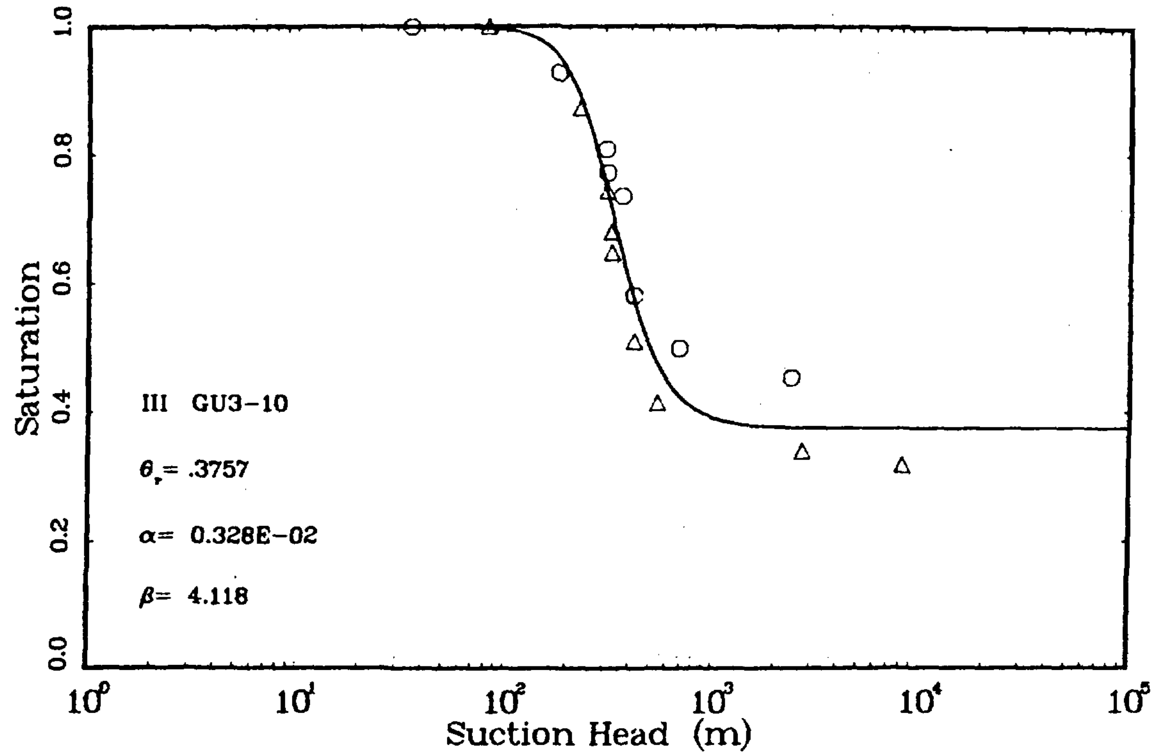


**Figure B.39**

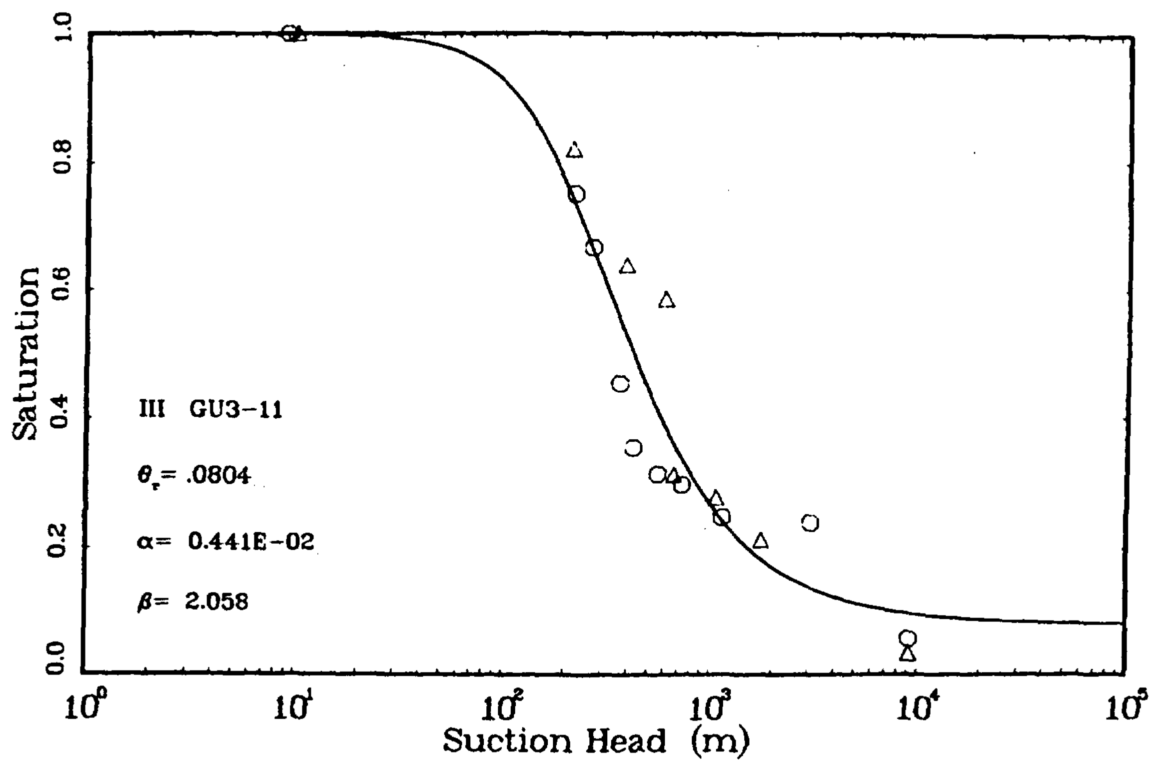


**Figure B.40**

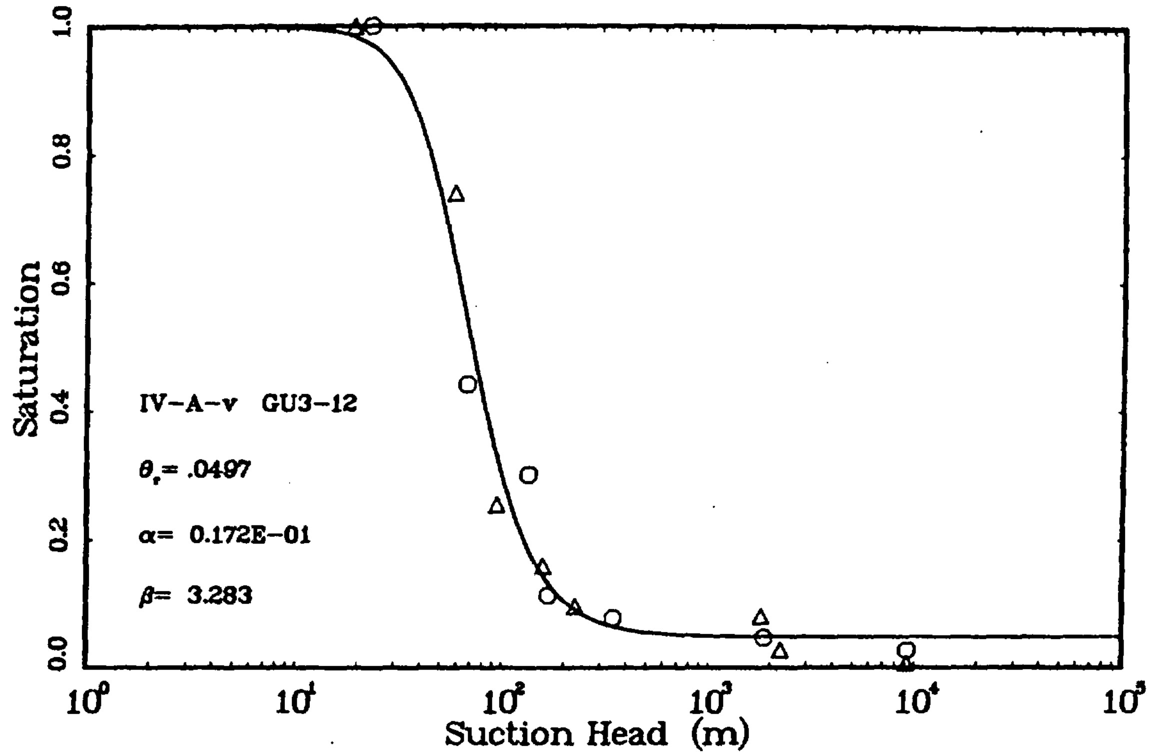


**Figure B.41**

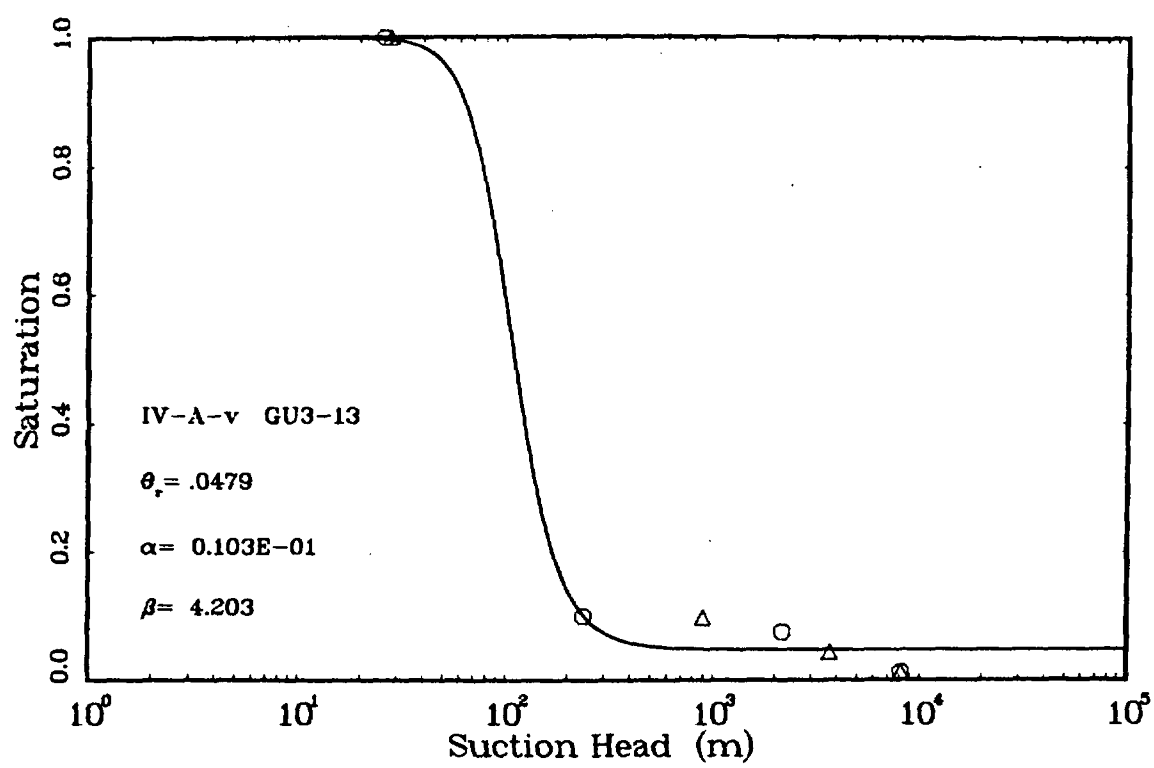


**Figure B.42**

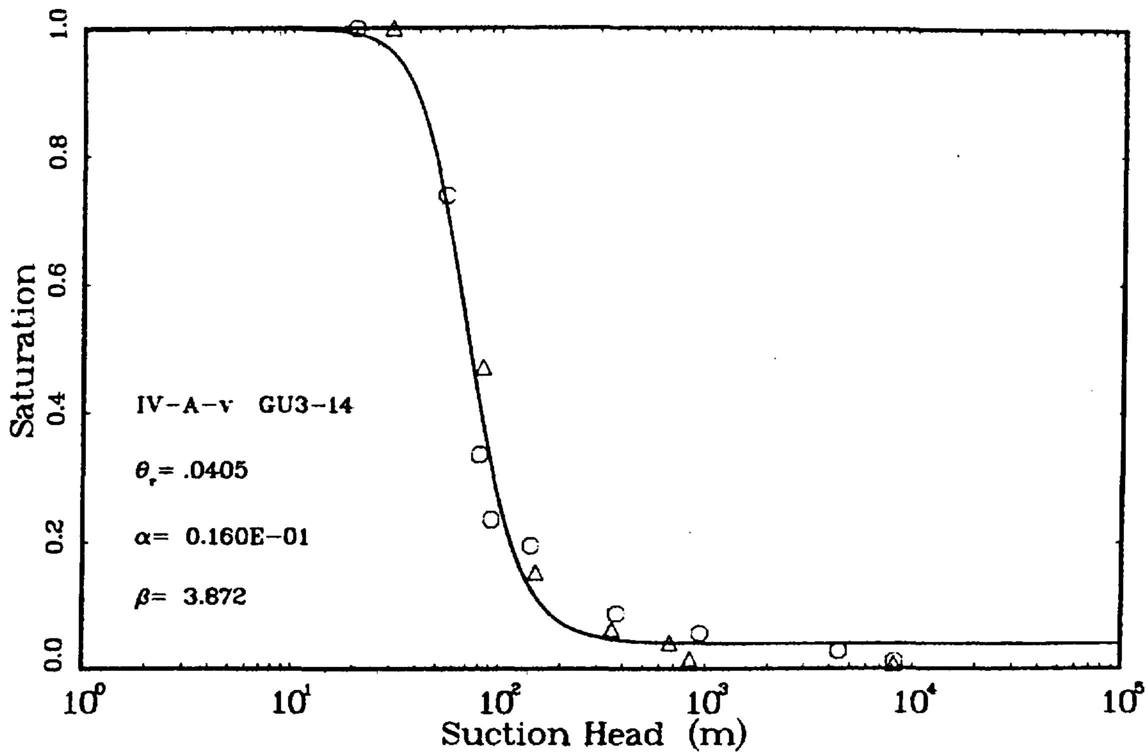


**Figure B.43**

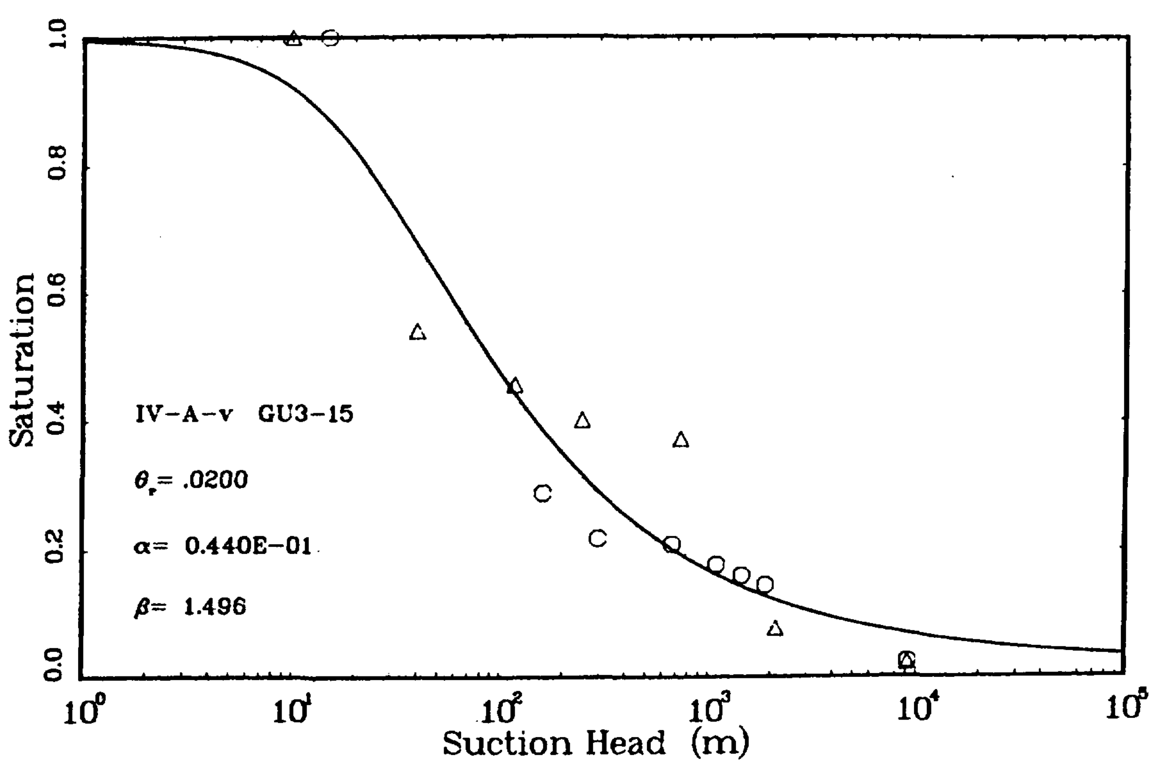


**Figure B.44**

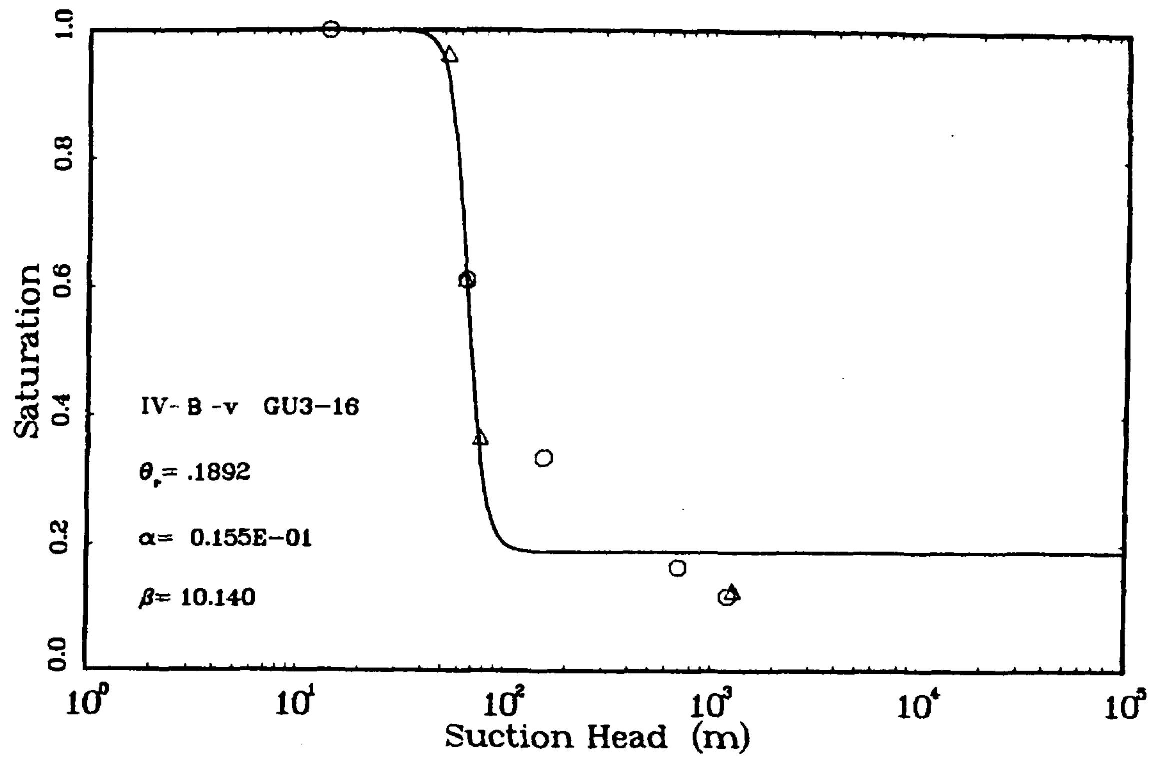


Figure B.45

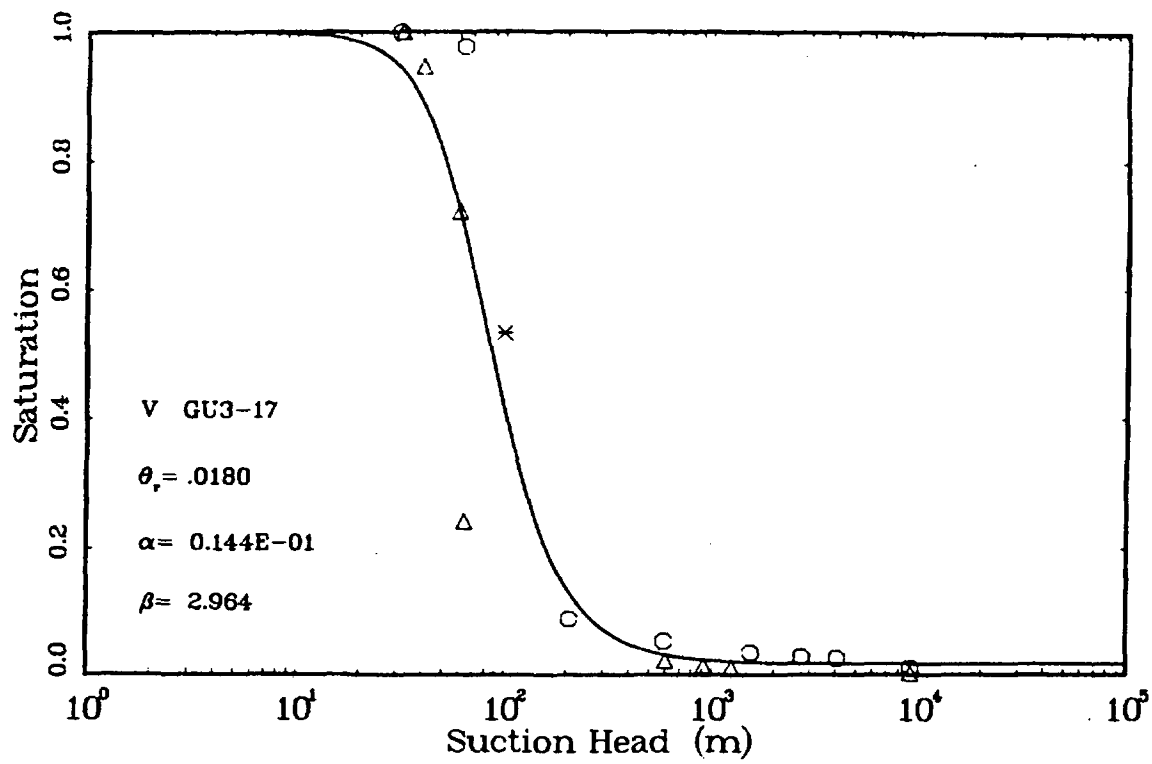


Figure B.46

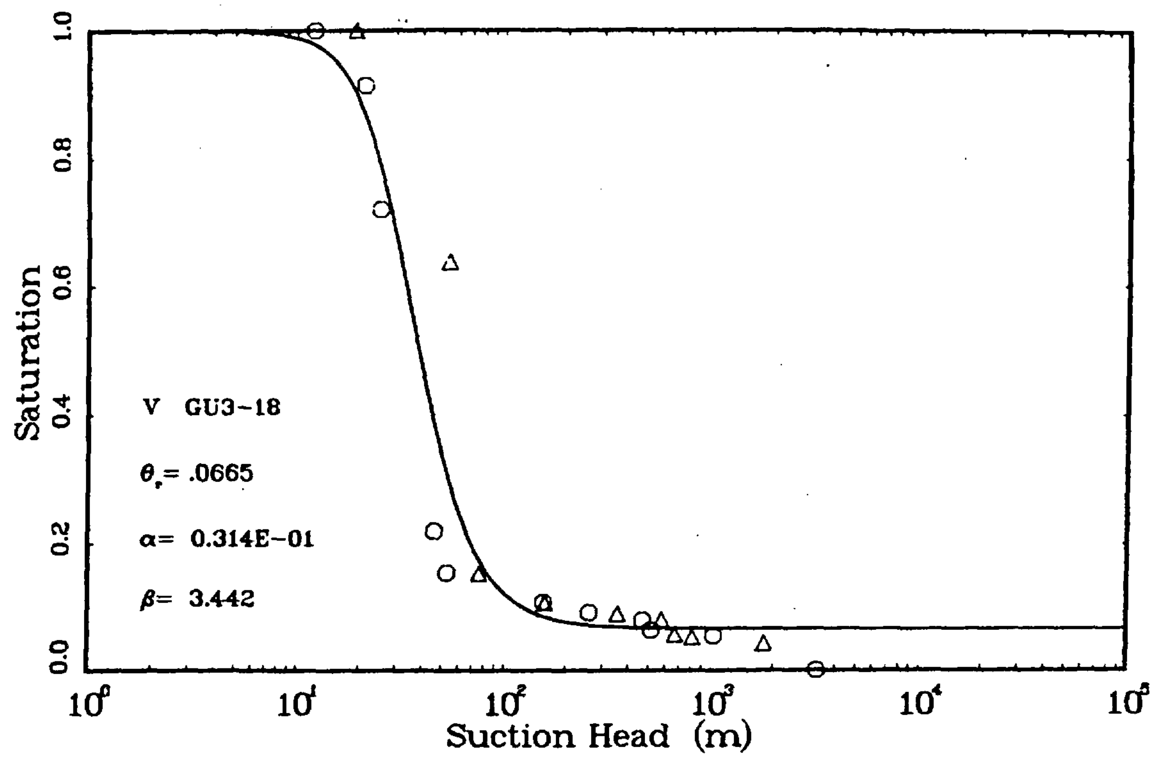


**Figure B.47**

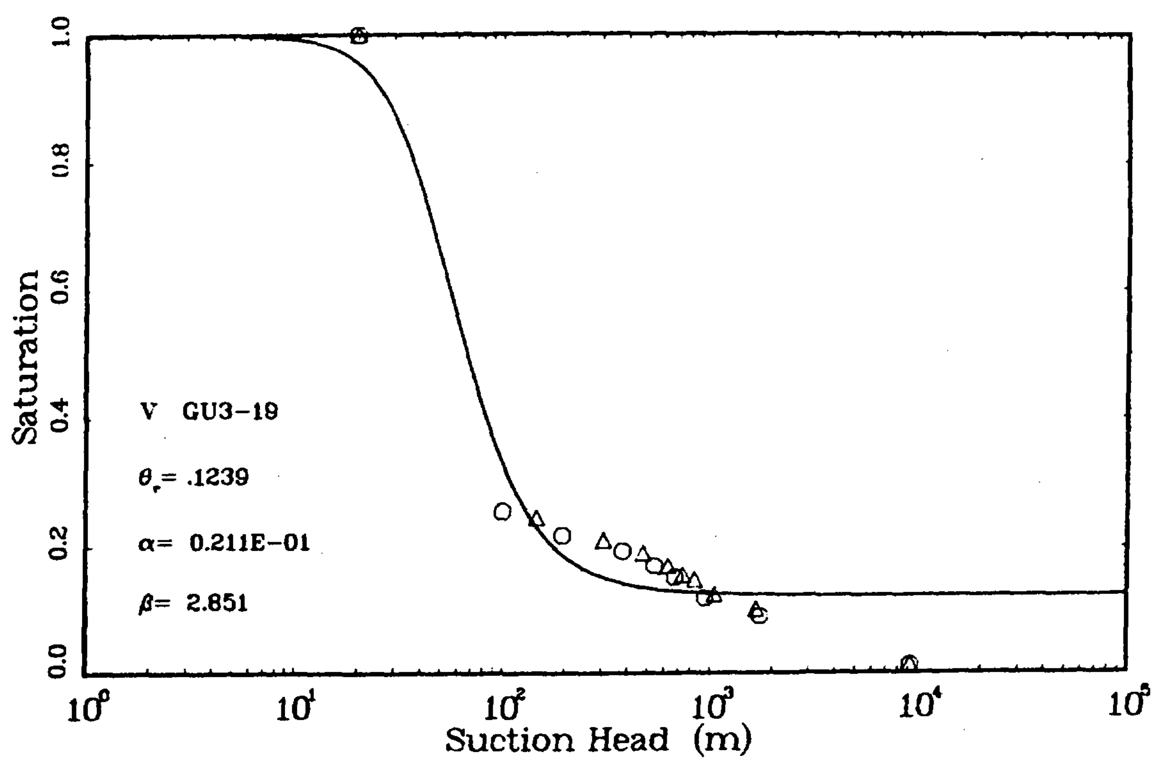


**Figure B.48**

# APPENDIX C

## COMPARISON OF SATURATION CURVES AS DETERMINED BY PSYCHROMETER DATA AND MERCURY-INTRUSION DATA

This appendix contains plots of the psychrometer data, the Van Genuchten curve fit of the psychrometer data, and the adjusted mercury-intrusion data. The manner in which these data were taken and analyzed is discussed in the text, particularly in the section TEST METHODS--WATER RETENTION and the first three subsections of RESULTS OF WATER RETENTION TESTING.

The root-mean-square (RMS) difference between the mercury-intrusion data points and the curve fit of the pyschrometer data in the suction head range of 10 to 3000 m (corresponding roughly to a pore size range of 50 to 15,000 angstroms) was calculated and the results are listed in Table C.1. The values listed in Table C.1 indicate the quantitative agreement between the mercury-intrusion data and the psychrometer data. The degree of agreement between the two testing methods indicated by this table agrees with that reached from a visual inspection of the figures. For example, the RMS difference for sample G4-5 is.05, which indicates good agreement; inspection of Figure C.4 confirms this conclusion. Sample G4-3 has a RMS difference of .37, which indicates poor agreement; inspection of Figure C.3 confirms this conclusion.

TABLE C.1 RMS Difference* Between the Mercury Intrusion Data and the Van Genuchten Fit of the Psychrometer Data

| Sample | Depth (ft) | Unit | RMS Difference |
|---|---|---|---|
| G4-1 | 43 | I-A | 0.174 |
| G4-2 | 124 | I-B | 0.139 |
| G4-3 | 208 | I-B | 0.369 |
| G4-5 | 864 | II-NL | 0.098 |
| G4-24 | 864 | II-NL | 0.425 |
| G4-6 | 1158 | II-NL | 0.079 |
| G4-7 | 1256 | II-NL | 0.079 |
| G4-8 | 1299 | III | 0.056 |
| G4-8 | 1299 | III | 0.070 |
| G4-10 | 1405 | IV-A-z | 0.088 |
| G4-11 | 1548 | IV-A-z | 0.097 |
| G4-12 | 1686 | IV-A-z | 0.113 |
| G4-13 | 1728 | IV-B-z | 0.275 |
| G4-14 | 1737 | IV-B-z | 0.103 |
| G4-15 | 1769 | IV-C-z | 0.111 |
| G4-16 | 1778 | IV-C-z | 0.128 |
| G4-17 | 1789 | IV-C-z | 0.208 |
| G4-18 | 1899 | V | 0.190 |
| G4-19 | 2006 | VI | 0.134 |
| G4-20 | 2101 | VI | 0.194 |
| G4-21 | 2401 | VII | 0.236 |
| G4-22 | 2407 | VII | 0.111 |
| G4-23 | Anaconda | 1010A | 0.138 |

$$*\text{RMS Difference} = \left( \frac{\sum_{h=10m}^{3000m} (Y_p(h) - Y_{Hg}(h))^2}{N} \right)^{\frac{1}{2}}$$

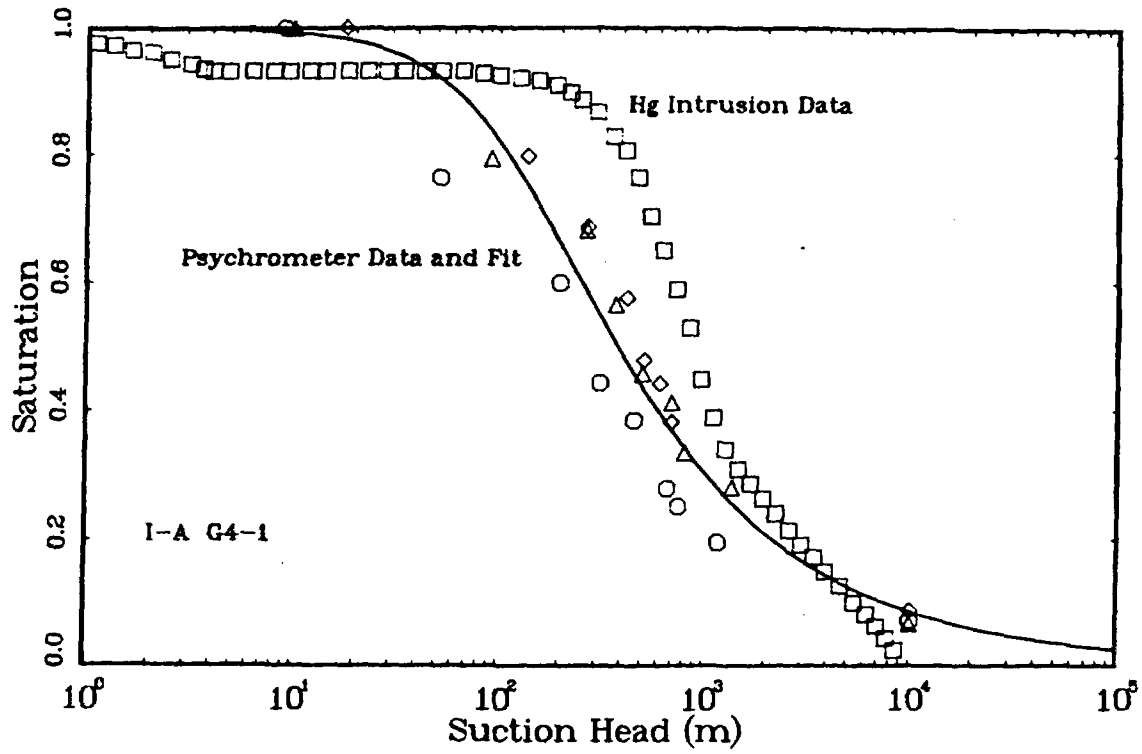


**Figure C.1**

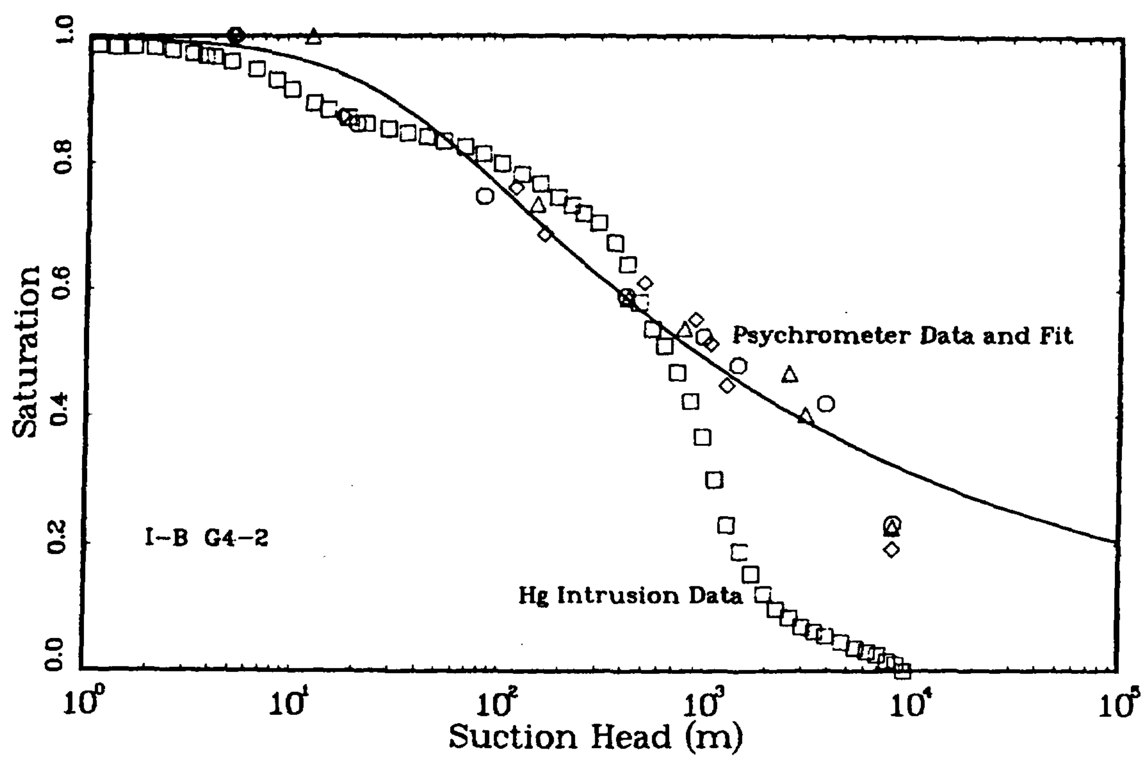


**Figure C.2**

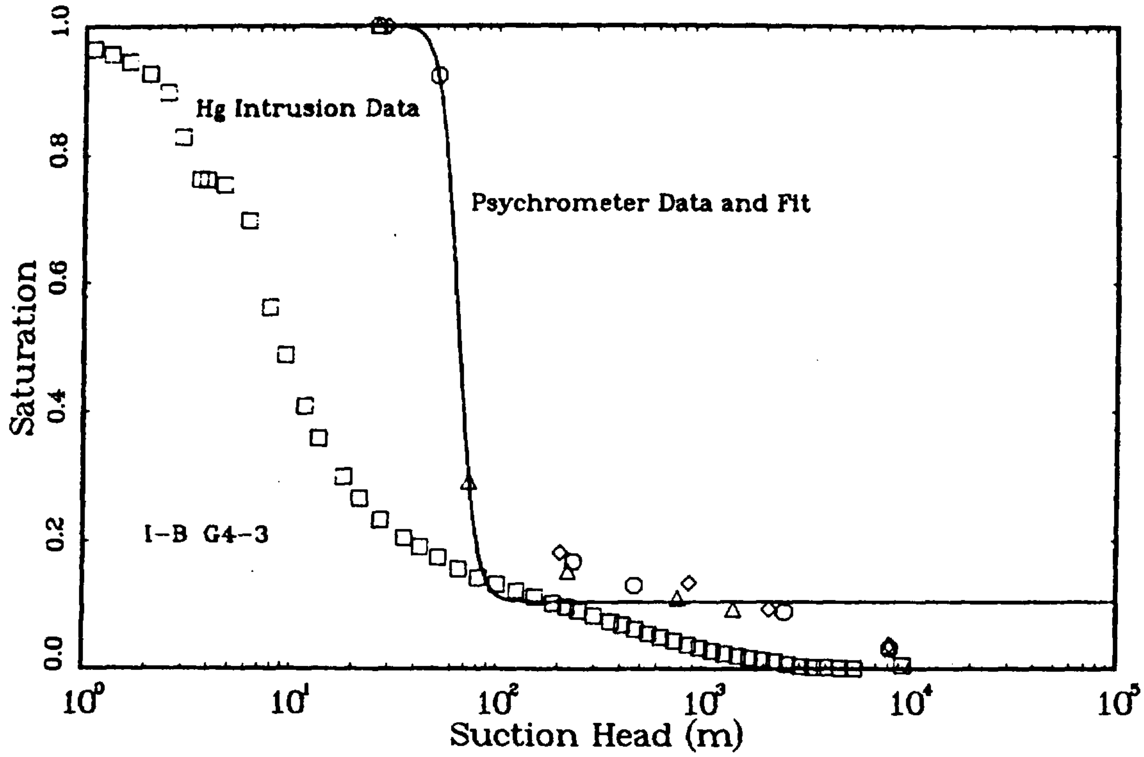


**Figure C.3**

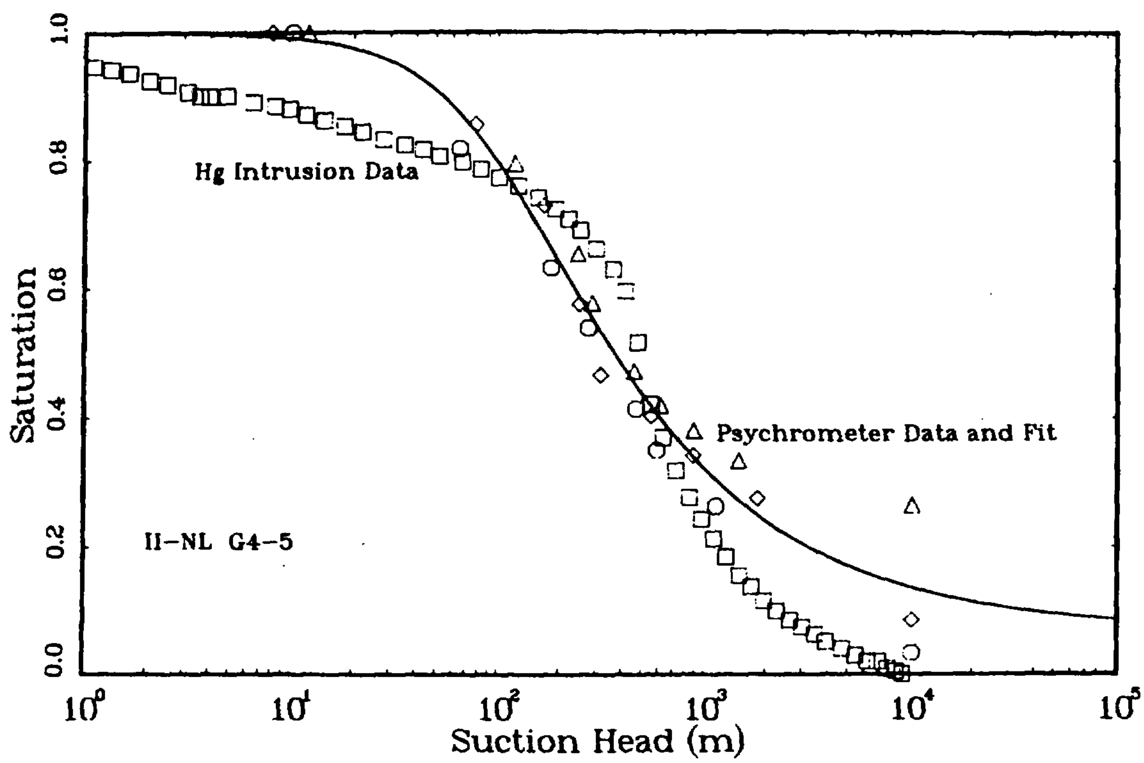


**Figure C.4**

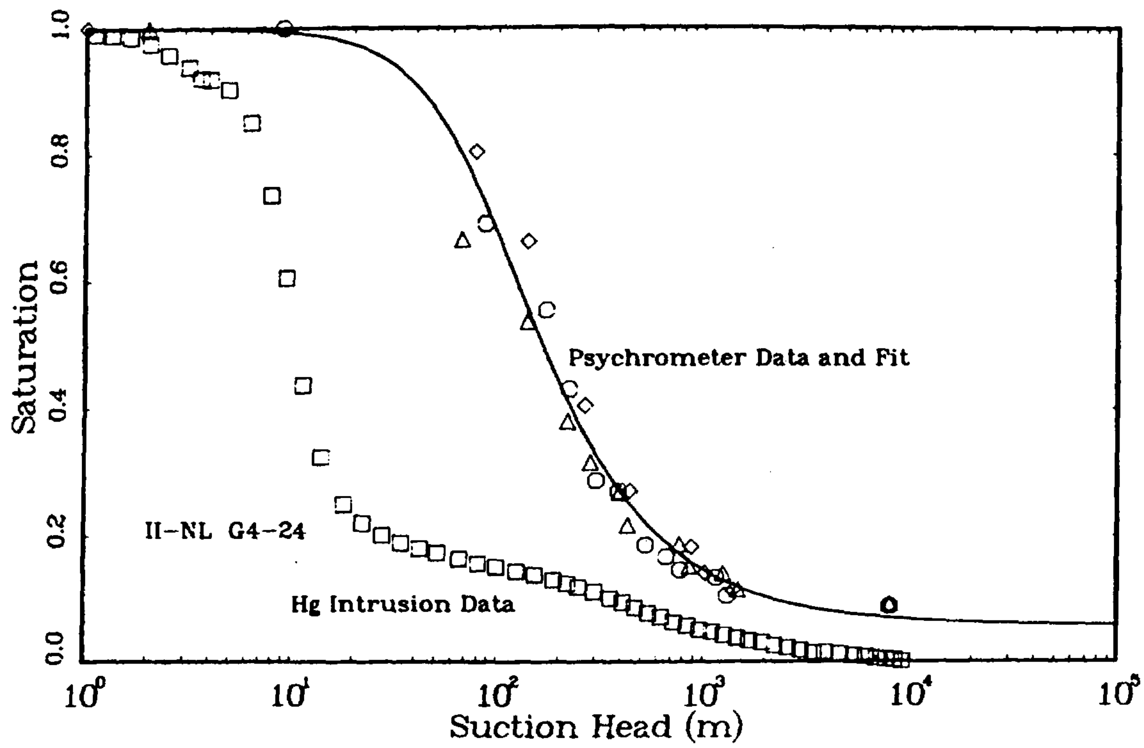


**Figure C.5**

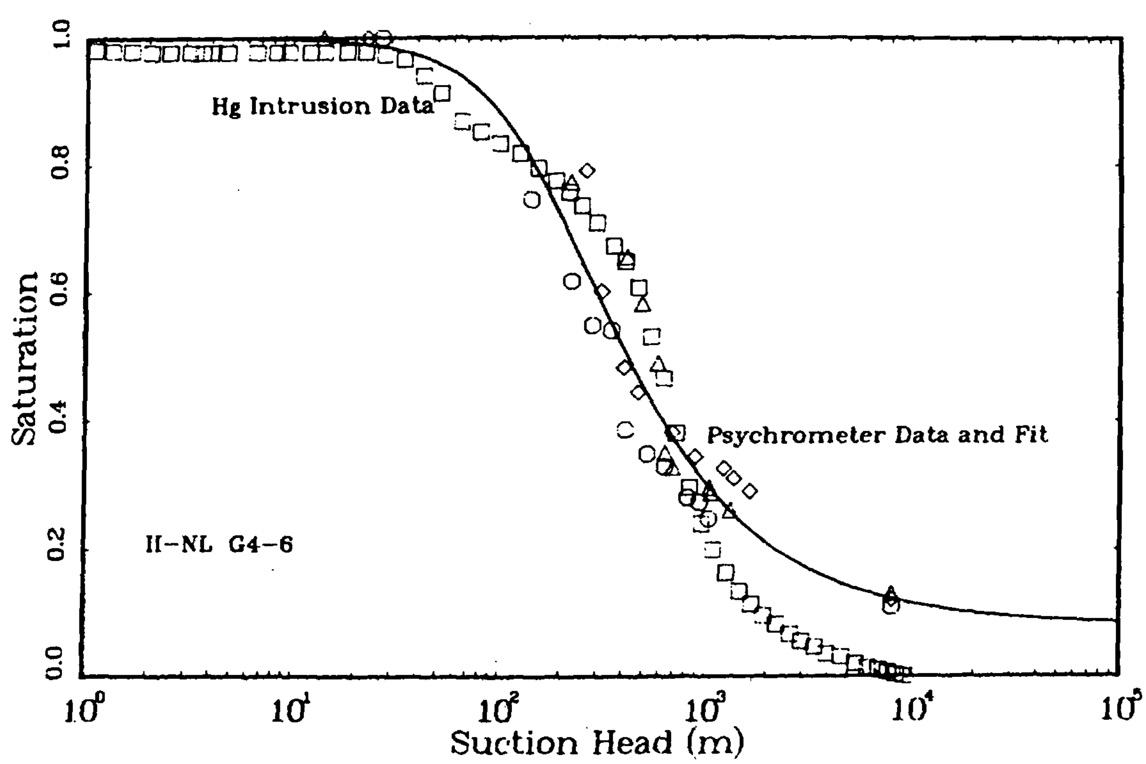


**Figure C.6**

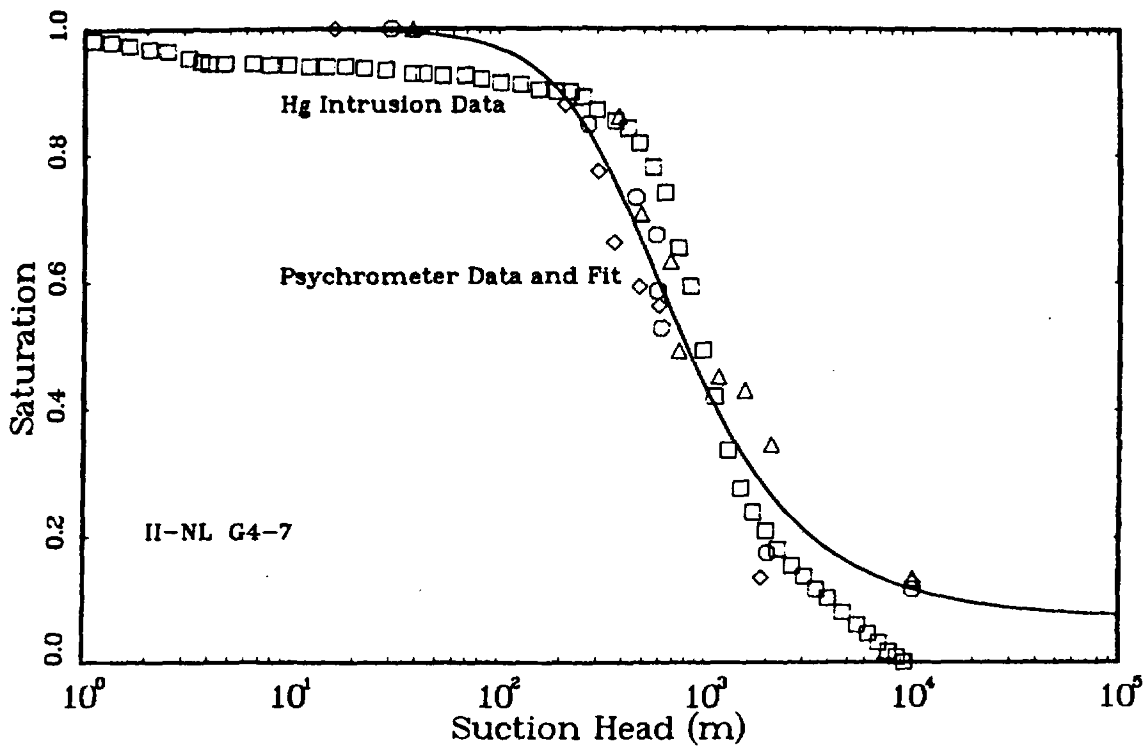


**Figure C.7**

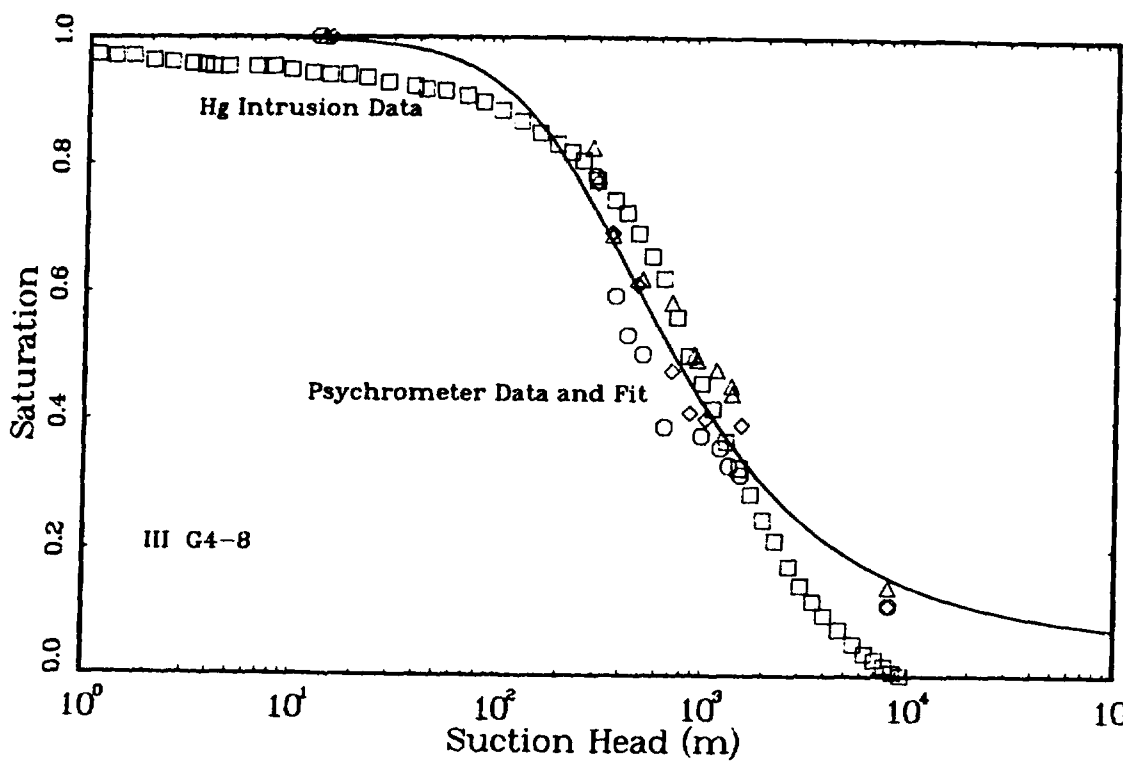


**Figure C.8**

**(Note: This is the result of the first of two Hg Intrusion tests on III G4-8)**

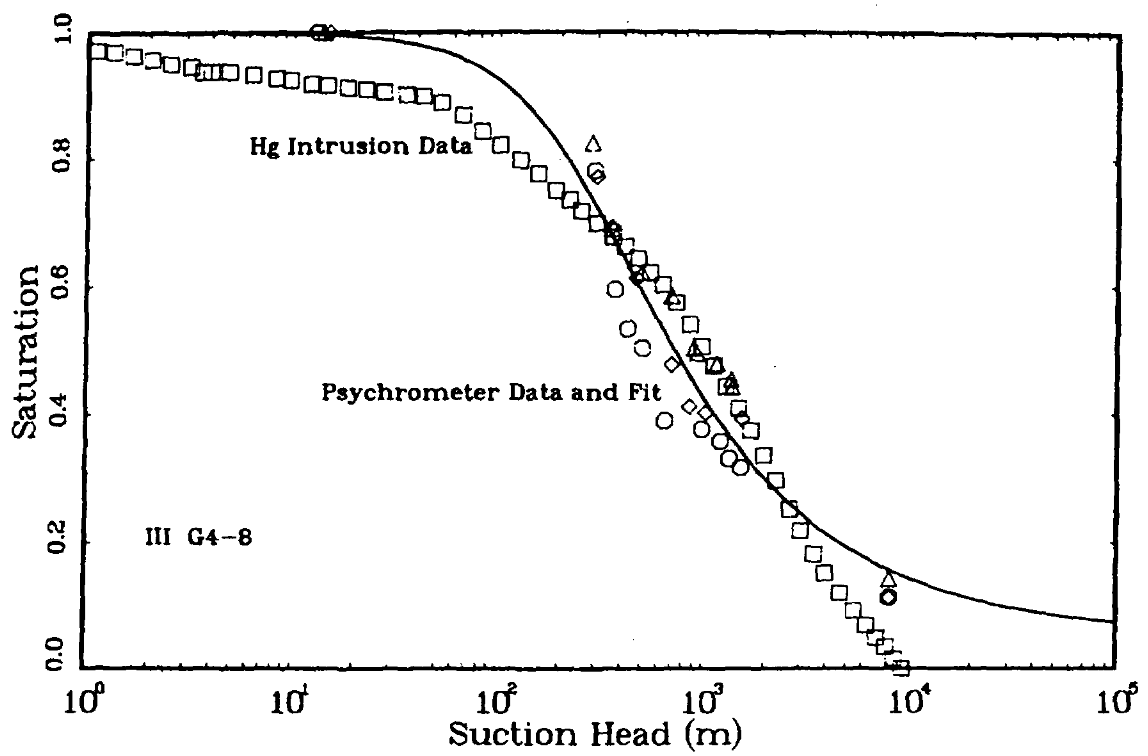


(Note: This is the result of the second of two Hg Intrusion tests on III G4-8)

Figure C.9

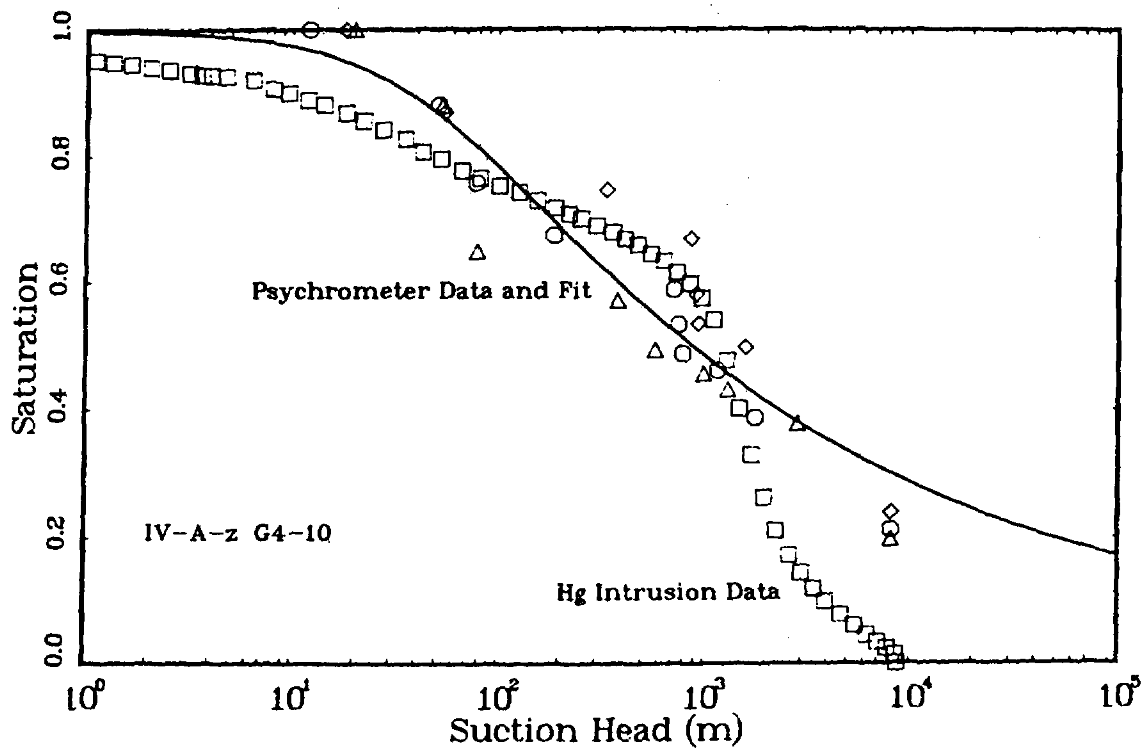


Figure C.10

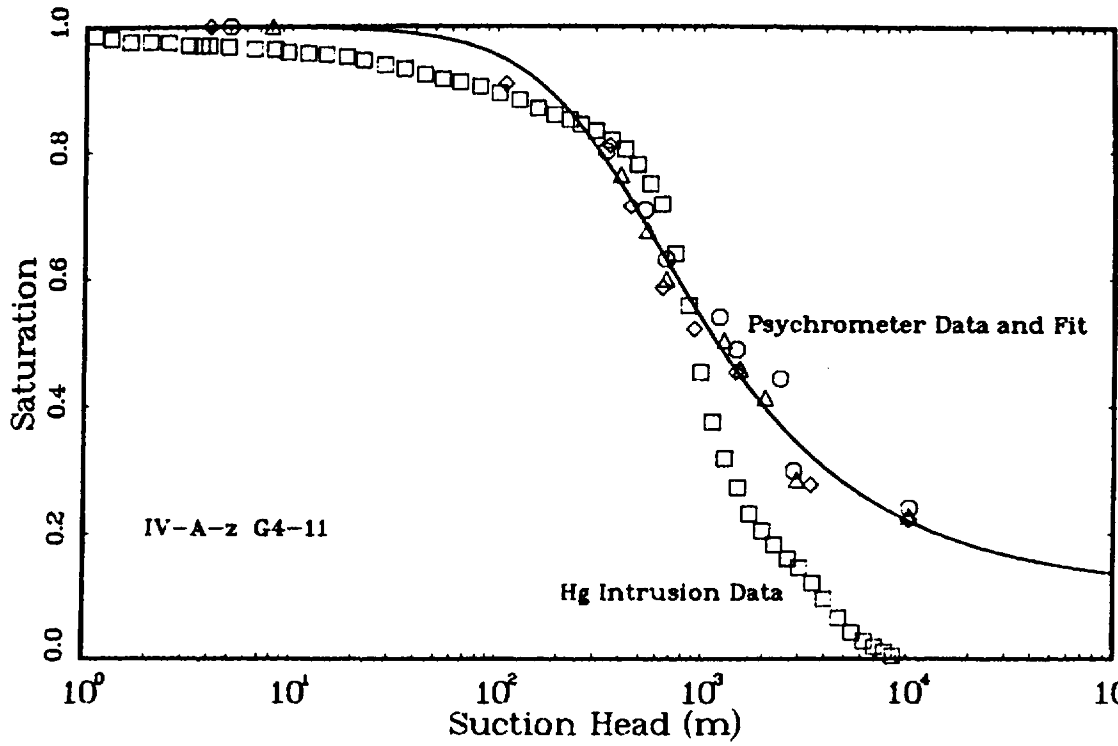


**Figure C.11**

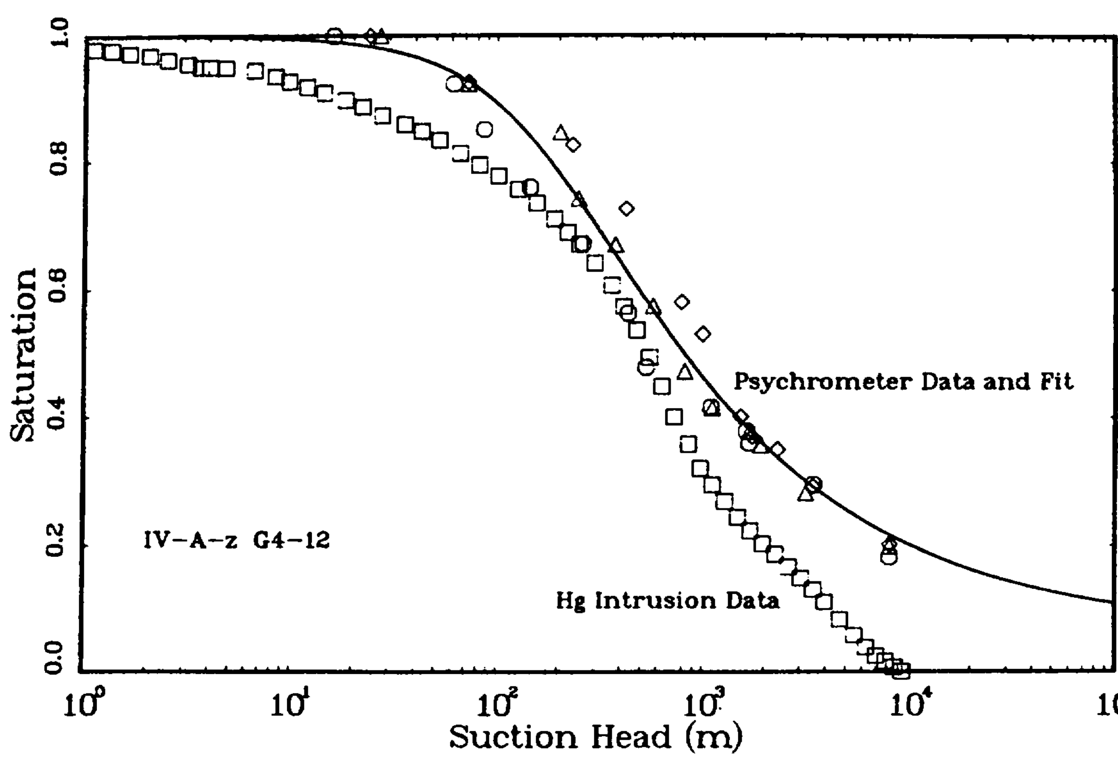


**Figure C.12**

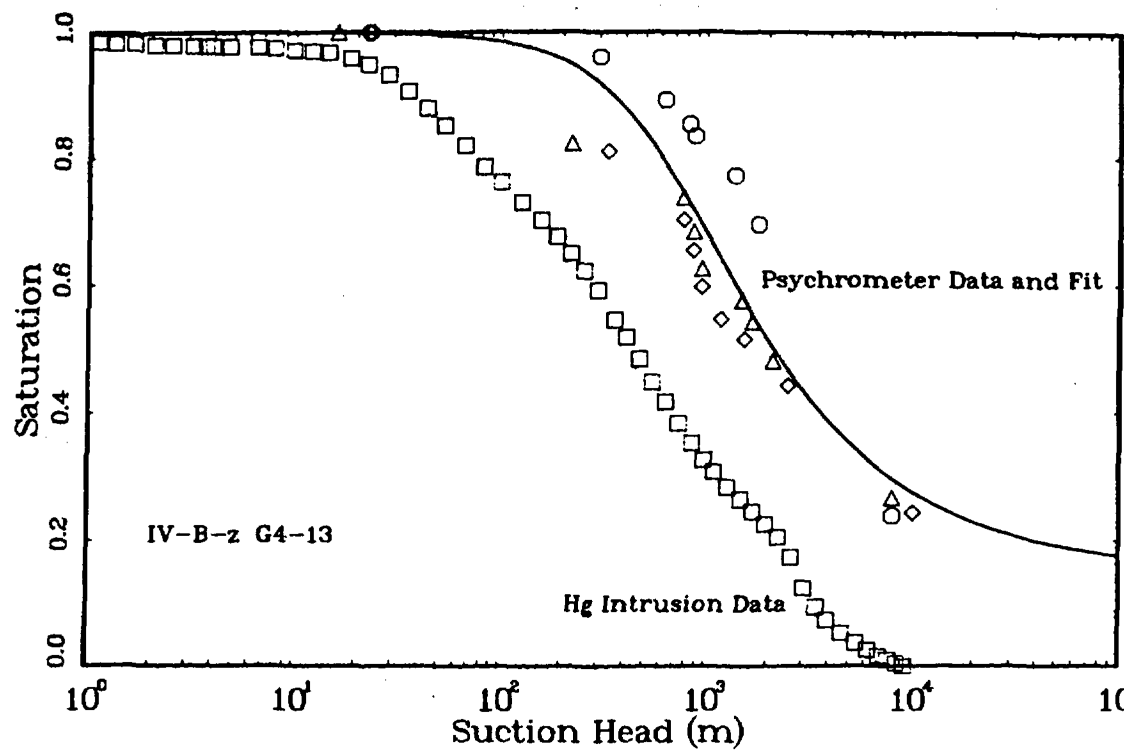


**Figure C.13**

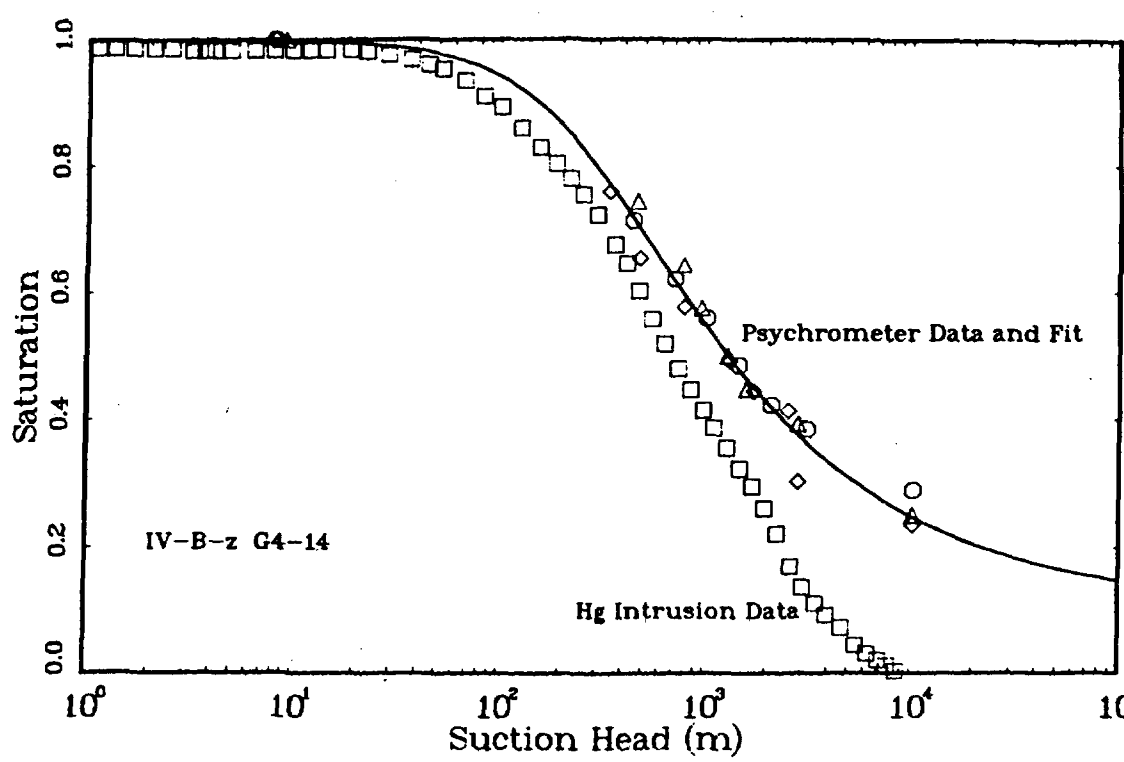


**Figure C.14**

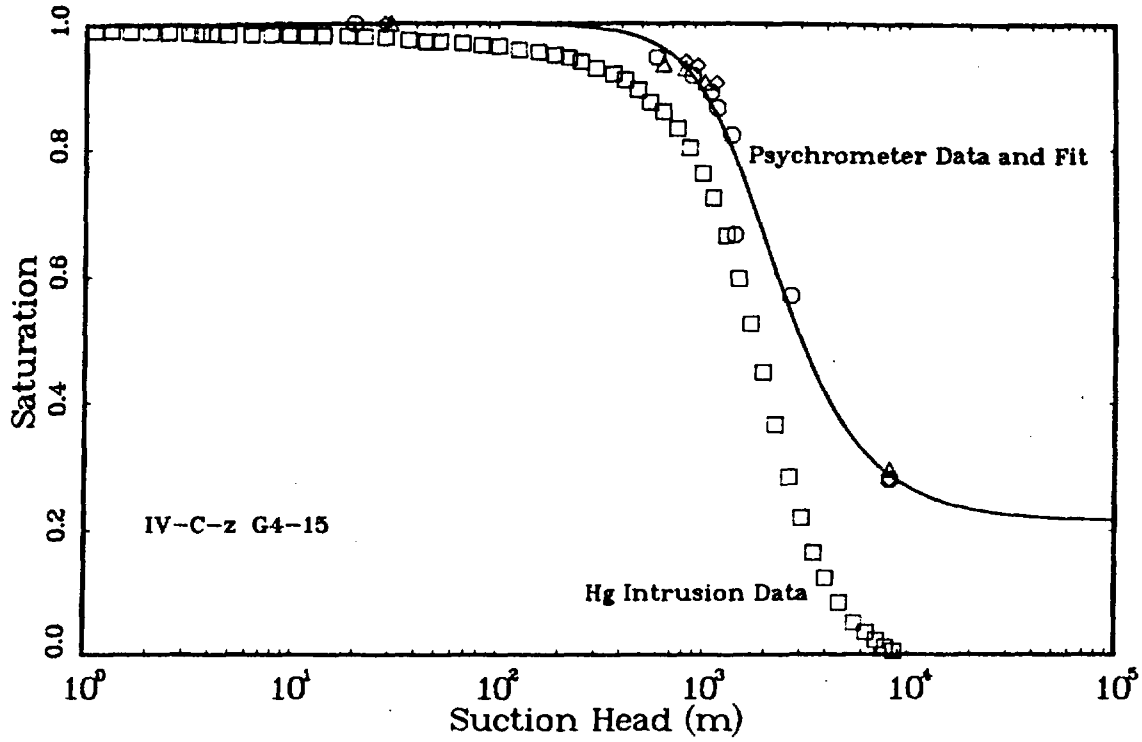


**Figure C.15**

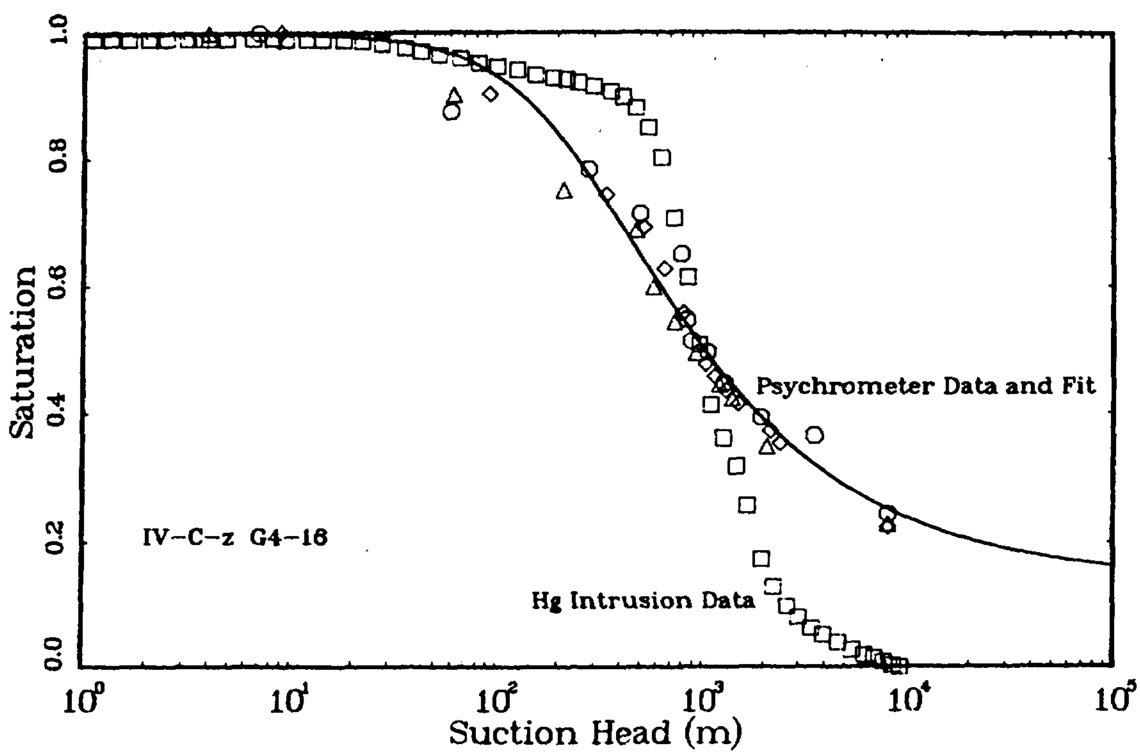


**Figure C.16**

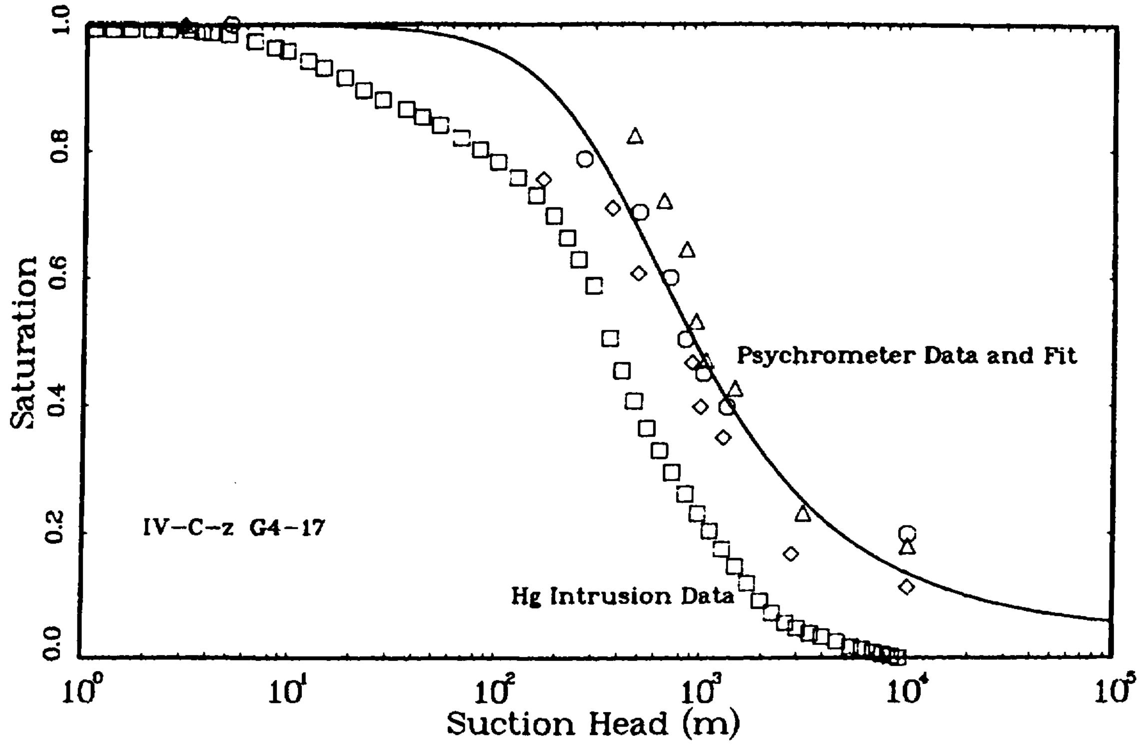


**Figure C.17**

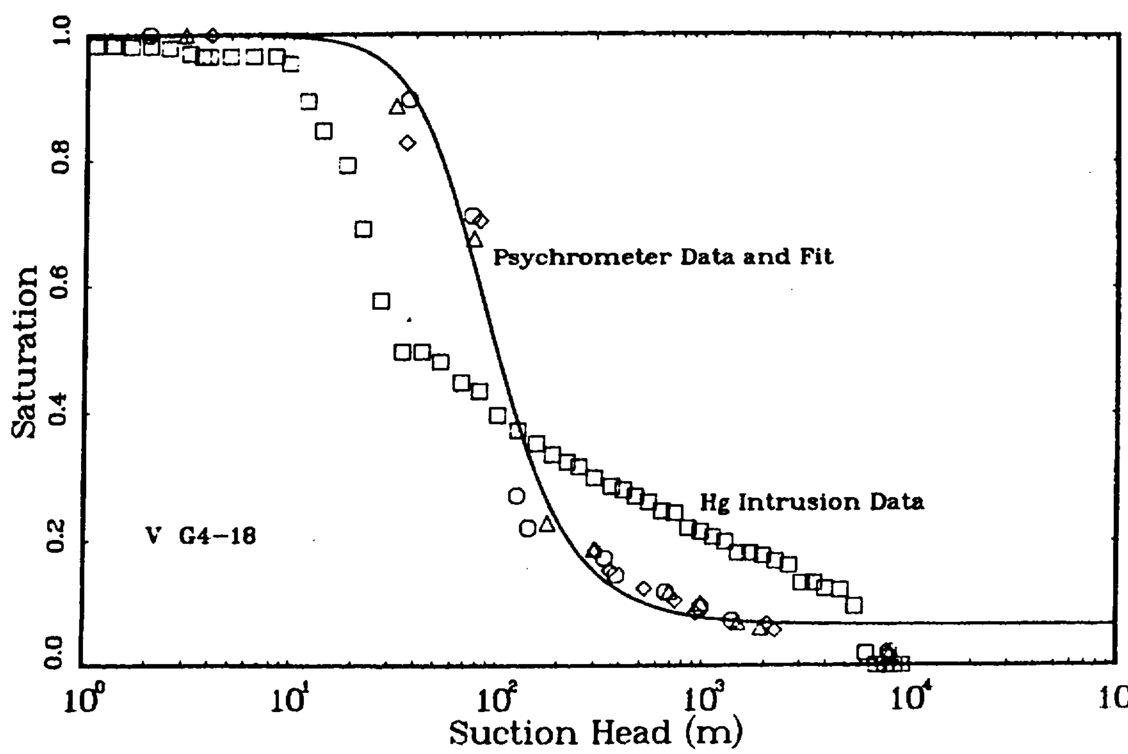


**Figure C.18**

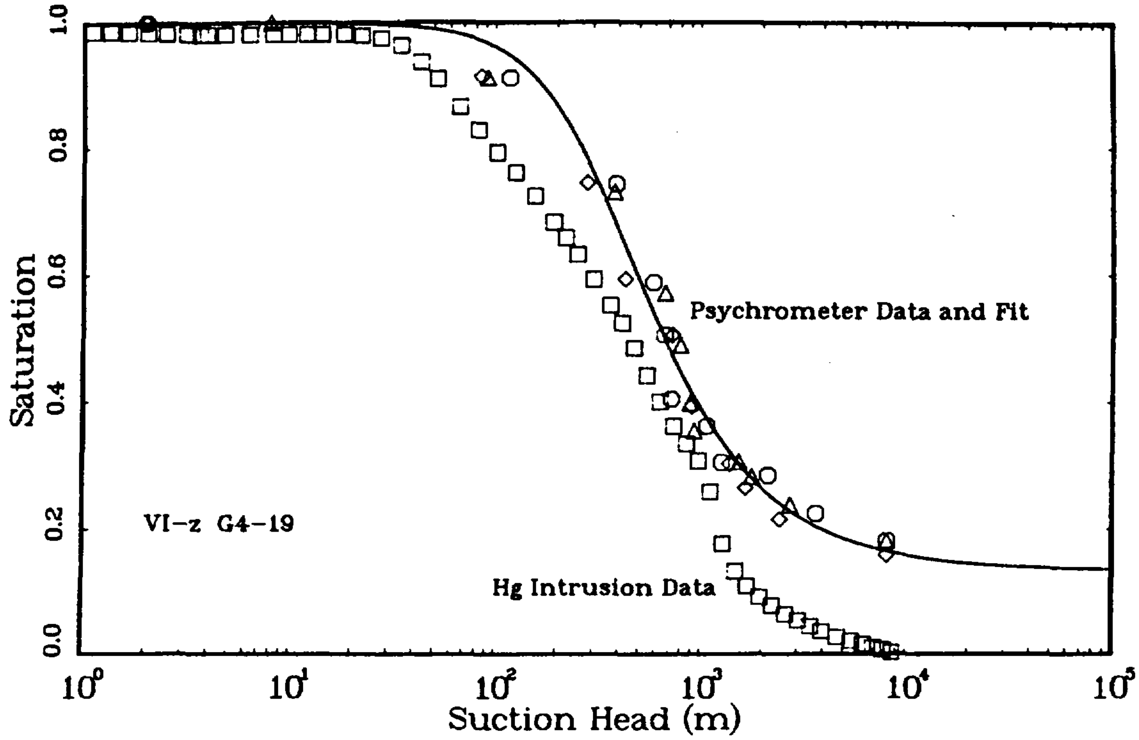


**Figure C.19**

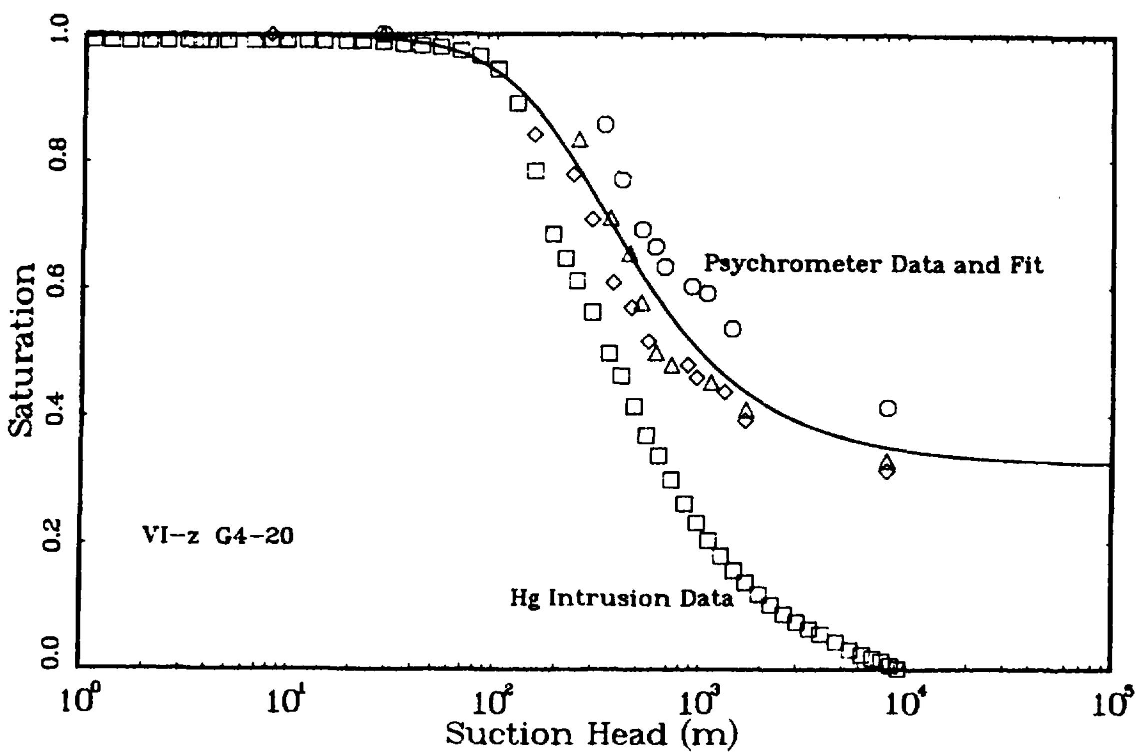


**Figure C.20**

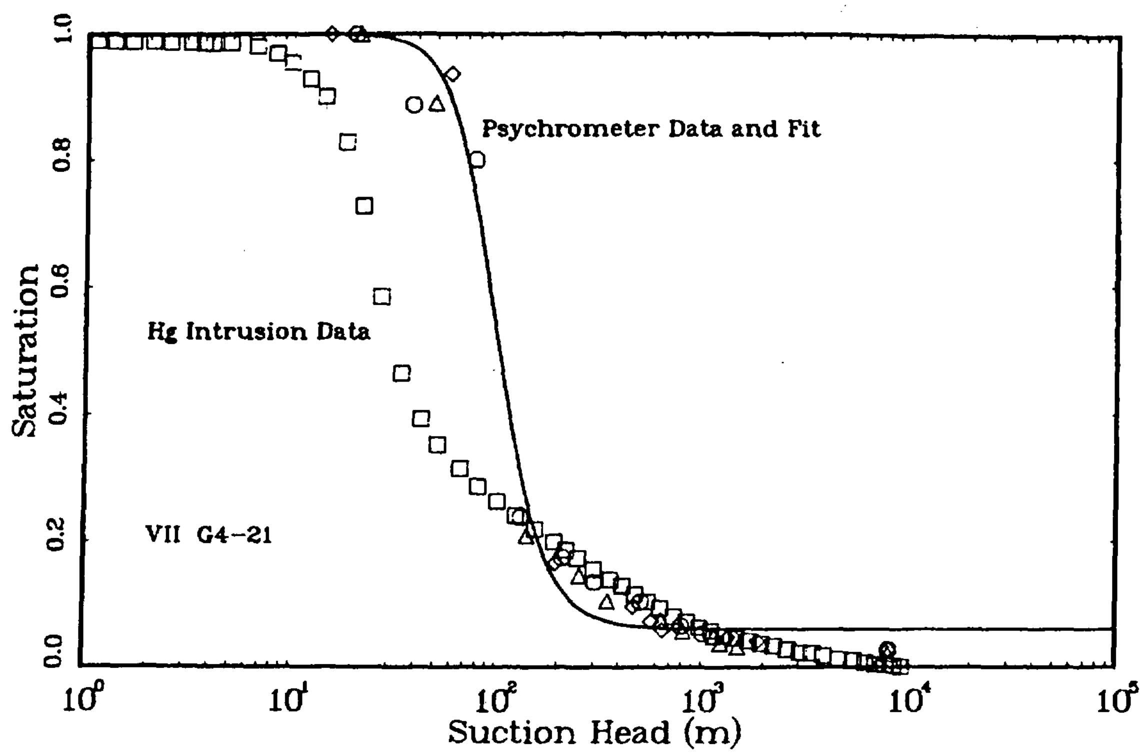


**Figure C.21**

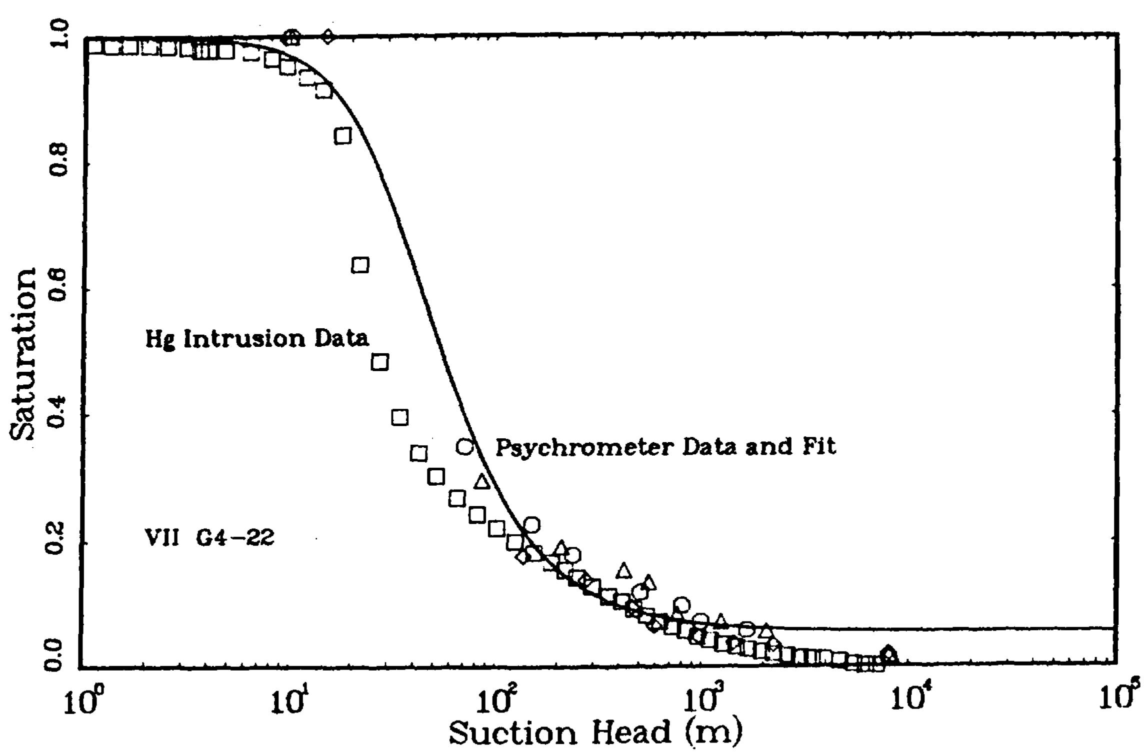


**Figure C.22**

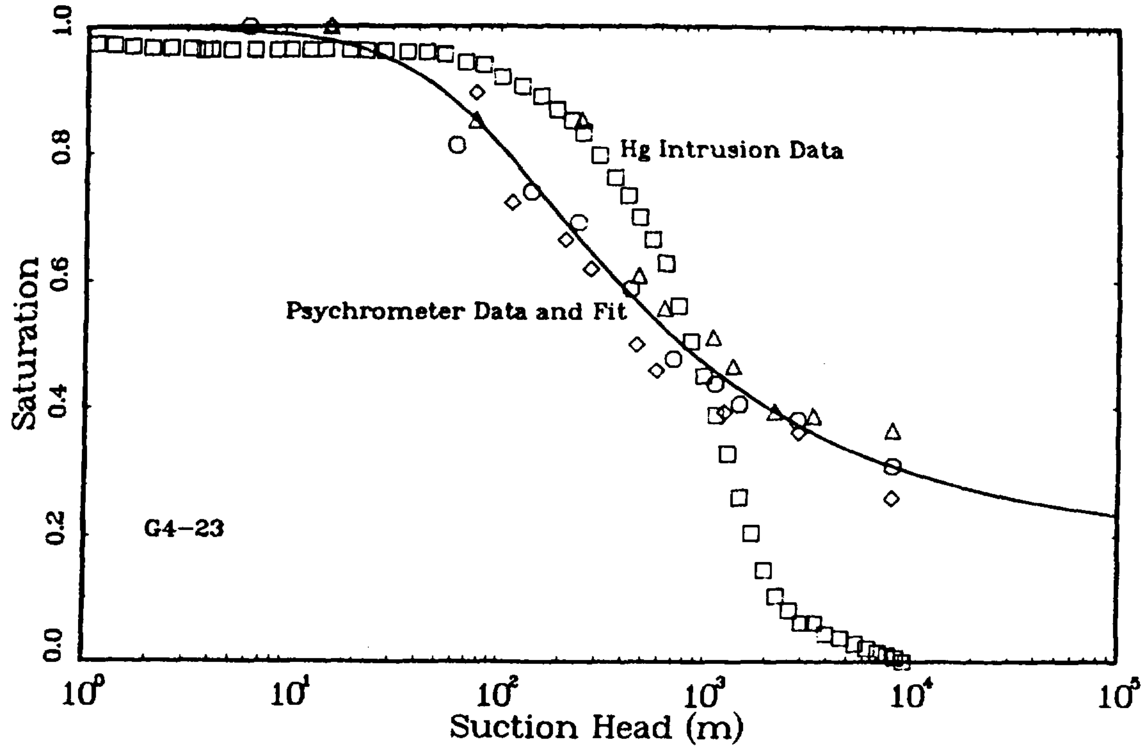

1.0
0.8
0.6
0.4
0.2
0.0
Saturation
Hg Intrusion Data
Psychrometer Data and Fit
G4-23
10^0
10^1
10^2
10^3
10^4
10^5
Suction Head (m)


**Figure C.23**

## APPENDIX D

## COMPARISON OF VAN GENUCHTEN AND HAVERKAMP SATURATION CURVE FITS AND CONDUCTIVITY CURVES

The Van Genuchten and Haverkamp curve fits of saturation data were compared for 14 different samples. The form of the equations is listed below. In the following figures, the Van Genuchten and Haverkamp curve fits and the saturation data are plotted for each sample investigated along with the relative conductivity curves calculated from the curve fits of the saturation data by the method of Mualem (1976). In general, when the shape of the curve was well defined by the data points (e.g., G4-1), the Haverkamp and Van Genuchten curve fits of the data were nearly identical, and the relative conductivity curve calculated from them was also nearly identical. The root-mean-square (RMS) errors for the two curve fits were also similar. The RMS error values are contained in Table D.1. The major difference between the two curve fits is in the estimation of the conductivity from them. If the Haverkamp saturation curve is used, the relative conductivity equation based on the work of Mualem (1976) must be numerically integrated to obtain the relative conductivity curve with the expression being undefined at the limits of integration. If the Van Genuchten curve is used, the relative conductivity equation can be analytically integrated. Relative conductivity curves using both saturation curve fits and the method of Mualem are included in the plots which follow.

The Van Genuchten curve was chosen as the standard method to fit the saturation data because it gave as good a fit (i.e., as low an RMS value) as other methods, and it yielded an analytical expression for the hydraulic conductivity when calculated using the method of Mualem.

The defining equations for the two curve fits follow.

Van Genuchten

$$S = (S_s - S_r)\left[\frac{1}{1 + |\alpha h|^{\beta}}\right]^{\lambda} + S_r$$

Haverkamp

$$S = (S_s - S_r)\frac{\alpha}{\alpha + (h)^{\beta}} + S_r$$

$h$ - Suction head

$S$ - Saturation as a function of pressure

$S_s$ - Maximum saturation ($\approx 1$)

$S_r$ - Residual saturation

$\lambda$ - $1 - 1/\beta$

$\alpha$ and $\beta$ are curve-fit parameters

**TABLE D.1.** RMS Error Values for Selected Haverkamp and Van Genuchten Curve Fits

| Sample | Unit | Van Genuchten RMS* Error ($x10^{-2}$) | Haverkamp RMS Error ($x10^{-2}$) |
|---|---|---|---|
| G4-1 | I-A | 6.7 | 6.3 |
| G4-4 | II-L | 8.9 | 9.6 |
| G4-7 | II-NL | 6.4 | 6.4 |
| G4-9 | III | 9.4 | 9.0 |
| G4-11 | IV-A-z | 3.1 | 3.1 |
| G4-14 | IV-B-z | 2.5 | 2.4 |
| G4-17 | V | 6.6 | 6.3 |
| GU3-2 | I-A | 13.0 | 12.0 |
| GU3-3 | I-A | 6.0 | 6.3 |
| GU3-7 | I-B | 8.9 | 13.0 |
| GU3-10 | I-B | 5.0 | 5.8 |
| GU3-14 | IV-A-v | 4.5 | 5.1 |
| GU3-16 | I-B-v | 6.1 | 10.0 |
| GU3-18 | V | 9.8 | 9.9 |

*RMS: Root-mean-square error between the curves predicted value ($Y_P$) and the measured value ($Y_M$). N is the number of data points.

$$\text{RMS Error} = \left( \frac{\sum_{i=1}^{N} (Y_{Pi} - Y_{Mi})^2}{N} \right)^{1/2}$$

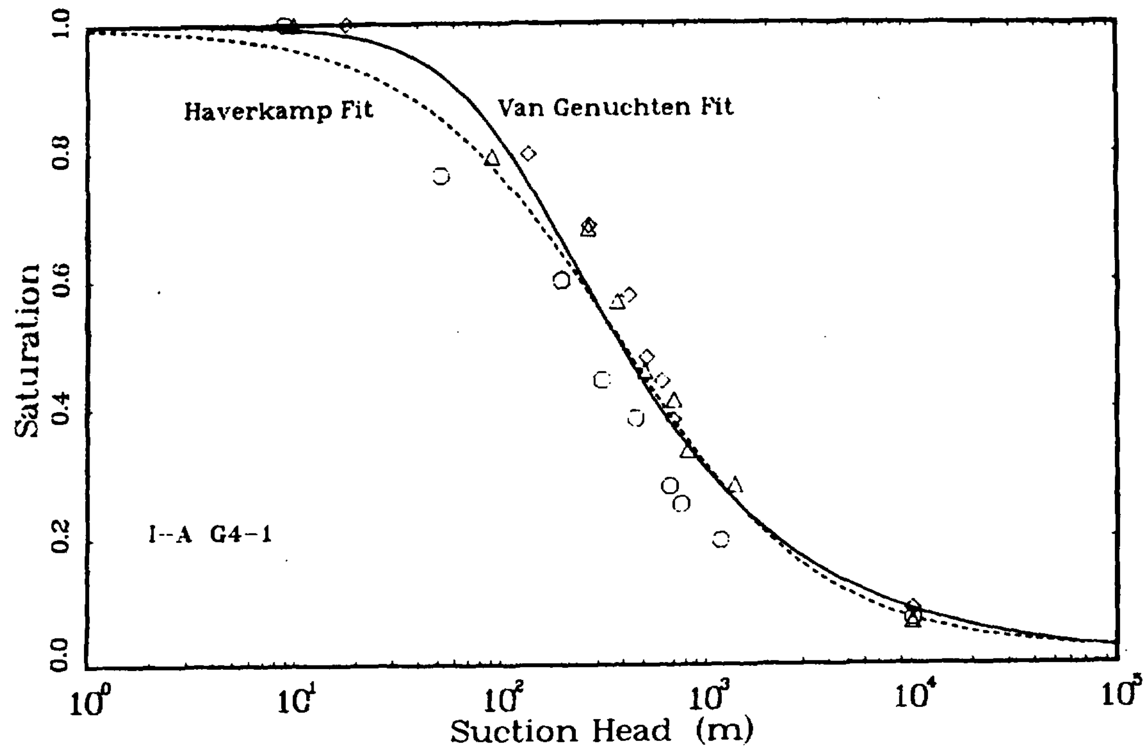


**Figure D.1**

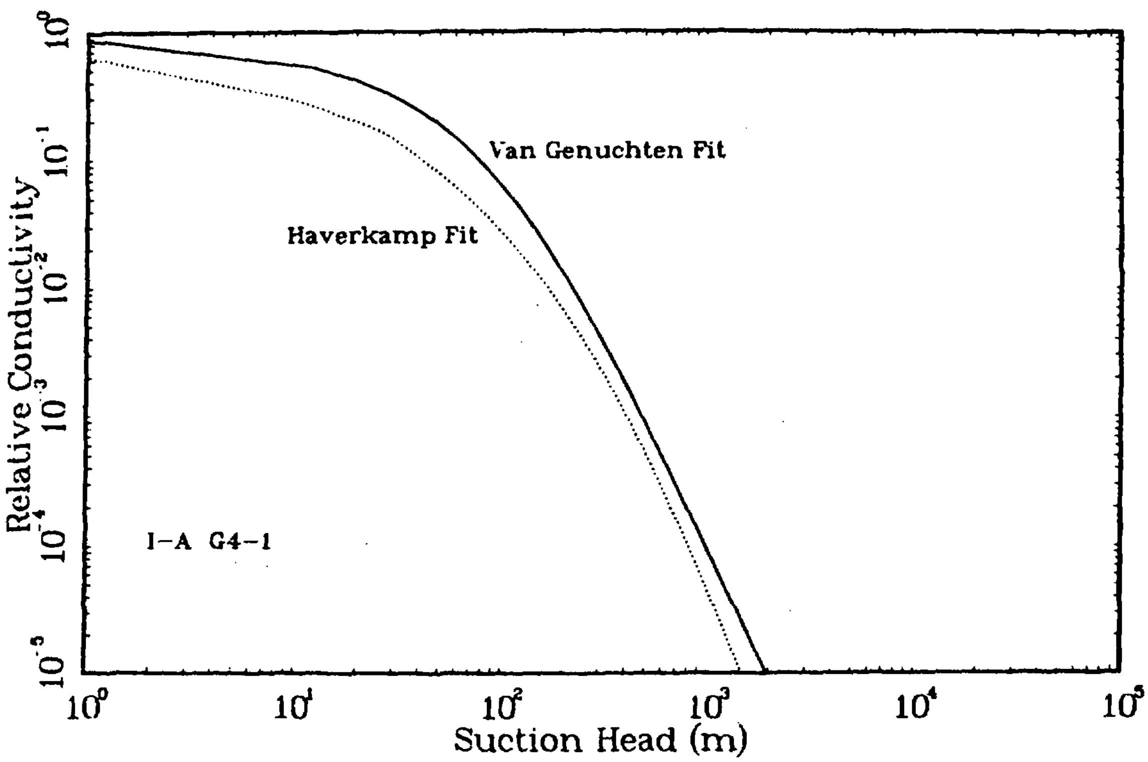


**Figure D.2**

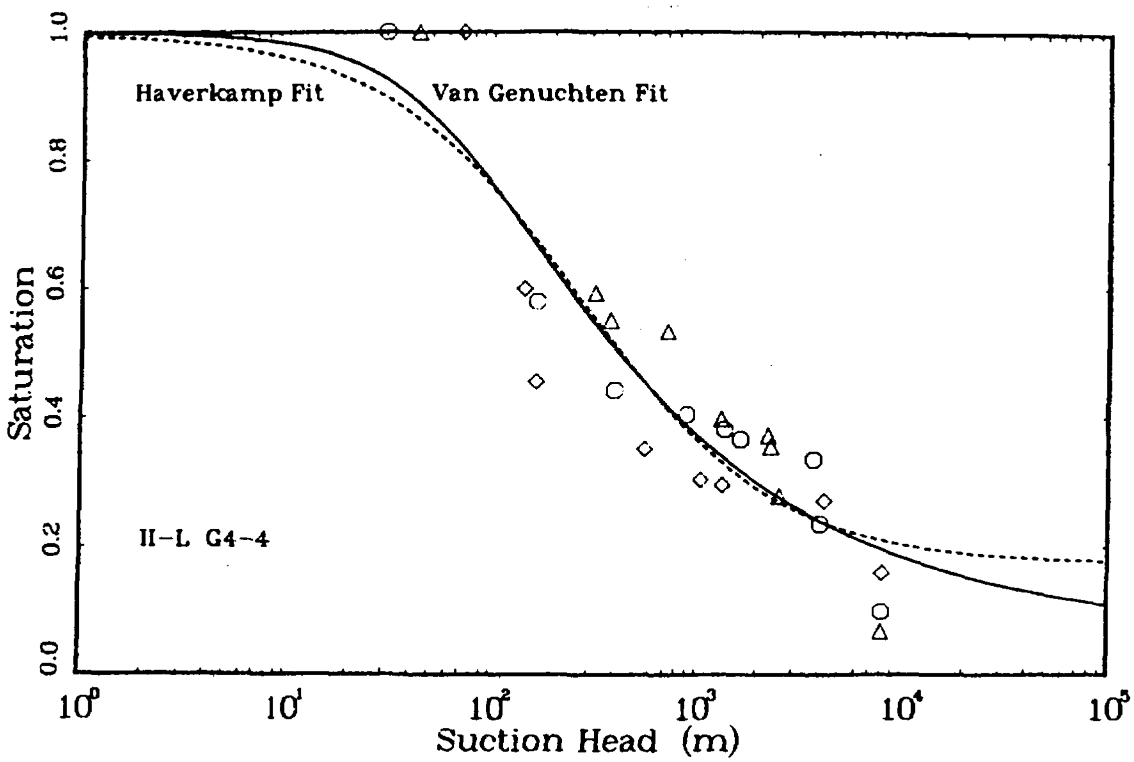


**Figure D.3**

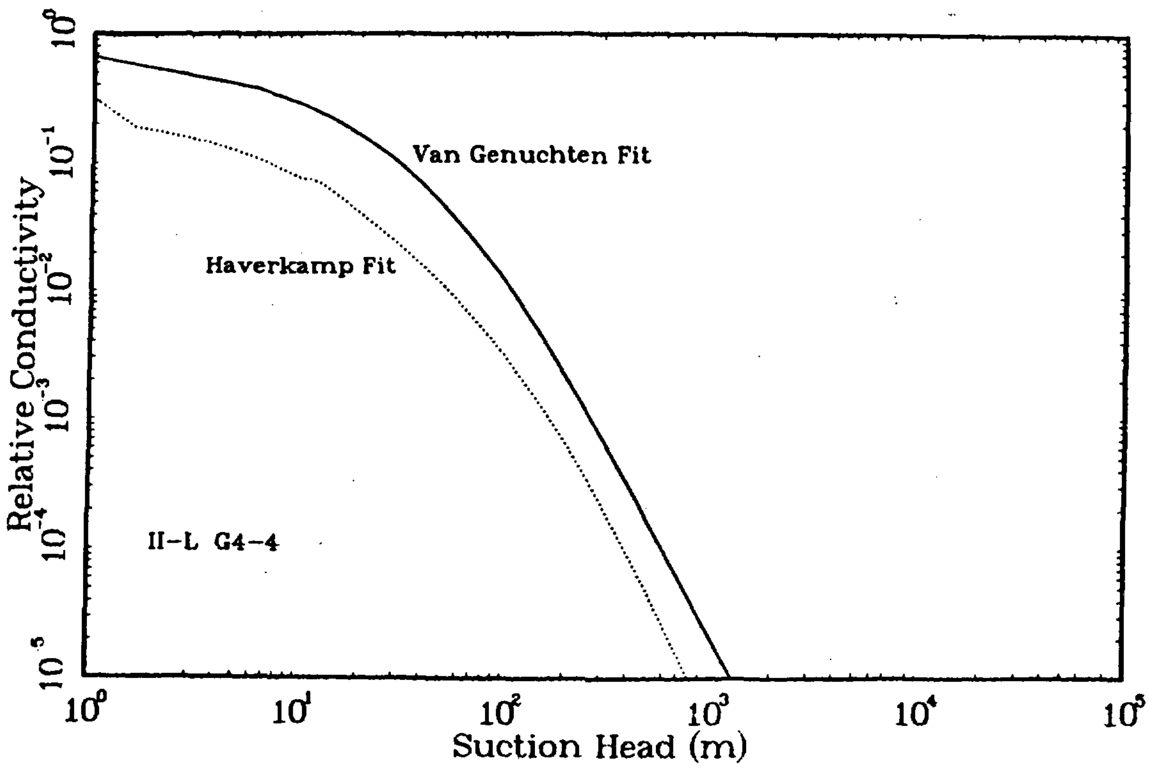


**Figure D.4**

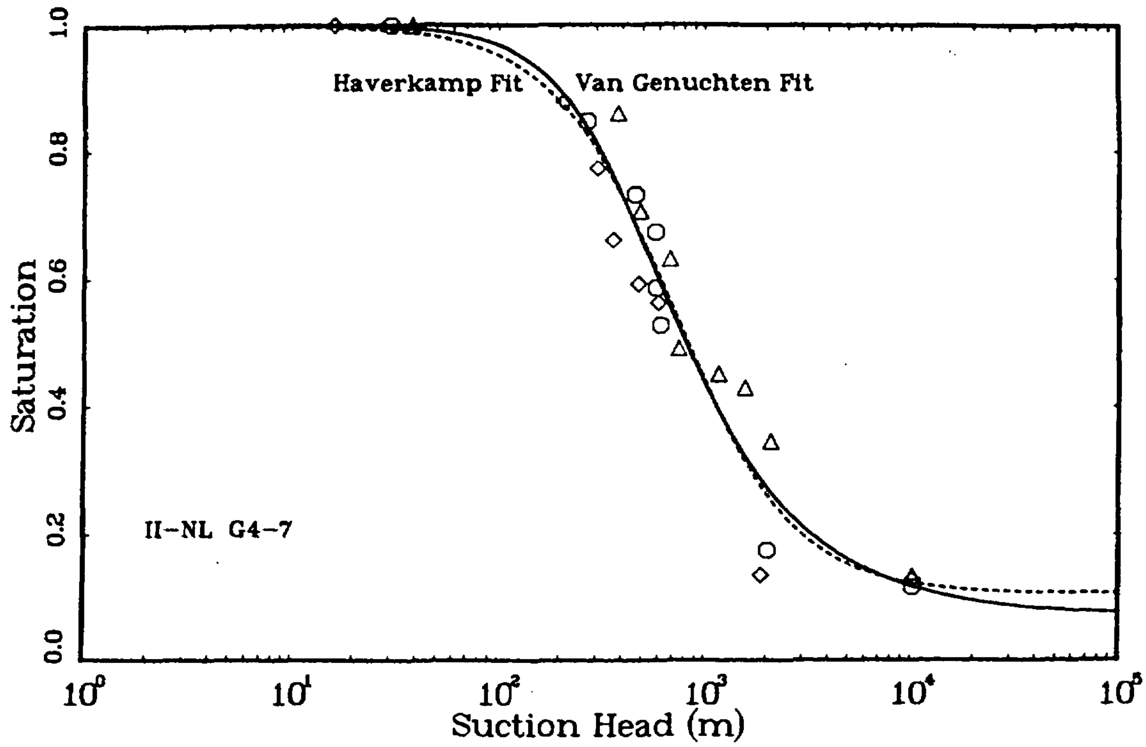


**Figure D.5**

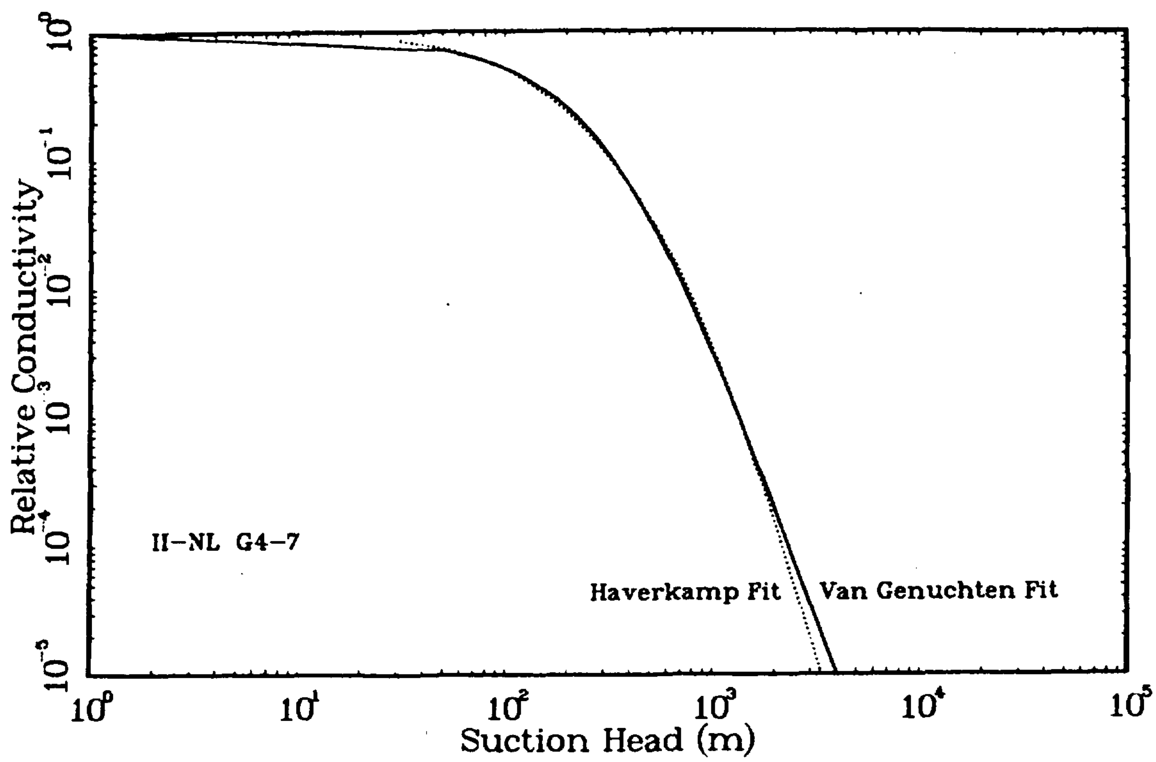


**Figure D.6**

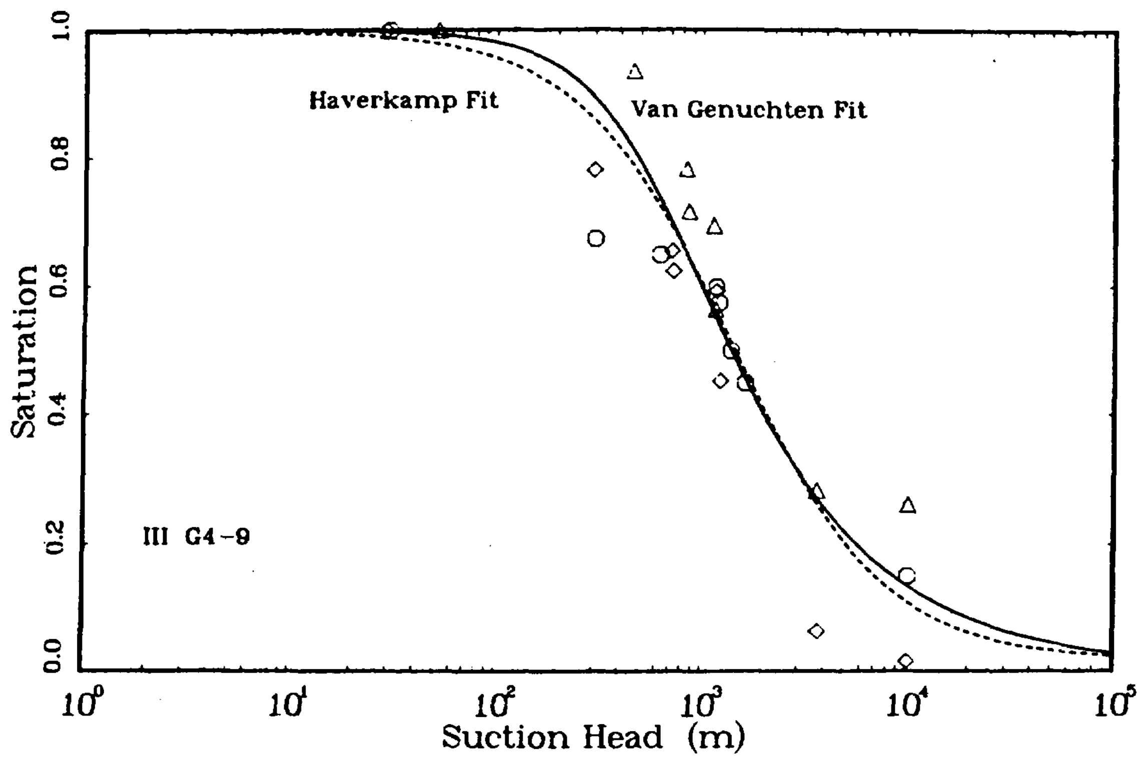


**Figure D.7**

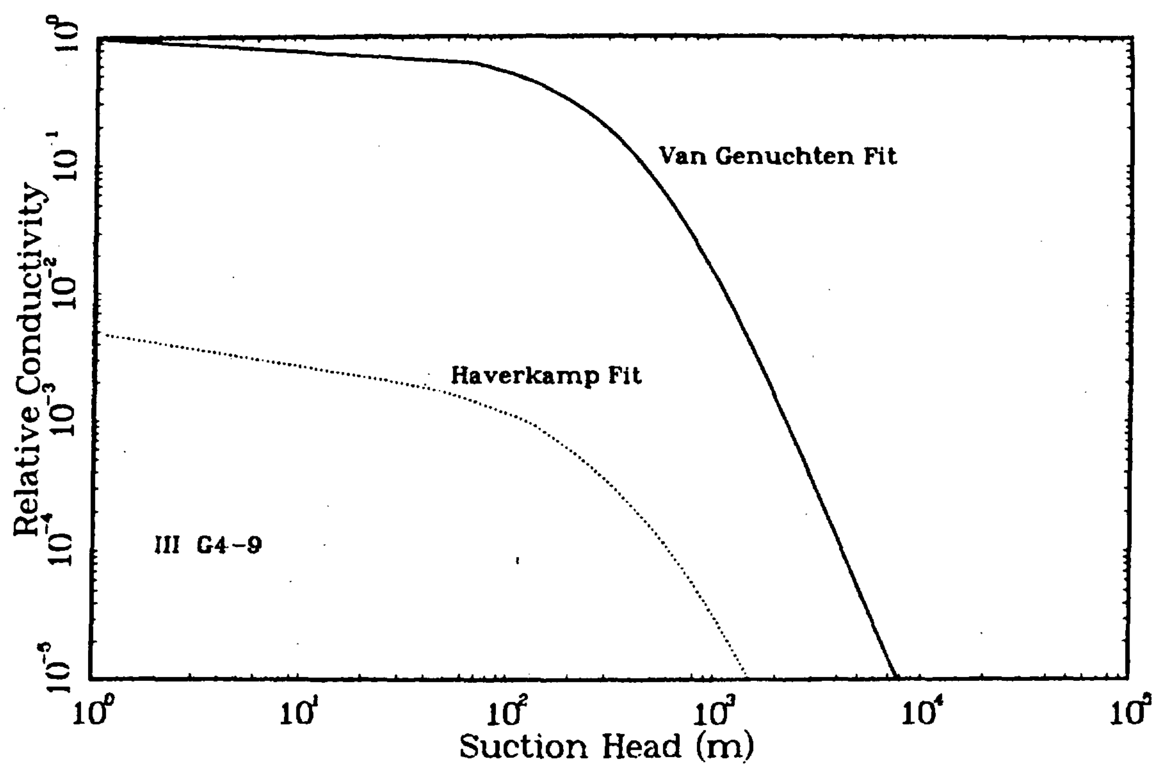


**Figure D.8**

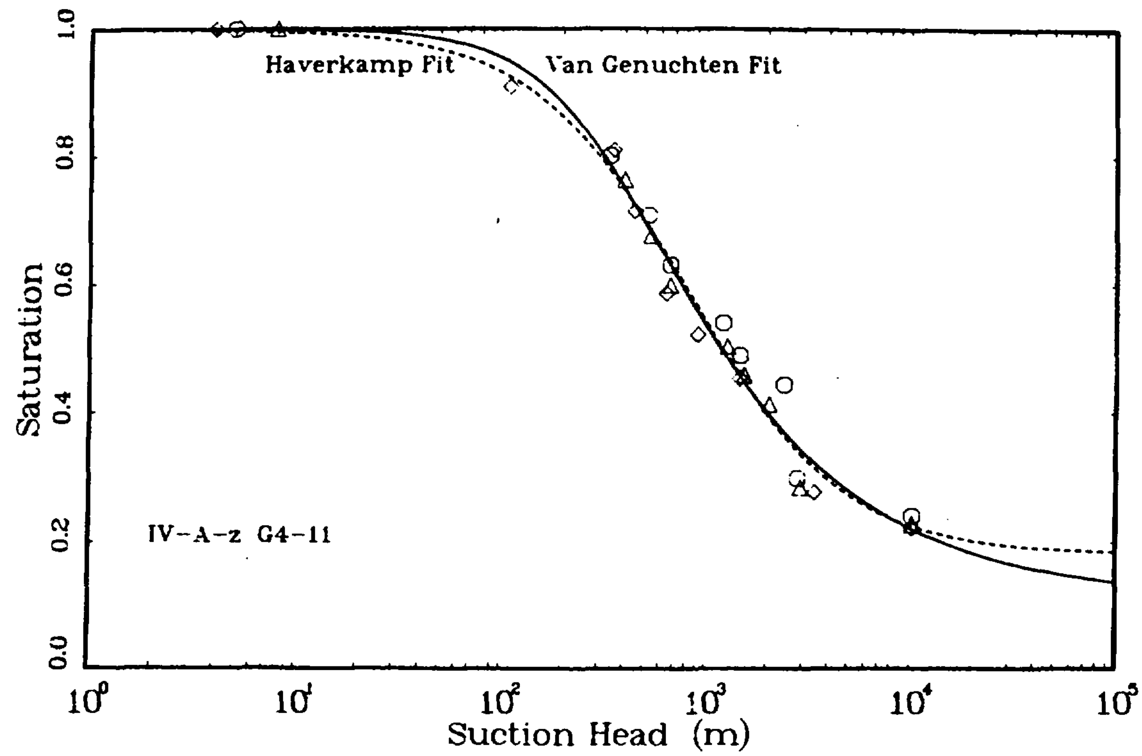


**Figure D.9**

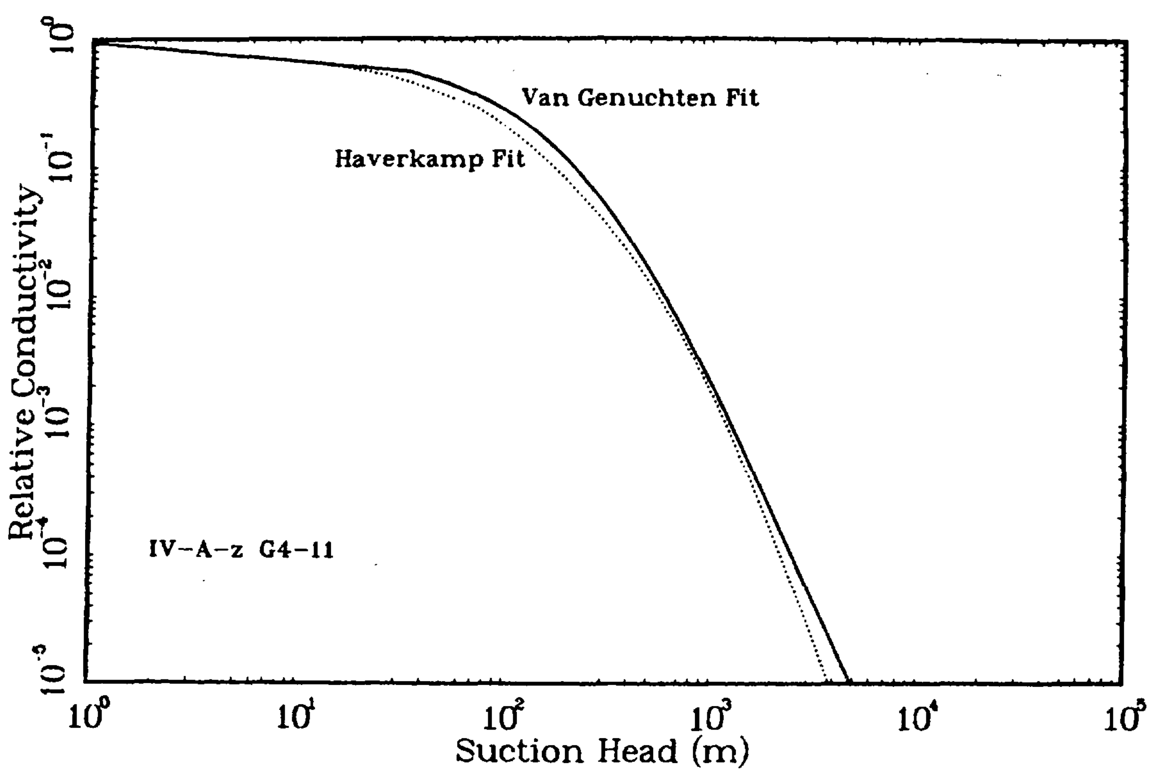


**Figure D.10**

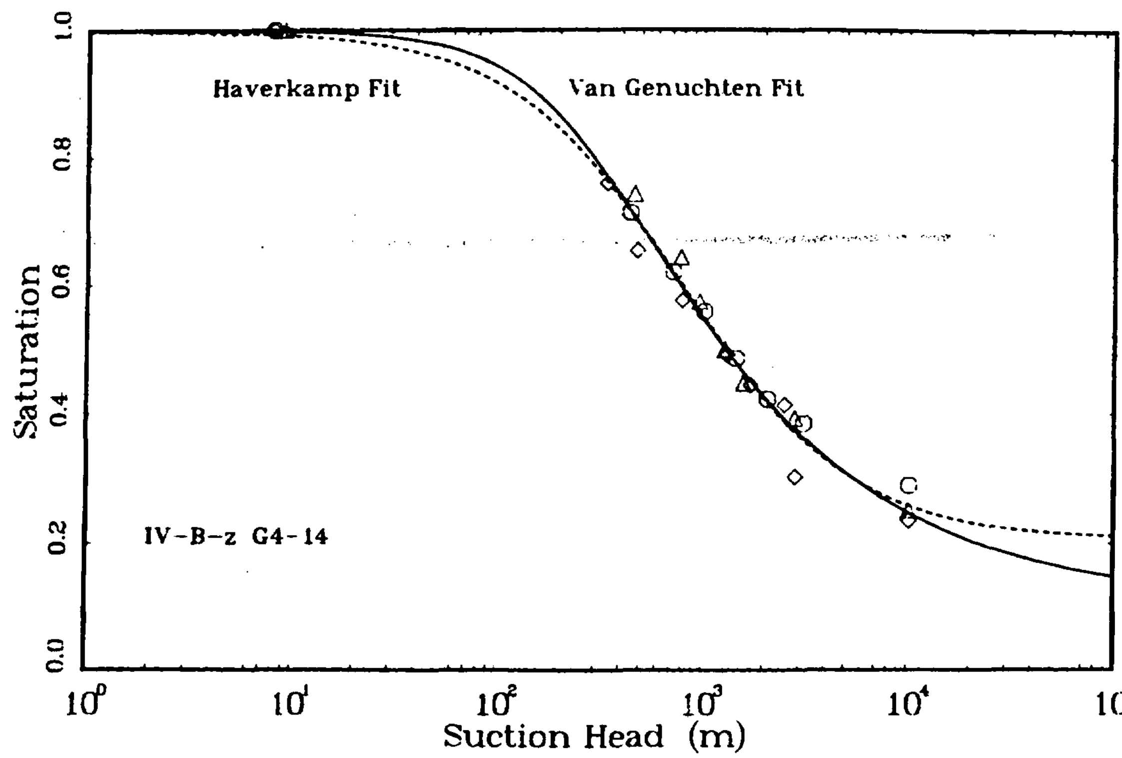


**Figure D.11**

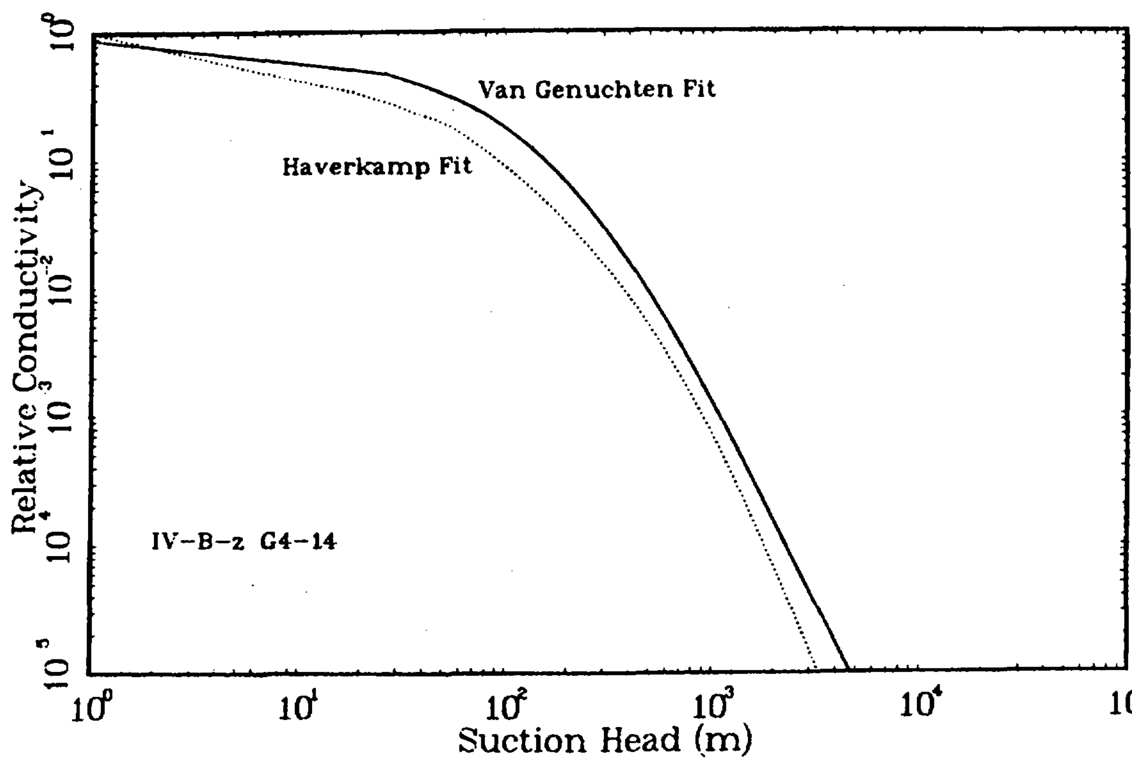


**Figure D.12**

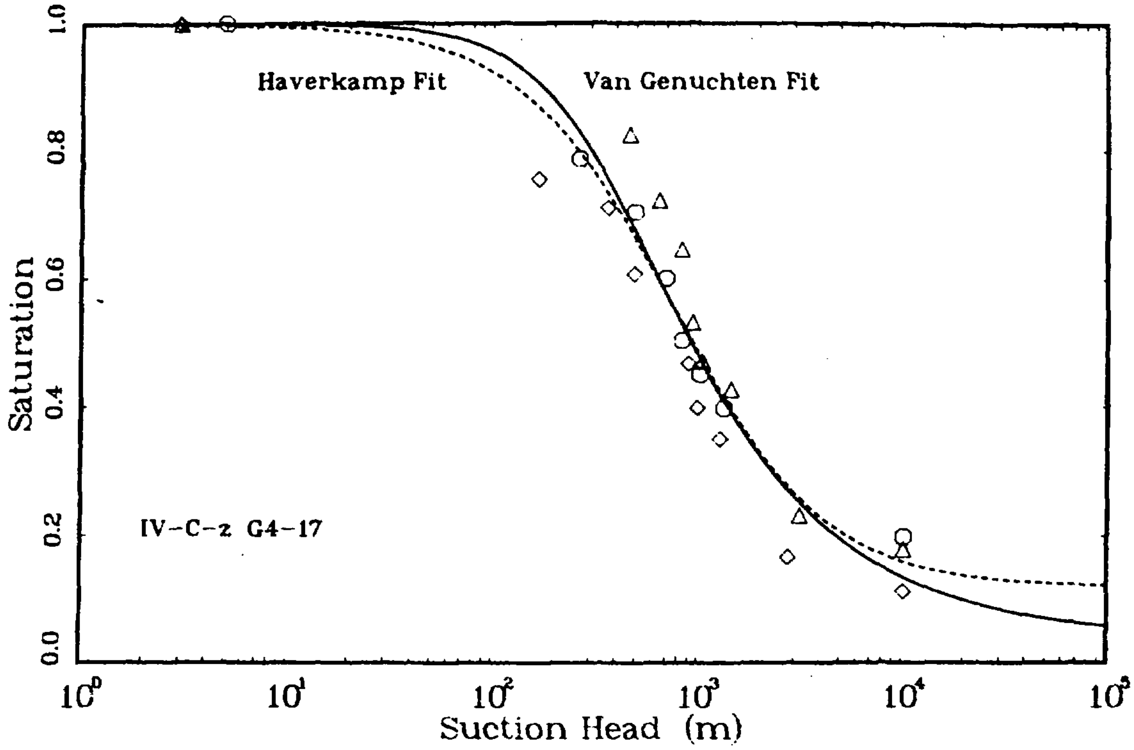


**Figure D.13**

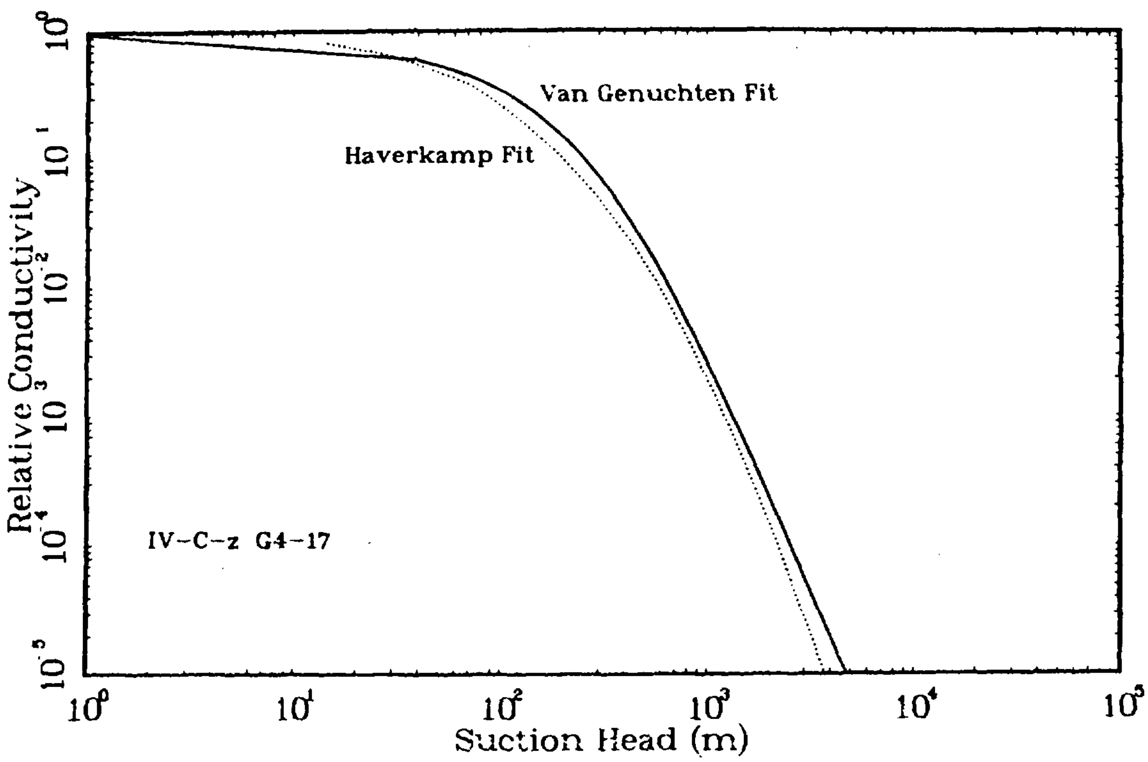


**Figure D.14**

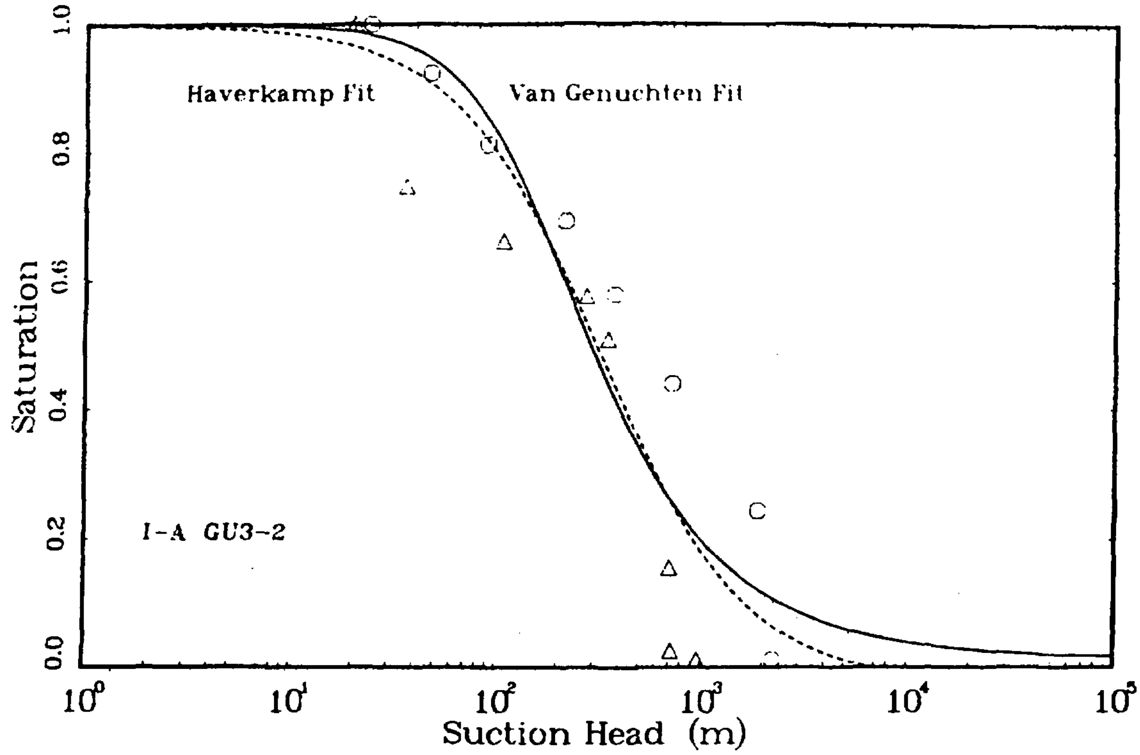


**Figure D.15**

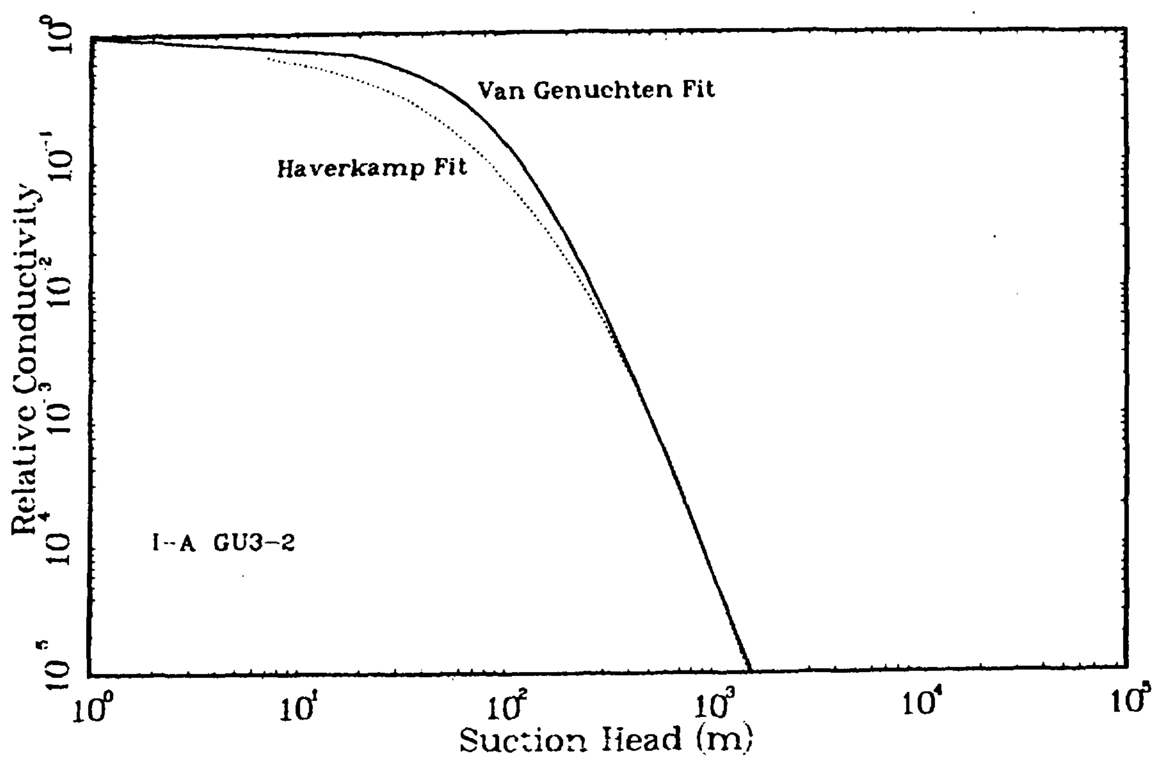


**Figure D.16**

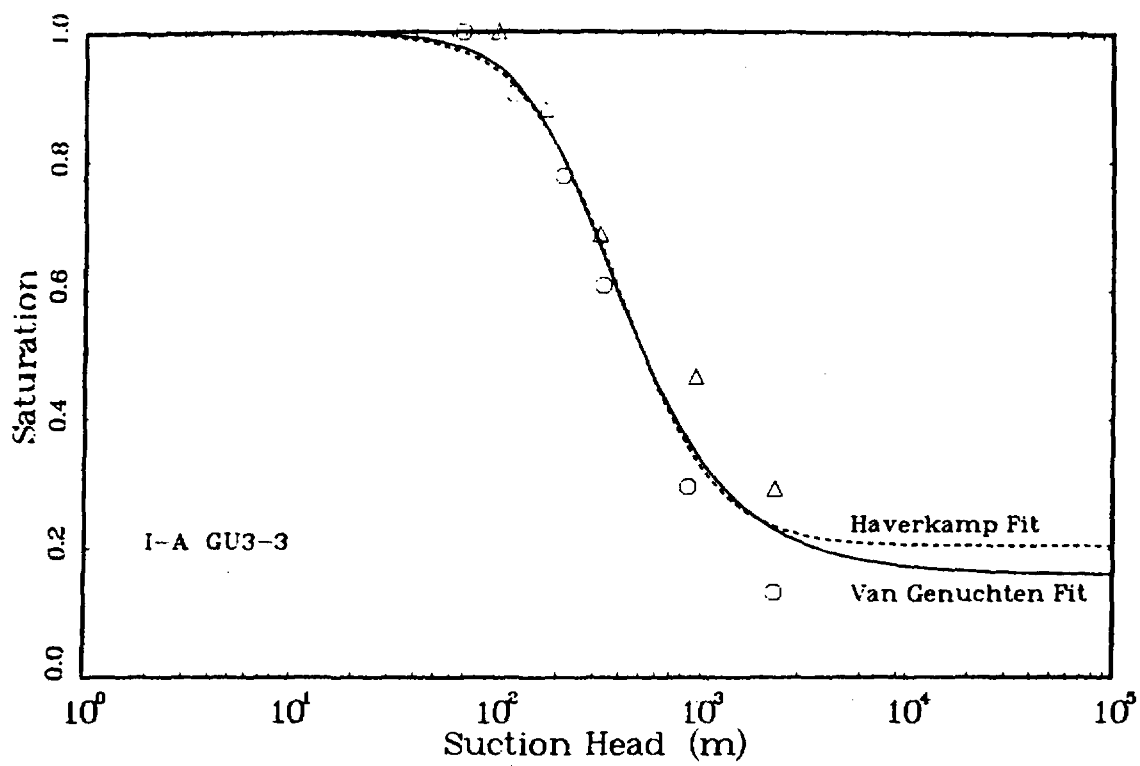


**Figure D.17**

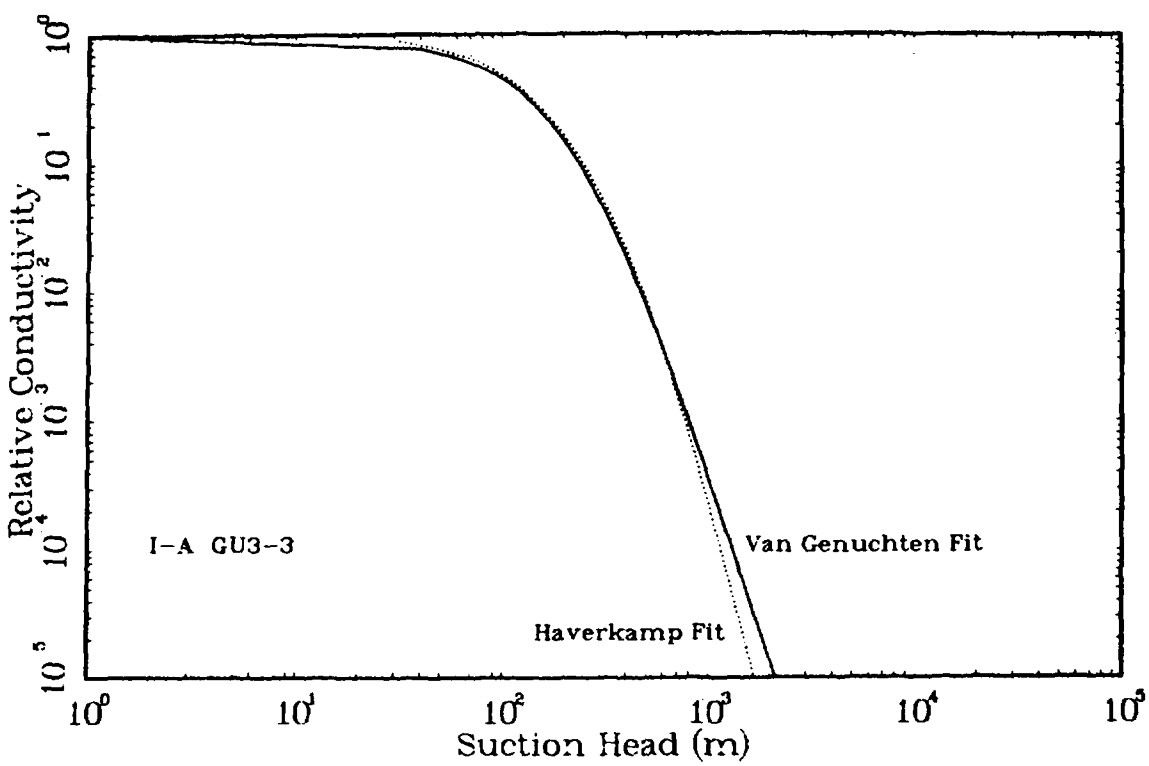


**Figure D.18**

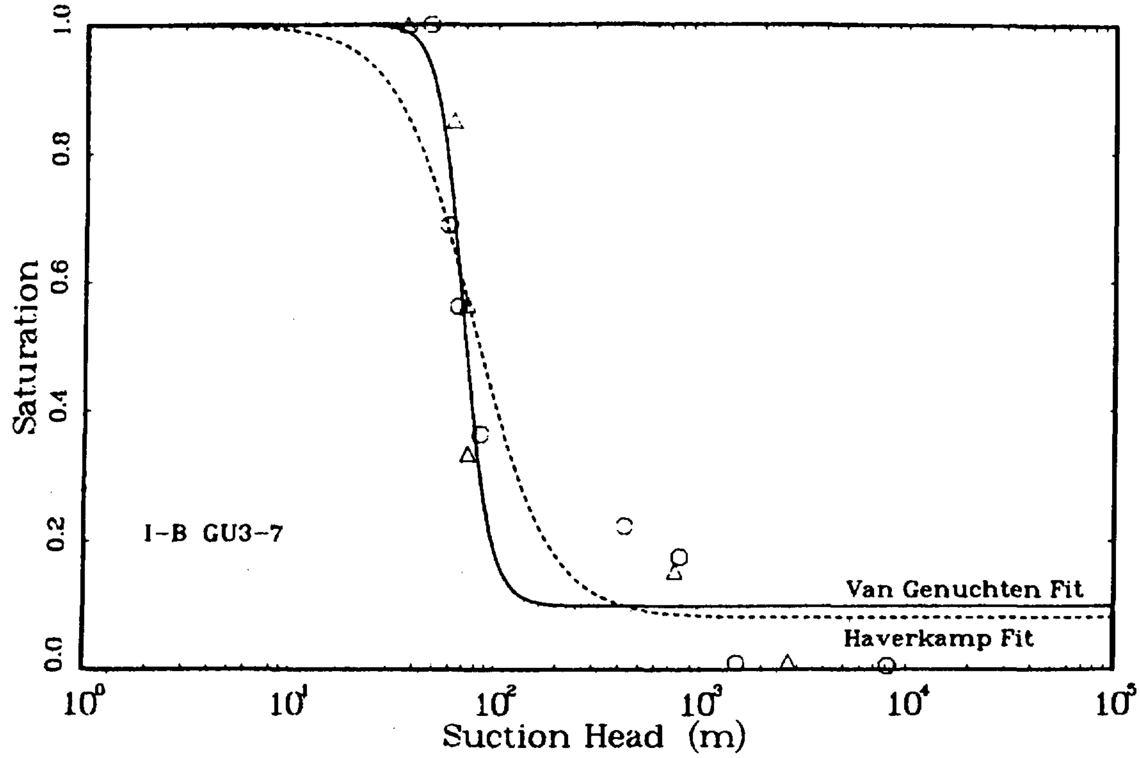


**Figure D.19**

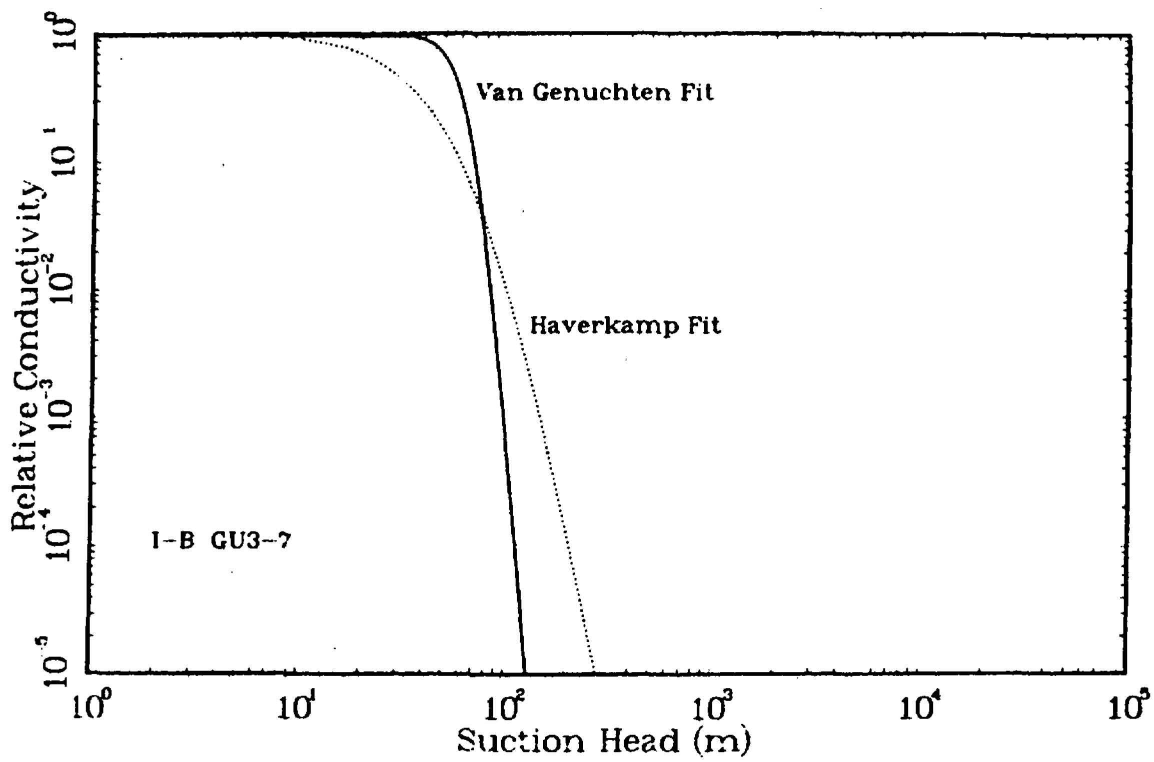


**Figure D.20**

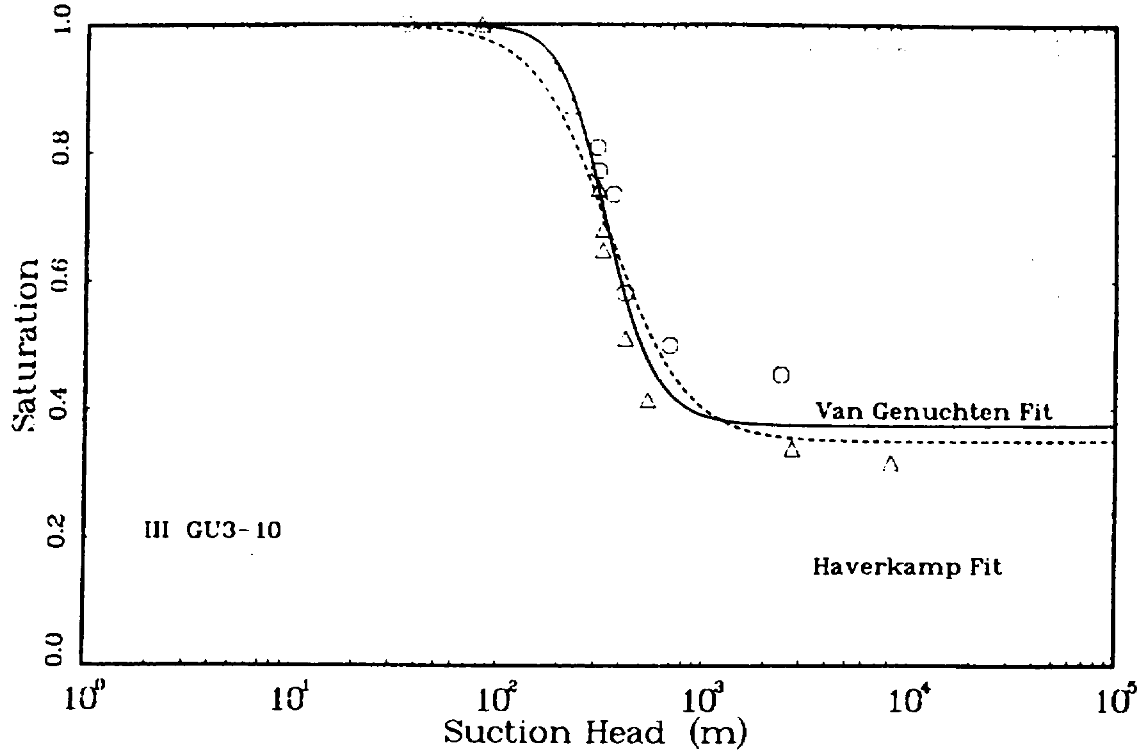


**Figure D.21**

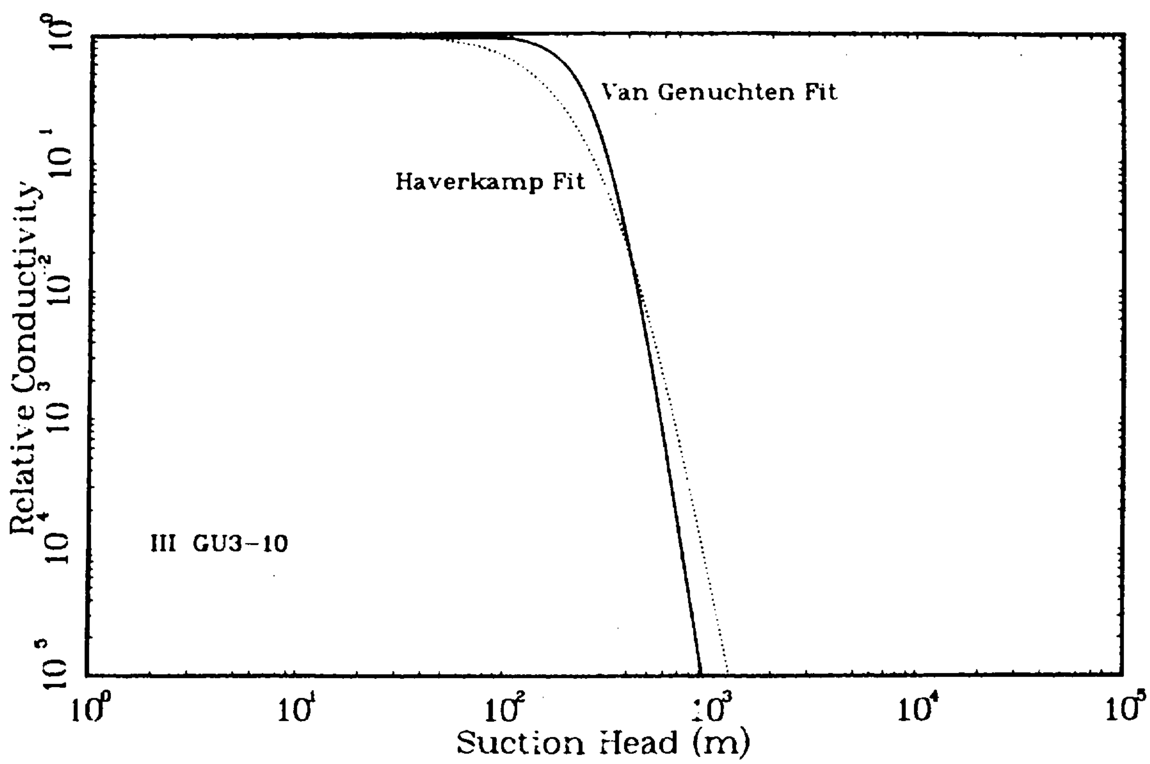


**Figure D.22**

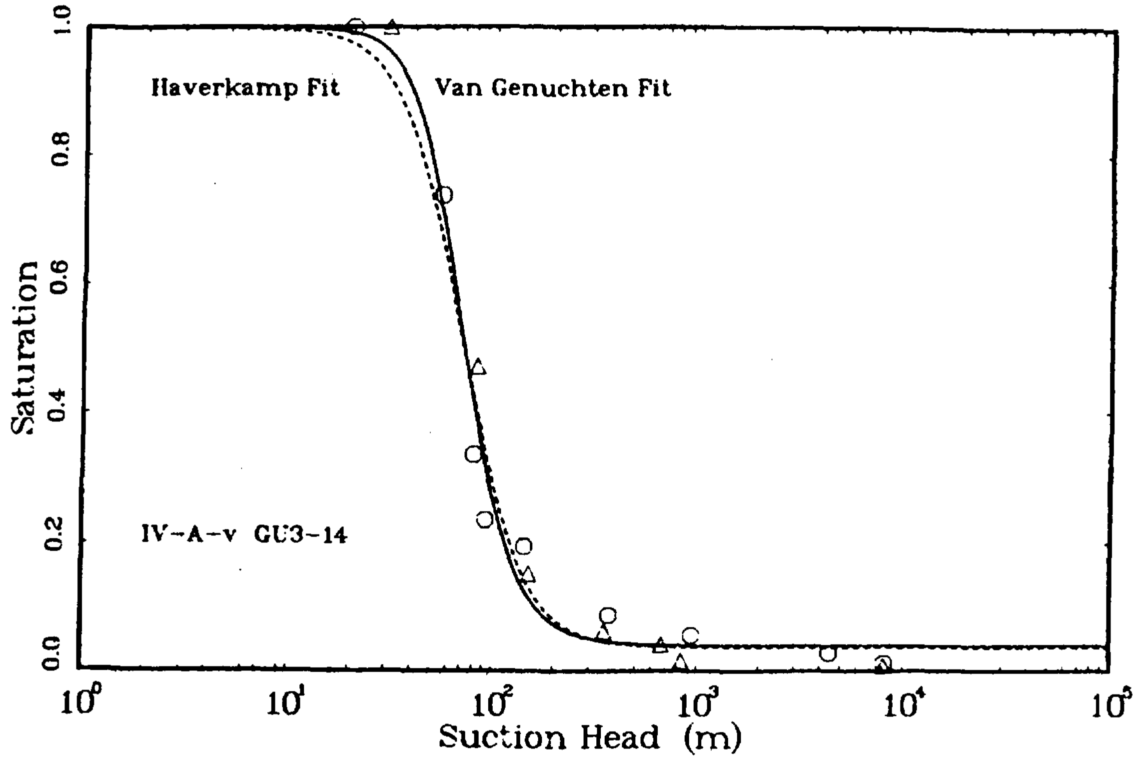


**Figure D.23**

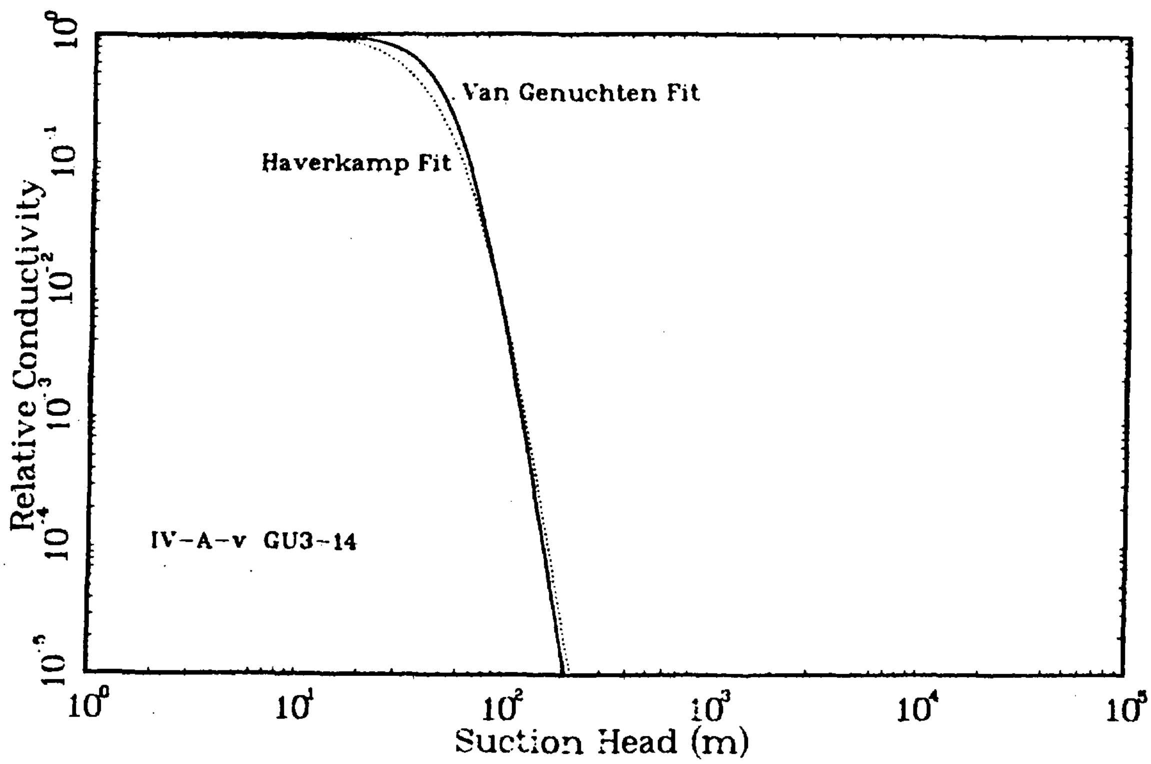


**Figure D.24**

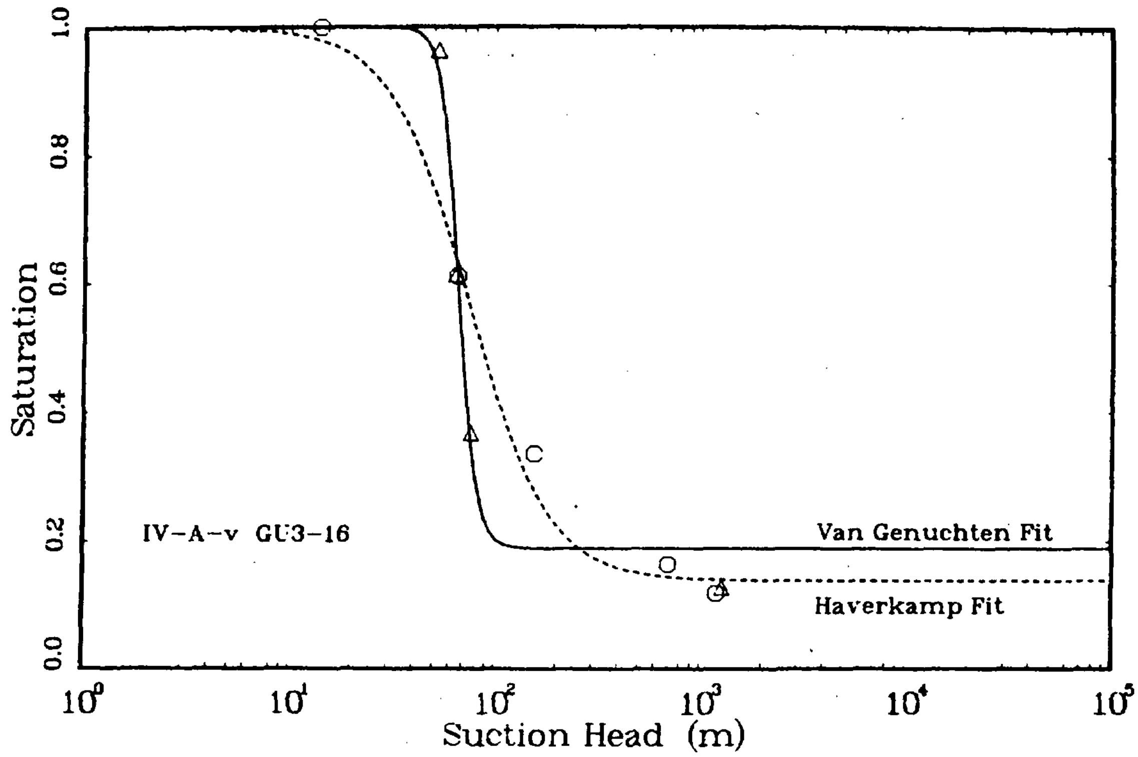


**Figure D.25**

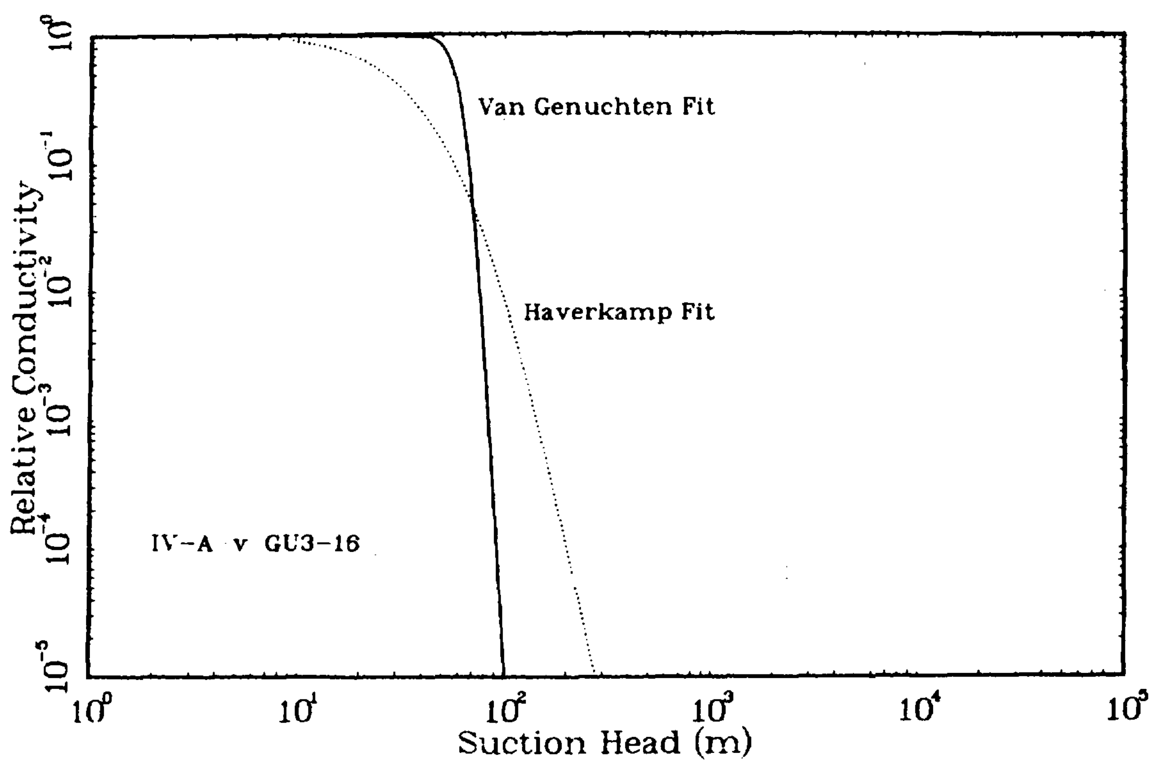


**Figure D.26**

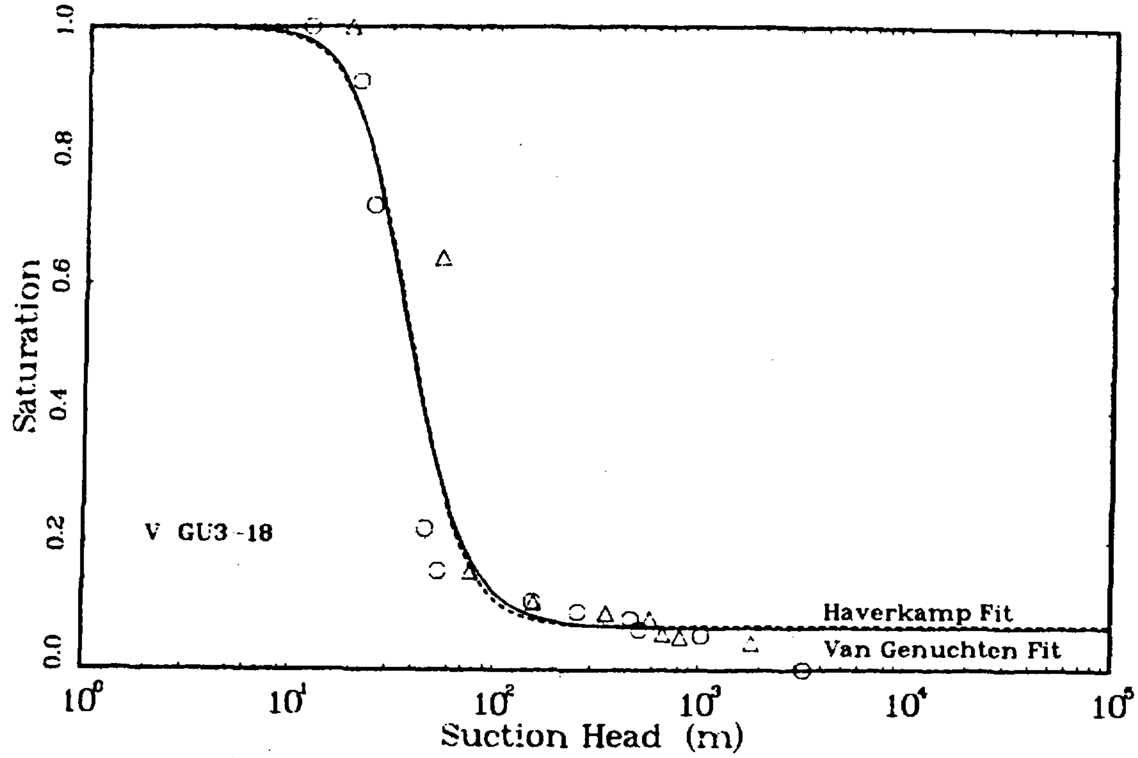


**Figure D.27**

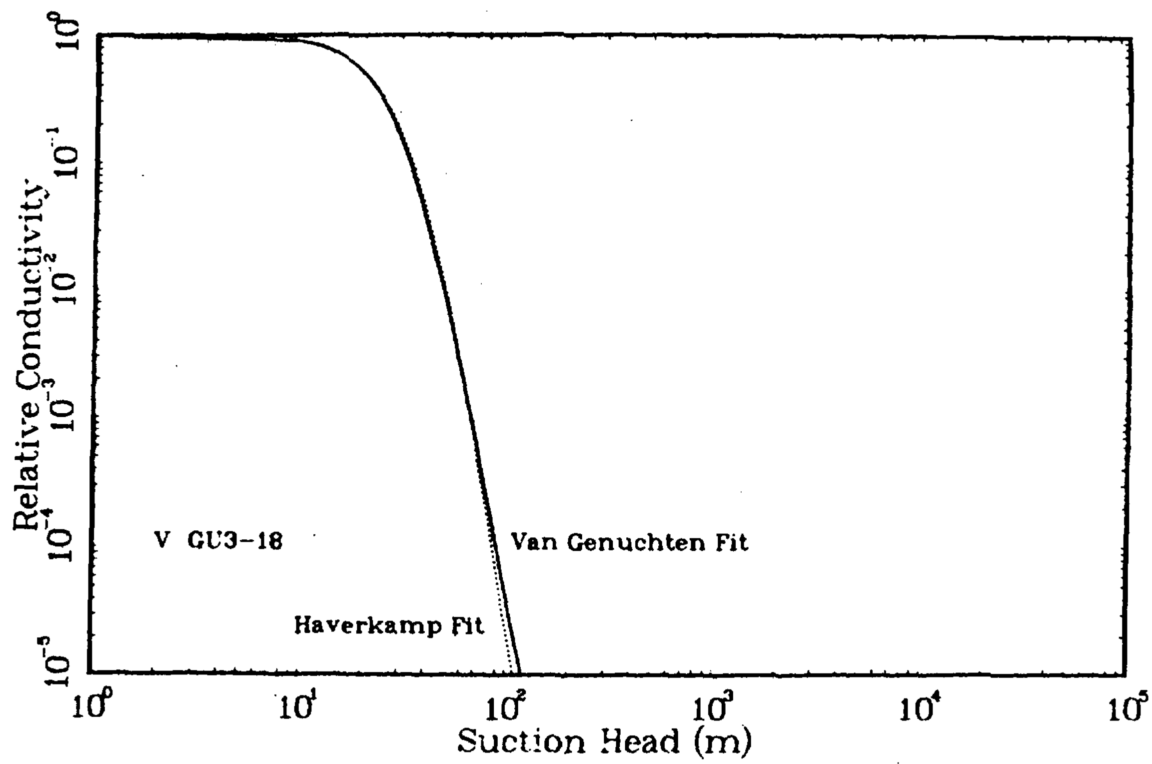


**Figure D.28**

## APPENDIX E

## DATA PLOTS FOR CONFINED SATURATED CONDUCTIVITY TESTS

This appendix contains plots of the results of the confined, saturated conductivity tests. Figures E.1 thru E.3 plot the results of the matrix testing [see Tables A.5 to A.7]. Figures E.4 thru E.18 plot the results of the fracture testing [see Tables A.8 - A.12] and the curve fit of the data [see Table 8].

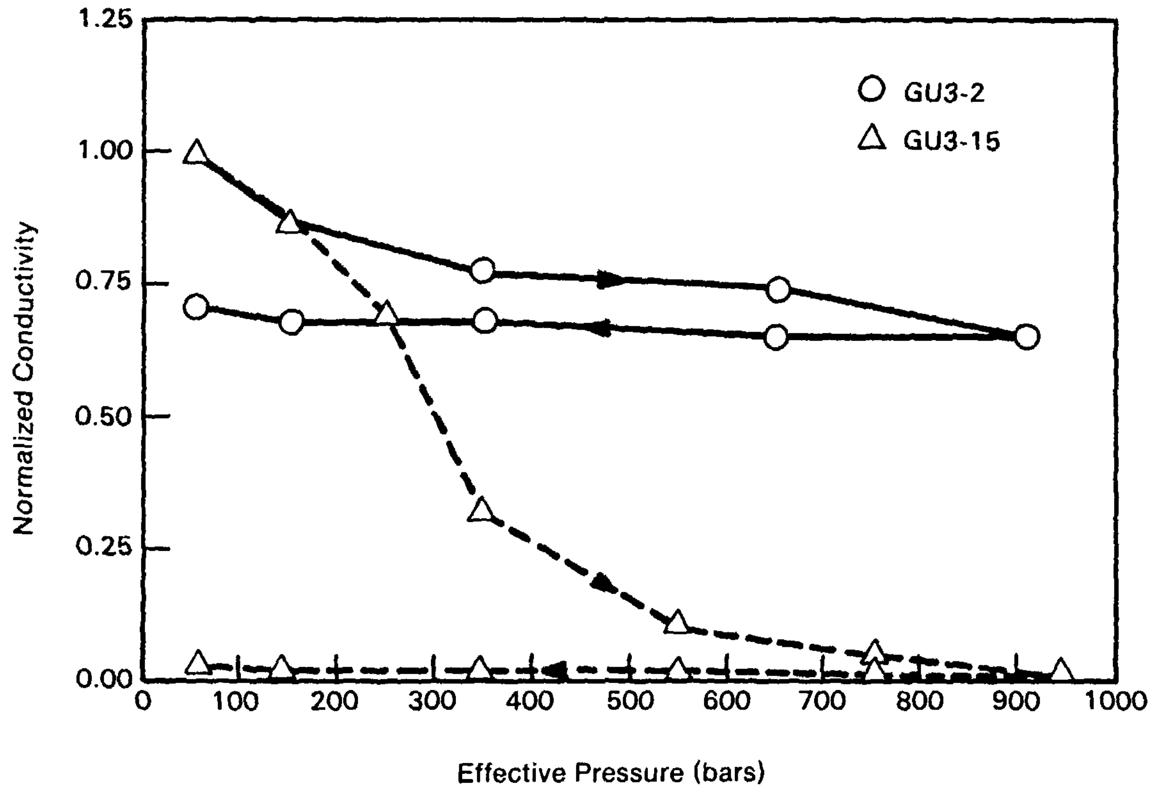


Figure E.1. Normalized Conductivity for Two Tuff Samples from Yucca Mountain as a Function of Increasing Effective Pressure

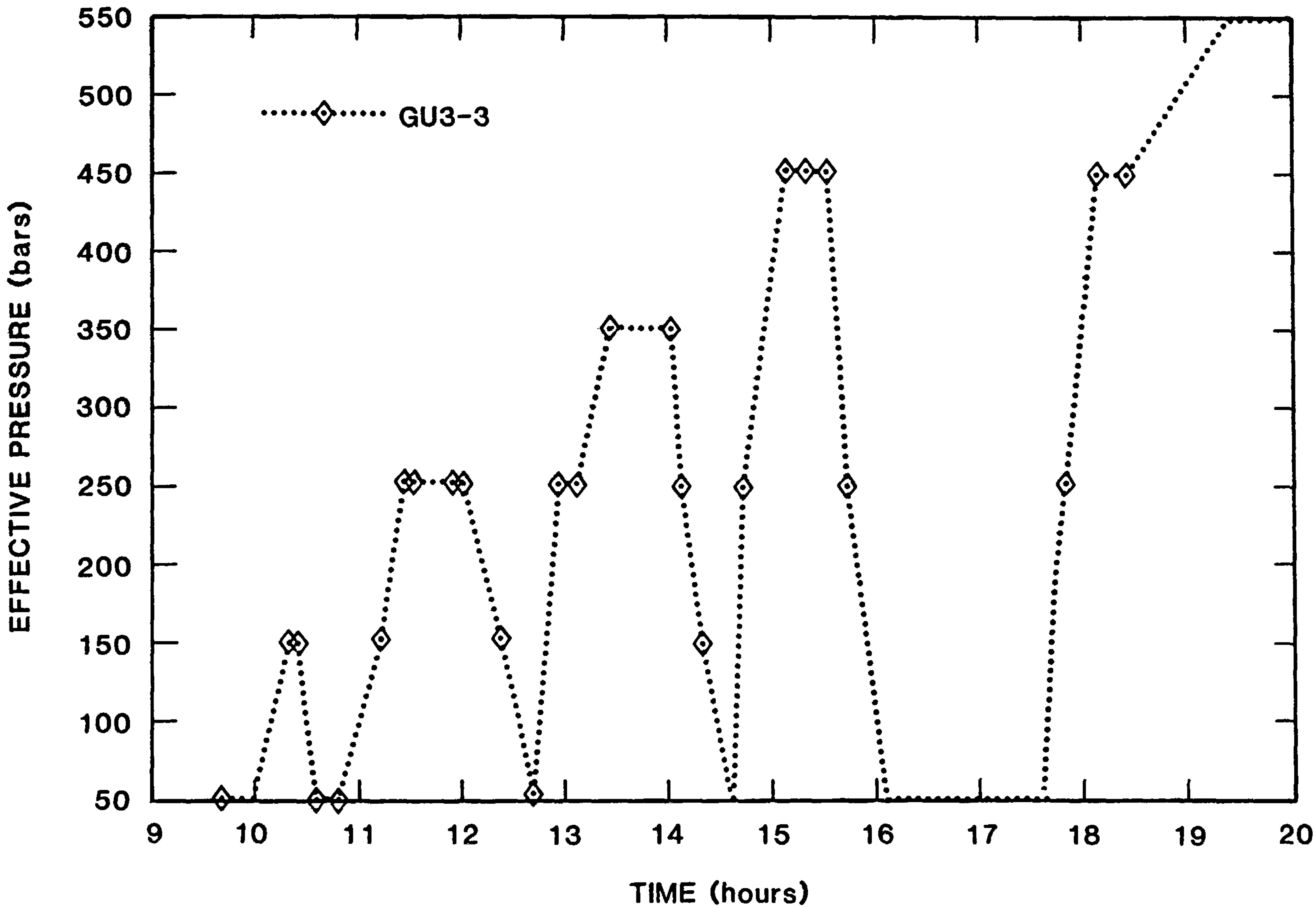


Figure E.2. Effective Pressure Versus Time for Tuff Sample GU3-3 from Yucca Mountain

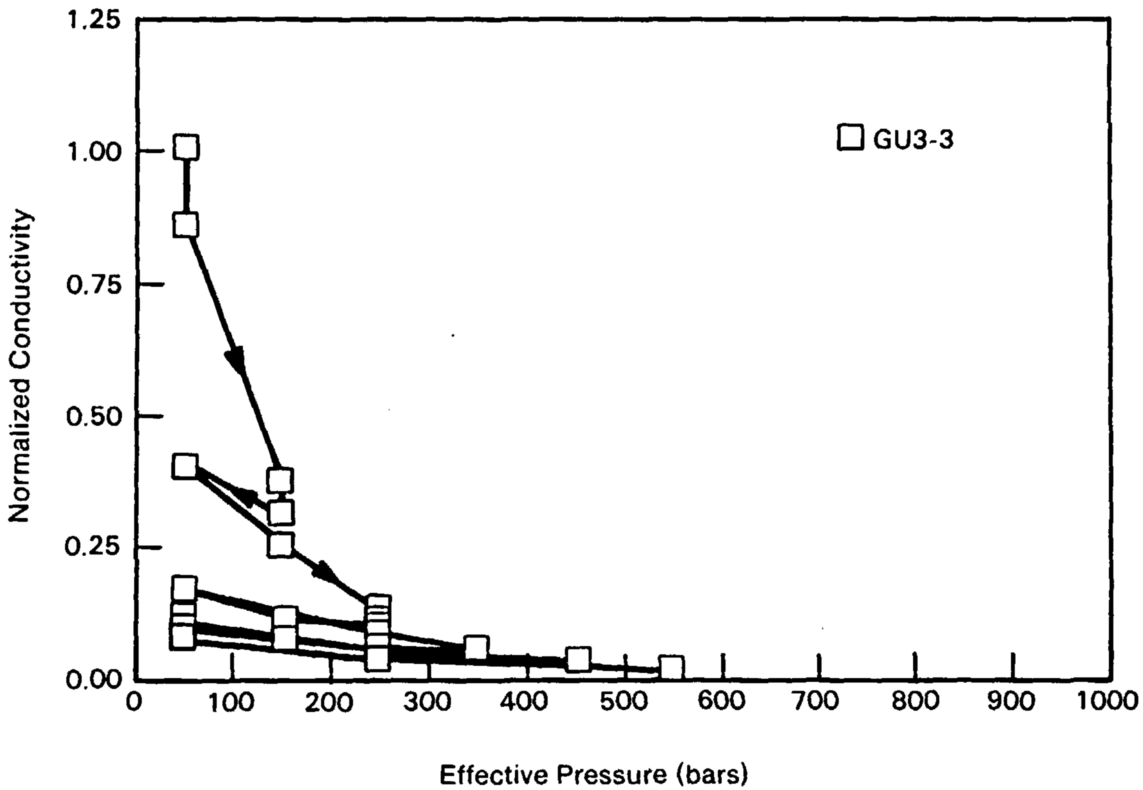


**Figure E.3. Normalized Conductivity for GU3-3 from Yucca Mountain as a Function of Increasing Effective Pressure**

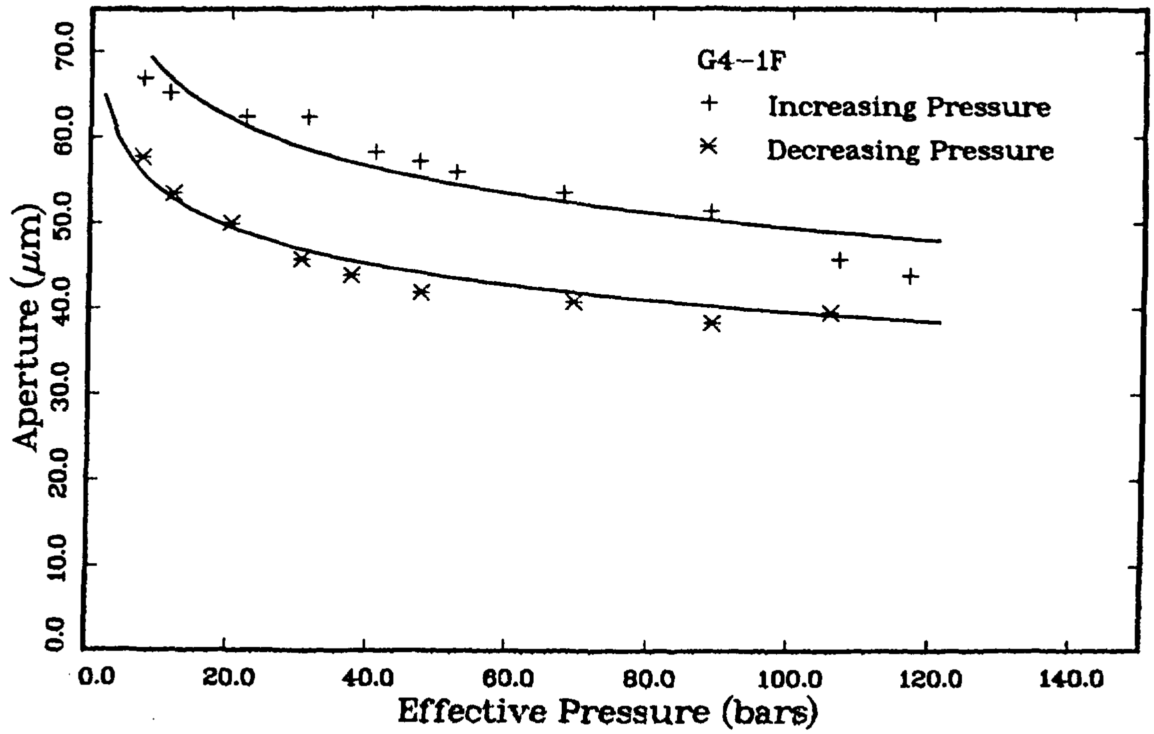


Figure E.4. Computed Aperture Versus Effective Pressure for Sample G4-1F

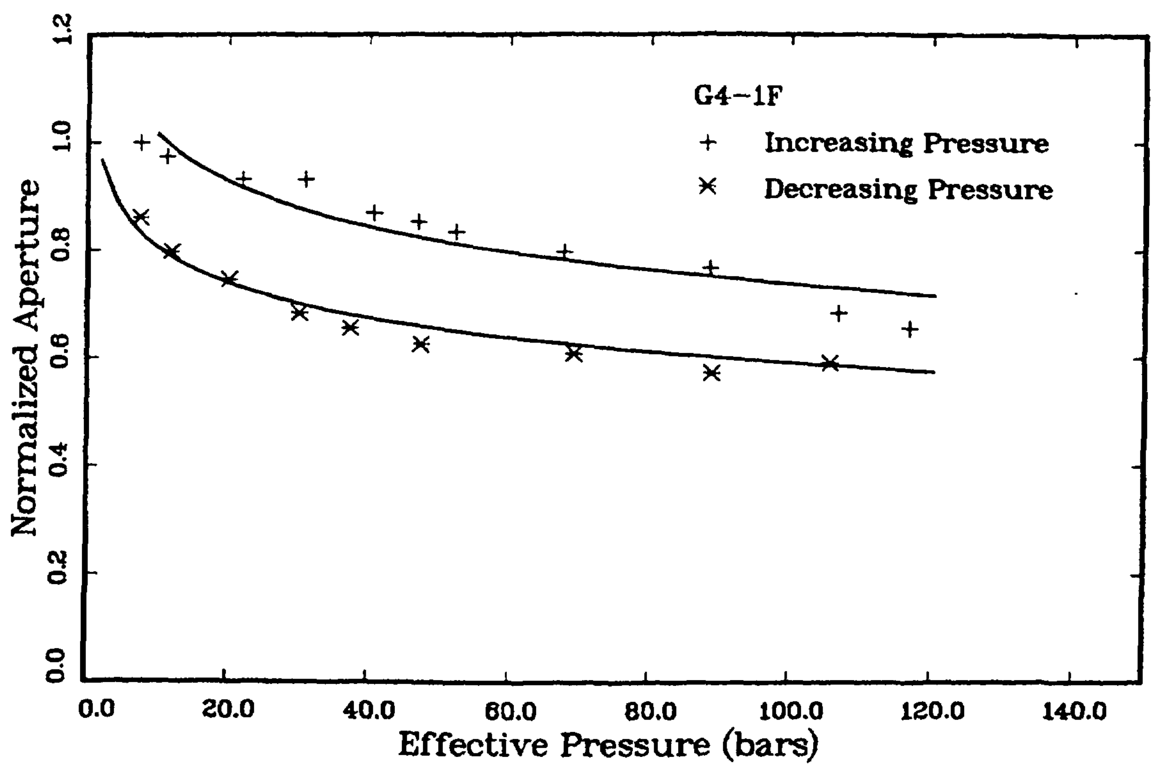


Figure E.5. Normalized Aperture Versus Effective Pressure for Sample G4-1F

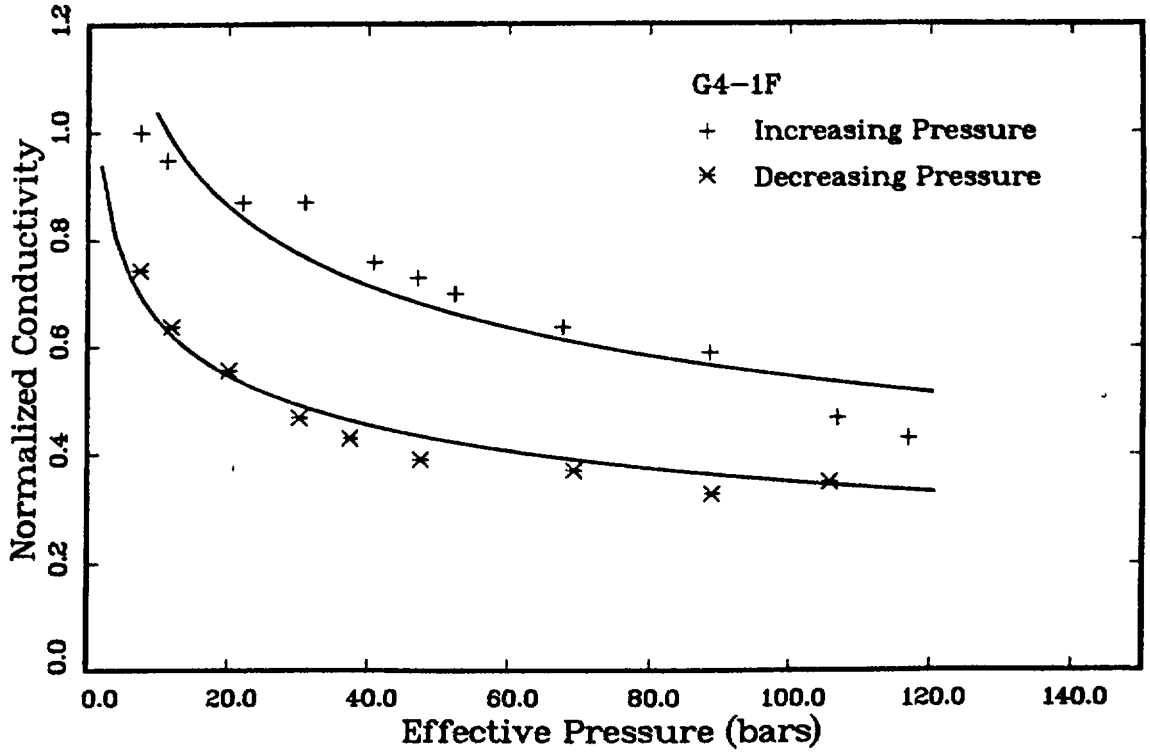


**Figure E.6.** Normalized Conductivity Versus Effective Pressure for Sample G4-1F

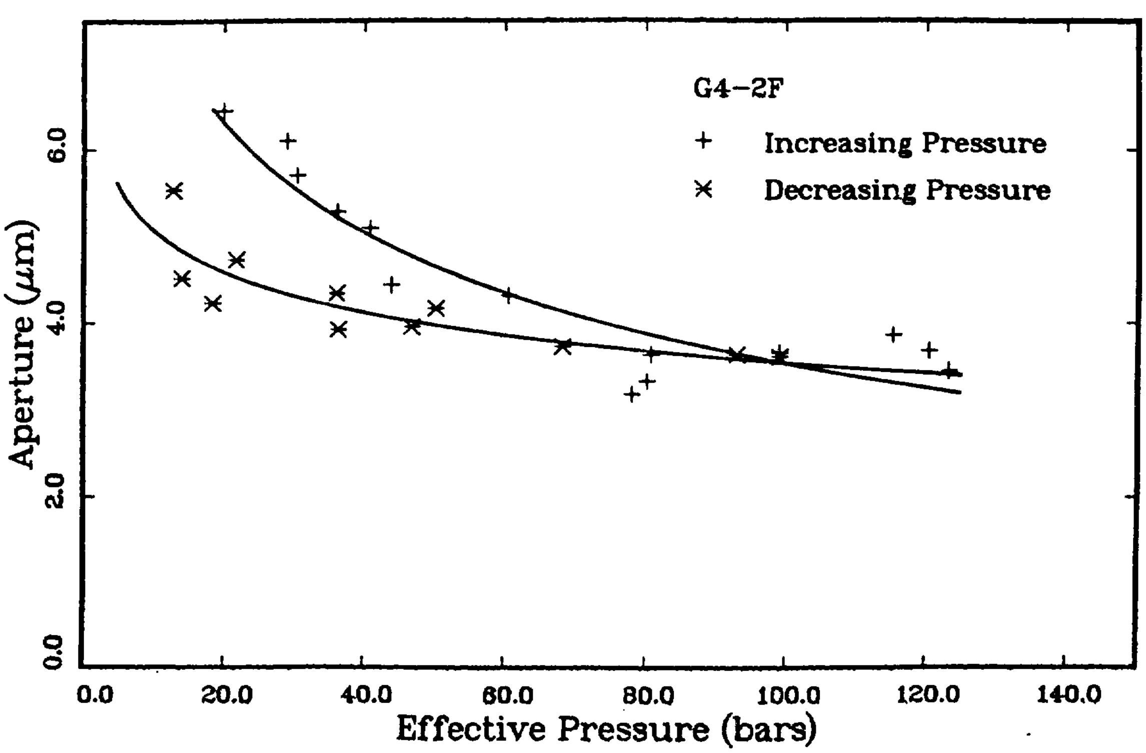


**Figure E.7.** Computed Aperture Versus Effective Pressure for Sample G4-2F

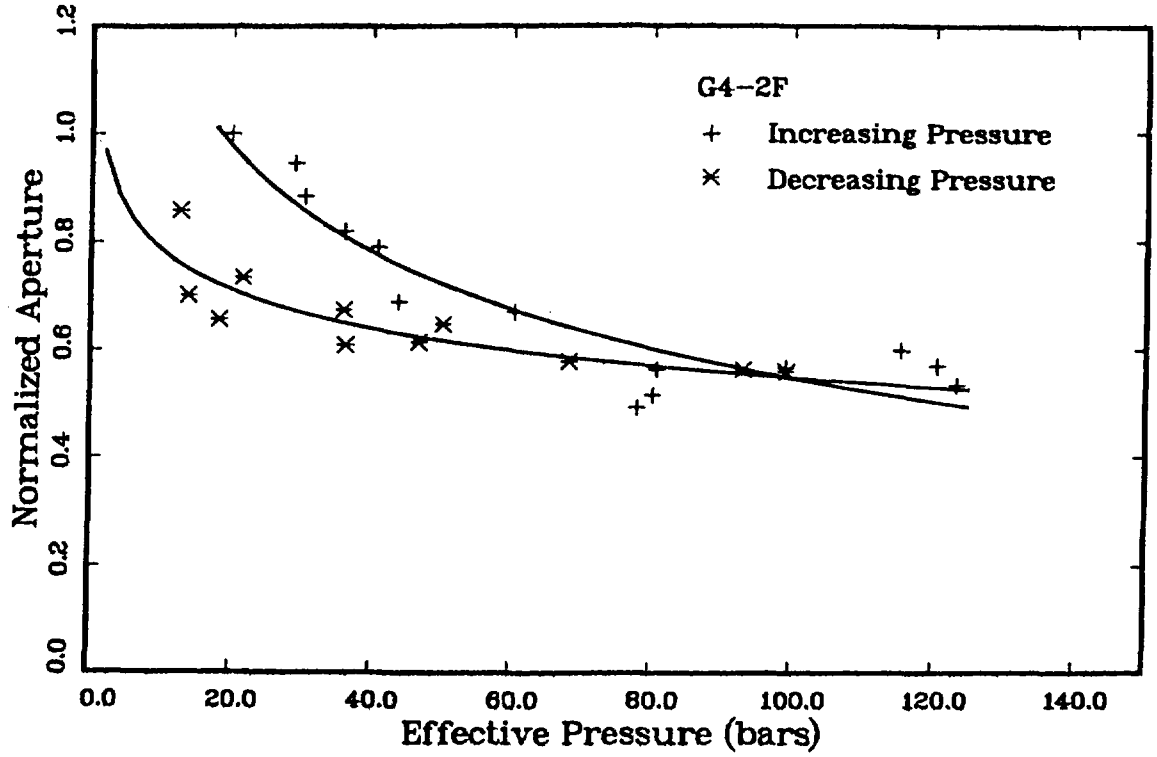


Figure E.8. Normalized Aperture Versus Effective Pressure for Sample G4-2F

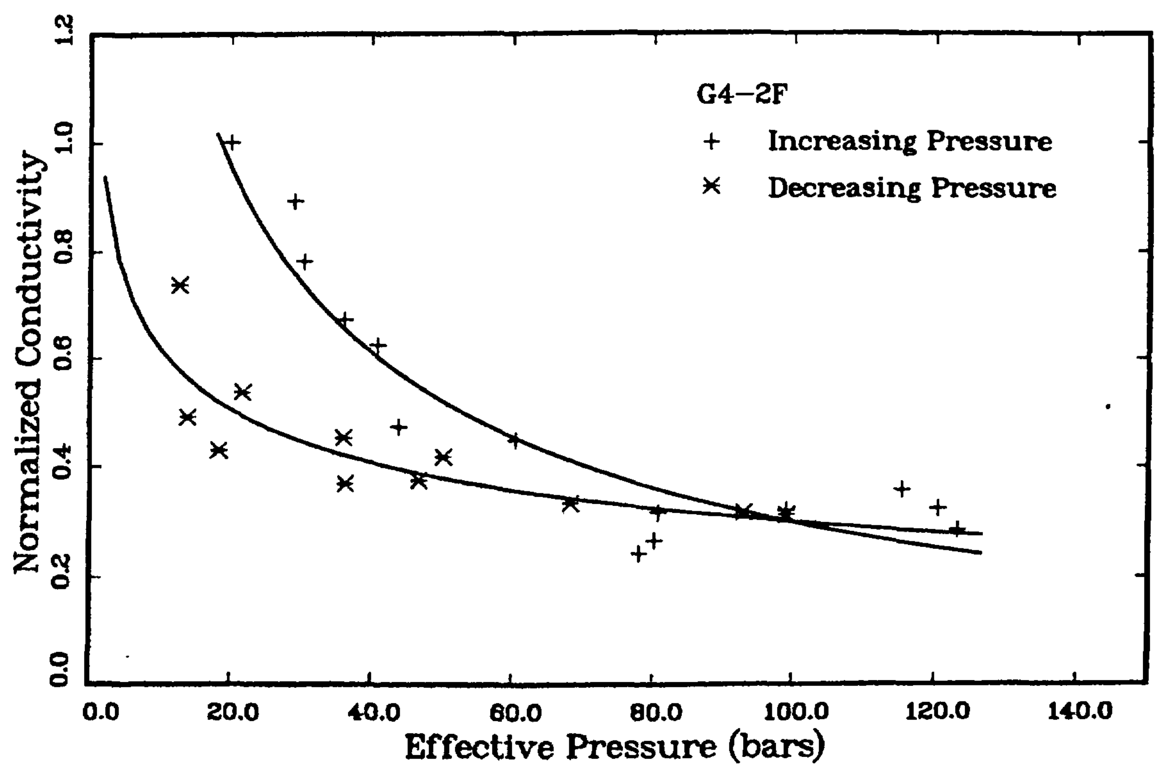


Figure E.9. Normalized Conductivity Versus Effective Pressure for Sample G4-2F

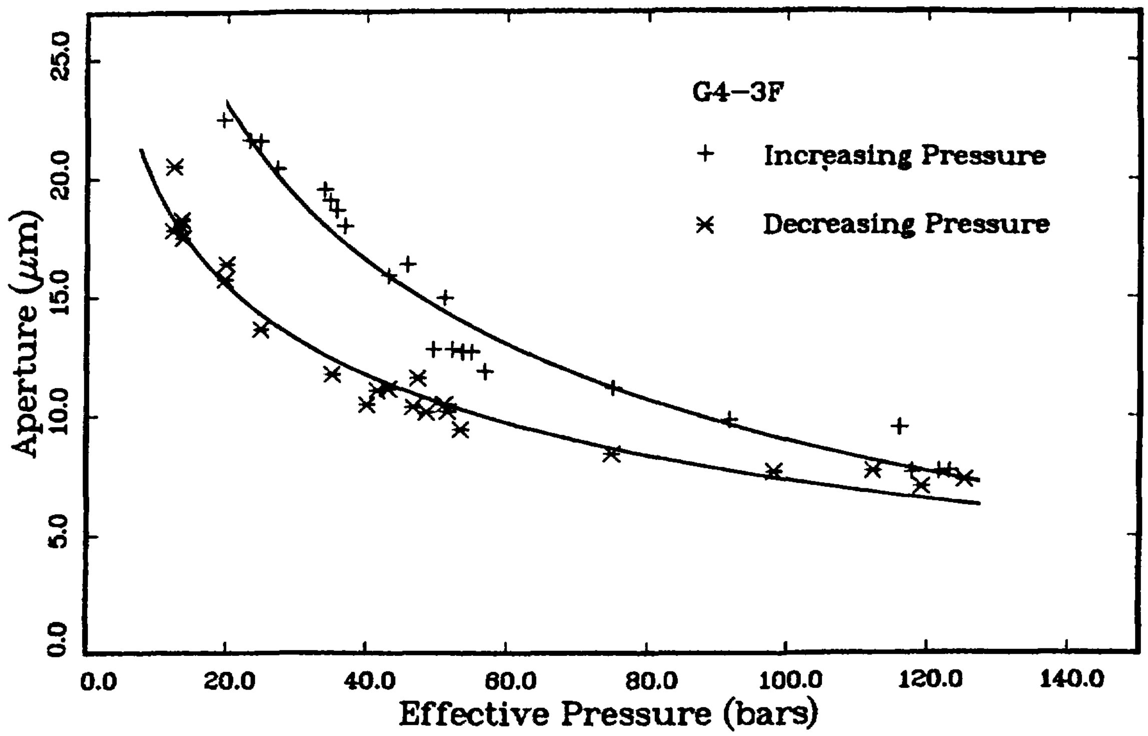


Figure E.10. Computed Aperture Versus Effective Pressure for Sample G4-3F

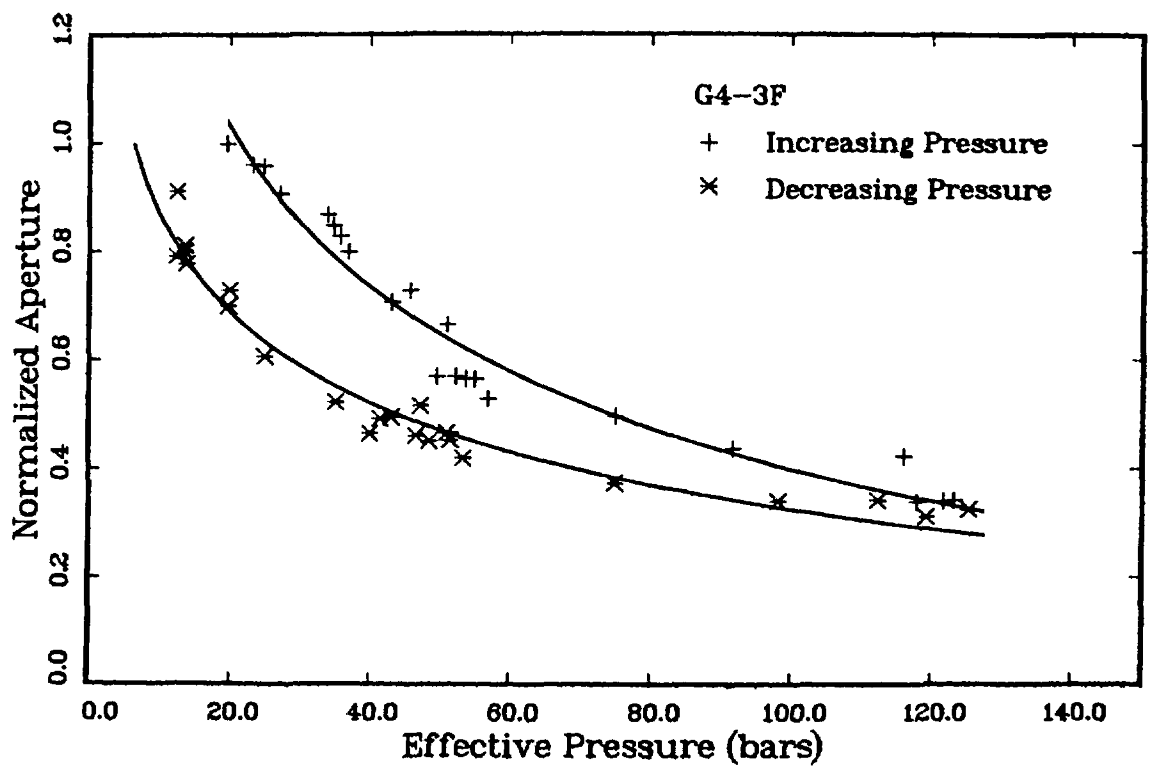


Figure E.11. Normalized Aperture Versus Effective Pressure for Sample G4-3F

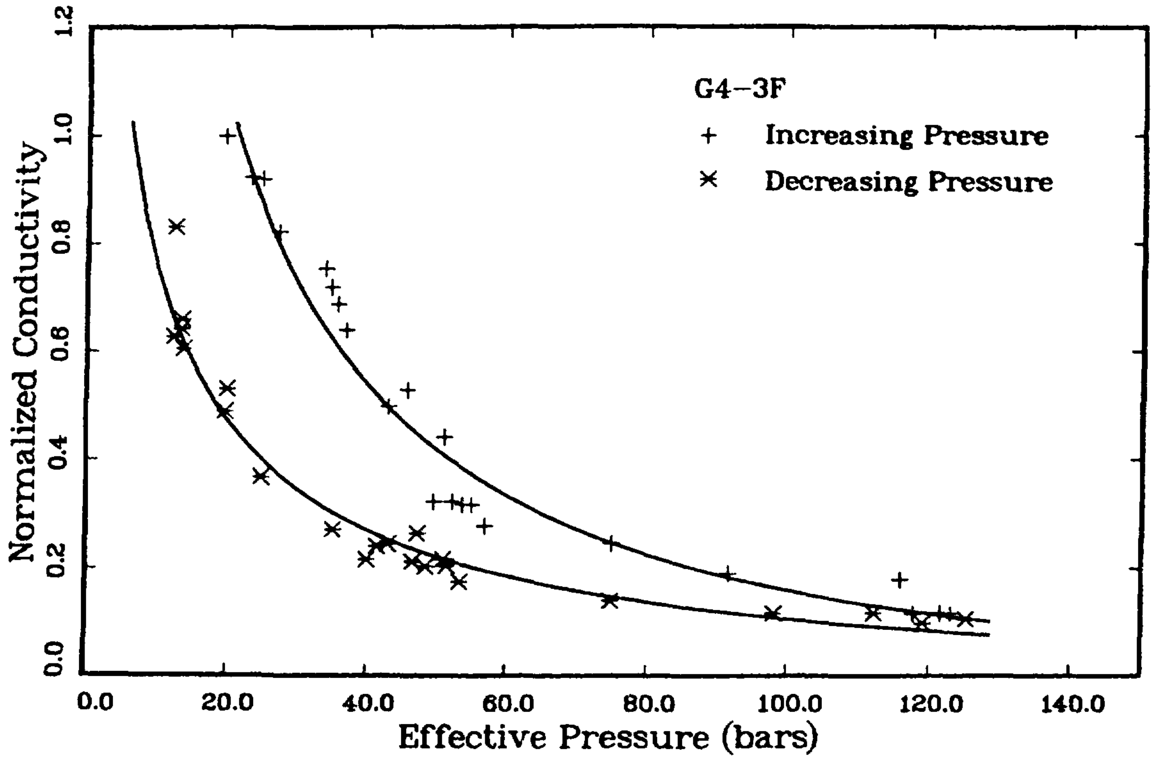


Figure E.12. Normalized Conductivity Versus Effective Pressure for Sample G4-3F

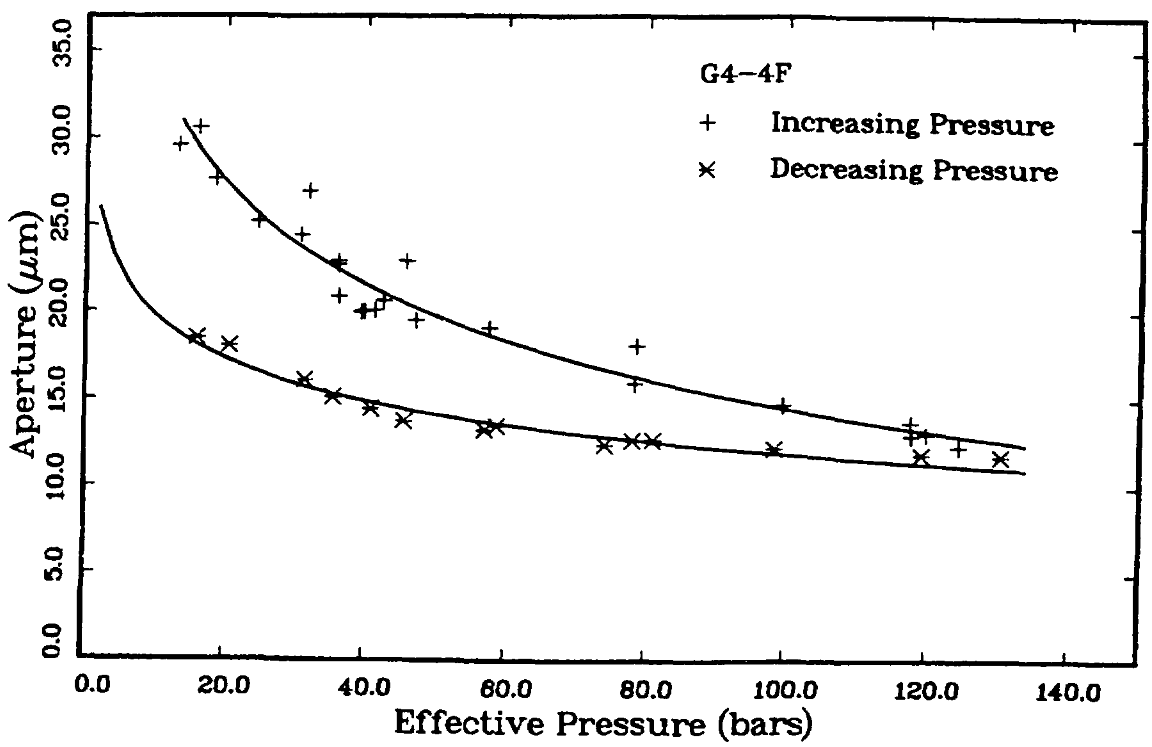


Figure E.13. Computed Aperture Versus Effective Pressure for Sample G4-4F

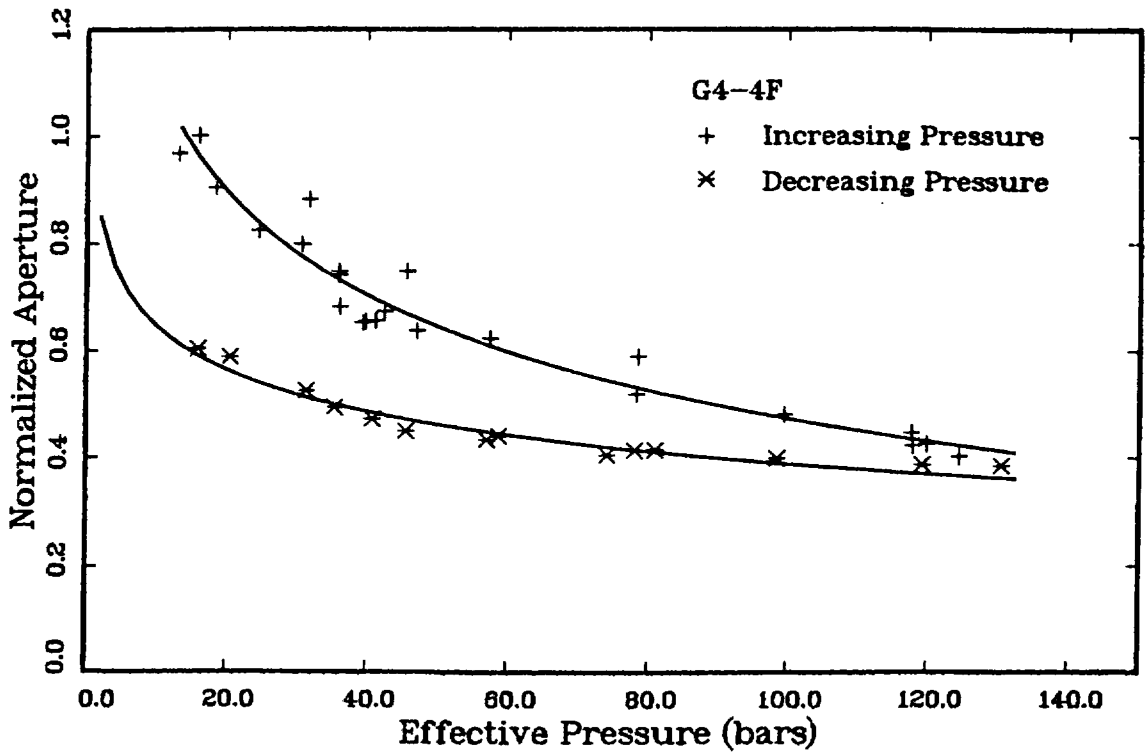


Figure E.14. Normalized Aperture Versus Effective Pressure for Sample G4-4F

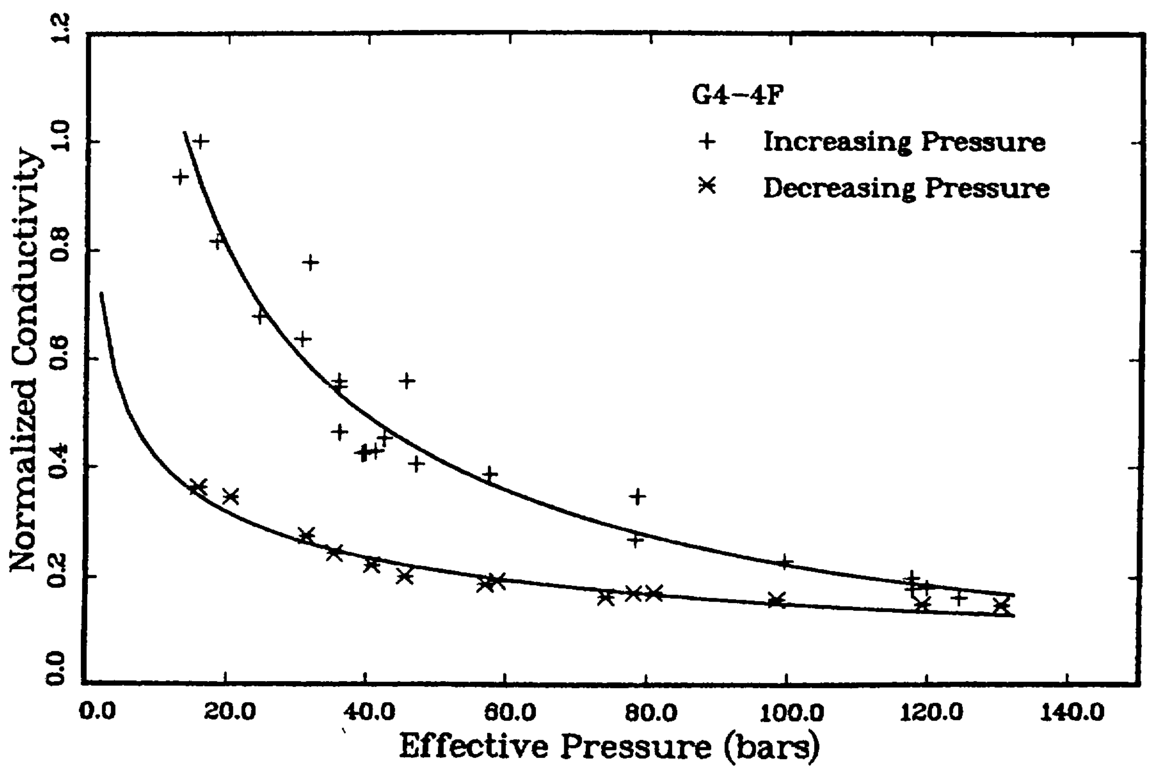


Figure E.15. Normalized Conductivity Versus Effective Pressure for Sample G4-4F

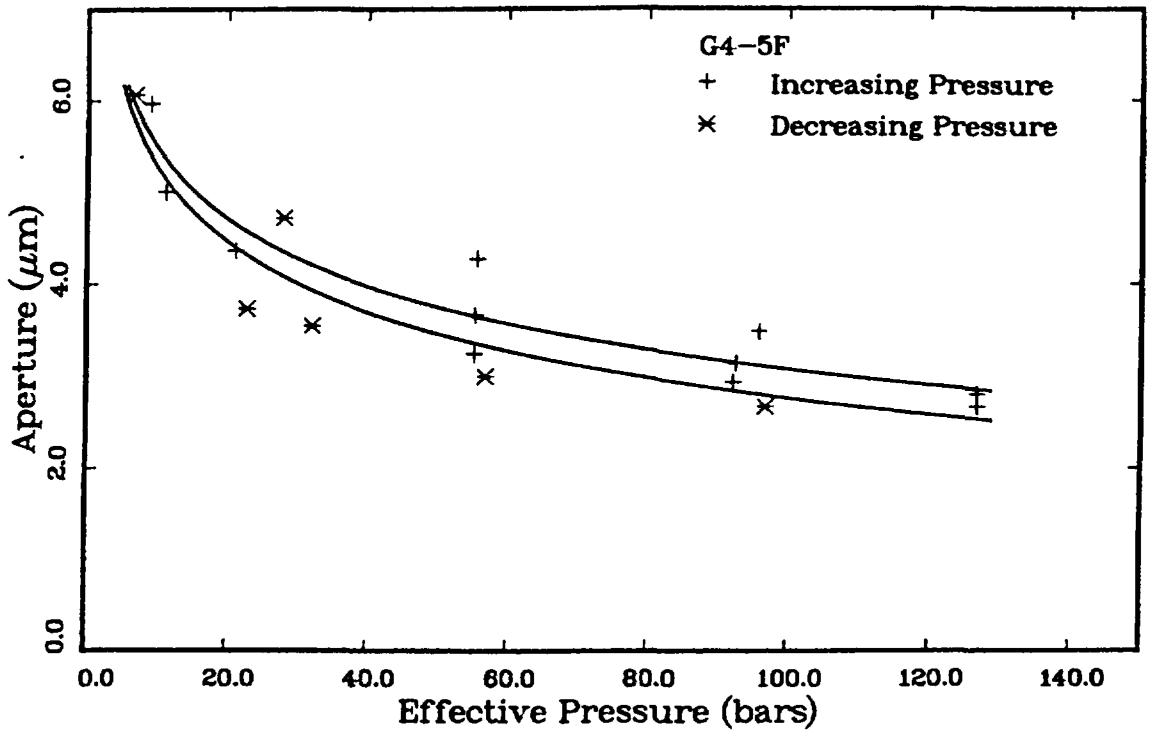


Figure E.16. Computed Aperture Versus Effective Pressure for Sample G4-5F

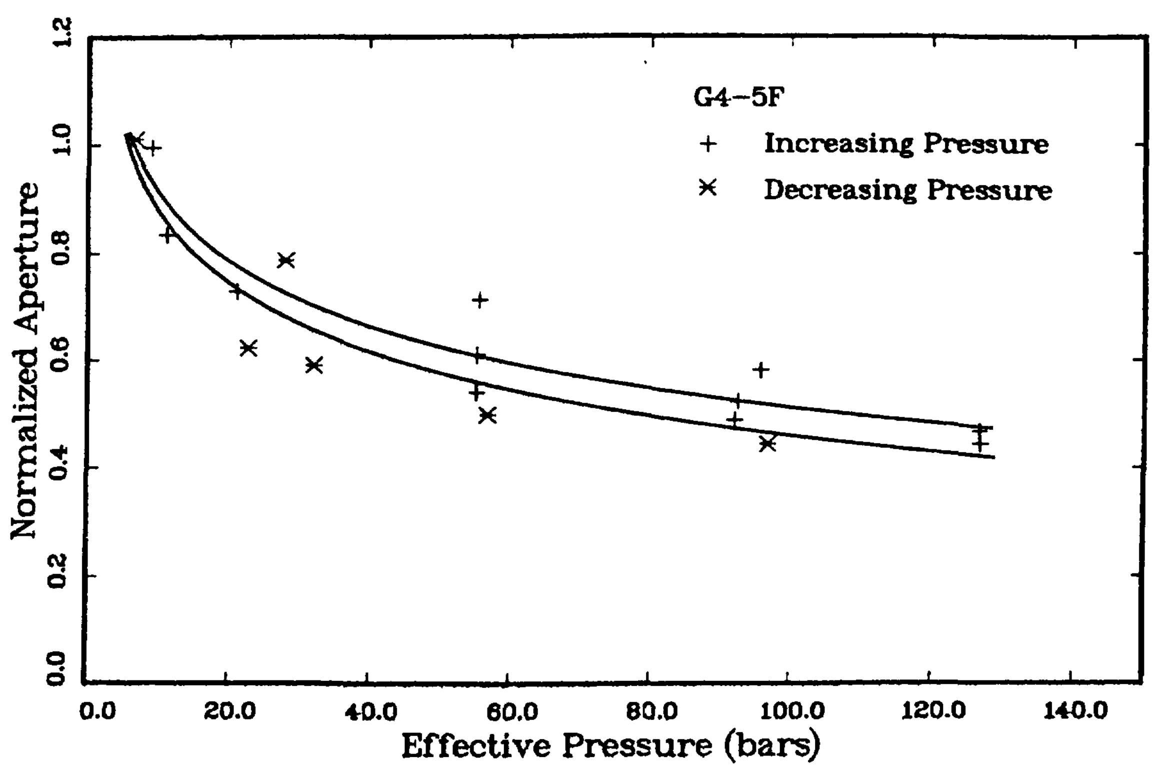


Figure E.17. Normalized Aperture Versus Effective Pressure for Sample G4-5F

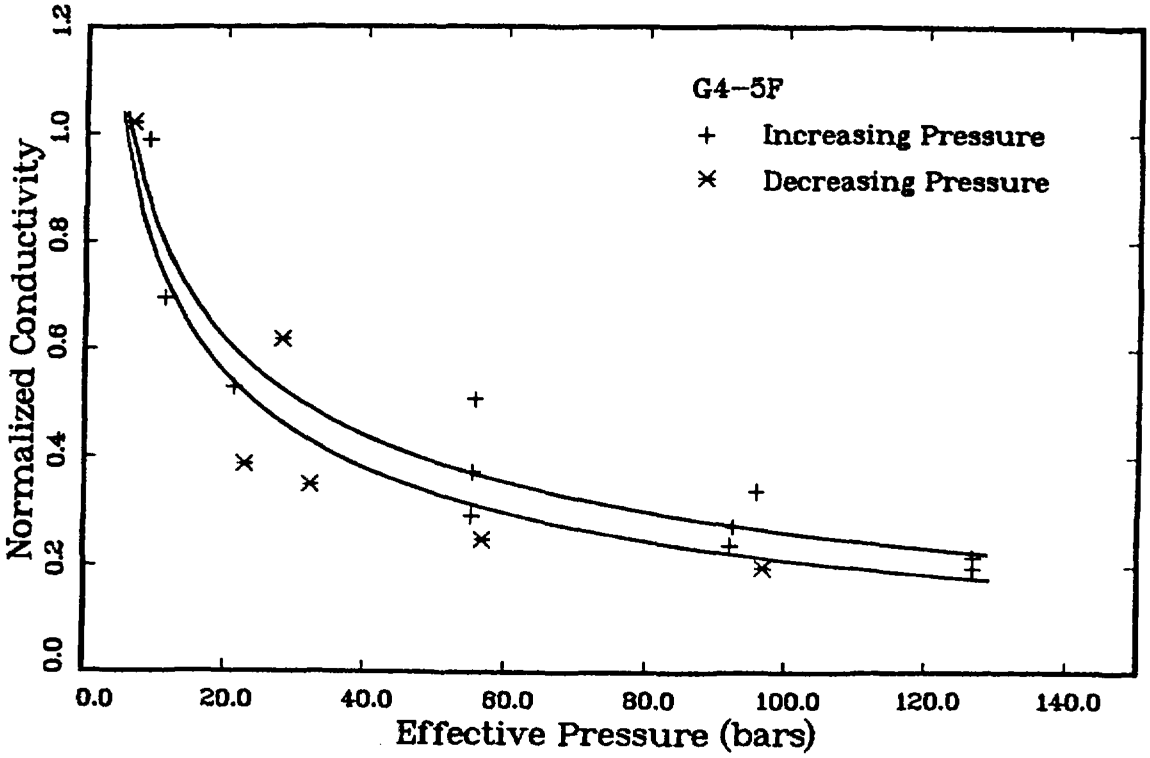


Figure E.18. Normalized Conductivity Versus Effective Pressure for Sample G4-5F

DISTRIBUTION LIST

B. C. Rusche (RW-1)
Director
Office of Civilian Radioactive
Waste Management
U.S. Department of Energy
Forrestal Building
Washington, DC 20585

J. W. Bennett (RW-20)
Office of Geologic Repositories
U.S. Department of Energy
Forrestal Building
Washington, DC 20585

Ralph Stein (RW-23)
Office of Geologic Repositories
U.S. Department of Energy
Forrestal Building
Washington, DC 20585

J. J. Fiore, (RW-22)
Program Management Division
Office of Geologic Repositories
U.S. Department of Energy
Forrestal Building
Washington, DC 20585

M. W. Frei (RW-23)
Engineering & Licensing Division
Office of Geologic Repositories
U.S. Department of Energy
Forrestal Building
Washington, DC 20585

E. S. Burton (RW-25)
Siting Division
Office of Geologic Repositories
U.S. Department of Energy
Forrestal Building
Washington, D.C. 20585

C. R. Cooley (RW-24)
Geosciences & Technology Division
Office of Geologic Repositories
U.S. Department of Energy
Forrestal Building
Washington, DC 20585

T. P. Longo (RW-25)
Program Management Division
Office of Geologic Repositories
U.S. Department of Energy
Forrestal Building
Washington, DC 20585

Cy Klingsberg (RW-24)
Geosciences and Technology Division
Office of Geologic Repositories
U. S. Department of Energy
Forrestal Building
Washington, DC 20585

B. G. Gale (RW-25)
Siting Division
Office of Geologic Repositories
U.S. Department of Energy
Forrestal Building
Washington, D.C. 20585

R. J. Blaney (RW-22)
Program Management Division
Office of Geologic Repositories
U.S. Department of Energy
Forrestal Building
Washington, DC 20585

R. W. Gale (RW-44)
Office of Policy, Integration, and
Outreach
U.S. Department of Energy
Forrestal Building
Washington, D.C. 20585

J. E. Shaheen (RW-44)
Outreach Programs
Office of Policy, Integration and
Outreach
U.S. Department of Energy
Forrestal Building
Washington, DC 20585

J. O. Neff
Salt Repository Project Office
U.S. Department of Energy
505 King Avenue
Columbus, OH 43201

D. C. Newton (RW-23)
Engineering & Licensing Division
Office of Geologic Repositories
U.S. Department of Energy
Forrestal Building
Washington, DC 20585

O. L. Olson, Manager
Basalt Waste Isolation Project Office
U.S. Department of Energy
Richland Operations Office
Post Office Box 550
Richland, WA 99352

D. L. Vieth, Director (4)
Waste Management Project Office
U.S. Department of Energy
Post Office Box 14100
Las Vegas, NV 89114

D. F. Miller, Director
Office of Public Affairs
U.S. Department of Energy
Post Office Box 14100
Las Vegas, NV 89114

D. A. Nowack (14)
Office of Public Affairs
U.S. Department of Energy
Post Office Box 14100
Las Vegas, NV 89114

B. W. Church, Director
Health Physics Division
U.S. Department of Energy
Post Office Box 14100
Las Vegas, NV 89114

Chief, Repository Projects Branch
Division of Waste Management
U.S. Nuclear Regulatory Commission
Washington, D.C. 20555

S. A. Mann, Manager
Crystalline Rock Project Office
U.S. Department of Energy
9800 South Cass Avenue
Argonne, IL 60439

K. Street, Jr.
Lawrence Livermore National
Laboratory
Post Office Box 808
Mail Stop L-209
Livermore, CA 94550

L. D. Ramspott (3)
Technical Project Officer for NNWSI
Lawrence Livermore National
Laboratory
P.O. Box 808
Mail Stop L-204
Livermore, CA 94550

J. E. Boudreau
Los Alamos National Laboratory
P.O. Box 1663
Mail Stop F-671
Los Alamos, NM 87545

D. T. Oakley (3)
Technical Project Officer for NNWSI
Los Alamos National Laboratory
P.O. Box 1663
Mail Stop F-671
Los Alamos, NM 87545

W. W. Dudley, Jr. (3)
Technical Project Officer for NNWSI
U.S. Geological Survey
Post Office Box 25046
418 Federal Center
Denver, CO 80225

NTS Section Leader
Repository Project Branch
Division of Waste Management
U.S. Nuclear Regulatory Commission
Washington, D.C. 20555

Document Control Center
Division of Waste Management
U.S. Nuclear Regulatory Commission
Washington, D.C. 20555

P. T. Prestholt
NRC Site Representative
1050 East Flamingo Road
Suite 319
Las Vegas, NV 89109

M. E. Spaeth
Technical Project Officer for NNWSI
Science Applications
International, Corp.
2769 South Highland Drive
Las Vegas, NV 89109

SAIC-T&MSS Library (2)
Science Applications
International, Corp.
2950 South Highland Drive
Las Vegas, NV 89109

W. S. Twenhofel, Consultant
Science Applications
International, Corp.
820 Estes Street
Lakewood, CO 80215

A. E. Gurrola
General Manager
Energy Support Division
Holmes & Narver, Inc.
Post Office Box 14340
Las Vegas, NV 89114

J. A. Cross, Manager
Las Vegas Branch
Fenix & Scisson, Inc.
Post Office Box 15408
Las Vegas, NV 89114

N. E. Carter
Battelle Columbus Laboratory
Office of Nuclear Waste Isolation
505 King Avenue
Columbus, OH 43201

V. M. Glanzman
U.S. Geological Survey
Post Office Box 25046
913 Federal Center
Denver, CO 80225

J. B. Wright
Technical Project Officer for NNWSI
Westinghouse Electric Corporation
Waste Technology Services Division
Nevada Operations
Post Office Box 708
Mail Stop 703
Mercury, NV 89023

ONWI Library (2)
Battelle Columbus Laboratory
Office of Nuclear Waste Isolation
505 King Avenue
Columbus, OH 43201

W. M. Hewitt, Program Manager
Roy F. Weston, Inc.
2301 Research Blvd., 3rd Floor
Rockville, MD 20850

H. D. Cunningham
General Manager
Reynolds Electrical &
Engineering Co., Inc.
Post Office Box 14400
Mail Stop 555
Las Vegas, NV 89114

T. Hay, Executive Assistant
Office of the Governor
State of Nevada
Capitol Complex
Carson City, NV 89710

R. R. Loux, Jr., Director (8)
Nuclear Waste Project Office
State of Nevada
Capitol Complex
Carson City, NV 89710

C. H. Johnson, Technical
Program Manager
Nuclear Waste Project Office
State of Nevada
Capitol Complex
Carson City, NV 89710

Len Anderson
U.S. Geological Survey
P.O. Box 25026
Denver Federal Center
Denver, CO 80225

E. Weeks
U.S. Geological Survey
P.O. Box 25046
Mail Stop 413
Denver Federal Center
Denver, CO 80225

T. R. Pigford
Dept. of Nuclear Engineering
University of California
Berkeley, CA 94702
Las Vegas, NV 89114

S. C. Blair (5)
Pacific Northwest Laboratory
P.O. Box 999
Richland, WA 99352

D. W. Dragnich
Pacific Northwest Laboratory
P.O. Box 999
Richland, WA 99352

G. W. Gee (3)
Pacific Northwest Laboratory
P.O. Box 999
Richland, WA 99352

P. R. Heller (3)
Pacific Northwest Laboratory
P.O. Box 999
Richland, WA 99352

D. Evans
Dept. of Hydrology and Water
Resources
University of Arizona
Phoenix, AZ 85721

D. D. Gonzalez
R.F. Weston, Inc.
5301 Central NE
Albuquerque, NM 87108

P. Montazer
U.S. Geological Survey
P.O. Box 25046
Mail Stop 416
Denver, CO 80225

J. L. Younker (15)
Science Applications, Inc.
2769 S. Highland Drive
Las Vegas, NV 89101

W. W. Owens
6269 S. Knoxville
Tulsa, OK 74136

F. H. Dove (3)
Pacific Northwest Laboratory
P.O. Box 999
Richland, WA 99352

M. D. Freshley
Pacific Northwest Laboratory
P.O. Fox 999
Richland, WA 99352

P. C. Hays
Pacific Northwest Laboratory
P.O. Box 999
Richland, WA 99352

S. B. Pahwa
Intera Technologies Inc.
11999 Katy Freeway, Suite, 610
Houston, TX 77079

H. W. Bentley
Hydro GeoChem, Inc.
1430 N. Sixth Av.
Tuscon, AZ 85705

M. R. Kreiter
Pacific Northwest Laboratory
P.O. Box 999
Richland, WA 99352

J. A. Stottlemyre
Pacific Northwest Laboratory
P.O. Box 999
Richland, WA 99352

L. L. Wendell
Pacific Northwest Laboratory
P.O. Box 999
Richland, WA 99352

Technical Information Library
Pacific Northwest Laboratory
P.O. Box 999
Richland, WA 99352

Publishing Coordination (2)
Pacific Northwest Laboratory
P.O. Box 999
Richland, WA 99352

John Fordham
Desert Research Institute
Water Resources Center
Post Office Box 60220
Reno, NV 89506

Dr. Martin Mifflin
Desert Research Institute
Water Resources Center
Suite 201
1500 East Tropicana Avenue
Las Vegas, NV 89109

Department of Comprehensive Planning
Clark County
225 Bridger Avenue, 7th Floor
Las Vegas, NV 89155

Planning Department
Nye County
Post Office Box 153
Tonopah, NV 89049

Lincoln County Commission
Lincoln County
Post Office Box 90
Pioche, NV 89043

Economic Development Department
City of Las Vegas
400 East Stewart Avenue
Las Vegas, NV 89101

D. Alexander
RW24 OCRWM
7F088 Forrestal Building
Washington, DC 20585

Community Planning and Development
City of North Las Vegas
Post Office Box 4086
North Las Vegas, NV 89030

| | |
|---|---|
| 6300 | R. W. Lynch |
| 6310 | T. O. Hunter |
| 6310 | NNWSICF |
| 6311 | L. W. Scully |
| 6311 | L. Perrine (2) |
| 6312 | F. W. Bingham |
| 6312 | A. L. Dudley |
| 6312 | N. K. Hayden |
| 6312 | S. R. Dengler |
| 6312 | J. W. Braithwaite |
| 6312 | J. Foster |

6312 J. H. Gauthier
6312 B. S. Langkopf
6312 Y. T. Lin
6312 T. S. Ortiz
6312 R. R. Peters (10)
6312 S. Sinnock
6312 M. S. Tierney (3)
6312 J. G. Yeager
6312 M. Wilson
6313 J. R. Tillerson
6313 S. J. Bauer
6313 R. M. Zimmerman
6313 F. B. Nimick
6313 J. A. Fernandez
6313 E. A. Klavetter (5)
6313 B. M. Schwartz
6313 Data Set File
6330 NNWSI CF
6331 A. R. Lappin
6332 L. D. Tyler
6332 WMP Library
6430 N. R. Ortiz
1511 R. R. Eaton
1511 N. E. Bixler
1512 D. C. Reda
1542 R. H. Price
7223 R. G. Easterling
7223 I. J. Hall (3)
3141 C. M. Ostrander (5)
3151 W. L. Garner (3)
8024 M. A. Pound
DOE/TIC (28)
(3154-3 C. H. Dalin)

| Org. | Bldg. | Name | Rec'd by | Org. | Bldg. | Name | Rec'd by |
|---|---|---|---|---|---|---|---|
| | | | | | | | |
| | | | | | | | |
| | | | | | | | |
| | | | | | | | |
| | | | | | | | |
| | | | | | | | |
| | | | | | | | |
| | | | | | | | |
| | | | | | | | |
| | | | | | | | |
| | | | | | | | |
| | | | | | | | |
| | | | | | | | |
| | | | | | | | |
| | | | | | | | |

Sandia National Laboratories